INCREASING DRUG RETENTION IN LUNG TISSUE THROUGH CONJUGATION WITH POLYETHYLENE-GLYCOL

FABRICE J.C. BAYARD

Thesis submitted to the University of Nottingham for the degree of Doctor of Philosophy

JULY 2013

Abstract

The pulmonary delivery of drugs is an attractive route of administration because of the large surface area and high permeability of the airway epithelium, the main barrier for drug absorption. The large majority of inhaled drugs are used to manage asthma and Chronic Obstructive Pulmonary Disorder (COPD), such as inhaled corticosteroids and β_2-adrenergic receptor agonists. Local delivery of small molecules often results in sub-optimal pharmacokinetics characterised by short absorption times (t_{max}) and high systemic concentrations (C_{max}). Numerous drug delivery strategies have been attempted to increase lung retention time, including drug encapsulation in microspheres, the use of polymeric excipients, or the formation of low solubility drugs. So far, drug conjugation strategies have been limited to decreasing the prodrug solubility. The non-permanent conjugation of small molecules to a large hydrophilic polymer has not been studied for pulmonary delivery. The rationale behind such a strategy is that small molecules are mainly absorbed through the epithelium by passive diffusion, the absorption rates being positively correlated to the drug lipophilicity and molecular weight.

This project has therefore been looking at the production, characterisation, *in vitro* and *ex vivo* evaluation of polyethylene glycol (PEG)-ester conjugates for the sustained delivery of drugs to the lung. This thesis presents the successful oxidation and subsequent esterification of PEG of various molecular weights with prednisolone (a corticosteroid) and salbutamol (a β_2-adrenergic receptor agonist). Overall, four ester conjugates of PEG and prednisolone were studied: three disubstituted PEG of 1000, 2000 and 3400 Da (PEG-$Pred_2$) and one monosubstituted PEG of 2000 Da (mPEG-$Pred_1$). Three ester conjugates of PEG

and salbutamol were also prepared but they were unstable in buffers at pH 6.2 to 8.0, and were not studied any further. The hydrolysis rates of PEG-prednisolone conjugates were pH dependant and the monosubstituted conjugate hydrolysed twice as slowly as the disubstituted ones. *In vitro* stability was not molecular weight dependant. Hydrolysis half lives of PEG-prednisolone conjugates were 35 and 70 h at pH 6.2, 3 and 6 h at pH 7.4 and 1 and 2 h at pH 8.0 for mPEG-$Pred_1$ and PEG-$Pred_2$ respectively. The cytotoxicity of PEG-prednisolone conjugates was assessed using the lactate dehydrogenase membrane integrity test on the human bronchial epithelial Calu-3 cell culture model. Conjugates of 1000 and 2000 Da were not cytotoxic to Calu-3 cells, up to 1000 μM. PEG_{3400}-$Pred_2$ however, was cytotoxic at concentrations above 1 μM and thus this compound was not studied any further. The three remaining conjugates were stable in the presence of Calu-3 cells, with half lives comparable to that of autohydrolysis. The local pharmacokinetics of esters of PEG_{2000} and prednisolone were compared to that of prednisolone alone in an isolated and perfused rat lung (IPRL). For the lead compound PEG-$Pred_2$, C_{max} was reduced by a factor 3 and t_{max} increased by 45%, compared to prednisolone. The apparent prednisolone absorption half life from the lung was 1 min with prednisolone and 8 min with PEG-$Pred_2$.

This study illustrated the feasibility of a polymeric drug conjugate strategy for sustained release of drugs to the lung. The conjugates exhibited good *in vitro* stability which was translated into improved pharmacokinetics and longer residence time *ex vivo* in the IPRL. Further studies must be conducted to fully assess the role of esterases in the pulmonary hydrolysis of the conjugates and *in vivo* experiments would be necessary to verify the safety of the conjugates and efficacy of the drug.

Acknowledgments

I would like to thank my academic supervisors Dr Cynthia Bosquillon (School of Pharmacy, Division of Drug Delivery and Tissue Engineering, The University of Nottingham), Dr Wim Thielemans (School of Chemistry and Process and Environmental Research division, Faculty of Engineering, The University of Nottingham), Prof Dave Pritchard (Division of Molecular Sciences, The University of Nottingham), Dr Stuart Paine (School of Veterinary Medicine and Science, The University of Nottingham), my industrial supervisors Dr Simon Young (Bioscience, AstraZeneca, Alderley Park, UK) and Dr Per Bäckman (Respiratory and Inflammation, Pharmaceutical and Analytical Research and Development department, AstraZeneca, Mölndal, Sweden).

Particularly, thank to Wim Thielemans' group, the Tissue Engineering and the Centre for Analytical Bioscience at the University of Nottingham. I am indebted to the Respiratory and Inflammation DMPK department at AstraZeneca, Mölndal (Sweden), and particularly, thanks to Dr Holger Adelmann and Dr François Guillou to facilitate my transfer to Sweden. I am very grateful to Dr Pär Ewing for his skilled surgical expertise and advices and to Dr Katarina Rubin for her training.

I would like to thank the Centre for Doctoral Training in Targeted Therapeutics and Formulation Science, particularly Prof Cameron Alexander, its operational director.

I am very grateful to AstraZeneca and the Engineering and Physical Sciences Research Council, who funded the project (grants EP/D501849/1 and EP/I01375X/1).

Table of contents

List of figures

List of tables

List of schemes

List of abbreviations

The following abbreviations, in alphabetical order, were used throughout the thesis:

ABC: Adenosine-5'-triphosphate Binding Cassette

amu: atomic mass uint

API: Active Pharmaceutical Ingredient

BHT: Butylated Hydroxytoluene

BSA: Bovine Serum Albumin

$CDCl_3$: deuterated chloroform

CE: Collision Energy

C_{max}: maximum blood concentration

COPD: Chronic Obstructive Pulmonary Disorder

CX: Cation exchange

CXP: Collision Cell exit Potential

DCC: N,N'-dicyclohexylcarbodiimide

DCM: Dichloromethane

DIC: N,N'-diisopropylcarbodiimide

DMAP: (dimethylamine)pyridine

DMPK: Drug Metabolism and Pharmacokinetic

DMSO: Dimethyl sulfoxide

DP: Declustering Potential

DPI: Dry Powder Inhaler

EA: Ethyl Acetate

ESI: Electrospray Ionisation

EtOH: Ethanol

FBS: Foetal Bovine Serum

FDA: Food and Drug Administration

FEV_1: Forced Expiratory Volume in one second

FTIR: Fourier Transformed Infra Red spectroscopy

HEPES: Hydroxyethyl Piperazineethanesulfonic acid

HFA: Hydrofluorocarbons

HMBC: Heteronuclear Multiple Bond Coherence

HMQC: Heteronuclear Multiple Quantum Coherence

HPLC: High Performance Liquid Chromatography

HSP: Hansen Solubility Parameters

IC: Inhaled Corticosteroids

ID: Internal Diameter

IPRL: Isolated and Perfused Rat Lung

IR: InfraRed

IUPAC: International Union of Pure and Applied Chemistry

LC-MS/MS: Liquid Chromatography tandem Mass Spectrometry

LDH: Lactate dehydrogenase

LLOQ: Lower Limit Of Quantification

MALDI: Matrix-Assisted Laser Desorption/Ionisation

MDI: Metered Dose Inhaler

$MEF_{75/50}$: Maximum Expiratory Flow at 75/50 % of the forced vital capacity

MeOH: Methanol

mPEG: monomethoxy Polyethylene Glycol

MRM: Multiple Reaction Monitoring

MW: Molecular Weight

NA: Not Applicable

NAD: Nicotinamide Adenine Dinucleotide

NMR: Nuclear Magnetic Resonance

OCT: Organic Cation Transporter

PBS: Phosphate Buffered Saline

PEG: Polyethylene Glycol

PLA: Poly(lactic acid)

PLGA: Poly(lactic-co- glycolide acid)

RT: Room Temperature

Salbutamol DS: Salbutamol Dodecyl Sulfate

Salbutamol FB: Salbutamol Free Base

SD: Standard Deviation

SDS: Sodium Dodecyl Sulfate

SF: Silica Filtration

$SOCl_2$: Thionyl chloride

TEA: Triethylamine

TEER: Transepithelial electrical resistance

TEMPO: 2,2,6,6-Tetramethylpiperidine-1-oxyl

THF: Tetrahydrofuran

TLC: Thin Layer Chromatography

t_{max}: Time to reach maximum blood concentration

TNF-α: Tumor Necrosis Factor alpha

TOF: Time Of Flight

UK: United Kingdom

ULOQ: Upper Limit Of Quantification

USA: United Sattes of America

UV: Ultraviolet

Chapter I. General Introduction

I.1. Structure of the lung

The pulmonary delivery of drugs is a challenging pathway because the lung is a complex organ, due to its geometry and high humidity content [1] (Fig.I.1). Weibel described the lung as a human bronchial tree, with 23 dichotomous generations terminated by the alveoli (respiratory sacs). The airways (trachea, bronchi and bronchioles) are the branches of the tree and the alveoli are the leaves [2].

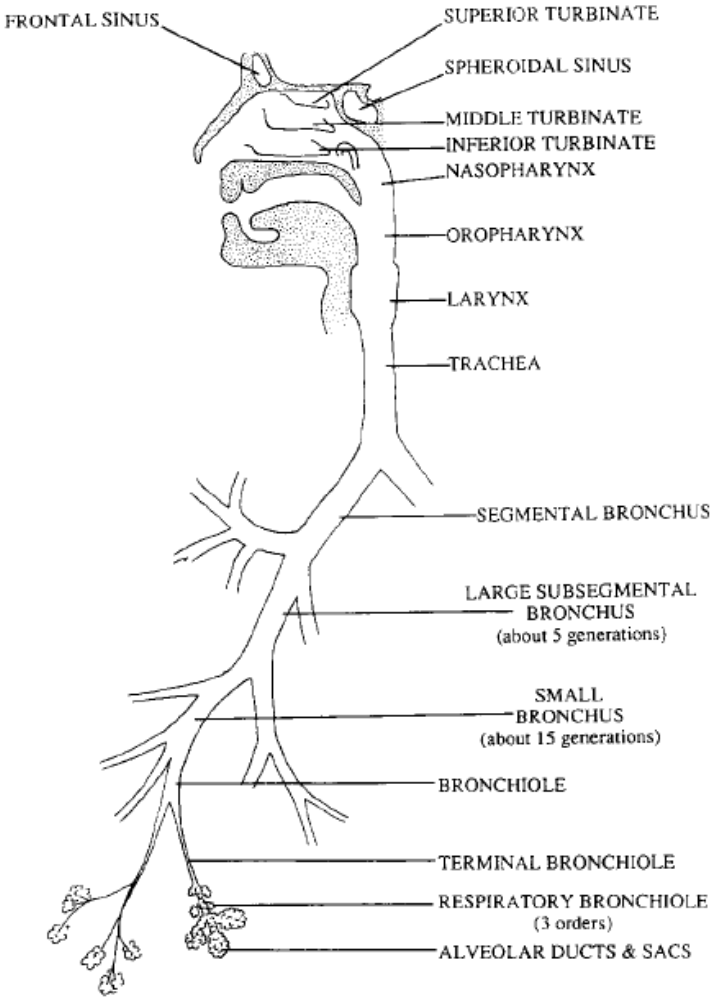

Fig.I.1. Schematic of the human respiratory tract, reprinted from [3]

The main barriers for drug absorption from the lung are the epithelia (Fig.I.2): thicker in the airway (58 μm) and thinner in the alveolar region (0.2 μm) [4, 5]. The airway epithelium is composed of four major classes of cells: basal cells (progenitor cells), ciliated cells, goblet cells and Clara cells. The alveolar epithelium, is composed of type I (broad and thin) and type II (small and compact) cells.

Nonetheless, the lung is a very attractive route of administration because of its large surface area (40-100 m^2) [6] and because of its permeable epithelium [7]. Drugs delivered via the pulmonary route are rapidly absorbed to the general circulation, avoiding gastrointestinal absorption and first pass metabolism [8].

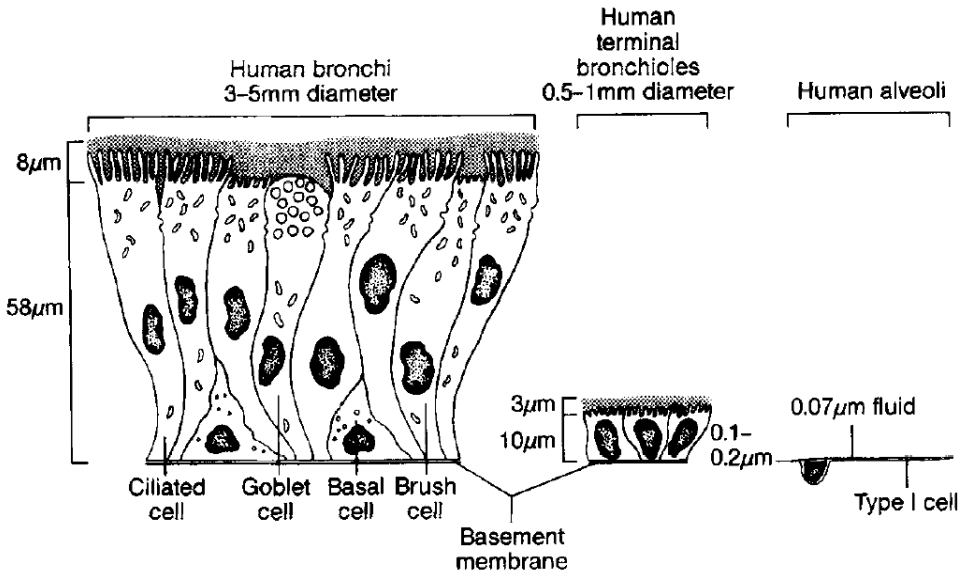

Fig.I.2. Schematic of the human airway epithelia, reprinted from [4]

I.2. Drug inhalation

Inhalation has been used to deliver medicines to the lung for more than 4000 years, when people smoked the leaves of Atropa belladona to suppress cough [9]. Nowadays, the large majority of inhaled drugs are used to manage asthma and Chronic Obstructive Pulmonary Disorder (COPD) [10].

Asthma is a chronic lung disease characterised by loss of breath and wheezing, it is life threatening if untreated. An asthma attack can be triggered by the environment (e.g. dust, pollen, smoke, irritants, ...), physical activity or during the night. The mechanisms or causes of an asthma attack are not fully understood but it seems airway hypersensitivity causes the smooth muscle to contract, reducing the airway diameter. According to the World Health Organisation (accessed 27 Aug 2012), 235 million people suffer from asthma worldwide.

COPD is a chronic life-threatening pulmonary disease characterised by a chronic cough, constant difficulties to breathe, a need for air. The primary cause of the disease is smoking which leads to a reduction in airway diameter, production of sputum (saliva and mucus) in the lung. It is not curable but can be managed. According to the World Health Organisation (accessed 27 Aug 2012), 64 million people suffer from COPD worldwide.

Other lung conditions are also treated by inhaled delivery of drugs. Pneumonia can be treated by increasing lung mucociliary clearance, using aerosolised saline solutions, by stimulating the production of antimicrobial proteins, by delivery of inhaled cytokines or antibiotics [11]. The delivery of antibiotics to the lung is also used to manage cystic fibrosis [12], and particularly fight against *Pseudomonas aeruginosa* and *Staphylococcus aureus* infections. *Pseudomonas aeruginosa* infection in patients with cystic fibrosis is currently managed by administration of nebulised antibiotics; however, there is a need for new devices and formulations of the antibiotics to improve patient compliance [13]. Inhaled Zanamir (Relenza) is currently used for both treatment and prophylaxis of influenza A and B. The drug has been approved by the Food and Drug Administration (FDA) in 1999 and works by binding to viral neuraminidase, thus inhibiting the virus ability to escape the

infected cell and limiting the viral spread [14]. Pulmonary arterial hypertension can be treated by treprostinil, a prostacyclin analog. For some patients, the inhalation route of administration is more convenient compared to continuous subcutaneous or intravenous infusions and the risk of blood stream infection and systemic exposure are minimised [15, 16].

Despite a great potential, the lung is only marginally used to deliver drugs systemically. Vaccines to prevent influenza [17, 18] and inhaled anaesthetics [19] are the two main classes of therapeutics systemically delivered to the the body via lung administration. Nicotine, a recreational drug, is rapidly delivered to the brain after smoking tobacco [20], a human practice since the Mayans [21].

Proteins have been administered by inhalation for local delivery (e.g. Dornase alfa, Genentech) to treat cystic fibrosis and for systemic delivery [22]. The development of the first inhaled insulin (Exubera$^{(c)}$) was a scientific success but a commercial failure and has been discontinued after a year on the US market [23]. Inhaled delivery of growth hormone in children has been investigated but due to low bioavailability, it is unlikely that the product will be further developed [24].

For both systemic and local delivery of drugs to or via the lung, there is a need to understand the fate of inhaled compounds.

I.3. Inhaler devices to administer drugs to the lung

Aerosols are generated with a nebuliser, metered dose inhaler (MDI) or dry powder inhaler (DPI) [5, 25]. A suspension or a solution of the active ingredient(s) is generally nebulised as a mist by a jet or ultrasonic nebuliser [26]. The jet nebuliser is based on the Bernoulli principle and the device produces a mist of the drug suspension or solution using a drop in pressure at the liquid surface, generated by the gas flow accelerated through a Venturi (Fig.I.3). The ultrasonic nebuliser uses the vibration of a piezoelectric crystal to generate waves at the liquid surface and produce fine aerosolised droplets (Fig.I.4).

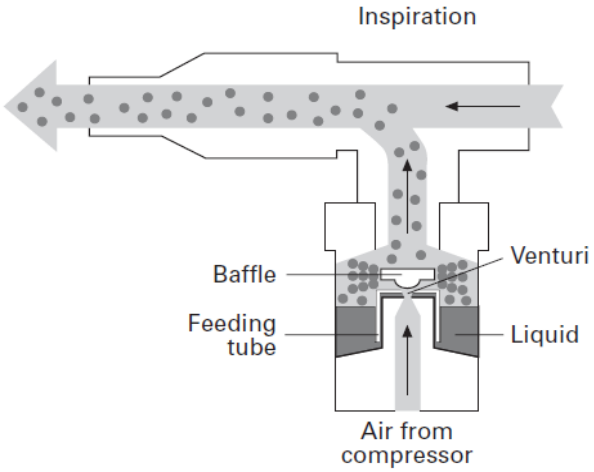

Fig.I.3. Schematic of a jet nebuliser, adapted from [26]

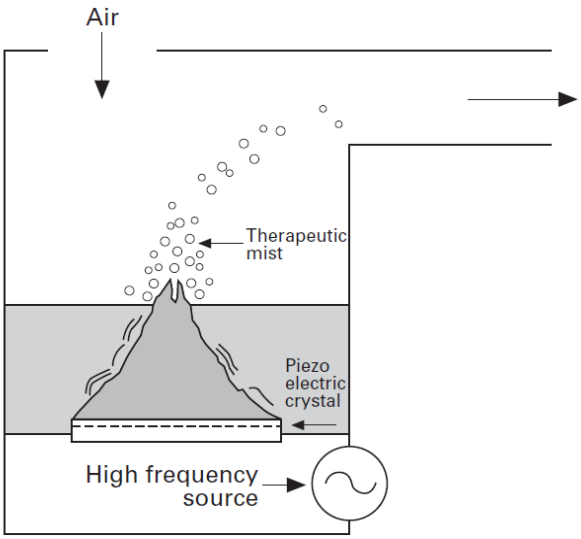

Fig.I.4. Schematic of an ultrasonic nebuliser, reprinted from [26]

Nebulisers are not easily transportable and require a long administration time; they are mainly used by people unable to operate other devices.

A pressurised metered dose inhaler delivers aerosol of the drug in solution or suspension in a propellant. The propellant is liquefied in the pressurised canister and depending on the drug physicochemical properties, the active ingredient can be dissolved or formulated as a suspension. A metered dose is dispensed and upon actuation, the liquid is expelled from the metering chamber generating an aerosol of the medicine (Fig.I.5). The propellant evaporates instantly due to its high vapour pressure (and low boiling point) [27]. Ozone depleting propellants have now been replaced by hydrofluorocarbons (HFA).

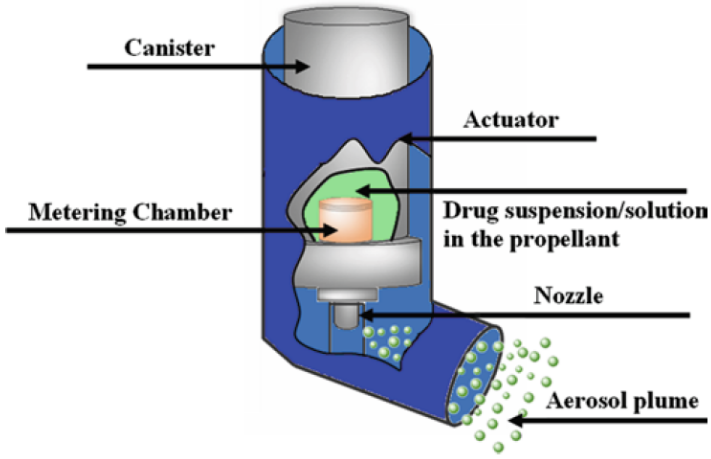

Fig.I.5. Schematic of a pressurised metered dose inhaled, reprinted from [28]

Dry powder inhalers are more recent delivery devices [29]. As the name suggests, the drug and excipients (often lactose) are stored in the device as dry powders and can be aerosolised by the patient's breath-actuation (passive DPIs) or by compressed air (active DPIs, e.g. Aspirair®). They can be single dose (e.g.

Handihaler®) or multi dose (e.g. Turbuhaler®, Fig.I.6). Aerosols are often generated by air flow turbulences created by the Venturi design of the chamber [30].

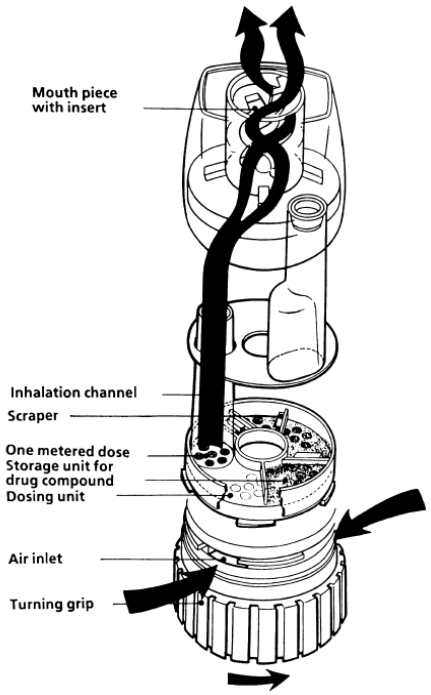

Fig.I.6. Schematic of Turbuhaler®: a multi dose, breathe-activated DPI, reprinted from [31]

These aerosol devices usually generate particles of around 1-35 μm in diameter [32], but the particle size can vary depending on the drug, the device and the user.

I.4. Deposition of drugs in the lung

The aerosolised particle aerodynamic diameter, shape and size influence the lung deposition pattern (Fig.I.7). Overall, small particles (aerodynamic diameter < 2 μm) penetrate the lung deeply and are mainly deposited in the lower respiratory tract. Such particles can be used to systemically deliver drugs via the lung. Large particles (aerodynamic diameter > 6μm) are mainly deposited in the upper airways and they have a limited clinical efficacy. Particles of intermediate size (2 μm < aerodynamic diameter < 6 μm) are mainly deposited in the central and small

airway. Such particles are the most relevant for local action of drugs. Several concomitant deposition mechanisms are taking place following inhalation of aerosolised particles. Small particles (aerodynamic diameter < 0.5 μm) are mainly deposited in the alveolar region of the airway by Brownian diffusion, random motion. Large particles (aerodynamic diameter > 5 μm) are mostly deposited by inertial impaction. Such particles are not affected by the airway airflow and due to their size, they follow their initial trajectories (inertia) and soon impact on an airway wall. Particles of intermediate size (1 μm < aerodynamic diameter < 8 μm), are mostly deposited by gravitational sedimentation. Particle size and residence time positively influence deposition by gravitational sedimentation. The particle shape greatly influences deposition by impaction and charged particles can be electrostatically attracted to the airway walls [33].

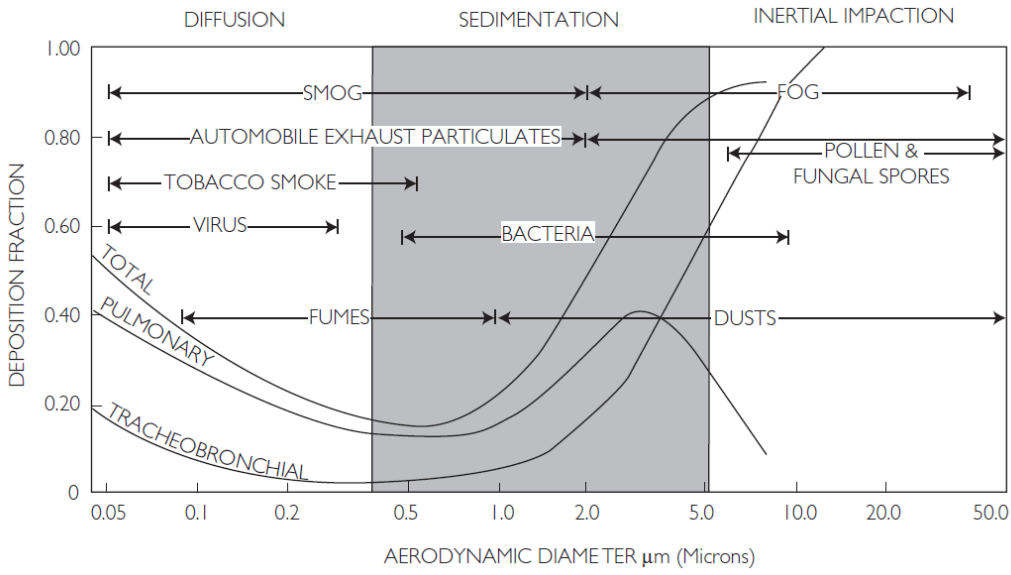

Fig.I.7. Influence of particle aerodynamic diameter and lung deposition, reprinted from [5]

Ultimately, the clinical efficacy of the drug is affected by the lung deposition pattern. For example, a study by P. Zanen et al. [34] determined the optimal particle

size of salbutamol and ipratropium bromide dry powder to be approximately 3 μm. They prepared monodisperse aerosols of 1.5, 2.8 and 5 μm particle size and treated a group of patients suffering from airflow obstruction. The treatment outcome was measured by lung function tests such as the mean forced expiratory volume in one second (FEV_1), or the maximum expiratory flow at 75/50 % of the forced vital capacity ($MEF_{75/50}$). The results indicated that out of the three particle sizes, aerosols of 2.8 μm induced statistically significant better improvements in lung function tests, with both salbutamol (20 μg) and ipratropium bromide (8 μg) [34].

The type of formulation (dry powder, solution or suspension) can influence the dissolution rate of the drug in lung fluids, alter the pharmacokinetic profile of the drug and ultimately modify the systemic exposure or clinical efficacy [35].

I.5. Fate of an inhaled aerosolised drug in the airways

Once deposited, the particles are solubilised in the lung fluids [3], Fig.I.8 illustrates the fate of an inhaled aerosol deposited in the airways. In the case of a nebulised solution, the drug is already solubilised and diffuses rapidly into the lung fluids. Other aerosolised drugs will take longer to diffuse into the lung surface depending on the drug solubility properties and the particle shape and composition. Large (> 6 μm), insoluble particles are rapidly cleared by mucocilliary clearance [36]. This defence mechanism is the result of the synchronised movement of the cilia (located on the apical surface of differentiated ciliated cells), and the resulting flow of mucus is propelled out of the airway, to the oropharynx where it is swallowed or expectorated [3]. A solubilised drug in the mucus is then available for local metabolism. Although the lung is not as metabolically active as the liver, there are

phase I, phase II and other enzymes in the lung. Regional distribution of these enzymes is heterogeneous and there are differences between cell types, even within the same airway section. There are metabolic differences between species and in particular between human and rodents [37]. Pulmonary absorption occurs when the drug solubilised in the mucus passes through to the epithelium and then permeates the epithelium [38]. Hydrophobic, mucus soluble small molecules rapidly diffuse through the epithelium by transcellular passive diffusion. It is believed that hydrophilic compounds are transported across the lung membrane by paracellular transport (between the cells), and the molecule charge may play a significant role in the absorption rate [39]. In vitro studies indicate that some small molecules could also be actively transported by so-called drug transporters. For example, the Adenosine-5'-triphosphate-binding cassette (ABC) transporters (such as P-glycoprotein), or Organic Cation Transporters (OCT) or even peptide transporters are thought to actively transport drugs *in vitro*, either as efflux transporter (i.e. back to the apical side of the epithelium) or uptake drug transporters (i.e. from apical to basal side) [40, 41]. ABC transporters are thought to be part of the defence mechanisms, preventing cellular accumulation of xenobiotics. OCTs transport positively charged molecules such as hormones, metabolites, in either direction.

Water solubility, lipophilicity and molecular weight play a significant role in the absorption rate of small molecules that are not actively transported [42]. Thus, a small, lipophilic, yet water soluble, molecule will cross the epithelium faster than a large hydrophilic one. Typical inhaled small molecules up to 1000 Da are passively absorbed through the epithelia resulting in rapid, high blood concentration [39].

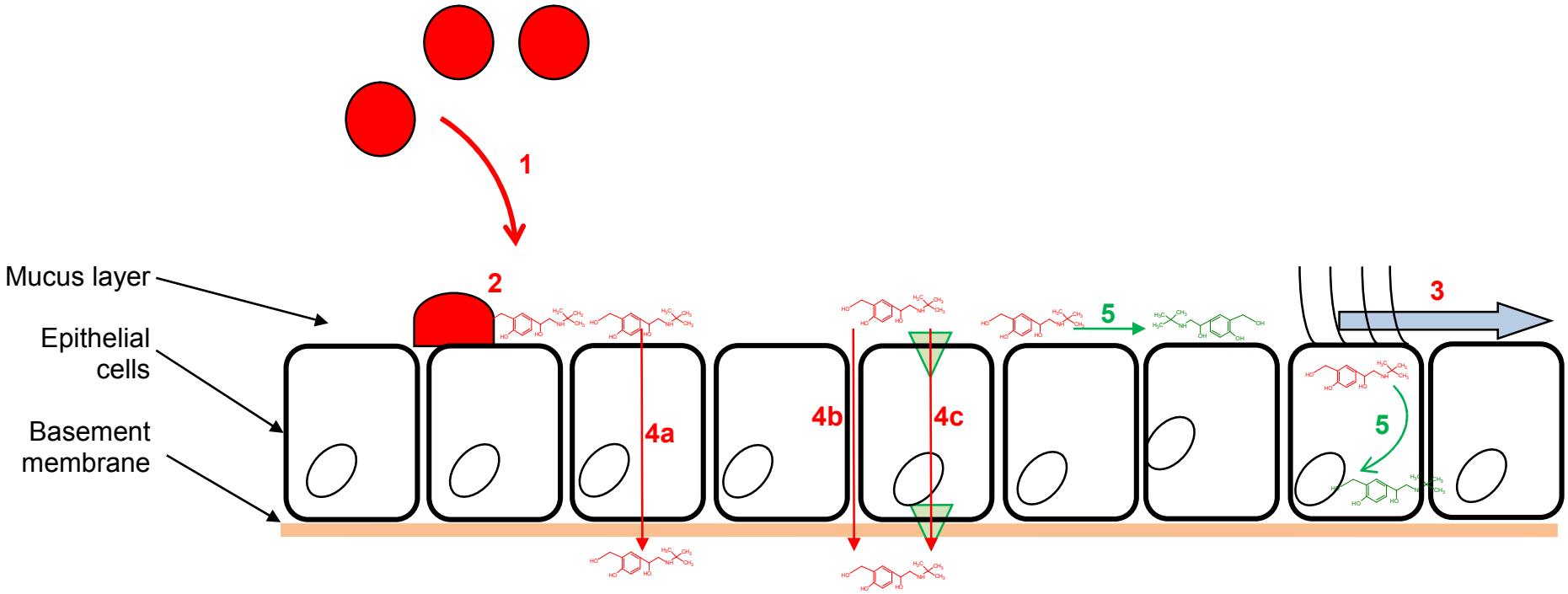

Fig.I.8. Fate of inhaled drugs in the lung

Aerosolised particles deposited (**1**) in the airways dissolve (**2**) in the mucus. Insoluble large particles may be removed from the airway by mucociliary clearance (**3**). Dissolved solutes are then absorbed across epithelial cells either passively by transcellular diffusion (**4a**) or by paracellular transport (**4b**) or actively, by drug transporters (**4c**). Throughout the process, drugs can be metabolised (**5**).

I.6. Pharmacokinetic profiles of drugs administered by inhalation

Because of high lung absorption rates, the resulting systemic delivery of inhaled drugs often offers a sub-optimal pharmacokinetic profile, characterised by a high maximum blood concentration (high C_{max}), that is quickly reached (short t_{max}). The resulting local effects are minimised because of the short residence time of drugs in the lung and the systemic side effects are increased because of high C_{max} [43].

The therapeutic index is defined as the ratio between the desired and undesired effects of a drug. A longer lung residence time would improve the overall therapeutic index of inhaled drugs for local effect [44-47] and for a given dose, an increased lung retention time would decrease the C_{max}. Rosenborg et al. [47] described for the first time in 2002 a relative therapeutic index between formoterol and salbutamol. They measured the FEV_1 as a positive outcome (desired effect) and potassium serum concentration as a side effect after inhalation of the drugs at different doses. They used 28 asthmatic patients and the results although not statistically significant (maybe due to the low number of patients), illustrated the principle of such a concept. Formoterol was 215 times more potent than salbutamol regarding FEV_1 increase (positive outcome) and 88 times more potent than salbutamol regarding suppression of serum potassium (negative outcome). The relative therapeutic index (ratio between positive outcome and side effect) was 2.5 in favour of formoterol [47].

The therapeutic index of inhaled corticosteroids can be clinically assessed by using the morning Peak Expiratory Flow rate as a desired effect of the treatment and systemic cortisol suppression as a side effect [44, 45]. The therapeutic index of a

glucocorticoid can be improved by limiting oral bioavailability, increasing lung and receptor affinity [46], concepts that are still the basis of new drug designs [48].

I.7. Controlled delivery of drugs administered to the lung

Extensive work has been carried out to optimise the delivery of inhaled small molecules and macromolecules. There are three main strategies to develop sustained release drug delivery to the airways. One can decrease the drug solubility in mucus, slow down the cellular uptake/permeation rate through the airway epithelium or use a sustained release formulation of the drug [49].

Fluticasone propionate, lipophilic (log P = 3.4), with low aqueous solubility (water solubility 0.51 $mg.L^{-1}$) and budesonide, less lipophilic (logP = 1.9) with higher aqueous solubility (27.98 $mg.L^{-1}$ [50]) are two inhaled corticosteroids (Fig.I.9).

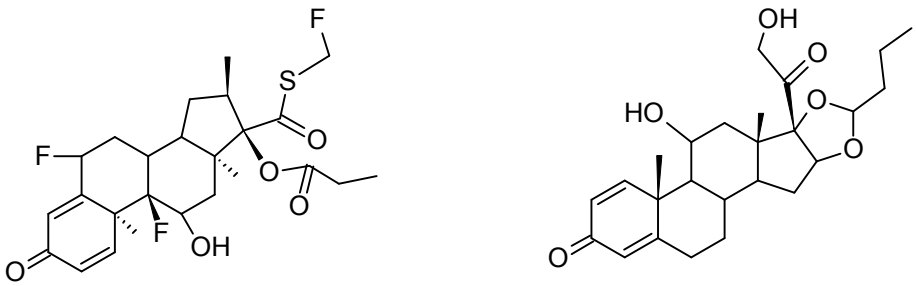

Fig.I.9. Fluticasone propionate (**A**) and budesonide (**B**)

When administered to healthy patients (1000 μg twice daily), using dry powder inhalers, the pharmacokinetic profiles of the two drugs were significantly different. Budesonide had a shorter t_{max} (17 min) and higher C_{max} (3.8 nmol) compared to fluticasone propionate (t_{max} 100 min, C_{max} 0.5 nmol). The fraction of the deposited dose absorbed by the lung was higher for budesonide (f_{lung}: 32%) compared to fluticasone propionate (f_{lung}: 12%) [51]. It was concluded that fluticasone

propionate exhibited a slower absorption due to its lower mucus solubility. The lower availability of fluticasone propionate was explained by mucociliary clearance extracting undissolved particles of fluticasone propionate away from the airways [52].

Drug conjugation of compounds delivered by inhalation was attempted in the late 1970's with esters of terbutaline such as ibuterol [53] and esters of isoproterenol such as bitolterol mesylate [54], the latter was approved by the FDA in 1984 (Fig.I.10). They were designed to reduce the drug solubility in lung fluids and therefore, slow down the absorption rate. They also prolonged lung exposure via increased circulation in blood after absorption by the lung. The active β_2-adrenergic receptor agonist were released upon hydrolysis of the ester link in lung, blood and other tissues. Lipid conjugation of inhaled corticosteroids was also used to modify the dissolution rate of the drug with similar results [55].

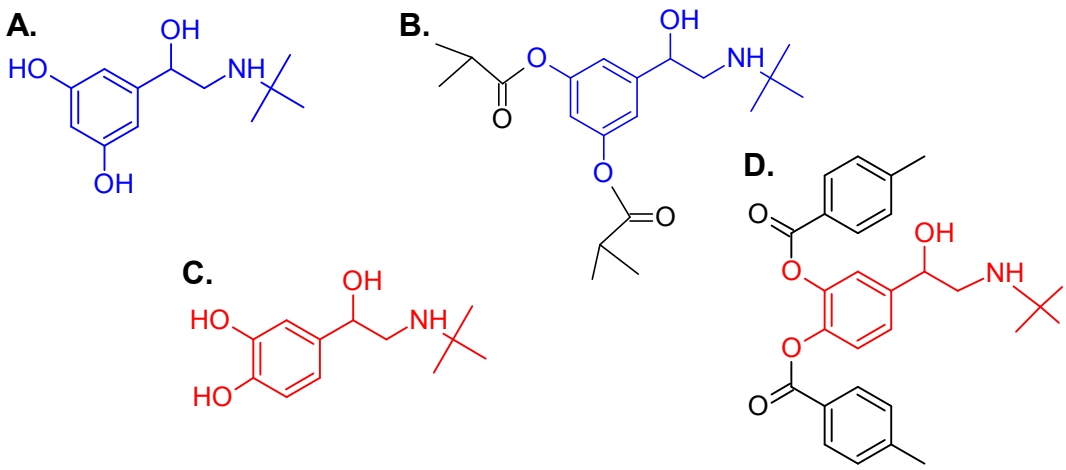

Fig.I.10. Terbutaline (**A**), ibuterol (**B**), isoproterenol (**C**) and bitolterol mesylate (**D**)

Sustained release formulations are based on the slow escape of drugs from a microsphere. Liposome-based formulations of drugs administered by injection have already been approved to treat cancer (e.g. DOXIL®, doxorubicin HCl liposomal

formulation). Liposomes are microspheres composed of a bilayer of amphiphilic molecules, with a hydrophilic core. They can encapsulate a wide range of molecules, hydrophilic drugs are trapped in the liposome core, lipophilic drugs can be located in the lipidic bilayer and nucleic acid based therapeutics at the liposome surface (Fig.I.11). Several studies have been performed to assess the potential of liposomal formulations of drugs for lung delivery. The results seem to be promising since liposomes have similar properties to the lung surfactant, they are stable suspensions, and they can target alveolar macrophages [56]. Liposomal formulations of drugs administered as dry powder or by nebulisation improved the pharmacokinetic profiles of drugs [57]. Tacrolimus, an immunosuppressive agent used after lung transplantation, was formulated as a liposomal dry powder and the resulting pharmacokinetic profile was improved after administration in rats [58]. The anaesthetic fentanyl was administered by nebulisation to a group of volunteers as a mixture of free and liposome-encapsulated formulation. The resulting pharmacokinetic profile was improved compared to intravenous injection of the free drug [59]. The anticancer drugs paclitaxel and camptothecin were prepared as liposome-based formulations and following inhalation of nebulised suspensions, sustained release profiles in the lung were obtained [60].

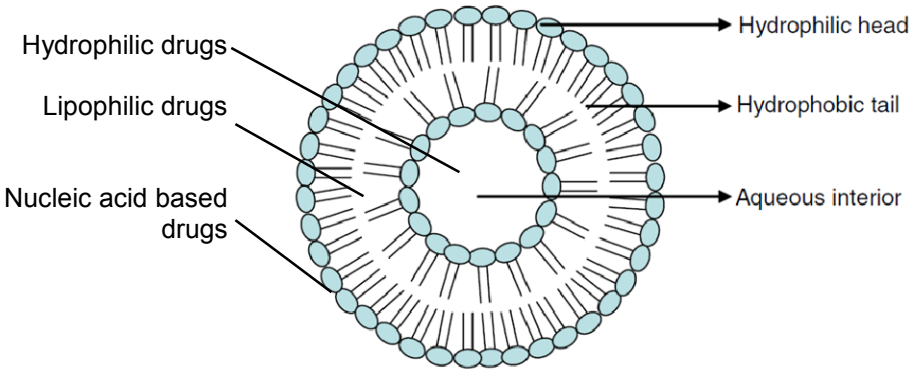

Fig.I.11. Structure of an unilamellar liposome, reprinted from [56]

Formulations of microparticles of an active ingredient and a polymer have been used to achieve sustained delivery of drugs following inhalation. The drugs escape from the polymer by three mechanisms: diffusion from the particle, swelling of the polymer and then diffusion of the drug out of the polymer, or following polymer degradation (Fig.I.12).

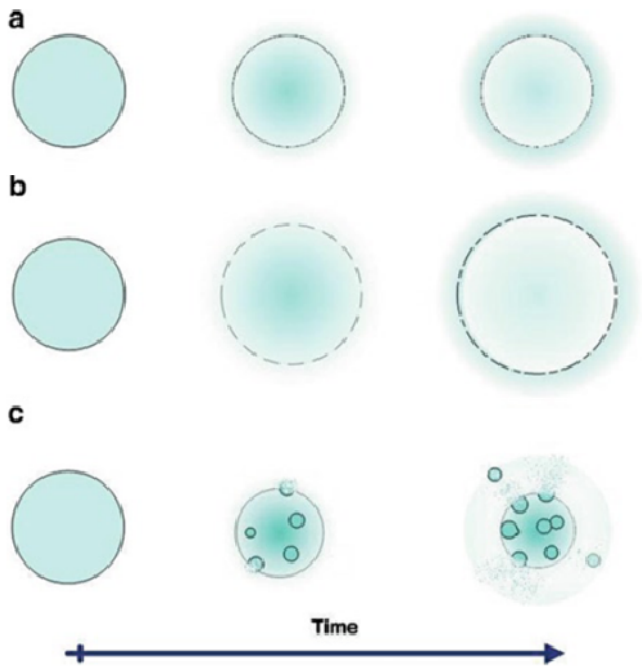

Fig.I.12. Drug escape from polymeric microspheres: diffusion (**a**), polymer swelling followed by drug diffusion (**b**), or microsphere degradation (**c**). Reprinted from [61]
The shading represents drug concentration, the darker, the greater the concentration

The polymers used are either natural (such as albumin, chitosan, hyaluronic acid) or synthetic polymers (such as Poly(lactic acid) (PLA), Poly(lactic-co- glycolide acid (PLGA), PEG) [62]. A systemic sustained delivery of a macromolecule was achieved using chitosan encapsulated insulin delivered by inhalation. Insulin was successfully encapsulated in chitosan microspheres and formulated as dry powder using lactose. After delivering the formulation *in vivo* to rats, the resulting hypoglycemic effect was prolonged when using the chitoasn-based formulation

compared to insulin alone [63]. A Korean group of researchers obtained a local sustained delivery of an anticancer small molecule using PLGA encapsulated doxorubicin, delivered by inhalation to mice. PLGA microparticles were successfully loaded with doxorubicin, formulated as dry powder and administered by insufflation to anaesthetised melanoma-bearing mice. The treated group showed significant tumour recession. Doxorubicin was detected in the lungs 14 days after drug delivery, illustrating the prolonged lung retention of the formulation [64]. Inorganic-based microparticles have also been investigated for sustained drug delivery of anti-inflammatory drugs. Dexamethasone phosphate was successfully loaded into calcium pyrosphate-based fibrous microspheres. Upon intratracheal instillation to rats, a sustained anti-inflammatory effect of 42 hours was obtained with the formulation as opposed to the drug alone [65].

I.8. Models to study drug delivery to the lung

Aerosol properties and capabilities to deliver drugs to the lungs can be tested *in vitro*. A large number of parameters can be measured to assess aerosol properties such as aerodynamic diameter, morphology, stability, density, solubility, drug content, zeta-potential [66]. The particle deposition pattern can be predicted using theoretical drug deposition models and experimentally assessed with cascade impactors. There are several mathematical models of the airways, differing in their assumptions and simplifications. The models of the human tree (Fig.I.13), proposed by Horsfield in 1971 are amongst the most realistic [67]. Briefly, two mathematical models of a normal bronchial tree were designed based on physiological measurements obtained after preparation of a human airway resin cast. The two proposed models took into account the lung asymmetry, and are based on the lung

dichotomous branching system: one parent branch divides into two branches creating a new daughter branch that can divide too. Each new division gives a new branch generation to which were associated measurements (such as airway diameter, angle of branching) [68]. The model is still used today to predict aerosol deposition in the human lung with modern computational mathematic.

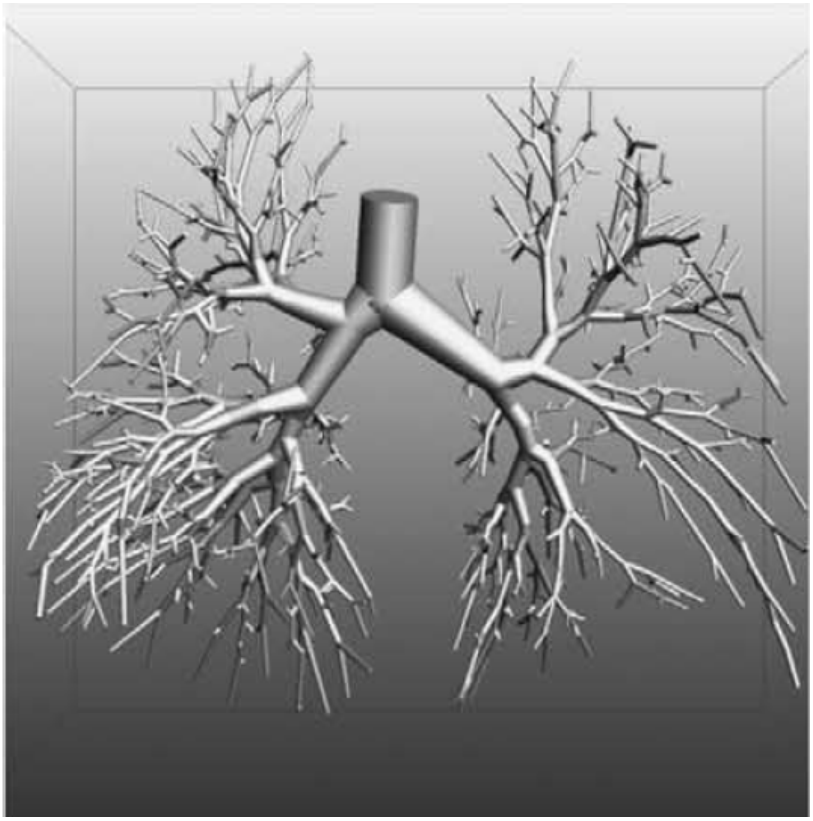

Fig.I.13. 3D visualisation of a bronchial tree model, reprinted from [69]

Cascade impaction is the recommended (US pharmacopeia) method of assessing aerosol aerodynamic diameter. The technique is a useful tool to simulate where not only the aerosol but more specifically the active pharmaceutical ingredient (API) is deposited. The general principle behind a cascade impactor is based on the tree model, where successive branches have decreasing diameters. The aerosol passes through nozzles of decreasing diameters, impacted particles are collected on plates and these can then be analysed to quantify the API Fig.I.14.

One of the most common systems is the Andersen cascade impactor, made of up to 8 stages. Mainly due to low flow rates, the next generation impactors were designed for the pharmaceutical industry [70].

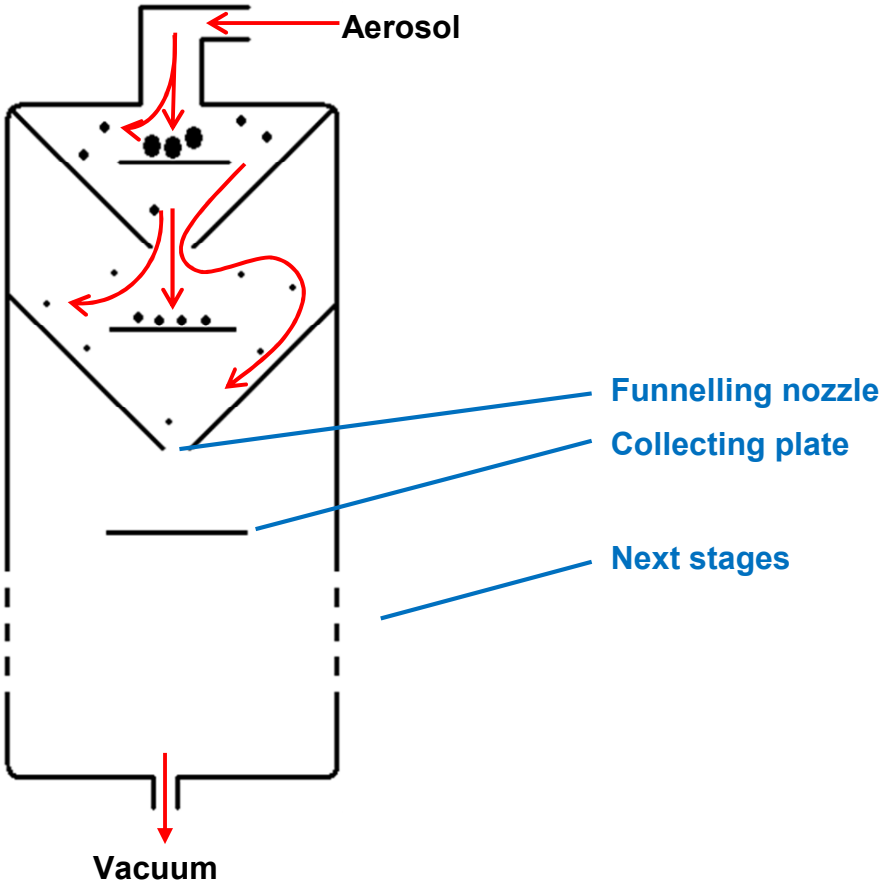

Fig.I.14. Schematic of a cascade impactor

Other *in vitro* systems are commonly used to assess drug activity on lung tissues. Cell culture systems are either based on primary cell culture or cell lines or co-cultures. Primary cell culture is the *in vitro* model closest to the *in vivo* situation since the tissue exhibits most of the native attributes. However, cost, donor availability and technical difficulties of working with such models often limit their use. They are the only reliable model of the alveolar region (type I or type II pneumocytes) since the human alveolar cell line A549 does not form tight junctions. Several *in vitro* models of human respiratory epithelia have been

developed such as the two human bronchial epithelial cell lines 16HBE14o- and Calu-3. These models, although useful to reduce the use of animal experiments, have to be characterised and proven to mimic the actual tissue [71]. These tissue culture models need to display epithelium-like phenotype, to grow at an air/liquid interface, and to behave as proper barriers, by forming functional tight junctions. Such barrier properties are measured by Transepithelial Electrical Resistance (TEER). Tissue cultured models have been investigated to assess drug permeability [72] with good correlations to the *in vivo* situation [73]. These models have also been extensively studied for their drug transporters such as P-glycoprotein [74], multidrug resistance proteins [75] and drug metabolism characteristics [76, 77].

The isolated and perfused lung is an *ex vivo* model. The lung of an anaesthetised animal (rat or guinea pig are the most common) is dissected, perfused with a buffered albumin solution and ventilated through the trachea. It can be maintained in an artificial thorax for up to three hours. Aerosols or solutions can be administered via the trachea and the perfusate is either recirculated or not (single pass). Permeation rate and drug absorption properties are directly determined by measuring the amount of drug in the perfusate. The structural integrity and functionality of the organ are maintained and the model is a close representation of the *in vivo* situation. Isolated and perfused lungs are particularly useful to determine permeation properties of drugs through the airways. Indeed, all the drug that has crossed the epithelium is recovered in perfusate, i.e. there is no excretion or metabolism once the drug has reached the perfusate, whereas *in vivo* the drug reaches the general circulation and it can be metabolised and excreted [73, 78].

Early pharmacokinetic *in vivo* studies following administration of drugs to the lung are usually conducted in rodents (often rat or mouse). The animals are sacrificed at

predetermined intervals, the blood concentration as well as the amount of drug remaining in the lung are measured and the pharmacokinetic profiles thus drawn [79].

I.9. Aim of the thesis

This thesis looked at the feasibility of a small drug conjugation strategy, with activation of the drug in the lung (Fig.I.15). The drug conjugate was designed to be more hydrophilic and larger than the active drug so that it would not be absorbed as quickly as the active compound. Release of the active drug from the conjugate should be controlled by the chemical nature of the linker.

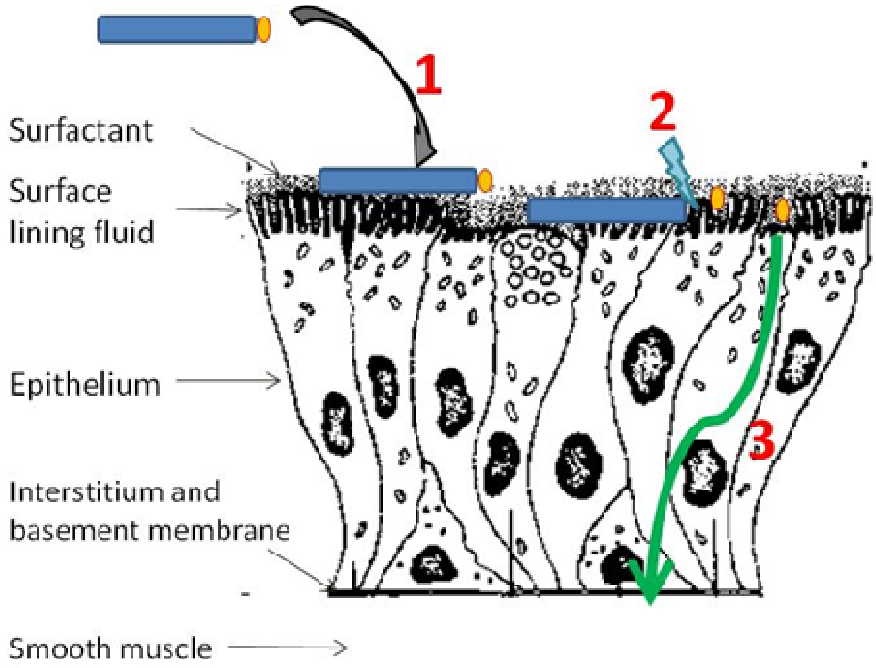

Fig.I.15. Schematic of the drug conjugation strategy to achieve a sustained drug delivery of a small molecule to the lung, modified from [4]
large, hydrophilic polymer, small inhaled drug, **1.** deposition of the drug conjugate in the airway, **2.** release of the active drug, **3.** absorption of the active compound

The lung possesses metabolic activity although lower than the liver [80] and in particular, the capacity to metabolise esters [81, 82], so an ester link was used to conjugate a polymer to inhaled model drugs.

Since asthma and COPD are the most common respiratory conditions, two model drugs administered to treat these diseases were used: a corticosteroid and a β_2-adrenergic receptor agonist. Inhaled corticosteroids (IC) are used locally for their immunosuppressive and anti-inflammatory properties [83]; their mechanism of action is complex [84] and they can result in topical (ear, nose and throat infections) and systemic side effects (such as nausea, viral gastroenteritis, cataracts, osteoporosis) [85]. β_2-adrenergic receptor agonists relax the smooth muscle and therefore decrease airway bronchoconstriction [86]. Local (e.g. pharyngitis, rhinitis) and systemic side effects (such as headache, tachycardia, pain, dizziness) can also be observed [87].

Prednisolone (11β,17,21-Trihydroxypregna-1,4diene-3,20-dione) as a model corticosteroid and salbutamol sulfate (α^1-[(*tert*-butylamino) methyl]-4-hydroxy-*m*-xylene-α,α'-diol sulfate (2:1) salt) as model β_2-adrenergic receptor agonist were chosen (Fig.I.16).

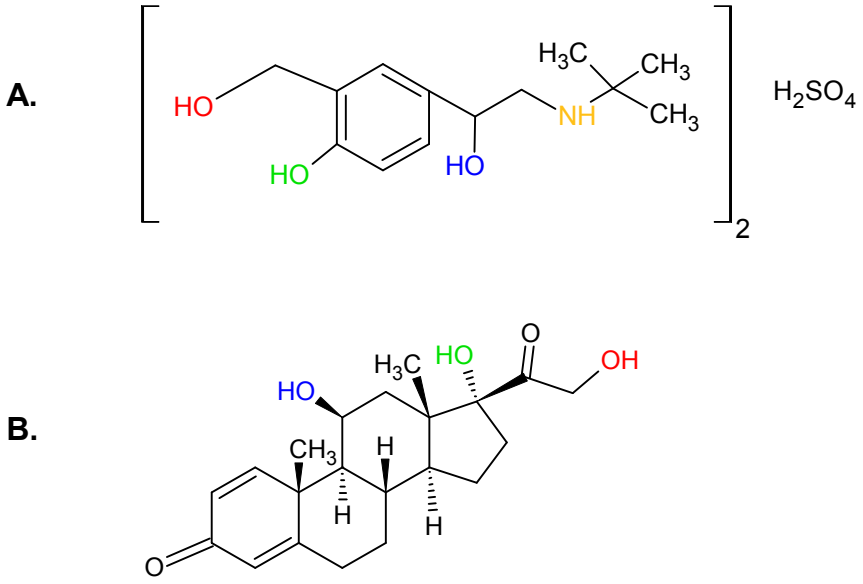

Fig.I.16. Chemical structures of salbutamol sulfate (**A**) and prednisolone (**B**)
Salbutamol possesses four reactive groups: one primary and one secondary hydroxyl group, one phenyl group and one amine group. Prednisolone possesses three reactive groups: one primary, one secondary and one tertiary hydroxyl group.

Natural, synthetic and pseudo-synthetic polymers have been used to produce drug conjugates of various molecular weights and with different linkers. Particularly, polyethylene glycol (PEG) is the most extensively used polymer for drug conjugation with either macromolecules or small drugs [88]. PEGylation of proteins has been used to increase the drug circulation time and decrease the protein immunogenicity. Several products are on the market since the first approval of PEG-Adenosine deaminase (Adagen®) in 1990. Polymer conjugation of small molecules is also currently investigated mainly for cancer therapies [89-91]. Enzon Pharmaceutical and Nektar Therapeutics are two leading companies in the field of polymer-drug conjugation. Greenwald reviewed the permanent and labile conjugations of small and large molecular weight PEG with macromolecules and small drugs. The conjugates improved delivery properties and therapeutic activities of the chemotherapeutic agents [92].

Polyethylene glycol was chosen as a polymeric drug carrier for the thesis since it possesses reactive hydroxyl group(s) (Fig.I.17) that can be coupled to drugs, it is commercially available in a wide range of molecular weights, and it is known to be biocompatible, and non toxic [93]. Native PEG (terminated with two hydroxyl groups) and monomethoxyPEG (mPEG, terminated with one hydroxyl and one methyl group) are thought to be mainly excreted in urine, with longer body residence time for higher molecular weight PEG [94, 95].

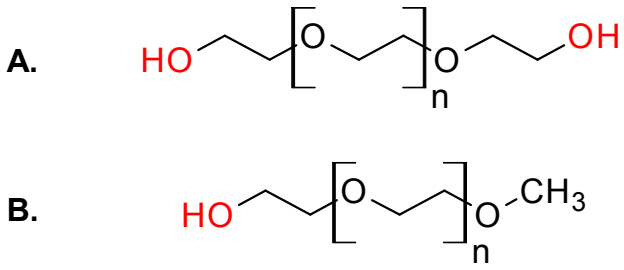

Fig.I.17. Chemical structures of native PEG (**A**) and monomethoxyPEG (**B**)

PEG (3350 Da) was found to be non toxic for the rat lung [96], and the lung permeability of mPEG-Fluorescein (thiourea bond) followed a first order decay, with a half life dependant of the polymer molecular weight up to 5 kDa. $mPEG_{2000}$-Fluorescein had a half life of 7.2 h and 99% of the dose was cleared from the airway after 48 h [97].

The overall aim of the thesis was to evaluate the influence of PEG ester conjugates of salbutamol and prednisolone on the local pharmacokinetic properties in the lung. The hydrophilic polymer PEG with a molecular weight of 1000, 2000 and 3400 Da and $mPEG_{2000}$ was used.

Chapter II deals with the production, purification and characterisation of the conjugates. In the first step, PEG hydroxyl groups were oxidised to carboxylic acids. Then, the drugs were reacted with oxidised PEG to form PEG ester

conjugates. The molecules were purified and characterised by Nuclear Magnetic Resonance (NMR), Fourier Transformed Infra-Red spectroscopy (FTIR), mass spectrometry and elemental analysis.

Chapter III illustrates the *in vitro* testing of the conjugates. Autohydrolysis in simple buffers at pH 6.2, 7.4 and 8.0 was studied. Cytotoxicity of the compounds was evaluated on Calu-3 cells, using a membrane integrity test and hydrolysis in the presence of the cells was studied. Simulations were performed to fully describe the hydrolysis pathways.

Chapter IV presents the *ex vivo* evaluation of the lead compounds, using an IPRL model. The local pharmacokinetics of ester conjugates were studied and compared to that of the drug alone. Simulations were also performed to measure the critical pharmacokinetic parameters C_{max} and t_{max}.

Chapter II. Conjugate synthesis

II.1. Introduction

Polyethylene glycol (PEG) ester conjugation is a widely used technique to manufacture prodrugs to treat cancer [98-100] or hypertension [101], with antiherpetic activities [102], or for ocular delivery [103]. The conjugates hydrolyse in the body and release the active drug. In most published studies, native PEG (i.e. terminated by hydroxyl groups) is conjugated to a carboxyl group of the drug to form an ester [100, 101, 103]. Inhaled corticosteroids and β_2-adrenergic receptor agonists do not have carboxyl groups; therefore, the polymer carrier has to provide the carboxyl group to be reacted with the drug hydroxyl group to form the desired ester linkage. A common strategy is to use a spacer between PEG and the drug, often an amino acid such as β-alanine, or an activating compound such as polyethylene glycol acetic acid N-succinimidyl ester (PEG-NHS) [92, 102, 104]. Oxidised PEG (i.e. PEG terminated by COOH) has also been directly conjugated to proteins or drugs. MonomethoxyPEG of 2000 Da ($mPEG_{2000}$) had been oxidised into mPEGCOOH in a three step reaction that lasted 36 hours [98, 105]. A more recent approach is to use TEMPO (2,2,6,6-Tetramethylpiperidine-1-oxyl) to turn hydroxyl groups into carboxylic acids [106].

There are a variety of ways to produces esters. The traditional Fisher esterification between an alcohol and a carboxylic acid is acid catalysed [107]. Nowadays, this historical chemical route is not widely used, as more efficient ways of condensation are available such as the use of acyl chloride that is much more reactive than carboxylic acid, or coupling reagents such as carbodiimides, or 2-chloro-

1methylpyridinium iodide (Mukaiyama reagent). In 1996, Greenwald, published two studies of drugs conjugated with oxidised poly(ethylene glycol) in dichloromethane (DCM), using the Steglich esterification [108], employing N,N'-diisopropylcarbodiimide (DIC) as coupling agent and (dimethylamine)pyridine (DMAP) as catalyst [98, 99].

The first part of this chapter will present PEG oxidation. The second and third parts will present esterifications of oxidised PEG with respectively prednisolone and salbutamol.

II.2. Material and methods

II.2.1. PEG oxidation

TEMPO oxidation of monomethoxy PEG was described in 2005 by Xing-Qi Li *et al.* and produced carboxymethylated PEG in high yields [109].

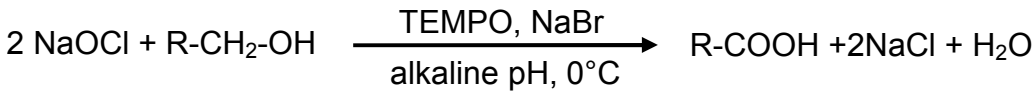

Scheme.II.1. TEMPO oxidation of primary hydroxyl group
TEMPO and Sodium bromide (NaBr) are used as catalysts

The same strategy was used (Scheme.II.1), with modifications, to produce oxidised PEG. The polymers were oxidised using TEMPO as catalyst, sodium hypochlorite (bleach solution, 13% available chlorine) and sodium bromide, in water, at pH 10 and 0°C. To improve the solubility of TEMPO, a fresh solution of the catalyst was prepared beforehand in warm (40°C) deionised water and thoroughly mixed until complete dissolution. An ice-cold bleach solution (adjusted to pH 10) was slowly added to an ice-cold mixture of PEG, NaBr and TEMPO. The pH was monitored

and maintained at 10 with addition of drops of NaOH as necessary. Table. II.1 sums up the different typical ratios used to produce oxidised PEG of various molecular weights. The products were then solvent extracted from the aqueous phase with DCM and precipitated or directly dried depending on their molecular weights.

Table. II.1. Conditions for PEG oxidations

PEG MW Da	PEG		TEMPO				NaBr			NaOCl			Deionised water
	g	mmol OH	mL	[TEMPO] M	mmol	eq OH	mg	mmol	eq OH	mL	mmol	eq OH	mL
1000	5	10	2.5	0.040	0.100	0.01	432	4.2	0.42	20	35	3.5	120
2000	20	20	3.52	0.057	0.200	0.01	830	8.1	0.40	35	61	3.1	150
2040*	10	4.9	1.21	0.04	0.040	0.01	239	2.3	0.48	14	25	5.1	50
3395	34	20	5.28	0.037	0.200	0.01	833	8.1	0.41	35	61	3.1	150

MW: Molecular Weight
eq OH: mol equivalent to PEG OH groups
**mPEG 2000 Da*

II.2.2.PEG-prednisolone

Prednisolone (Fig.II.1) is a corticosteroid that possesses one primary hydroxyl group, likely to be the most reactive toward esterification. The molecule also has a secondary and a tertiary hydroxyl group, which are less reactive. Its molecular weight is 360.44 Da, it is a white crystalline powder insoluble in water and slightly soluble in methanol and non polar organic solvents.

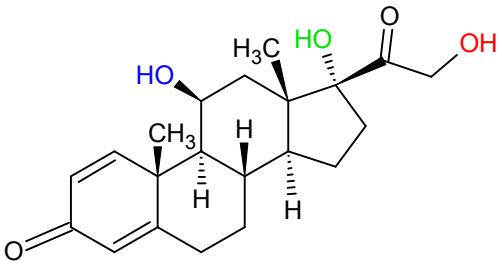

Fig.II.1. Prednisolone

II.2.2.2. Acyl chloride

The first esterification route investigated consisted of a two step synthesis starting with chlorination of oxidised PEG to turn the free carboxylic acids into a highly reactive acyl chloride, using thionyl chloride ($SOCl_2$), Scheme.II.2. PEG acyl chloride was then reacted with prednisolone in the presence of a tertiary amine base, acting as an HCl scavenger, thus accelerating the reaction (Table. II.2). The reaction was followed by NMR. The purification of the products was carried out by silica gel chromatography, filtration over silica, solvent extraction and precipitation. The choice of solvents was selected by Thin Layer Chromatography (TLC) and rationalised by the Hansen Solubility Parameters (HSP) of the solvent mixtures used.

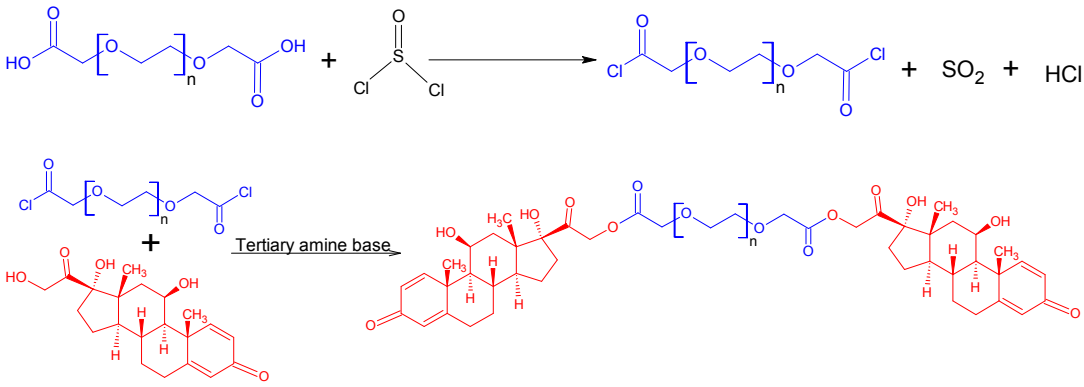

Scheme.II.2. PEG-prednisolone through acyl chloride route

The first set of reactions concerned the production of PEG-prednisolone ester of various molecular weights using a standard methodology for acyl chloride preparation and esterification (Table. II.2). Particularly, PP11 and PP14 illustrate the conjugation of $PEG_{3400}COOH$ and prednisolone and the development of a purification methodology. PP08, PP16 and PP13 illustrate the production of respectively $mPEG_{2000}COOH$, $PEG_{2000}COOH$ and $PEG_{1000}COOH$ and prednisolone and their purification (Table. II.3). Schematics of the purification strategies are presented in Fig.II.2, they consisted of filtrations over silica, precipitations, cation exchange and silica gel chromatography.

The second set of reactions (using $PEG_{3400}COOH$) dealt with optimisation of the chemical reactions. Pyridine (pKa 5.25) was used instead of triethylamine (pKa 10.75) as it is a weaker amine base (PP17). The way the three reactants (PEG acyl chloride, prednisolone, and pyridine) were mixed together was investigated in PP20/PP21. The ratio of prednisolone was tested in PP22/PP23. A lower excess of thionyl chloride (10×) was used in PP26/PP27 to produce PEG acyl chlorides.

Table. II.2. Experimental conditions for the use of thionyl chloride for esterification of PEGCOOH and prednisolone

Batch	PEG type	PEGCOOH [COOH] mmol/L	Prednisolone / COOH	Thionyl chloride / COOH	Triethylamine / Pyridine / COOH	Solvents, temperature	Time min
PP11	PEG_{3400}	40	1.4	27.5	2.6	75 mL of dry THF, 50 mL of dry DCM, 40°C	1200
PP14		30	1.4	28.1	2.4	70 mL of dry THF, 30 mL of dry DCM, 40°C	1580
PP08	$mPEG_{2000}$	34	1.4	28.2	2.7	25 mL of dry THF, 25 mL of dry DCM, 40°C	1260
PP16	PEG_{2000}	30	1.5	45.8	3.1	60 mL of dry THF, 40 mL of dry DCM, 45°C	1105
PP13	PEG_{1000}	38	1.4	22.5	2.6	40 mL of dry THF, 25 mL of dry DCM, 40°C	1600
PP17	PEG_{3400}	30	1.8	34.7	11.5	20 mL of dry THF, 20 mL of dry DCM, 45°C	1010
PP20		15	1.5	69.8	2.1	15 mL of dry THF, 22.5 mL of dry DCM, 45°C	1410
PP21		14	1.4	69.8	2.1	20 mL of dry THF, 22.5 mL of dry DCM, 45°C	1380
PP22		26	2.1	69.3	12.5	15 mL of dry THF, 8 mL of dry DCM, 50°C	100
PP23		26	1.0	69.3	12.5	15 mL of dry THF, 8 mL of dry DCM, 50°C	100
PP25		24	1.0	10.5	19.0	15 mL of dry THF, 10 mL of dry DCM, 40°C	1245
PP26		20	2.1	10.5	19.0	15 mL of dry THF, 15 mL of dry DCM, 40°C	1185

THF: tetrahydrofuran

Table. II.3. Purification steps for PEG-prednisolone of various molecular weights

Product	PEG type	Crude product		Purification 1	Purification 2
PP11	PEG_{3400}	Filtration, evaporation of solvents	PP11BS1	S.F: EA → [*PP11SFA-D*] DCM/MeOH 90/10 → [*PP11SFE-K*]	-
PP14	PEG_{3400}	Filtration, evaporation of solvents	PP14S1	S.F: ether/EA 50/50 [PP14SF1-3] THF/DCM 40/60 [PP14SF4-7] precipitation ether → *PP14SF4p* THF/DCM 50/50 [PP14SF8-9] precipitation ether	[PP14SF4-9p]: cation exchange in acetone overnight → *PP14SFDC1S*
PP08	$mPEG_{2000}$	Filtration, evaporation of solvents	Precipitation in ether PP08P2	Cation exchange in THF/DCM, overnight → *PP08DC2*, precipitation cyclohexane	S.F: Ether/EA 90/10 A DCM/MeOH 80/20 → *PP08DC2DF1B*
PP16	PEG_{2000}	Filtration, evaporation of solvents	PP16S1	HCl wash (15 mL at 0.5M) → *PP16HCl*	S.F: Ether/EA 50/50 Column: 1- THF/EA 50/50 2- THF → SGA precipitated in ether→ *PP16SGAp*
PP13	PEG_{1000}	Filtration, evaporation of solvents	PP13S1	Cation exchange in acetone, overnight, then in DCM, 2h → *PP13DC2*	S.F: Ether/EA 90/10 [A] DCM/MeOH 80/20 → [*PP13DC2DFB*]

S.F: silica filtration, TEA: triethylamine, EA: ethyl acetate, THF: tetrahydrofuran, DCM: dichloromethane, MeOH: methanol. Column: silica gel chromatography. separation of prednisolone and PEG-TEA, separation of $TEAH^+Cl^-$ *Intermediate samples names are in italic e.g. PP11SFA* is the first fraction collected after Silica filtration of PP11BS1

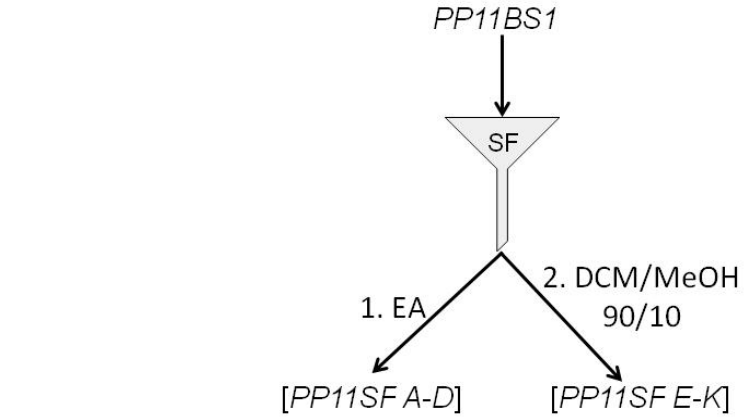
PP11BS1
SF
1. EA
2. DCM/MeOH
90/10
[PP11SF A-D]
[PP11SF E-K]

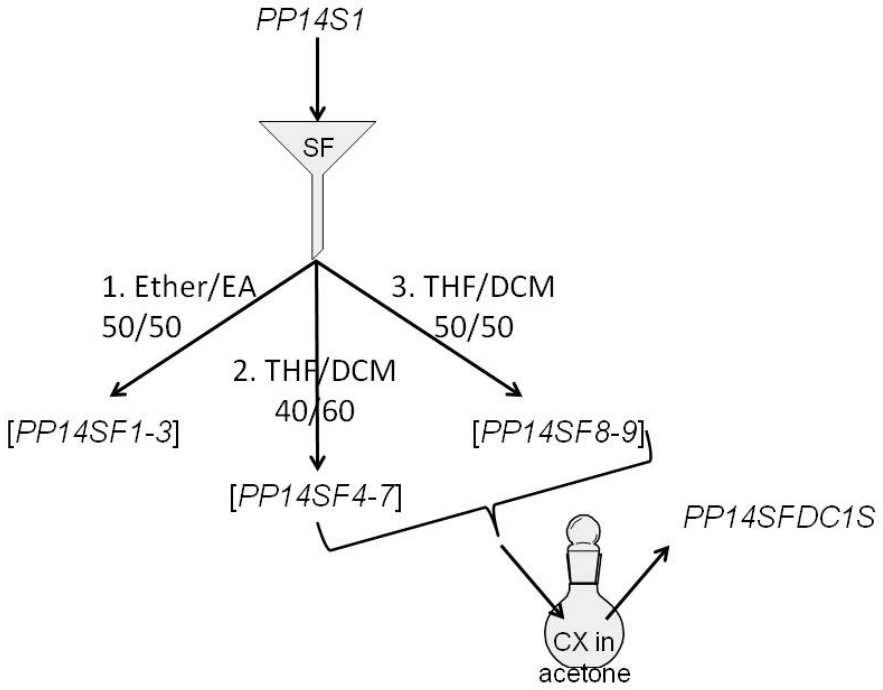
PP14S1
SF
1. Ether/EA
50/50
2. THF/DCM
40/60
3. THF/DCM
50/50
[PP14SF1-3]
[PP14SF4-7]
[PP14SF8-9]
PP14SFDC1S
CX in
acetone

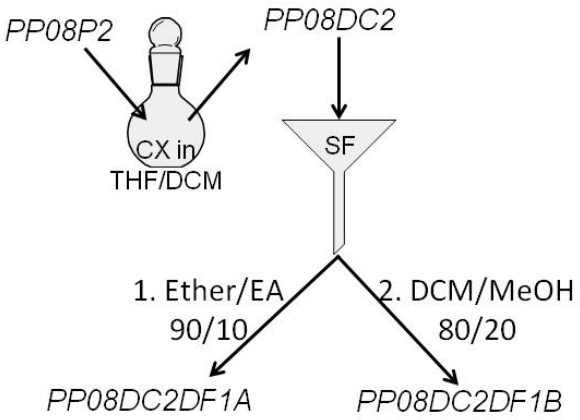
PP08P2
CX in
THF/DCM
PP08DC2
SF
1. Ether/EA
90/10
2. DCM/MeOH
80/20
PP08DC2DF1A
PP08DC2DF1B

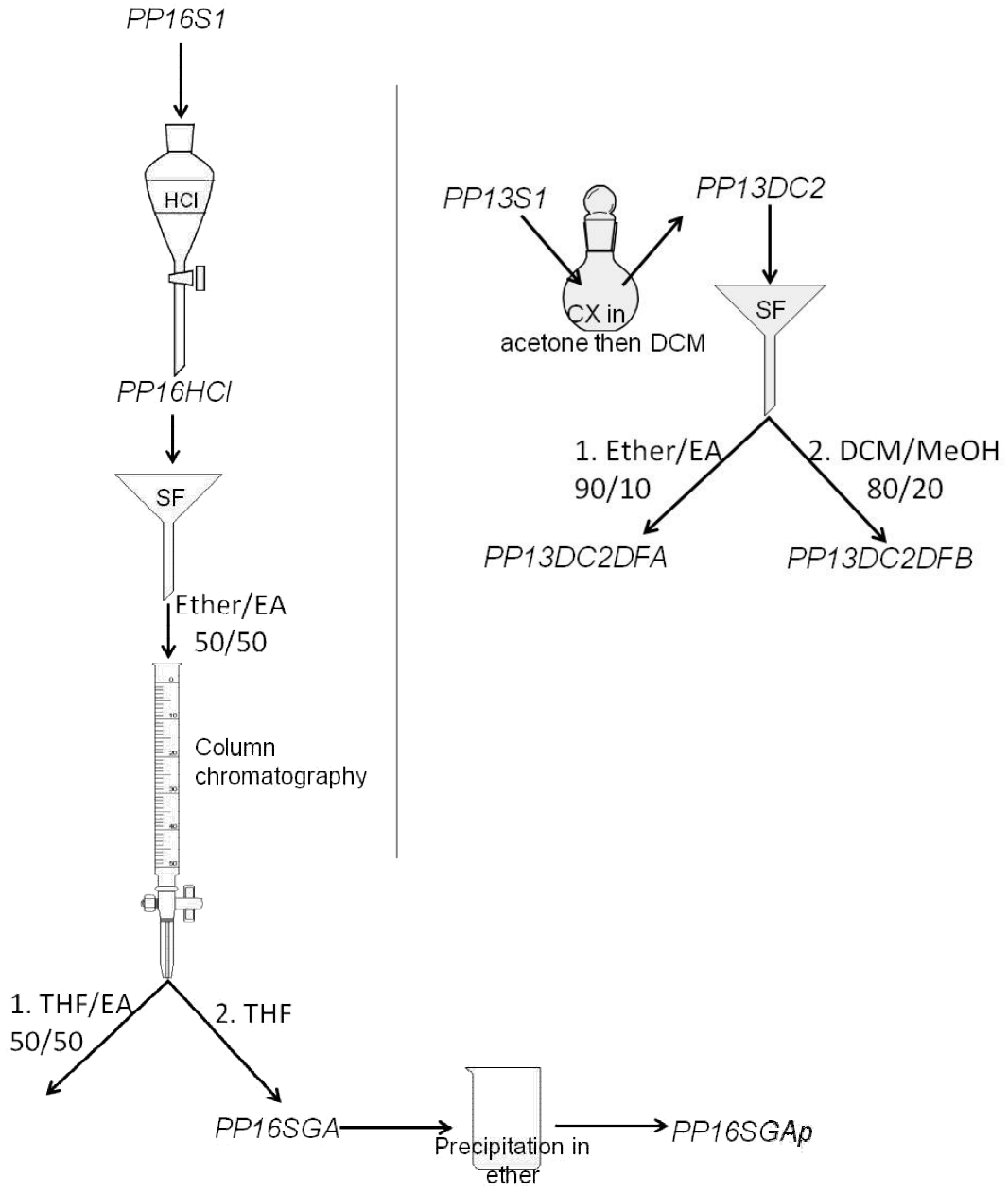

Fig.II.2. Purification steps for PEG-prednisolone products resulting of PEG-acyl chloride and prednisolone conjugation
EA: Ethyl acetate, DCM: Dichloromethane, MeOH: Methanol, THF: Tetrahydrofuran, HCl: HCl wash, SF: Silica filtration, CX: Cation exchange

Esters of PEG and prednisolone were successfully prepared via the acyl chloride route but due to low conversion rates and the need for extensive purification, the overall yields were poor and these results called for a more efficient esterification route. The use of a coupling reagent was therefore investigated.

II.2.2.3. Mukaiyama reagent

In 1977, T. Mukaiyama published a new method for the preparation of carboxylic esters, and described the use of 2-chloro-1-methylpyridinium iodide (Mukaiyama reagent) to conjugate a wide range of carboxylic acids and alcohols, in the presence of tertiary amine base, in a wide range of solvents such as ether, dichloromethane, tetrahydrofuran, acetonitrile, 1,2-dimethoxyethane, pyridine and toluene [110]. In 1998, Greenwald compared the coupling of PEG diacid and camptothecin with DIC and Mukaiyama reagent [104]. The use of the Mukaiyama reagent led to 90% of diester whereas the use of DIC yielded to a mixture of mono and diester.

In this work, the use of Mukaiyama reagent to conjugate oxidised PEG and prednisolone (Scheme.II.3) was investigated using triethylamine as amine base, in DCM and THF. Several ratios of the three components, initially based on previous publications [104, 110], were investigated to optimise the reaction (Table. II.4), followed by NMR.

Once the conditions were optimised with PEG_{3400}, other PEG molecular weights were used using the optimised conditions (Table. II.5).

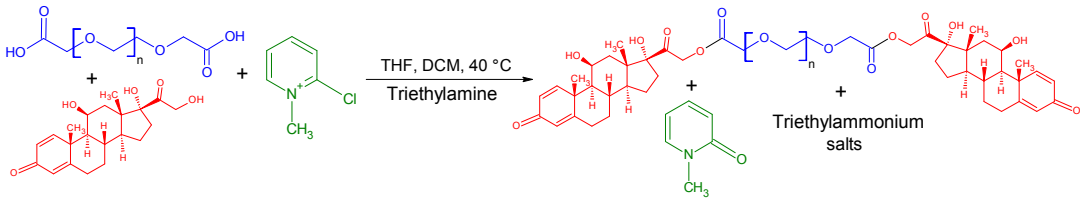

Scheme.II.3. PEG-prednisolone via Mukaiyama reagent route

Purification of the products was carried out according to the PEG molecular weight: PEG_{3400} and $mPEG_{2000}$ afforded products that recrystallised in isopropanol. Conjugates obtained with PEG_{2000} and PEG_{1000} were purified by silica gel chromatography.

Table. II.4. Experimental optimisation of the use of Mukaiyama reagent for esterification of PEG_{3400} and prednisolone

Batch	$PEG_{3400}(COOH)_2$ [COOH] mmol/L	Prednisolone / COOH	Mukaiyama reagent / COOH	Triethylamine / COOH	Solvents, temperature	Time min
PP04	5	1.3	1.3	3.5	45 mL of dry DCM, 45°C	250
PP01	6	1.2	1.3	2.6	70 mL of dry THF, 50°C	2440
PP24	15	1.5	1.5	4.3	10 mL of dry THF, 30 mL of dry DCM, 50°C	1250
PP27	13	1.5	3.0	6.1	12 mL of dry THF, 32 mL of dry DCM, 50°C	2460

Table. II.5. Experimental conditions for the production of PEG-prednisolone ester of various molecular weights

Batch	Oxidised PEG Type	Oxidised PEG [COOH] mmol/L	Prednisolone / COOH	Mukaiyama reagent / COOH	Triethylamine / COOH	Solvents, temperature	Time min
PP33	PEG_{1000}	57	1.4	3.0	5.9	50 mL of dry THF, 20 mL of dry DCM, 50°C	4320
PP28	$mPEG_{2000}$	49	1.4	3.1	6.3	20 mL of dry THF, 20 mL of dry DCM, 40°C	4110
PP32	PEG_{2000}	50	1.4	3.0	6.1	20 mL of dry THF, 20 mL of dry DCM, 40°C	4245
PP31	PEG_{3400}	40	1.4	3.1	6.1	20 mL of dry THF, 30 mL of dry DCM, 40°C	4380

II.2.3.PEG-salbutamol

Salbutamol (Fig.II.3) is a β_2-adrenergic receptor agonist, sold as a salt of salbutamol sulfate of molecular weight 576.71 Da. It is a white crystalline powder. The molecule which possesses one primary hydroxyl group, which is the most reactive. It also has one secondary and one tertiary (phenol) hydroxyl group, less reactive. The amine group, being nucleophilic as well as a base, is likely to react during esterification to form an amide bond.

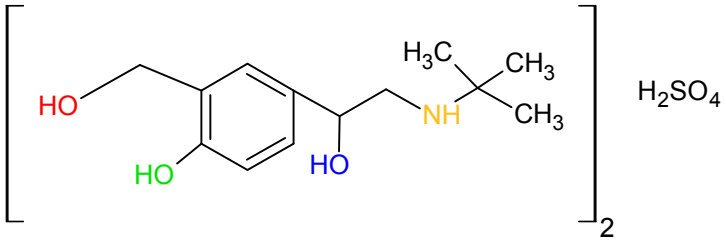

Fig.II.3. Salbutamol sulfate

Ijzerman et al. characterised the ionisation scheme of salbutamol (Fig.II.4) and calculated the macroscopic pKa values of amine (pKa_1= 9.07) and phenol (pKa_2=10.37) groups, in aqueous solutions [111] [112].

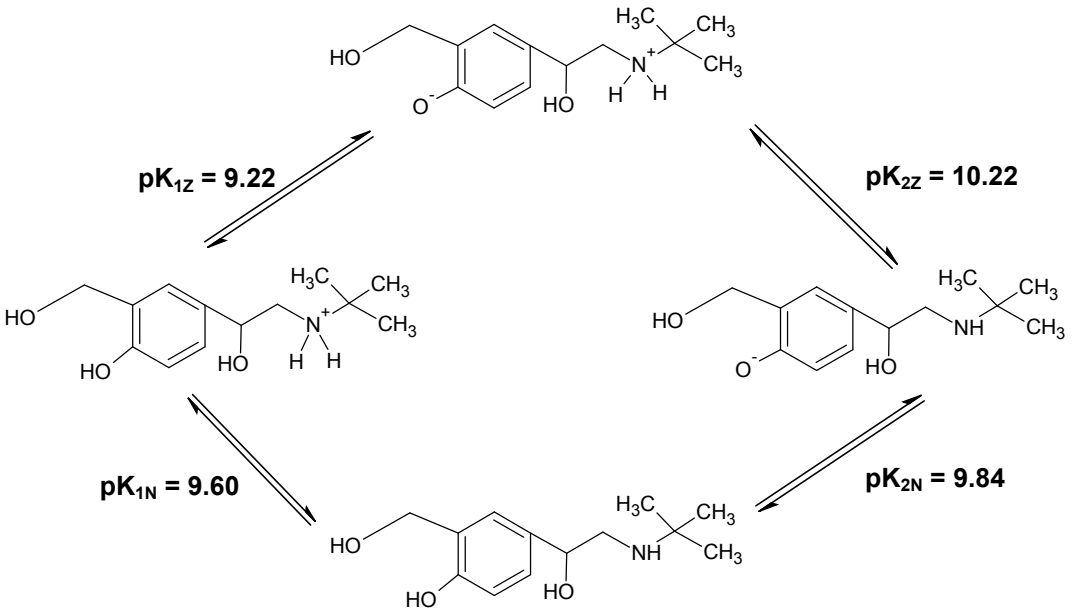

Fig.II.4. Ionisation scheme of salbutamol

II.2.3.2. Modification of salbutamol

Commercially available salbutamol is usually sold as the salt salbutamol sulfate, which is soluble in water and slightly soluble in alcohol, both unsuitable solvents for esterification purposes. Therefore, we produced a free base form of salbutamol to improve the drug solubility in non polar organic solvents, by isolating the neutral form of the molecule (Scheme.II.4). This was achieved by solubilising salbutamol sulfate in water and increasing the pH of the solution to deprotonate the amine group. Then, the water was removed and salbutamol free base was recovered in THF. In salbutamol free base, the amine is deprotonated and the nitrogen carries a free electron pair, likely to react in place of the hydroxyl group through amidation.

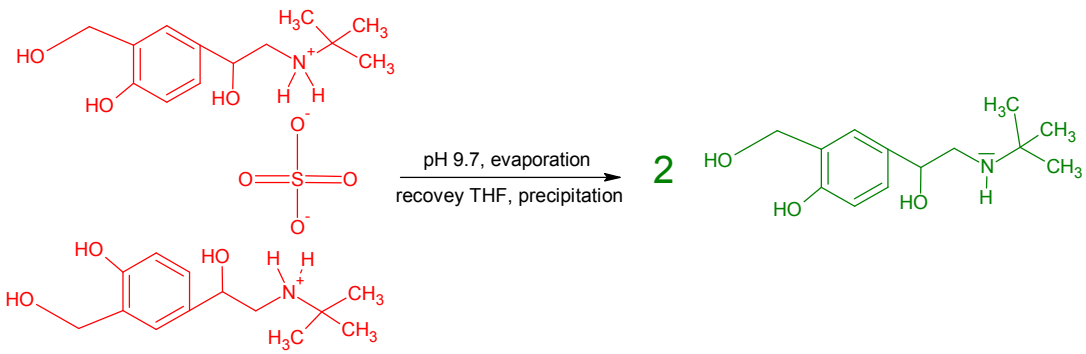

Scheme.II.4. Production of salbutamol free base

To improve the drug solubility in non polar organic solvents while maintaining the protonation of the amine group, a new salt of salbutamol was produced by mixing protonated dodecyl sulfonic acid (pKa = 2.3 [113]) and salbutamol free base to produce salbutamol dodecyl sulfate (salbutamol DS), Scheme.II.5.

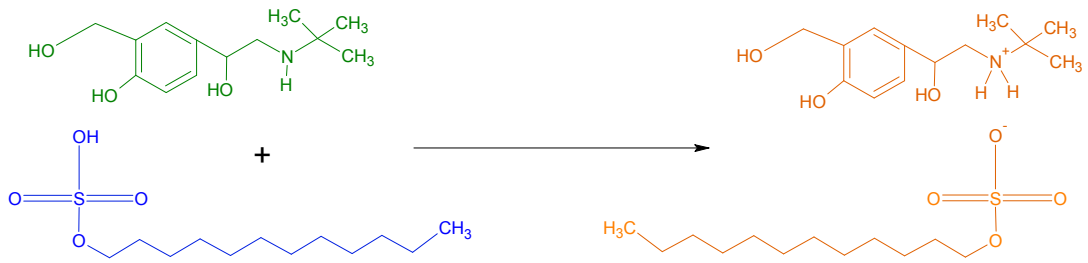

Scheme.II.5. Production of salbutamol dodecyl sulfate

The alkyl chain of salbutamol DS aids in solubilising the new salbutamol salt in non polar organic solvents while the protonated amine was prevented from interfering in the esterification reaction.

II.2.3.3. Esterification of oxidised PEG and salbutamol DS

The experimental design space of the experiments conducted to optimise the reaction conditions of esterification of oxidised PEG and salbutamol was defined by the variation of three parameters:

– the type of salbutamol employed (salbutamol sulfate, free base, dodecyl sulfate)

– the synthesis route (coupling reagent such as Mukaiyama reagent, N,N'-dicyclohexylcarbodiimide (DCC), or direct esterification through acyl chloride)

– the tertiary amine base used (triethylamine, DMAP, pyridine, 2,6 lutidine), of different pKa and steric hindrance

Upon optimisation, the acyl chloride route using 2,6 lutidine as tertiary amine base was employed to produce esters of oxidised $mPEG_{2000}$, PEG_{2000}, PEG_{3400} and salbutamol dodecyl sulfate (Scheme.II.6). The experimental conditions are summarised in Table. II.6.

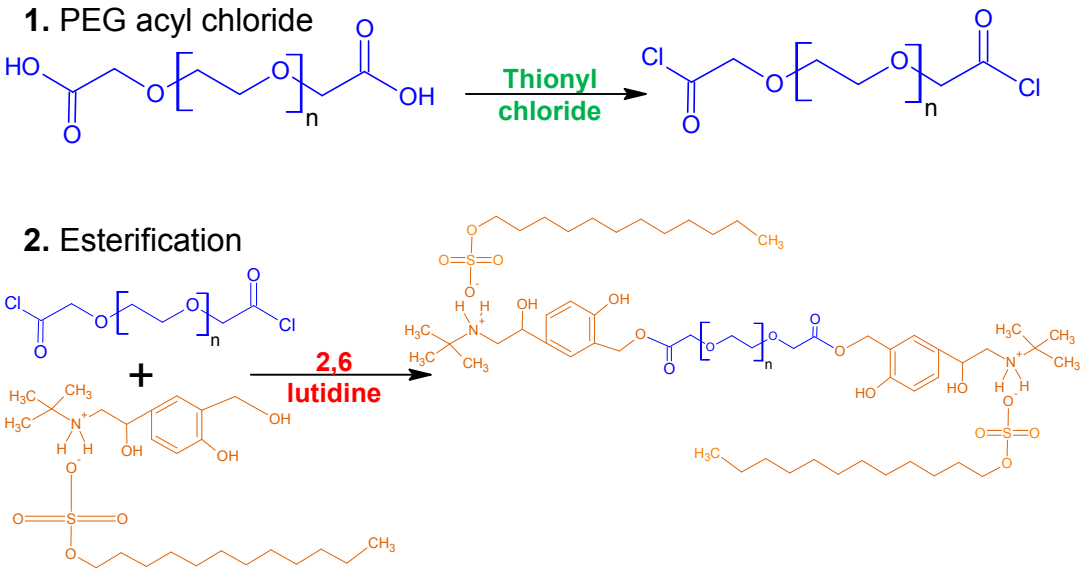

Scheme.II.6. Production of PEG-salbutamol ester conjugates

Table. II.6. Optimised conditions for PEG-salbutamol ester conjugation

Oxidised PEG		$SOCl_2$	Salbutamol DS	2,6 lutidine	Solvents, temperature	Time
Type	[COOH] mmol/L	/ COOH	/ COOH	/ COOH		min
$mPEG_{2000}$	19	6.3	2.4	5.6	22 mL of dry THF, 11 mL of dry DCM, 50°C	42
PEG_{2000}	20	5.3	2.2	5.2	44 mL of dry THF, 20 mL of dry DCM, 50°C	45
PEG_{3400}	20	5.5	2.3	5.4	44 mL of dry THF, 20 mL of dry DCM, 50°C	37

Purification of the conjugates was performed by anion exchange to eliminate dodecyl sulfonate ions (replaced by chloride ions), excess salbutamol was washed with dilute HCl and the purified product precipitated in diethyl ether to remove the excess 2,6 lutidine (Scheme.II.7). Two dimensions NMR, FTIR and elemental analysis were conducted to determine the conjugates chemical structure and purity.

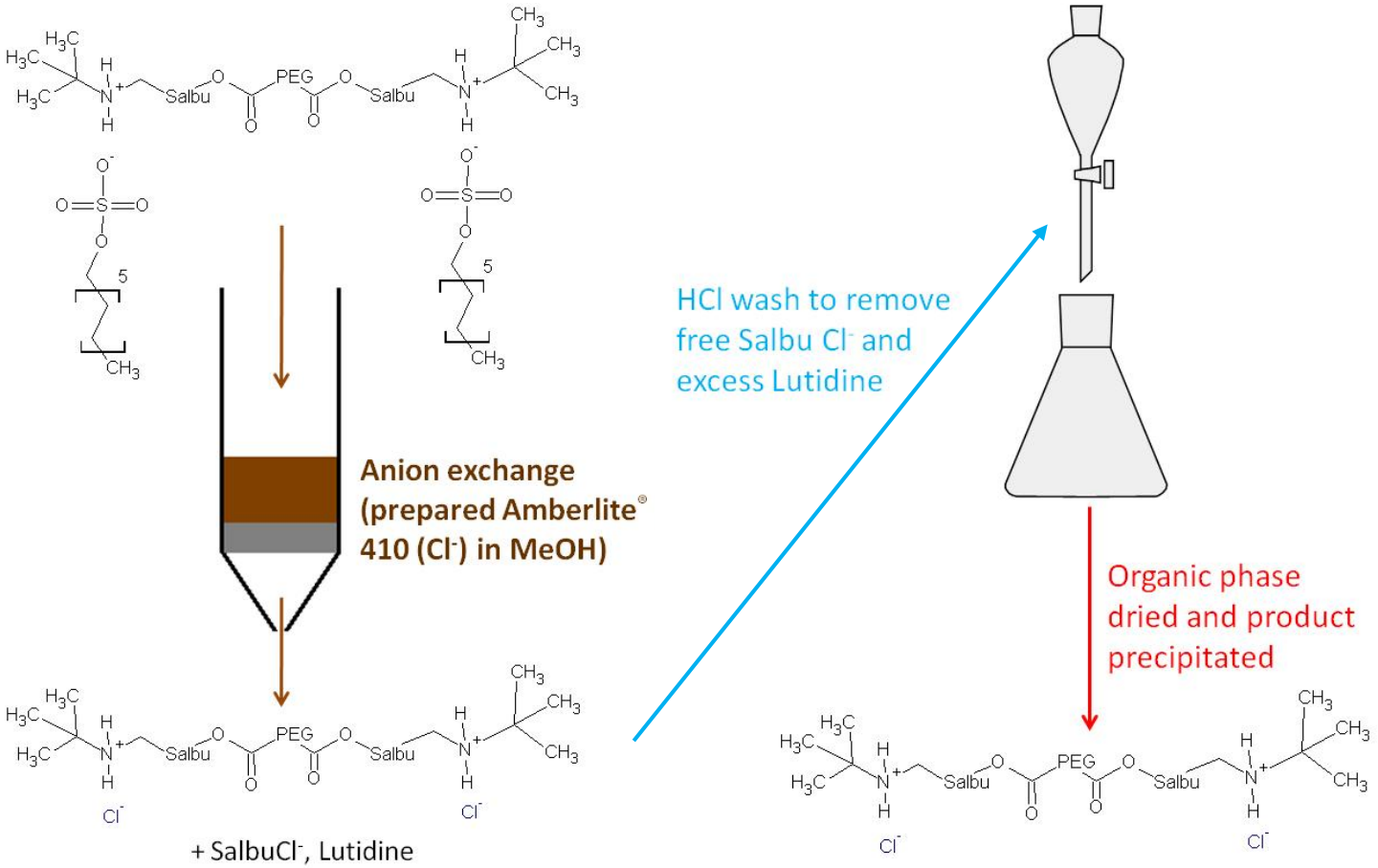

Scheme.II.7. Schematic of PEG-salbutamol ester conjugate purification

II.2.4. Analytical techniques

II.2.4.1. Acid titration

Oxidised products were analysed by acid titration. A known amount of dried oxidised PEG (e.g. 569.62 mg of oxidised PEG_{3400}) was dissolved in approximately 50 mL of deionised water. Total carboxylic acid content was titrated against sodium hydroxide by measuring the pH of the solution with addition of sodium hydroxide (200 µL of 0.1 M solution or 0.03 M closer to equivalence). The amount of carboxylic acid in solution was equal to the amount of sodium hydroxide added to get to the equivalence point, determined as the inflection point in the graph of pH *vs* amount of NaOH. Excel software was used to calculate $\frac{\Delta pH}{\Delta NaOH}$ (slope of the plot pH *vs* NaOH, approximation of the first derivative of the function pH = f(NaOH)) and to determine its maximum, defining the equivalence point.

II.2.4.2. Infra Red spectroscopy

Infra Red spectrometry was performed by grinding 2 mg of product with 200 mg of potassium bromide (spectroscopic grade) using an agate mortar and pestle. FTIR spectra were then acquired using a Nicolet 380 FTIR spectrometer (Thermo Fisher, Waltham, MA, USA), and spectra were processed by OMINIC software (Thermo Fisher).

II.2.4.3. Nuclear Magnetic Resonance spectrometry

For NMR analyses, the sample (20 mg for ^{1}H NMR, 50 mg for ^{13}C NMR) was dissolved in deuterated solvent (methanol MeOD, chloroform $CDCl_3$, deuterium oxide D_2O or dymethyl sulfoxide $DMSO_{d6}$). One Dimensional Nuclear Magnetic Resonance (1D NMR) spectra were acquired on a Bruker DPX300, or a Bruker DPX400, using the standard pulse sequence zg 30, 0.1 s

relaxation delay, 2.9846 s acquisition time, 16 or 64 scans. Two Dimensional NMR spectra were acquired on a Bruker AV(III)400 NMR spectrometer. Heteronuclear Multiple Quantum Coherence (HMQC, showing one-bond correlations from ^{1}H to ^{13}C nuclei), using the inv4gptp pulse sequence, 8 transients, acquisition times (0.2540, 0,0305 ^{1}H, ^{13}C). Heteronuclear Multiple Bond Coherence (HMBC, showing over 2 or 3 bonds correlations from ^{1}H to ^{13}C nuclei), spectra were recorded using Bruker hmbcetgpl2nd pulse sequence, 16 transients, acquisition time (0.5079, 0,0221 ^{1}H, ^{13}C). Spectra were then processed using ACD Labs software v12.

II.2.4.4. Reaction completion follow up

To follow the reaction progress, approximately 500 µL of the reaction mixture was sampled under inert atmosphere and the solvents evaporated to dryness using a rotary evaporator. The crude solid was resuspended in deuterated NMR solvent and spectra were acquired and processed.

II.2.4.5. Mass spectrometry

For mass spectrometry measurement, samples were prepared in MeOH at 10 $ng.L^{-1}$ and analyses were conducted using ESI (Electrospray Ionisation) with a Bruker MicroTOF (in-house analytical service) or an API 4000 (Applied Biosystem) mass spectrometer or Matrix-Assisted Laser Desorption/Ionisation (MALDI) using a Bruker Ultraflex III and measuring Time Of Flight (TOF).

II.2.4.6. Elemental analysis

For elemental microanalysis, 2 mg of product were used to measure C, N and H content using an in-house analytical service (CE-440 Elemental Analyzer from Exeter Analytical).

II.3. Results

II.3.1. PEG oxidation

The TEMPO mediated oxidation of polyethylene glycol of various molecular weights was successfully carried out and the oxidised polymers were characterised by Infra Red spectroscopy, acid titration and NMR. The following describes in detail the analysis of oxidised PEG_{3400}. The same characterisation was carried out for PEG of other molecular weights and after optimisation, 100% oxidation could be achieved consistently for all molecular weights. PEG oxidation results for all molecular weights are combined in Table. II.8. Supportive information for oxidised PEG_{1000}, PEG_{2000} and $mPEG_{2000}$, such as, IR spectra, acid titration and NMR are available in Appendix 1.

Infra Red spectroscopy: A carbonyl stretch at 1745 cm^{-1} appeared in the Infra red spectrum of oxidised PEG_{3400} when compared to native PEG (Fig.II.5), whereas the rest of the spectrum conformed to that of the starting material.

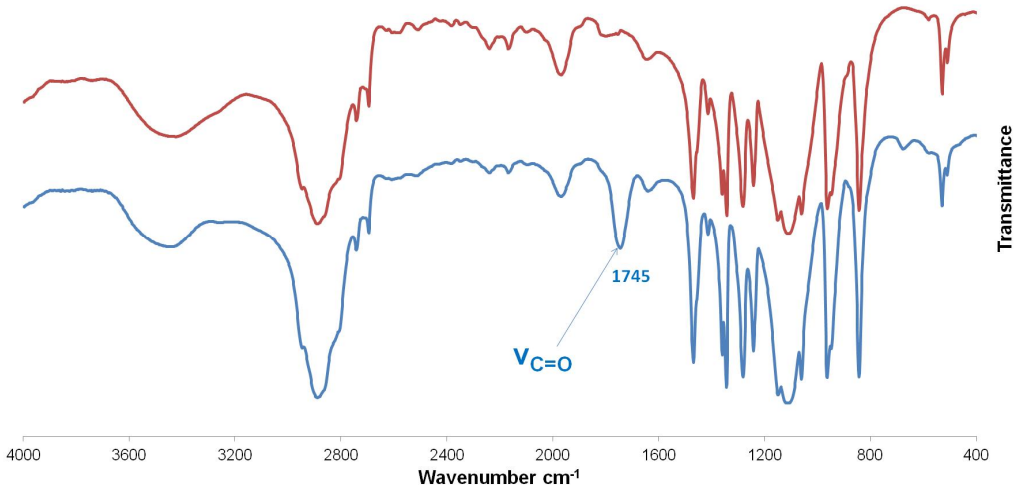

Fig.II.5. Infra Red Spectrum of unmodified and oxidised PEG_{3400}
— $PEG_{3400}OH$, —$PEG_{3400}COOH$

Acid titration: During acid titration of 569.62 mg of oxidised PEG with sodium hydroxide, the equivalence point was reached after addition of 322 µmol of NaOH (Fig.II.6). Fully oxidised PEG has gained 2 oxygen atoms (16 Da) and lost 4 protons (1 Da) compared to native PEG. Therefore, the molecular weight of oxidised PEG_{3400} was:

(II.1) Mn(PEGCOOH)=Mn(PEG)+2×16-4×1

(II.2) Mn (PEGCOOH) = 3395 + 28

(II.3) Mn(PEGCOOH) = 3423 Da

The starting number of moles of PEG_{3400} was 166 µmol ($\frac{569.62\ mg}{3423 Da}$) and therefore **the number of carboxylic acid per molecule of PEG was 1.94** ($\frac{322\ \mu mol}{166\ \mu mol}$).

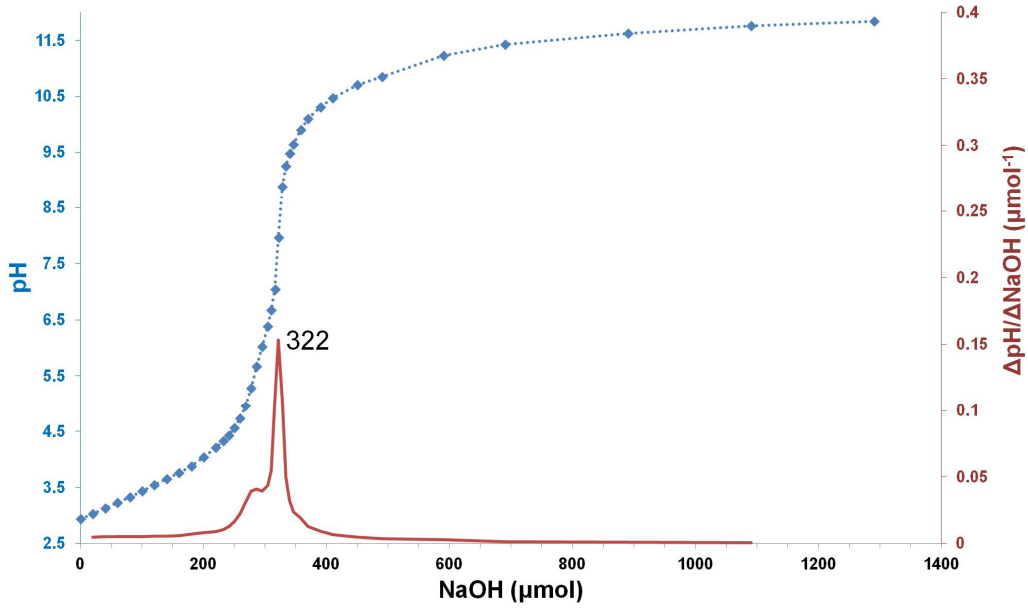

Fig.II.6. Acid titration for $PEG_{3400}COOH$
-♦- pH, —ΔpH/ΔNaOH

NMR spectroscopy: A new signal at 4.12 ppm appeared on the proton NMR of oxidised PEG. Considering a molecular weight of 3423 Da, the number of PEG unit was calculated and thus the total number of protons for the signal in position 1 (Fig.II.7). A general formula for oxidised PEG was $C_4H_6O_5(C_2H_4O)n$, and the molecular weight can be calculated according to the number of PEG units n and the atomic mass of each of its atom (ma(atom)):

(II.4) Mn (PEG_{COOH}) = 4 m_a(C)+6 m_a(H)+5 m_a(O)+n (2 m_a(C)+4 m_a(H)+m_a(O))

$3423 = ((4\times12.011+6\times1.008+5\times15.999) + n\times(2\times12.011+4\times1.011+15.999))$

$3423 = 134.09 + n\times44.05$

$n = 74.66$.

With an average of 74.66 units per molecule of PEG, the average number of protons in position 1 was 299 (4×74.66). This number of protons was then used as a reference to integrate the signals in NMR spectra and therefore integrations for other signals gave the number of protons per molecule of PEG. Two dimensional NMR studies in MeOD were conducted on oxidised PEG and the assignment of the spectra allowed the deduction of the following structure (Fig.II.7):

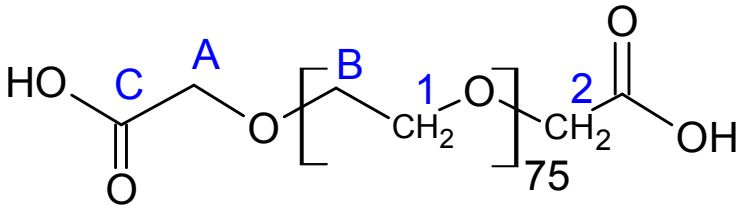

Fig.II.7. Position numbering of PEG
Different numbers refer to different proton environments and letters refer to different carbon environments

Oxidised PEG_{3400} ^{1}H NMR (400 MHz, methanol-d_4) δ 4.12 (s, 4H), 3.64 (br. s., 299H). The proton NMR spectrum of oxidised PEG was characterised by a broad signal for 299 protons in position 1 (δ 3.64 (br. s., 299H)) and the appearance of a signal for 3.79 protons in position 2 (δ 4.12 (s, 4H)) (Fig.II.8). **On average, 1.90 carboxylic acid groups per PEG were calculated**, this is consistent with acid titration results and within the margin of error for complete oxidation.

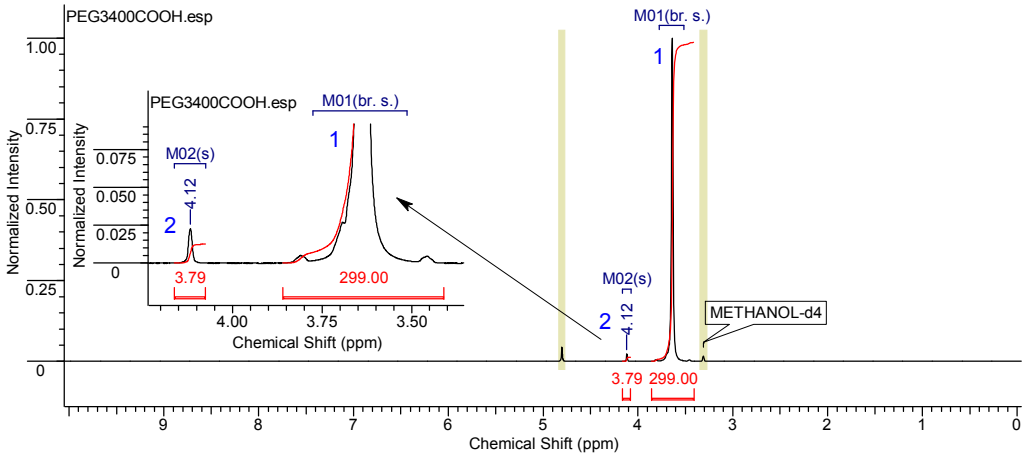

Fig.II.8. Proton NMR spectrum for oxidised PEG_{3400}
Spectrum acquired on a Bruker AV(III)400 spectrometer, 16 scans, in MeOD

The HMQC spectrum (showing one bond correlation between ^{1}H and ^{13}C) of oxidised PEG displayed the values for carbon chemical shifts in positions A and B. Where the signal 1/B was positioned, the ordinate value gave the chemical shift for the carbon atom in position B (71.2 ppm), directly bonded to the protons in position 1. The correlation 2/A gave the value for the carbon atom in position A (69.2 ppm), directly bonded to protons in position 2 (Fig.II.9).

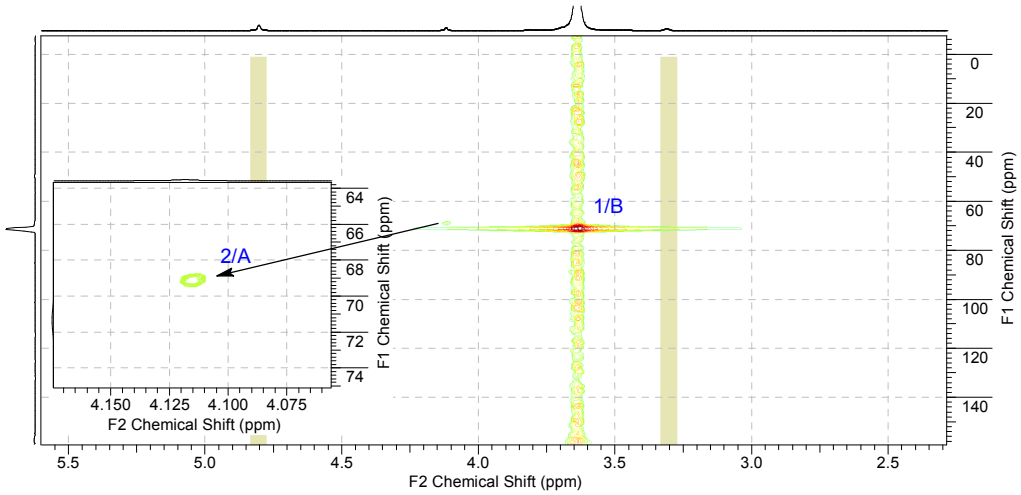

Fig.II.9. 2D HMQC spectrum for oxidised PEG
Spectra acquired on a Bruker AV(III)400 spectrometer in MeOD

The HMBC spectrum (showing multiple correlation between ^{1}H and ^{13}C) of oxidised PEG showed the correlations 1/A and 2/B.

The correlation 2/C produced a typical carbonyl chemical shift for carbon in position C (172.3 ppm) (Fig.II.10).

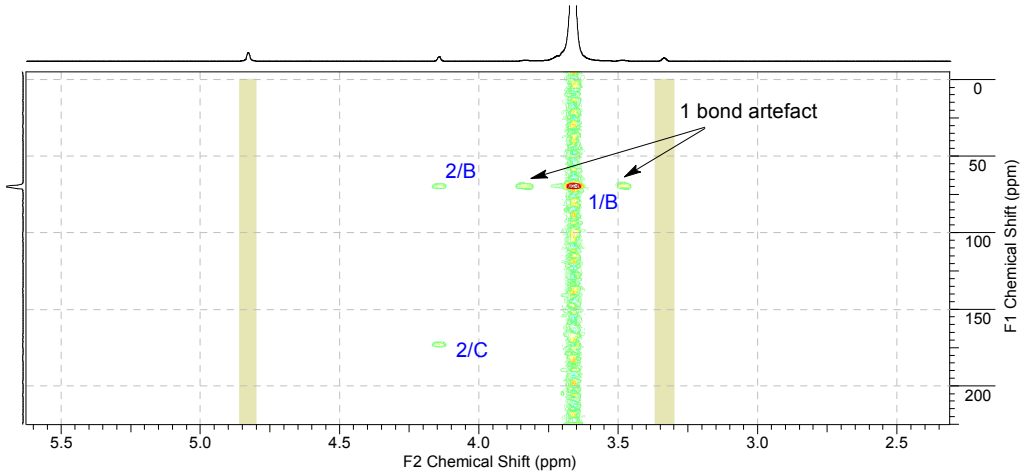

Fig.II.10. 2D HMBC spectrum for oxidised PEG
Spectra acquired on a Bruker AV(III)400 spectrometer in MeOD

The structure of oxidised PEG_{3400} was therefore confirmed by NMR, and the findings for NMR study are in Table. II.7.

Table. II.7. Full assignment of 2D NMR spectra of oxidised PEG.

#	Atom	Chemical shift (ppm)	Type	Integral
1	H	3.64	s	299
2		4.12	s	3.79
A	C	69.2	NA	NA
B		71.2		
C		172.3		

Spectra were recorded in MeOD, using an AV(III)400 Bruker spectrometer. s: singlet, d: doublet, dd: doublet of doublets, m: multiplet, br: broad, NA: Not Applicable.

Oxidised PEG of other molecular weights were analysed likewise and Table. II.8 combines the results of PEG oxidations for various molecular weights.

PEG_{1000}: The IR spectrum showed a carbonyl stretch at 1743 cm^{-1} with the rest of the spectrum conformed to PEG (Appendix 1, Fig.VI.1). ^{1}H NMR (400 MHz, chloroform-d) δ 4.16 (s, 4H), 3.65 (s, 81H) (Appendix 1, Fig.VI.2). The molecular weight of oxidised PEG_{1000} was calculated with equation (II.1) and the general formula for PEG $C_4H_6O_5(C_2H_4O)n$ to give 1028 Da. The number of PEG units, n was calculated with equation (II.4). There was an average of n = 20.29 units of PEG ($\frac{1028-134.09}{44.05}$) in $PEG_{1000}COOH$, which gave 81 protons (4 × 20.29) for the signal in position 1 (δ 3.65 (s, 81H)). With this reference set, the integral for the signal in position 2 was measured at 3.91 protons (δ 4.16 (s, 4H)), or **1.96 mol of carboxylic acid per mol of polymer**. Acid titration was conducted on 257.8 mg of oxidised PEG_{1000} (250.8 µmol) and the equivalence point was reached after addition of 500 µmol of NaOH (Appendix 1, Fig.VI.3). The number of carboxylic acids per mol of PEG was therefore 1.99 ($\frac{500}{250.8}$), confirming the total oxidation of PEG_{1000}.

PEG_{2000}: The IR spectrum showed a carbonyl stretch at 1743 cm^{-1} with the rest of the spectrum conformed to PEG (Appendix 1, Fig.VI.1). ^1H NMR (400 MHz, chlorofom-d) δ 4.07 (s, 4H), 3.58 (br. s., 172H), Appendix 1, Fig.VI.4. The molecular weight of oxidised PEG_{2000} was calculated with equation (II.1) and the general formula for PEG $C_4H_6O_5(C_2H_4O)n$ to give 2028 Da. The number of PEG units, n was calculated with equation (II.4). There was an average of n = 43 units of PEG ($\frac{2028-134.09}{44.05}$) in $PEG_{2000}COOH$, which gave 172 protons (4 × 43) for the signal in position 1 (δ 3.58 (br. s., 172H)). With this reference set, the integral for the signal in position 2 was measured at 4.15 protons (δ 4.07 (s, 4H)), or **2.08 mol of carboxylic acid per mol of polymer**. Acid titration was conducted on 264.97 mg of oxidised PEG_{2000} (130.7 µmol) and the equivalence point was reached after addition of 280 µmol of NaOH (Appendix 1, Fig.VI.5). **The number of carboxylic acids per mol of PEG was therefore 2.14** ($\frac{280}{130.7}$), confirming the total oxidation of PEG_{2000}.

$mPEG_{2000}$: The IR spectrum showed a carbonyl stretch at 1742 cm^{-1} with the rest of the spectrum conformed to that of mPEG (Appendix 1, Fig.VI.6).

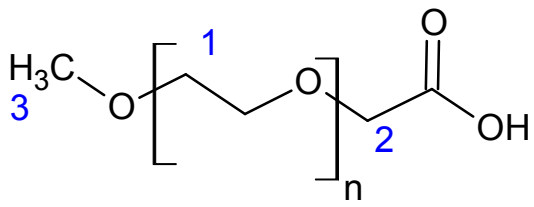

Fig.II.11. Proton numbering of mPEG

^1H NMR for $mPEG_{2000}COOH$: (400 MHz, chloroform-d) δ 4.08 (s, 2H), 3.58 (s, 178H), 3.32 (s, 3H) (Appendix 1, Fig.VI.7). The actual molecular weight of

$mPEG_{2000}COOH$ (Fig.II.11) was calculated with the $^{1}HNMR$ spectrum. The integration for the methyl group in position 3 was used as a reference and set at 3 protons (δ 3.32 (s, 3H)). The total number of protons for the main PEG unit chain in position 1 was measured at 178.34 protons (δ 3.58 (s, 178H)). **The number of carboxylic acid groups per molecule of mPEG was 1.24** since the integration for the signal of position 2 gave 2.47 protons (δ 4.08 (s, 2H)).

The general formula for mPEG was $C_3H_6O_3(C_2H_4O)n$, with n = 44.59 ($\frac{178.34}{4}$) on average for $mPEG_{2000}COOH$. The molecular weight of oxidised $mPEG_{2000}$ was therefore:

(II.5) Mn = 3 ma(C)+6 ma(H)+3 ma(O)+n (2 ma(C)+4 ma(H)+ma(O))

(II.6) Mn = (3×12.011+6×1.008+3×15.999) +

44.59×(2×12.011+4×1.011+15.999)

(II.7) Mn ($mPEG_{2000}COOH$) = 2054 Da

Acid titration was conducted on 252.89 mg of oxidised $mPEG_{2000}$ (123.1 µmol) and the equivalence point was reached after addition of 137 µmol of NaOH (Appendix 1, Fig.VI.8). **The number of carboxylic acids per mol of PEG was therefore 1.11** ($\frac{137}{123.1}$), confirming the total oxidation of $mPEG_{2000}$.

Table. II.8. Results for PEG oxidation

PEG MW (Da)	COOH/PEG		FTIR	Yield
	NMR	Acid titration	cm^{-1}	%
1000	1.96	1.99	1743	45
2000	2.08	2.14	1743	87
2000*	1.24	1.11	1742	76
3400	1.90	1.9	1745	93

**mPEG 2000 Da, yield after purification*

Summary

All products were 100% oxidised, and the synthetic yields were influenced by the polymer molecular weights. The recovery for $mPEG_{2000}$, PEG_{2000} and 3400 Da was greater than 75%, while it was 45% for PEG_{1000}(Table. II.8). The physical properties of PEG were clearly molecular weight dependent. PEG_{1000} was a white waxy paste that melted at 37-40°C whereas with increasing molecular weighs, the polymers became more powder-like and less waxy, PEG_{3400} melted at 54-58°C. Aqueous and organic solubility were also molecular weight dependant, water solubility decreasing with increasing molecular weight. PEG_{3400} was efficiently extracted from the aqueous phase and crystallised, yielding a good recovery. PEG_{1000} was not efficiently solvent extracted, it was not crystalline, giving poor recovery. The recovery was ranked as follows: $PEG_{3400} > PEG_{2000} > PEG_{1000}$.

II.3.2.PEG-prednisolone

II.3.2.1. Analysis of prednisolone.

Carbon atoms of prednisolone were lettered and protons numbered for reference in the NMR analysis (Fig.II.12). The reader must be aware that the numbering and lettering system referred respectively to protons and carbons of the molecules and this nomenclature is different to the position numbering proposed by the International Union of Pure and Applied Chemistry (IUPAC) [114]. The following assignment was performed with the use of ^{1}HNMR, 2D HMQC and 2D HMBC (Fig.II.13, Fig.II.14, Fig.II.15). The proton and carbon chemical shifts were combined in Table. II.9.

a.

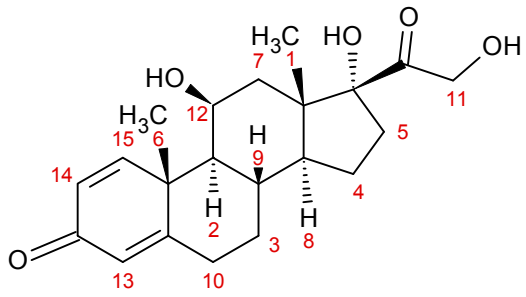

b.

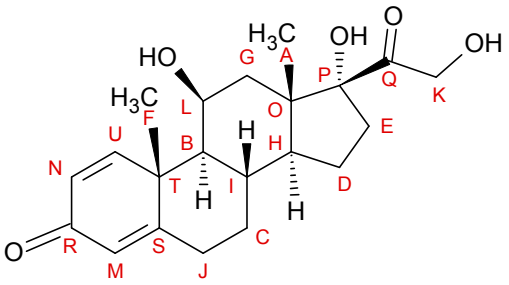

c.

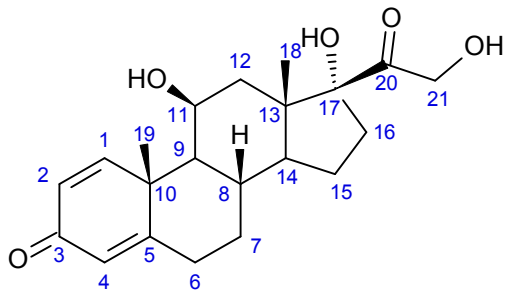

Fig.II.12. Proton numbering (a), carbon lettering (b) of prednisolone used in the thesis, position numbering (c) of prednisolone according the IUPAC nomenclature

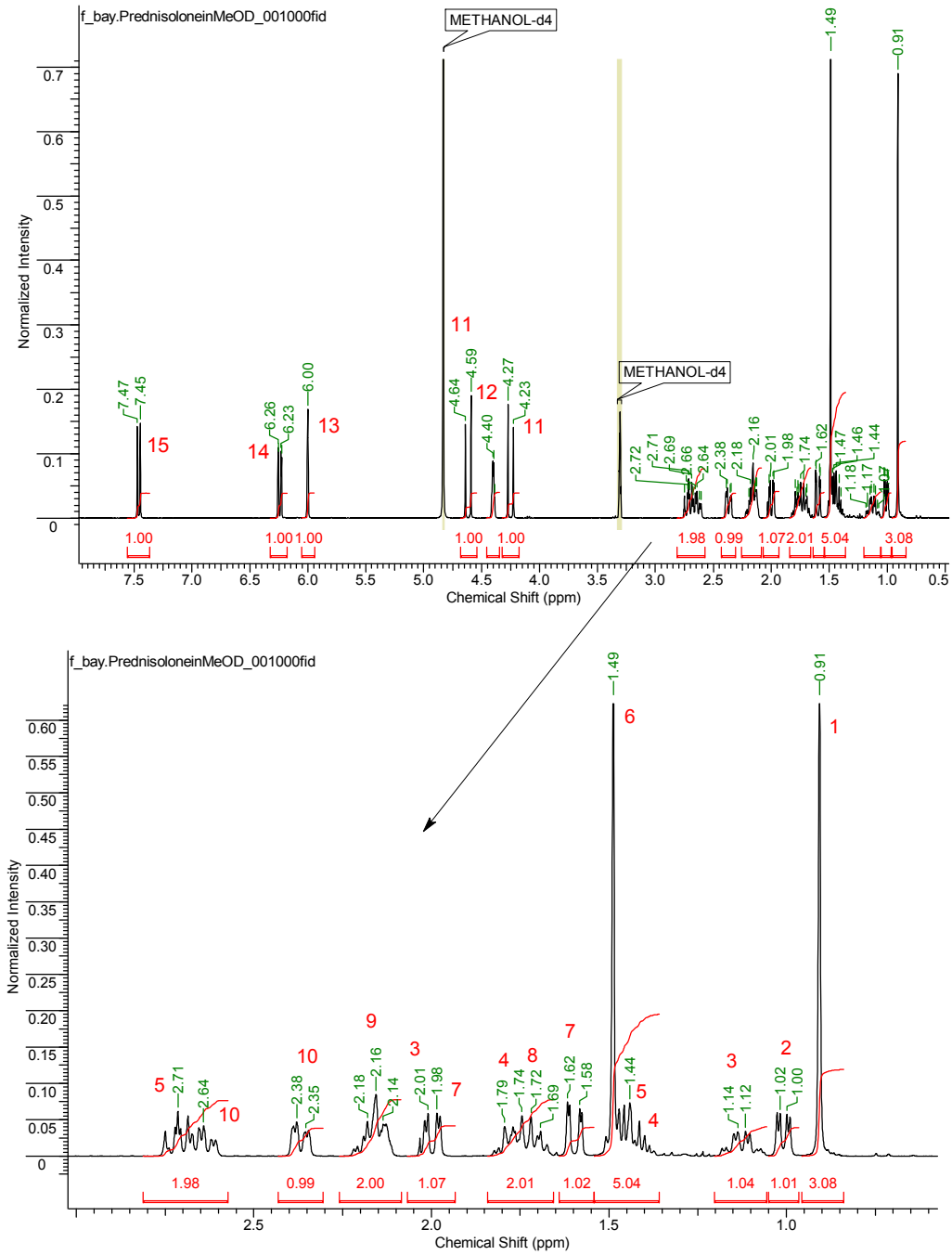

Fig.II.13. ^{1}HNMR of prednisolone and signal assignment
Spectrum acquired on a Bruker AV(III)400 spectrometer, 16 scans, in MeOD

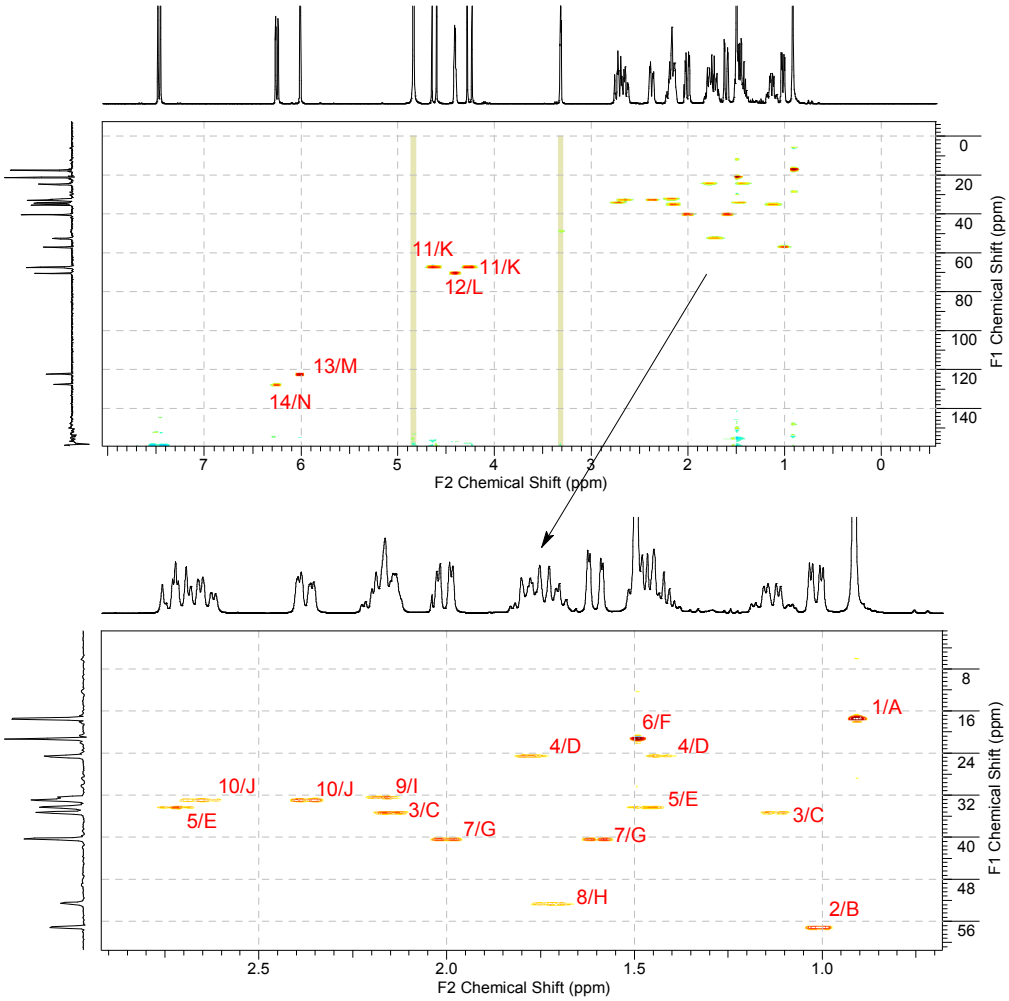

Fig.II.14. 2D HMQC of prednisolone and correlation assignment
Spectra acquired on a Bruker AV(III)400 spectrometer in MeOD

Signals for carbon atoms in positions O to U were not assigned using HMQC. The 2D HMBC granted the full assignment of these signals (Fig.II.15).

In this spectrum, seven carbon signals, not seen in HMQC spectrum, appeared at 44.7, 47.1, 88.8, 158.6, 173.3, 187.5 and 211.4 ppm, corresponding to the chemical shifts for the unassigned positions O to U. Using the proton signal to which they were correlated, it was possible to fully assign the chemical shifts for prednisolone (Table. II.9), and the results conformed to the supplier specifications (Sigma) and a previous NMR assignment performed in deuterated chloroform by Rachwal et al. [115].

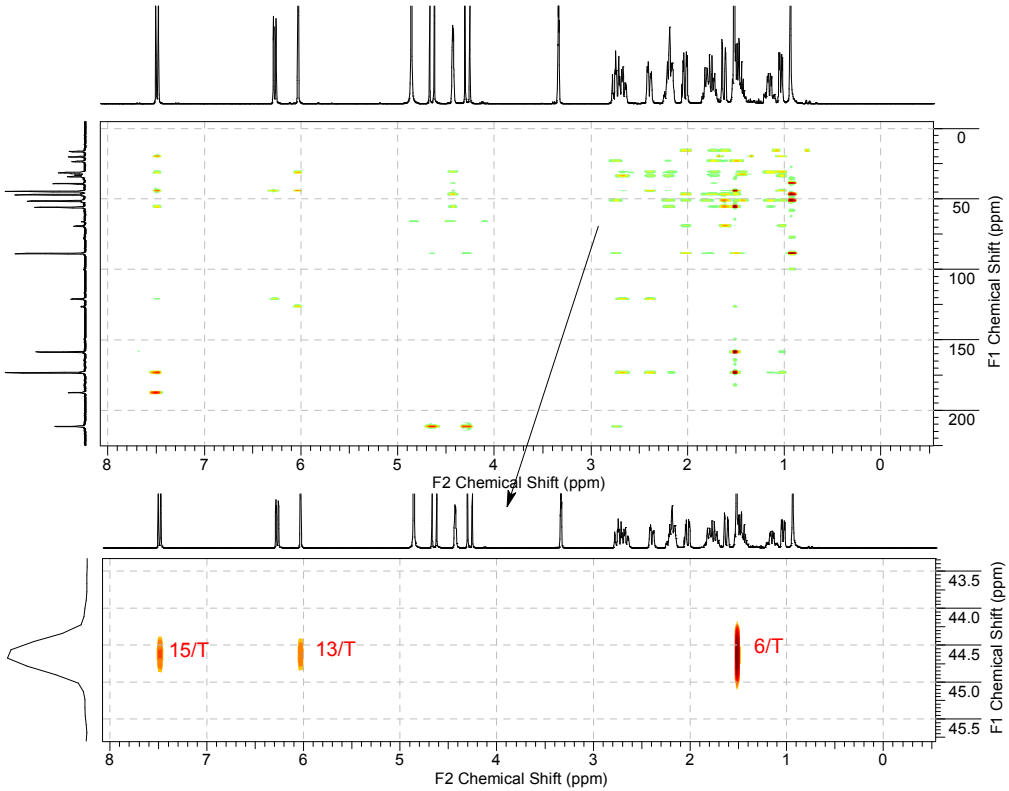

Fig.II.15. 2D HMBC of prednisolone
Spectra acquired on a Bruker AV(III)400 spectrometer in MeOD

The NMR analysis of prednisolone gave a rather complex set of spectra to analyse, especially ^{1}H-NMR and HMBC. The study of prednisolone NMR spectra was nonetheless essential in order to analyse the products of esterification between oxidised PEG and prednisolone. The hydroxyl groups of prednisolone has been particularly scrutinised with an emphasis on the primary hydroxyl group of the molecule which was the more likely to react to form an ester bond. Particularly, any changes in the signal for positions 11/K (for primary hydroxyl group), 12/L (for secondary hydroxyl group) and P (for tertiary hydroxyl group) were monitored. Integrity of the rest of the structure was assessed by tracking any changes in the remaining parts of the spectrum.

Table. II.9. Prednisolone full assignment of proton and carbon chemical shifts

Proton position	Chemical shift (ppm)	Carbon position	Chemical shift (ppm)
1	0.91	A	16.3
2	1.01	B	55.9
3	1.13 / 2.13	C	34.1
4	1.41 / 1.78	D	23.4
5	1.44 / 2.71	E	33.1
6	1.49	F	20.1
7	1.60 / 2.00	G	39.2
8	1.73	H	51.4
9	2.16	I	31.2
10	2.36 / 2.65	J	31.7
11	4.25 / 4.61	K	66.2
12	4.40	L	69.3
13	6.00	M	121.1
14	6.24	N	126.5
15	7.46	O	47.1
		P	88.8
		Q	211.4
		R	187.5
		S	173.3
		T	44.7
		U	158.6

II.3.2.2. Reaction with PEG acyl chloride

PP11: NMR analysis of the crude product PP11 was conducted as follow:

The usual NMR solvent traces were observed: THF ((1.87, m, 11.49 H) and (3.72, m, merged with PEG signal 1)), and DCM (5.51 ppm, s). Triethylammonium chloride signals were also present ((1.32 ppm, t, J=7.3 Hz, 25H) and (3.21, q, J=7.3 Hz, 14H) and (3.35, q, J=7.3 Hz, 2H)), Fig.II.17.

In the region 3.1-5.3 ppm, the peak for PEG signal 1 was broad with satellite peaks and set at 299 protons (PEG chain ($C\underline{H_2}$-$C\underline{H_2}$-$O)_n$). The signal at 4.30 ppm (2') was directly correlated to a carbon at 67.6 ppm (A',Fig.II.18) and along the molecule to B (70.1 ppm) and to C' shifted to 170.6 ppm (Fig.II.19). The doublet of doublets at 5.05 ppm (J = 17.57, 56.97 Hz, 2.7 H), corresponded to prednisolone position 11' when conjugated to PEG as it was correlated to position K' at 67.9 ppm (Fig.II.18) and Q (205.2 ppm) and PEG position C (170.6 ppm) (Fig.II.19). This correlation 11'/C' was a definite proof that PEG and prednisolone were conjugated via an ester link. There were 1.39 mol of conjugated prednisolone per mol of PEG (PEG-$C\underline{H_2}$-CO-O-Pred, δ 4.3, (s, 2.78 H)). The other signals conformed to unreacted prednisolone: signals for position 11 (Pred-CO-$C\underline{H_2}$-OH, 4.43 ppm (dd, J = 19.07, 147.57 Hz, 1.83 H)) and 12 (4.43 ppm, m, 2.51 H).

The other signal for PEG position 2 was shifted to 3.95 ppm and therefore likely to be related to a deprotonated form of oxidised PEG (PEG-$C\underline{H_2}$-COO^-, δ 3.95 ppm). The integration value could not be used as the signal was merged with one of PEG unit satellite signal.

A third form of oxidised PEG was present in the mixture. The foreign singlet i at 4.69 ppm (PEG-$C\underline{H_2}$-N^+-$(CH_2$-$CH_3)_3$, s, 0.59 H) was directly bonded to a

carbon a at 83.9 ppm (Fig.II.18) and along the molecule to carbon atoms b (49.9 ppm) and e (71.1 ppm) (Fig.II.19). The signal b was also correlated to a proton signal in position ii (3.38 ppm), close to triethylamine, in both HMBC and HMQC spectra. The proton signal ii was correlated further along the molecule to a, confirming a link with proton signal i and to carbon signal c (5.8ppm). This signal c was found on HMQC as being directly bonded to triethylamine signal iii (Fig.II.18), which in turn was linked to b in HMBC spectrum (Fig.II.19).

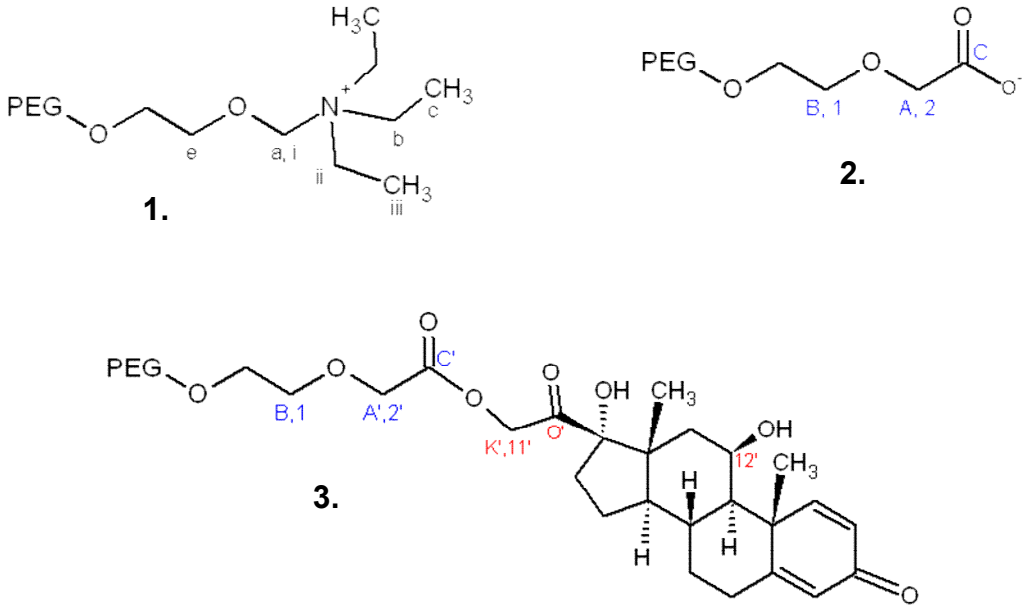

Fig.II.16. Different forms of PEG present in crude PP11
1.PEG-triethylammoium, 2. deprotonated PEG, 3. PEG-prednisolone

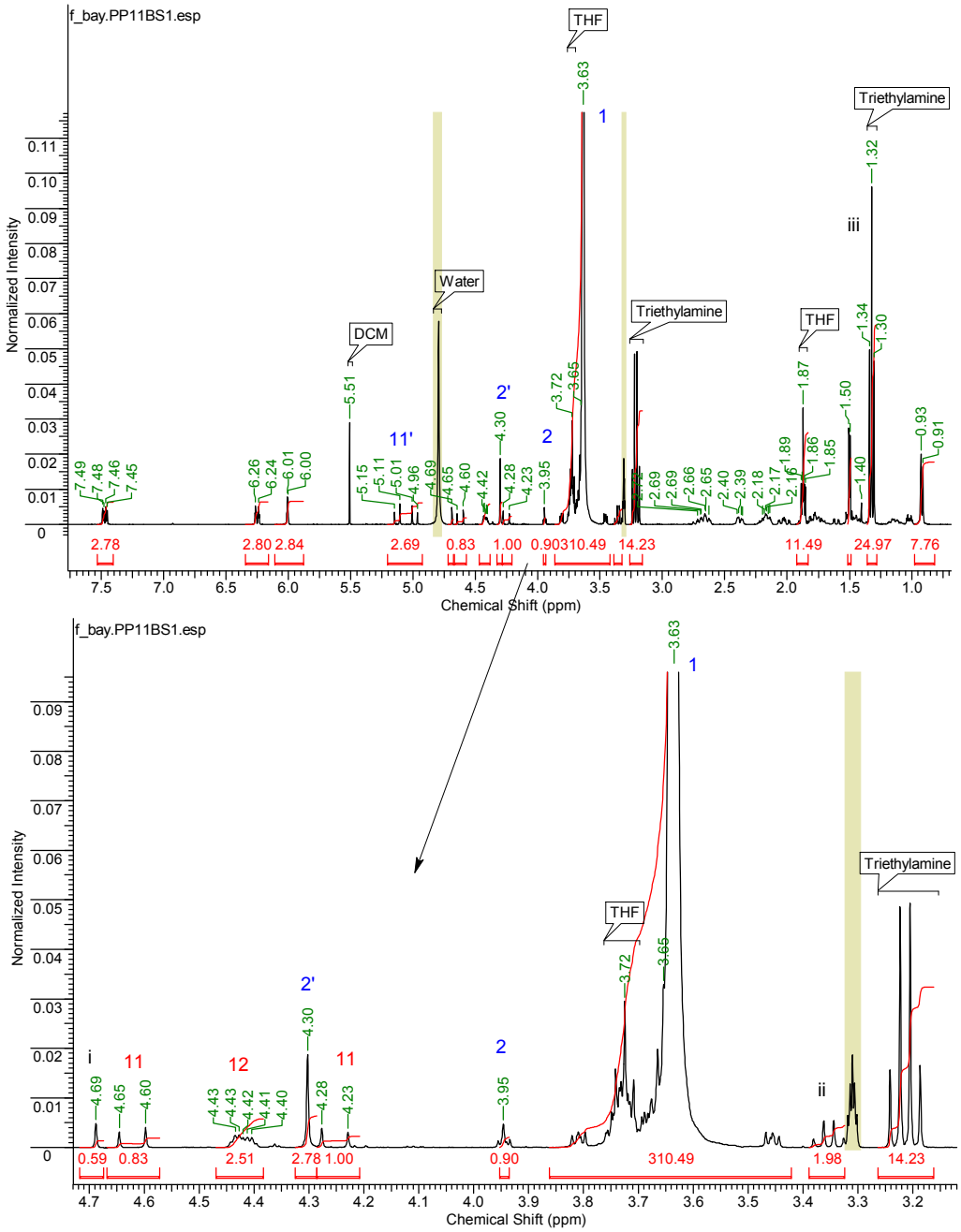

Fig.II.17. [1]HNMR for crude PP11
Spectrum acquired on a Bruker AV(III)400 spectrometer, 16 scans, in MeOD

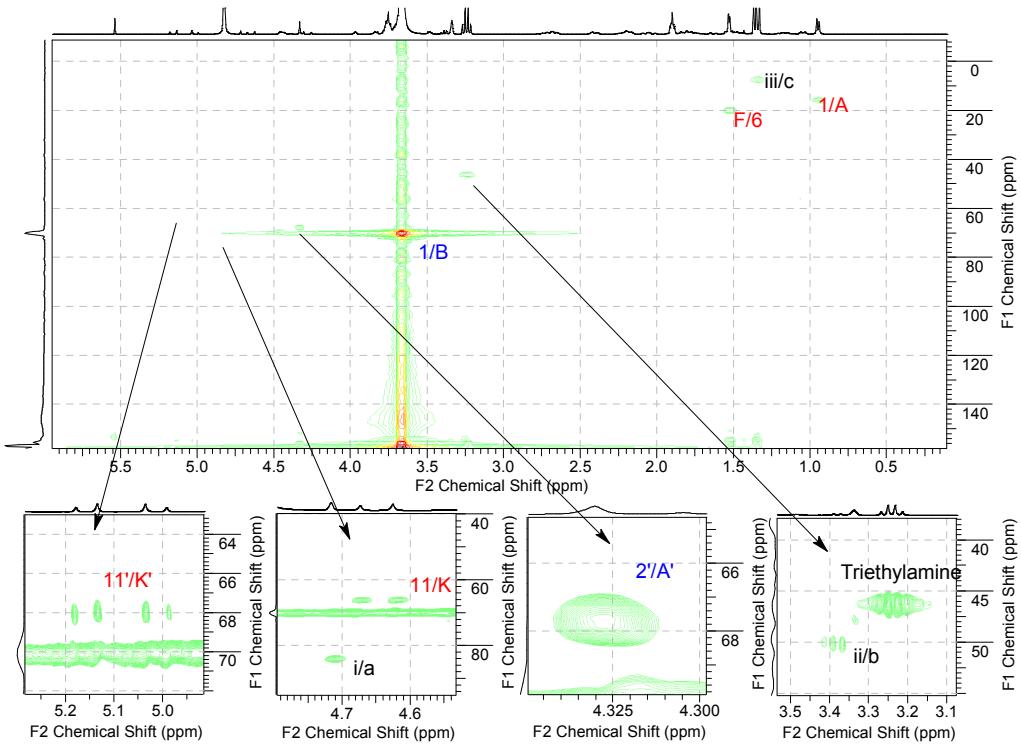

Fig.II.18. HMQC for crude PP11
Spectra acquired on a Bruker AV(III)400 spectrometer in MeOD

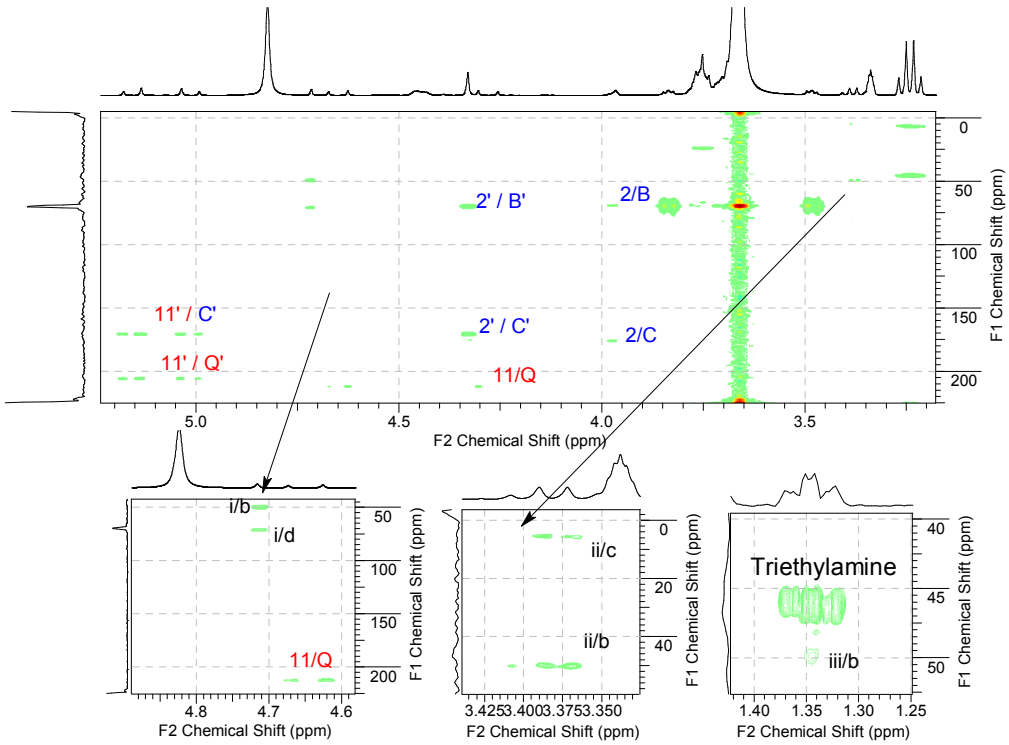

Fig.II.19. HMBC for crude PP11
Spectra acquired on a Bruker AV(III)400 spectrometer in MeOD

In conclusion, crude PP11 was a mixture of triethylammonium chloride, unconjugated $PEGCOO^-$ (0.3 mol), PEG-prednisolone ester (1.4 mol), PEG-triethylamonium (0.3 mol), and unreacted prednisolone (Fig.II.16).

PP11SFAD: after clearing the NMR spectrum of the solvent traces (Fig.II.20), the analysis revealed that this fraction contained only unreacted prednisolone, no trace of PEG or triethylamine.

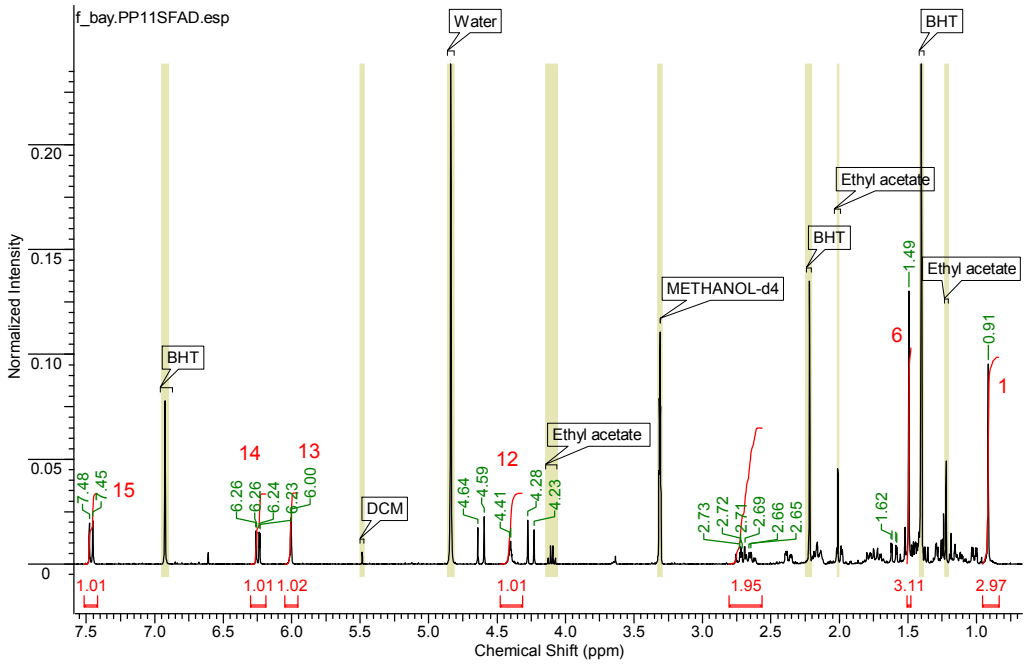

Fig.II.20. ^{1}HNMR spectrum for PP11SFAD
Spectrum acquired on a Bruker AV(III)400 spectrometer, 16 scans, in MeOD

PP11SFEK: According to NMR spectroscopy (Fig.II.21), there was no free prednisolone in this fraction, only a mixture of 0.19 mol of PEGCOOH (δ 4.10, s, 0.37 H, PEG-C<u>H$_2$</u>COOH), 1.52 mol of PEG-prednisolone (δ 4.30, s, 3.04 H, PEG-C<u>H$_2$</u>-CO-Pred) and 0.21 mol of PEG-triethylammonium (δ 4.68, s, 0.42 H, PEG-C<u>H$_2$</u>-N^+-(CH_2-CH_3)$_3$).

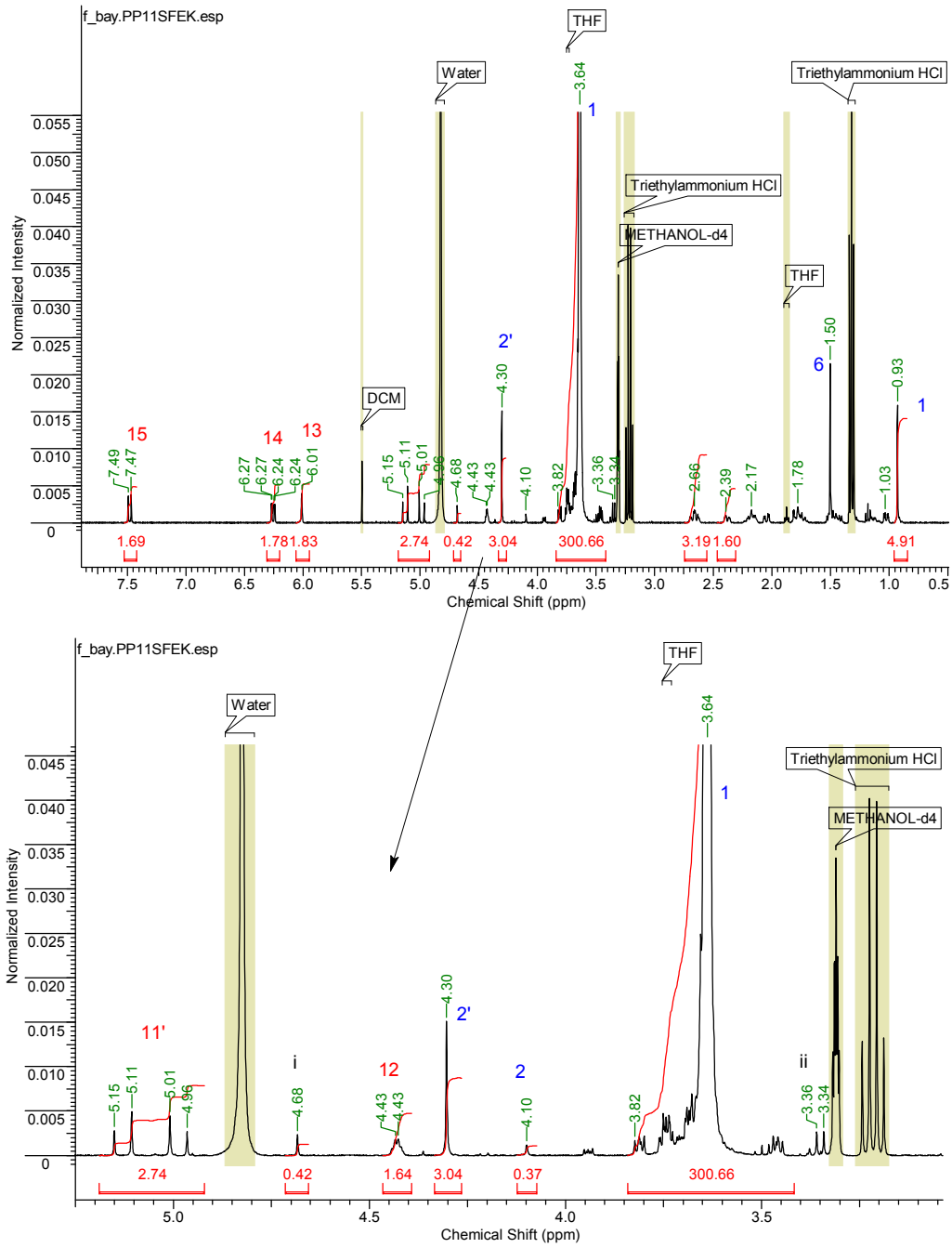

Fig.II.21. [1]HNMR spectrum for PP11SFEK
Spectrum acquired on a Bruker AV(III)400 spectrometer, 16 scans, in MeOD

This simple filtration over silica allowed separating prednisolone (eluted with ethyl acetate) from the rest of the mixture but triethylammonium chloride and PEG-triethylammonium were still contaminating the sample PP11SFEK (eluted with DCM/MeOH 90/10 v/v).

PP14: ^{1}HNMR analysis (Appendix 2, Fig.VI.9) of the crude product revealed a similar mixture as obtained for PP11, there were 1.32 mol of PEG-prednisolone (δ 4.30, s, 2.64 H, PEG-C<u>H</u>$_2$-CO-O-Pred), 0.29 mol of PEGCOOH (δ 4.00, s, 0.57 H, PEG-C<u>H</u>$_2$-COO-), 0.38 mol of PEG-triethylammonium (PEG-C<u>H</u>$_2$-N$^+$(CH$_2$-CH$_3$)$_3$), 3.24 mol of triethylammonium chloride (δ 3.21, q, 19.41 H, $^+$N-(C<u>H</u>$_2$-CH$_3$)$_3$) and 1.5 mol of free prednisolone.

PP14SF1P: ^{1}HNMR analysis revealed the fraction contained only prednisolone (Appendix 2, Fig.VI.10).

PP14SF4P contained PEG that was 100% conjugated to prednisolone (δ 4.30, s, 4H, PEGC<u>H</u>$_2$-COO-Pred) and 1.2 mol of triethylammonium chloride (δ 3.21, q, 6.9 H, N$^+$(C<u>H</u>$_2$-CH$_3$)$_3$) and (δ 1.32, t, 10.7 H, N+(CH$_2$-C<u>H</u>$_3$)$_3$). This fraction was free of unreacted prednisolone and PEG-triethylammonium (Appendix 2, Fig.VI.11).

Similarly to PP11, the filtration over silica allowed separating prednisolone in the first fractions (diethyl ether/ethyl acetate 50/50 v/v) and recovering PEG-prednisolone and triethylammonium chloride in the last fractions (eluted with THF/DCM 40/60 v/v). The less polar solvent mixture afforded a good separation of free prednisolone from the mixture. The undesired triethylammonium chloride was successfully removed by cation exchange and in *PP14SFDC*, there was no trace of the contaminants, the sample contained pure PEG$_{3400}$-prednisolone$_2$ (Appendix 2, Fig.VI.12).

PP08P2 (esterification of $mPEG_{2000}COOH$) contained 0.15 mol of mPEG-triethylammonium, 0.10 mol of unreacted mPEG and 0.80 mol of mPEG-prednisolone. The mixture was also contaminated with 1.16 mol of triethylammonium chloride (Appendix 2, Fig.VI.13). Cation exchange was effective in removing triethylammonium base contaminants from the mixture as *PP08DC2* was free of PEG-triethylammonium and contained only 0.11 mol of triethylammonium chloride (Appendix 2, Fig.VI.14). After filtration over silica, the product (*PP08DC2DF1B*) was virtually free of contaminants and consisted in 0.94 mol of mPEG-prednisolone, and 0.05 mol of unreacted mPEGCOOH. The amount of triethylammonium chloride was 0.02 mol (Appendix 2, Fig.VI.15).

PP16S1 (esterification of $PEG_{2000}COOH$) was a mixture similar to the previous experiments and contained 0.10 mol of unreacted PEG, 0.63 mol of PEG-triethylammonium, 1.22 mol of PEG-prednisolone, 1.86 mol of free prednisolone and 2.38 mol of triethylammonium chloride (Appendix 2, Fig.VI.16). The mixture washed with HCl (*PP16HCl*) contained less triethylammonium chloride (0.77 mol) and less PEG-triethylammonium, the proportion for the other species was similar to the crude product (Appendix 2, Fig.VI.17). After silica filtration, silica gel chromatography and precipitation *PP16SGAp* was pure PEG-prednisolone (Appendix 2, Fig.VI.18).

PP13S1 (esterification of $PEG_{1000}COOH$) was a mixture of 1.14 mol of PEG-prednisolone, 0.12 mol of unreacted oxidised PEG, 0.77 mol of PEG-triethylammonium. The sample also contained 1.89 mol of triethylammonium

chloride and 2.05 mol of free prednisolone (Appendix 2,Fig.VI.19). Similarly to PP08 purification, cation exchange allowed the removal of triethylammonium chloride (*PP13DC2*) and PEG triethylammonium chloride proportion was lowered to 0.11 mol (Appendix 2,Fig.VI.20). Silica filtration allowed once again the removal of free prednisolone and the recovery of purified PEG-prednisolone. The final product *PP13DC2DFB* contained 0.14 mol of unreacted PEG, 0.09 mol of PEG-triethylammonium and 1.72 mol of PEG-prednisolone (Appendix 2Fig.VI.21) and the overall yield was 25%.

The previous procedure: acyl chloride and esterification with triethylamine was optimised to get pure PEG-prednisolone. However, this chemical route and subsequent purification process was not satisfactorily efficient and afforded yields so low that it was difficult to accurately determine them. These low yields were explained by several reasons:

- The succession of purification steps: the more steps, the lower the yield. eg 3 steps at 85% gives a theoretical 61.4% yield (100×0.85^3)
- The low conjugation rates: 80% for mPEG (PP08) and 61% on average for PEG (PP14, PP16 and PP13).

Therefore there was a need to improve the chemistry of the reaction to reduce undesired conjugation between PEG and the tertiary amine base triethylamine. By doing so, the aim was to facilitate the recovery and decrease the number of purification steps but also to improve the synthetic yield and increase the proportion of conjugated PEG-prednisolone in the crude mixture. The following experiments dealt with the optimisation of a better esterification procedure, starting with the use of pyridine, a weaker amine base (pKa 5.25) than triethylamine (pKa 10.75).

PP17S2 was analysed by 2D NMR and similarly to PP11, the study of ^{1}HNMR (Fig.II.23), HMQC and HMBC revealed that PEG was conjugated to pyridine (0.35 mol), and prednisolone (1.39 mol) with a fraction unreacted (0.35 mol). Some pyridine (4.35 mol) and free prednisolone (2.40 mol) also remained. According to 2D NMR, several chemical products were present in the crude product *PP17S2* (Fig.II.22).

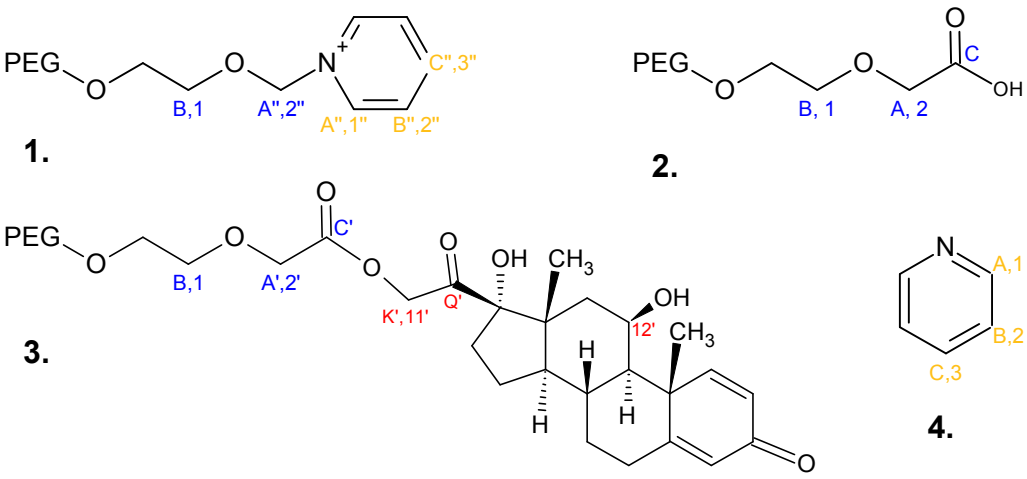

Fig.II.22. Chemical structures of PP17 mixture products
1. PEG-pyridinium, 2. unreacted oxidised PEG, 3. PEG-prednisolone, 4. pyridine

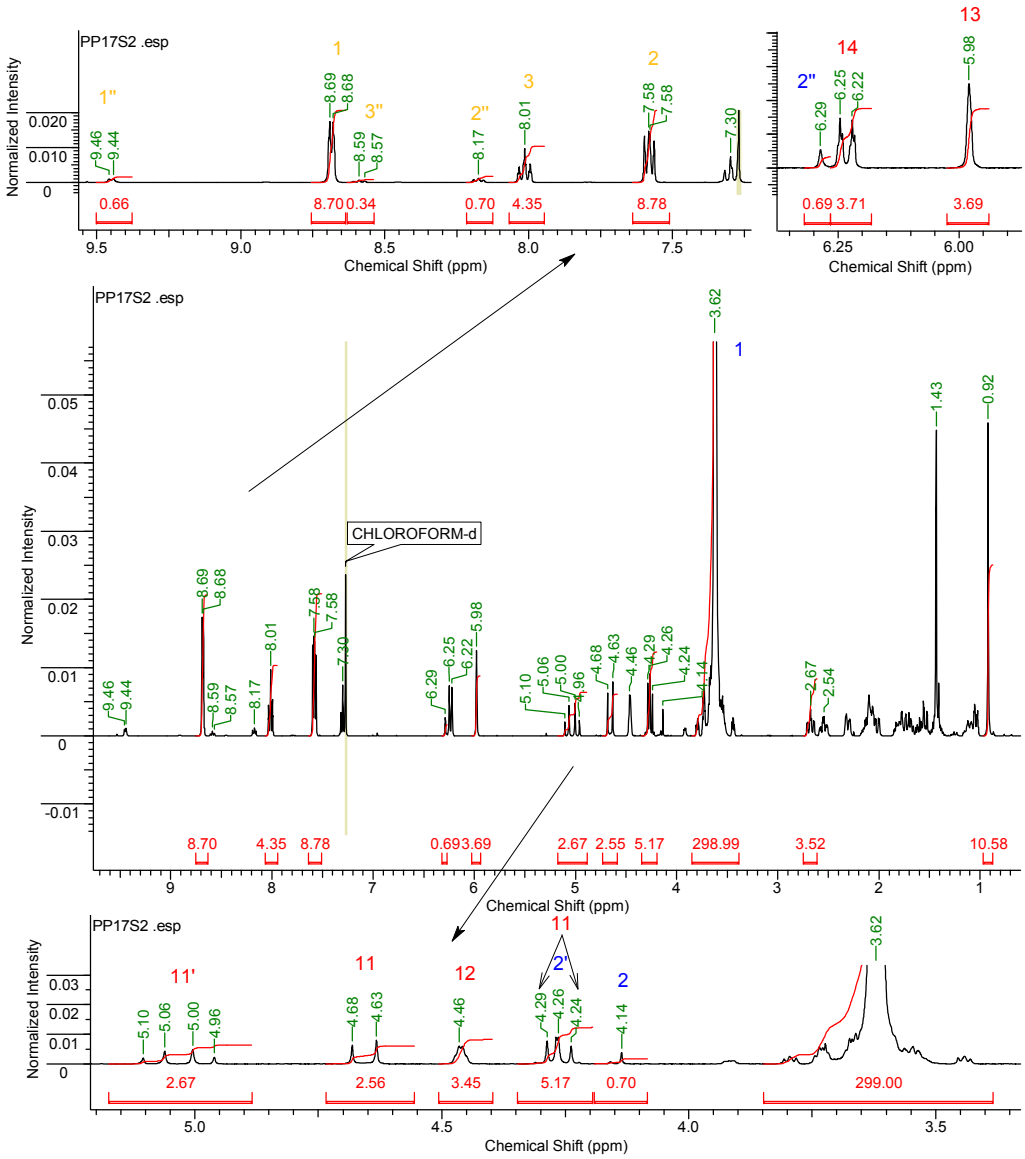

Fig.II.23. ^{1}HNMR of PP17S2
Spectrum acquired on a Bruker AV(III)400 spectrometer, 16 scans, in $CDCl_3$

The study of both HMQC and HMBC spectra afforded the determination of the relevant proton and carbon signals (Table. II.10). The correlation 11'/C' (HMBC) confirmed the conjugation between PEG and prednisolone and the correlation 2'/ A'' illustrated the conjugation between PEG and pyridine.

Table. II.10. Proton and carbon signals of PP17S2 crude product

Proton position	Chemical shift (ppm)	Carbon position	Chemical shift (ppm)
1	8.69	A	146.2 *
2	7.58	B	125.3 *
3	8.01	C	140.0 *
1''	9.45	A''	143.6 *
2''	8.17	B''	127.9 *
3''	8.58	C''	146.2 *
1	3.62	B	70.5 *
2	4.14	A	68.6 *
		C	171.9 **
2'	4.26	A'	68.2 *
		C'	170.1 **
2''	6.29	A''	88.5 *
11	4.26/4.65	K	67.7 *
		Q	212.4 **
11'	5.03	K'	68.6 *
		Q'	204.8 **

** Determined using HMQC correlation with corresponding proton signal, ** determined using HMBC correlation*

In conclusion, there was no difference between the two types of amine bases used. The cross-reaction between PEG and the amine base took place with both triethylamine and pyridine.

PP20/21: Despite the relative low proportion of pyridine used (2.1/COOH), both crude products had the same relative amount of undesired PEG-pyridinium (0.68-0.69 mol) (Appendix 2, Fig.VI.22 and Fig.VI.23). The proportion of PEG-prednisolone in *PP20S2* (1.08 mol) and in *PP21S2* (0.91 mol) were similar. In conclusion, the type of addition did not change the

relative amount of PEG-pyridinium in the crude product neither did it change the proportion of the desired ester.

PP22/PP23: The two reactions ended up with a similar mixture of PEG-prednisolone (1.08, 1.04 mol resp.), unreacted PEG (0.17, 0.18 mol resp.) and PEG-pyridinium (0.76, 0.80 mol resp.). Here the relative amount of prednisolone did not influence the final conjugation efficiency and the proportion of PEG-pyridinium was still high (Appendix 2, Fig.VI.24, Fig.VI.25).

PP25/PP26: When decreasing the relative amount of thionyl chloride used to produce PEG acyl chloride, there was no decarboxylation of PEGCOOH taking place and the crude products were free of PEG-pyridinium. In *PP25S2*, produced with one prednisolone per acyl chloride, there were 1.28 mol of PEG-prednisolone (and 0.75 mol of unreacted PEG) (Appendix 2, Fig.VI.26). In *PP26S1*, produced with two molecules of prednisolone per acyl chloride, there were 1.38 mol of PEG-prednisolone (and 0.63 mol of unreacted PEG) (Appendix 2, Fig.VI.27). The lower excess of thionyl chloride used in these reactions had the beneficial effect to avoid decarboxylation of oxidised PEG but it also increased the relative amount of unreacted PEG.

Table. II.11 summarises the compositions of the crude and purified products obtained after esterification of oxidised PEG of various molecular weights and prednisolone using thionyl chloride. Table. II.12 illustrates the compositions of the crude mixtures obtained after esterification of oxidised PEG 3400 and prednisolone using acyl chloride at different ratios.

Table. II.11. PEG-prednisolone crude mixture and purified product compositions according to NMR for various PEG molecular weights

Signal / Product	PEG type	Unreacted PEGCOOH / PEGCOO$^-$	PEG-TEA	PEG-prednisolone	TEA HCl	Free prednisolone	∫CH_2 (PEG unit)
		#2 (4.14 ppm) (4.00 ppm)	#i (4.68 ppm)	#2' (4.30 ppm)	(1.32 ppm)	#13 (6.00 ppm)	#1 (3.63 ppm)
PP11SB1		0.32	0.30	1.39	2.77	1.41	299+11.49(THF)
PP11SFEK		0.19	0.21	1.52	283	0	299+1.66(THF)
PP14S1	PEG_{3400}	0.29	0.38	1.32	3.71	1.48	299+16(THF)
PP14SF4P		0	0	1.99	1.19	0	299
PP14SFDC		0	0	2.0	0.11	0	299
PP08P2		0.10	0.15	0.80	1.16	0.67	178
PP08DC2	$mPEG_{2000}$	0.06	0	0.87	0.11	0.45	178
PP08DC2DF1B		0.05	0	0.94	0.02	0	178
PP16S1		0.10	0.63	1.22	2.38	1.86	172
PP16HCl	PEG_{2000}	0.17	0.49	1.27	0.77	1.73	172+4.60(THF)
PP16SGAp		0	0	2.17	0	0	172
PP13S1		0.12	0.77	1.14	1.89	2.05	81+18.28(THF)
PP13DC2	PEG_{1000}	0.15	0.11	1.64	0	3.42	81+1.57(THF)
PP13DC2DFB		0.14	0.09	1.72	0	0	81+1.47(THF)

The number of moles of each species is calculated relative to one mole of PEG. One mole of PEG is used as reference using the appropriate number of protons for PEG signal in position 1. (e.g. 299H for PEG_{3400}, 172H for PEG_{2000}, 178H for $mPEG_{2000}$ or 81H for PEG_{1000}). ^{1}HNMR spectra recorded in MeOD or $CDCl_3$

Table. II.12. PEG-prednisolone crude mixture composition according to NMR for PEG_{3400}

Signal / Product	PEG type	Unreacted PEGCOOH	PEG-pyridine	PEG-prednisolone	Pyridine	Free prednisolone	∫CH_2 (PEG unit)
		#2 (4.14 ppm)	#2'' (6.05 ppm) (6.29 ppm)	#2' (4.26 ppm)	aromatic	#13 (5.98 ppm)	#1 (3.62 ppm)
PP17S2		0.35	0.35	2.40	4.35	1.39	299
PP20S1		0.29	0.69	2.40	18.5	1.08	299+10.54(THF)
PP21S2		0.43	0.68	2.08	13.8	0.91	299+8.58(THF)
PP22S2	PEG_{3400}	0.17	0.76	3.01	4.34	1.08	299
PP23S2		0.18	0.80	1.01	2.6	1.04	299
PP25S1		0.75	0	1.58	5.56	1.28	299
PP26S1		0.63	0	2.49	5.93	1.38	299

The number of moles of each species is calculated relative to one mole of PEG. One mole of PEG is used as reference using 299 protons for PEG_{3400} unit signal in position 1. ^{1}HNMR spectra recorded in MeOD or $CDCl_3$

Discussion

For the previous reactions, the relative amount of thionyl chloride used to generate PEG acyl chloride was 10, 30 or 70 times excess (relative to carboxylic acid). The resulting amount of PEG-amine produced as a result was respectively 0, 0.30 and 0.75 mol per mol of PEG. There was therefore a linear relationship (Fig.II.24) between the amount of acyl chloride and the resulting decarboxylation of oxidised PEG and the ensuing production of PEG-amine (Fig.II.24).

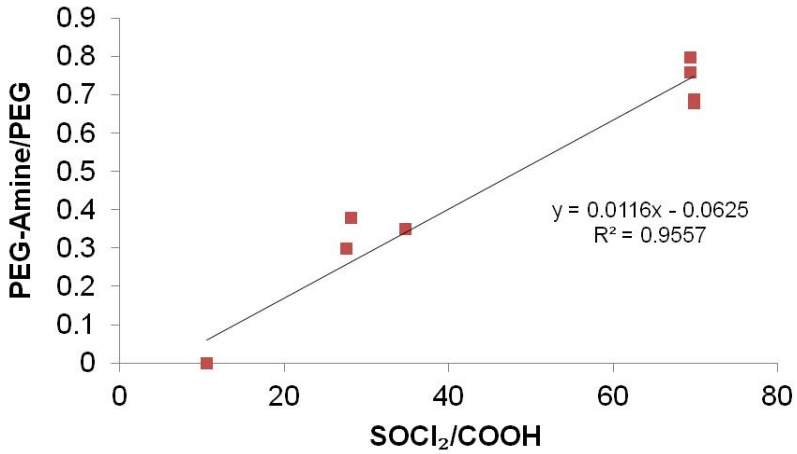

Fig.II.24. Relationship between acyl chloride excess and relative amount of PEG_{3400}-amine

In this system, the balance between the production of sufficient acyl chloride to get maximum conjugation and excessive acyl chloride leading to PEGCOOH decarboxylation could not result in complete PEG conjugation to prednisolone while avoiding PEG decarboxylation.

Despite the 69% conversion in PP26, and the possibility of purifying the products to a satisfactory grade (PP14, PP08, PP16 and PP13), these results called for a better, more efficient route to produce PEG-prednisolone ester conjugates. The use of coupling reagent 2-chloro-1-methyl pyridinium iodide (Mukaiyama reagent) was investigated to overcome these difficulties as discussed in the following section.

II.3.2.3. Mukaiyama reagent

The use of Mukaiyama reagent was investigated using DCM, THF, and then a mixture of the two solvents, and varying ratios of prednisolone and tertiary amine base. PP04 was produced by reacting oxidised PEG_{2000} and prednisolone with Mukaiyama reagent and triethylamine, in DCM at 40°C. After 250 min, a first sample (PP04S1) was withdrawn and analysed by 2D NMR. The full assignments of the corresponding spectra are detailed below and the same methodology was used to deduce the reaction completion for the following reactions (PP01, PP24, PP27).

a. Experimental optimisations

PP04: For one mole of $mPEG_{2000}$, the crude product PP04S1 contained 0.67 mol of ester of PEG-prednisolone, unreacted oxidised PEG (0.35 mol), and 1.23 mol of reacted Mukaiyama reagent (1-methylpyridin-2(1*H*)-one). There was also some unreacted prednisolone (0.43 mol) and triethylammonium HCl (2.73 mol) (Fig.II.25). According to NMR spectra (Fig.II.26, Fig.II.27, Fig.II.28), the following chemical entities were present in the crude product PP04S1 (Fig.II.25).

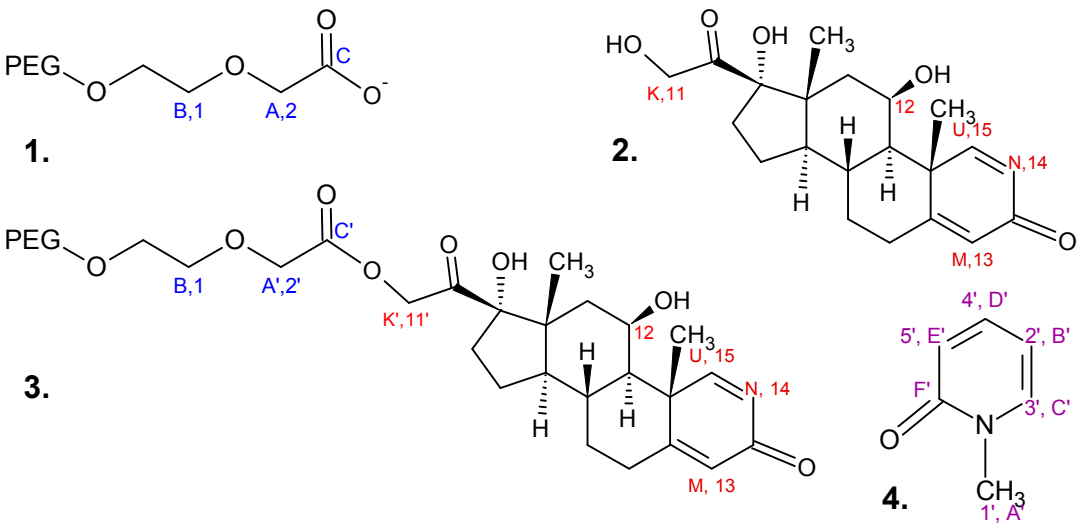

Fig.II.25. Chemical structures of PP04 mixture products
1. Oxidised PEG. 2. Unreacted prednisolone, 3. PEG-prednisolone, 4. Reacted Mukaiyama reagent.

Proton and carbon chemical shifts of the crude mixture are presented in 0.

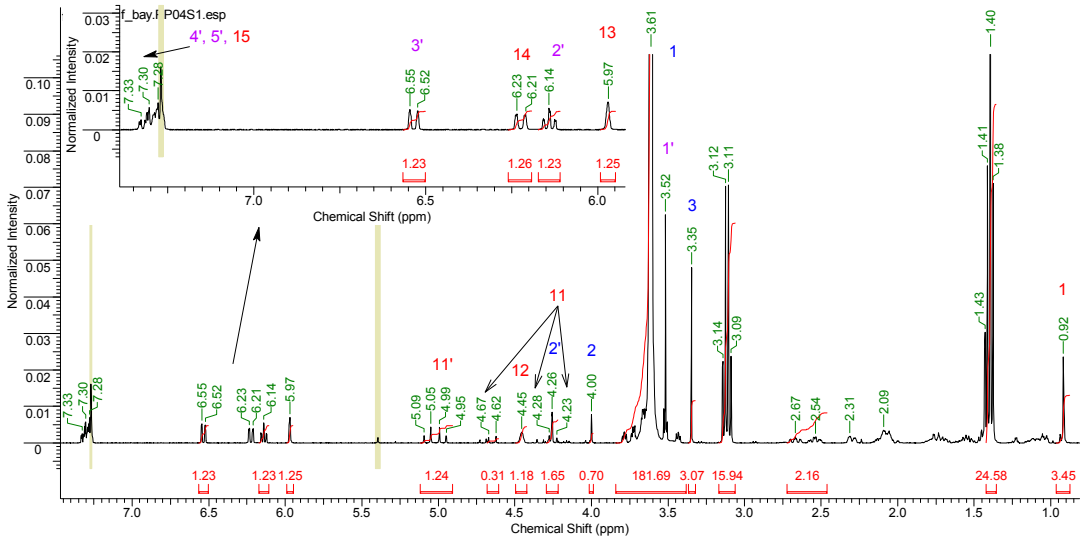

Fig.II.26. ^{1}HNMR spectrum of PP04S1
Spectrum acquired on a Bruker AV(III)400 spectrometer, 16 scans, in $CDCl_3$

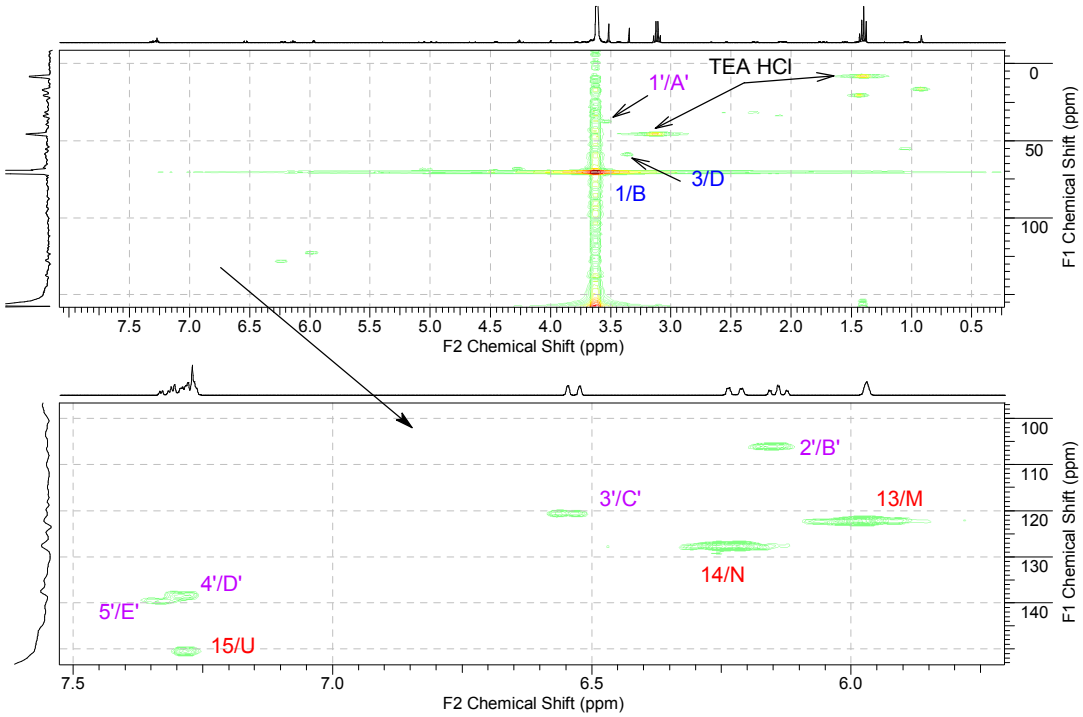

Fig.II.27. HMQC of PP04S1
Spectra acquired on a Bruker AV(III)400 spectrometer in $CDCl_3$

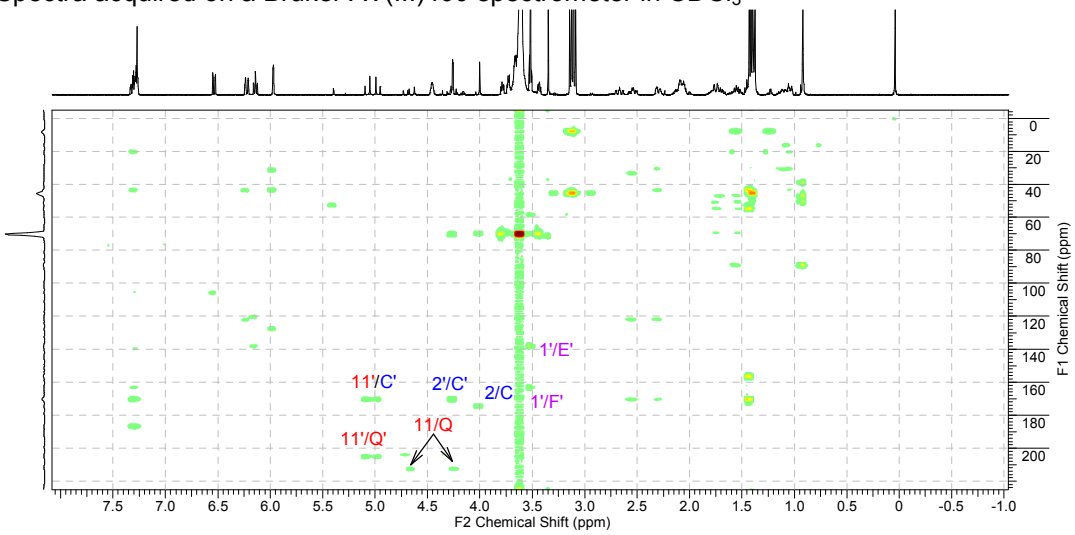

Fig.II.28. HMBC of PP04S1
Spectra acquired on a Bruker AV(III)400 spectrometer in $CDCl_3$

Table. II.13. Proton and carbon signals of PP04S1 crude products

Proton position	Chemical shift (ppm)	Carbon position	Chemical shift (ppm)
1'	3.52	A'	37.6 *
		F'	138.1 **
2'	6.14	B'	106.1 *
3'	6.53	C'	120.8 *
4'	7.33	D'	139.7 *
5'	7.30	E'	138.4 *
		F'	162.9 **
1	3.61	B	70.3 *
2	4.00	A	68.9 *
		C	174.6 **
3	3.35	D	58.6 *
2'	4.26	A'	68.2 *
		C'	170.1 **
11	4.65 / 4.25	K	67.2 *
13	5.97	M	122.4 *
14	6.22	N	127.6 *
15	7.28	U	150.4 *
11'	5.02	K'	68.2 *

** Determined using HMQC correlation with corresponding proton signal, ** determined using HMBC correlation*

After 250 min of reaction, 67% of the starting carboxyl groups were conjugated to prednisolone, and the coupling reagent was entirely consumed.

PP01: When conducted in THF, using oxidised PEG_{3400}, the reaction yielded comparable results: Mukaiyama reagent was entirely consumed, and the conjugation efficiency was 63.5% after 2440 min (Appendix 3, Fig.VI.28).

PP24: After 60 min (PP24S1), according to ^{1}HNMR of the crude product (Appendix 3, Fig.VI.29), 50% of the carboxyl groups were conjugated to

prednisolone. The reaction was not finished since 0.45 mol of unreacted Mukaiyama reagent was detected, (e.g. signal at 8.31 ppm). The reaction was complete (no trace of coupling reagent) after 1250 min (PP24S2) and resulted (Appendix 3, Fig.VI.30) in the conjugation of 1.67 of an original 2 mol of carboxyl groups conjugated to prednisolone (83.5%). The increasing amount of prednisolone, Mukaiyama reagent and triethylamine significantly improved the synthetic yield. Since the Mukaiyama reagent was entirely consumed at the end of the reaction and the conjugation was not complete, one could assume that the coupling reagent was limiting the reaction completion. The starting relative amount of Mukaiyama reagent was therefore doubled in the following experiment.

PP27: The first sample was withdrawn after 1000 min (PP27S1) and the synthetic yield was 91.5% (Appendix 3, Fig.VI.31). After 2460 min, the reaction was complete and every PEG carboxyl group was conjugated to prednisolone (Appendix 3, Fig.VI.32). A small amount of unreacted Mukaiyama reagent was left (0.8 mol) while 3.76 mol of Mukaiyama reagent had reacted. Triethylammonium chloride (11.28 mol) and unreacted prednisolone (0.92 mol) were also present in the crude product. After silica gel chromatography, the fraction recovered in THF (PP27FB) contained 0.72 mol of reacted Mukaiyama reagent and 1.19 mol of butylated hydroxytoluene (BHT) from evaporated THF as contaminant (Appendix 3, Fig.VI.33). When recrystallised from isopropanol, the product PP27C1 was a pure ester conjugate of PEG_{3400}-$Pred_2$ (Fig.II.29).

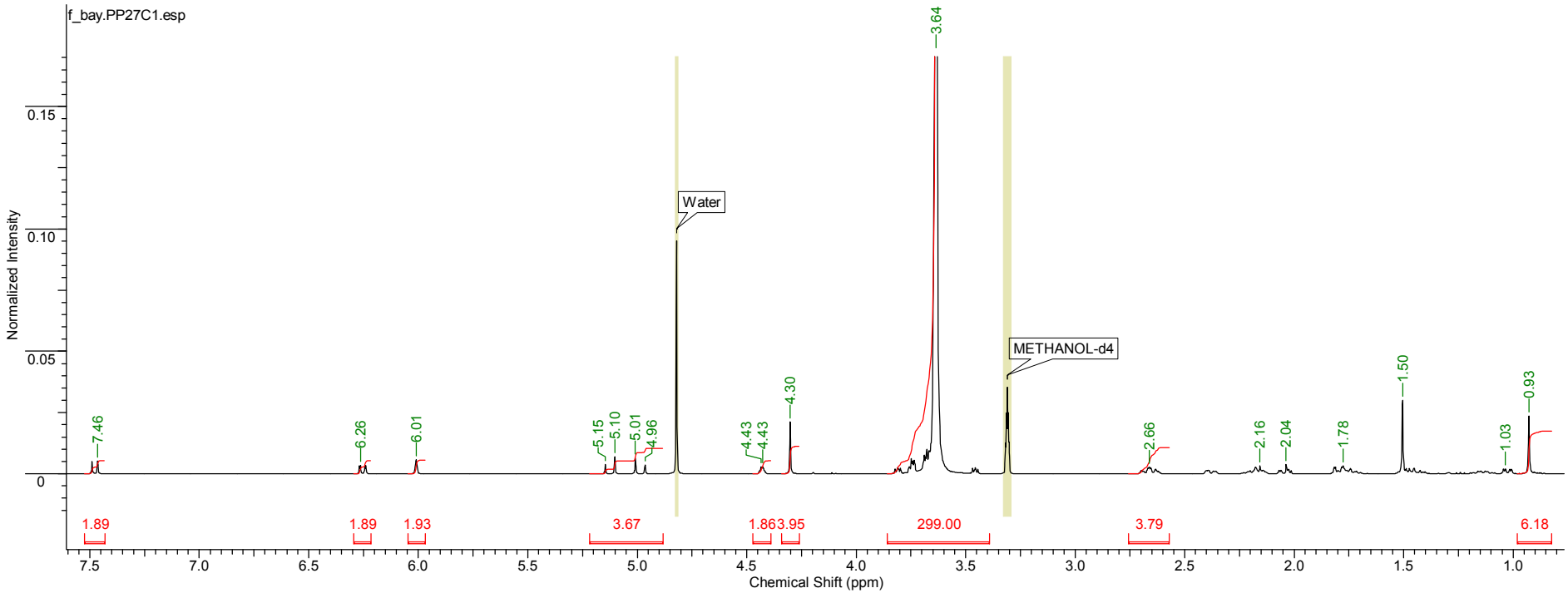

Fig.II.29. ^{1}HNMR for PP27C1
Spectrum acquired on a Bruker AV(III)400 spectrometer, 16 scans, in MeOD

b. Production and purification of $mPEG_{2000}$-prednisolone using optimised conditions

PP28: Oxidised $mPEG_{2000}$ was successfully conjugated to prednisolone after 4110 min of reaction. The crude product PP28S1 (Appendix 3, Fig.VI.34) was contaminated by reacted and unreacted Mukaiyama reagent (1.47 and 0.23 mol respectively), triethylammonium chloride (2.63 mol) and unreacted prednisolone (0.22 mol). After crystallisation from propan-2-ol, and successive washes in diethyl ether, ethanol, and diethyl ether, the product PP28C1 was obtained free of contamination (Fig.II.30). In the purified product, 0.99 mol of prednisolone was conjugated (per mol of $mPEG_{2000}$).

The product purity was confirmed by elemental analysis since the measured relative weight amounts of carbon, nitrogen and hydrogen agreed with calculated values (Table. II.14).

FTIR confirmed the presence of prednisolone with the characteristic prednisolone peaks (1659 cm^{-1}, 1614 cm^{-1}, 1419 cm^{-1}), but also the ester link with the carbonyl shifting from 1747 cm^{-1} in the oxidised PEG to 1761 cm^{-1} in the ester (Fig.II.31). The carbonyl stretch of prednisolone at 1707 cm^{-1} was shifted to 1726 cm^{-1} after conjugation, which conformed to the spectrum of prednisolone acetate [116].

Mass spectrometry analysis was performed and a mass difference of 342 Da (between oxidised $mPEG_{2000}$ and PP28C1) was measured, confirming the product molecular formula (Fig.II.32). Briefly, the mass spectrum for $mPEG_{2000}COOH$ showed several overlapping mass distribution patterns. The maximum intensity was obtained for 635.5 atomic mass units (amu), the surrounding peaks were separated by 14.7 amu on average. Since PEG monomer weights 44 Da, the maximum peak

at 635.5 amu corresponded to mPEGCOOH triply charged ($\frac{44}{14.7} = 3$). Under the same ionisation conditions, the triply charged signal of PP28C1 was measured at 749.7 mass units. The mass difference of the triply charged species was therefore 114.2 amu (749.7-635.5). Assuming the two compounds did ionise in the same way and produced the same ionic complexes, the mass difference between $mPEG_{2000}COOH$ and PP28C1 was 342.6 Da (3×114.2) compared to the theoretical mass difference being 342.4 Da (addition of prednisolone at 360.4 Da and loss of water at 18 Da). The synthetic yield was 58% (II.4.2.2).

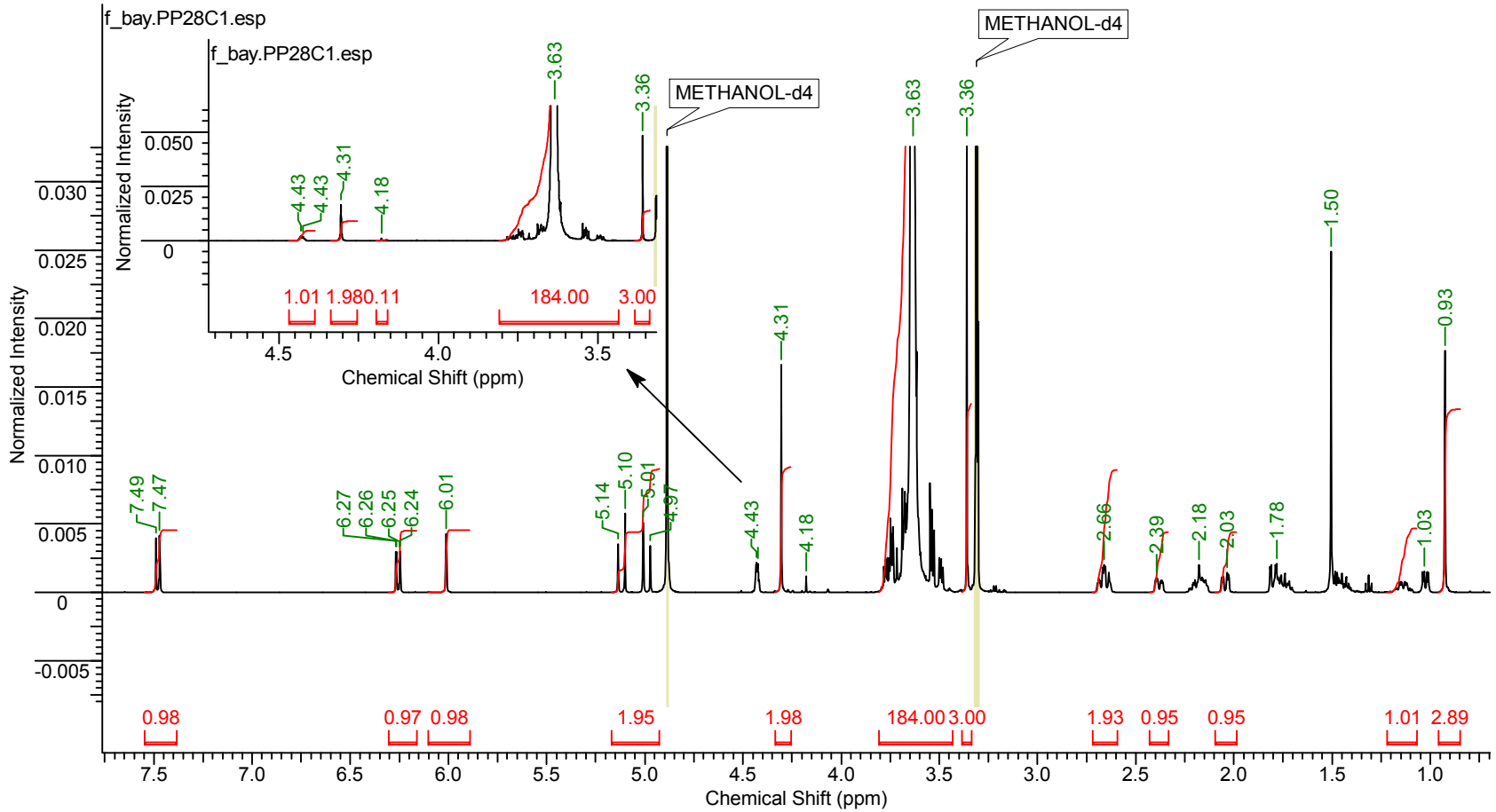

Fig.II.30. [1]HNMR of purified PP28C1
Spectrum acquired on a Bruker AV(III)500, 16 scans, in MeOD

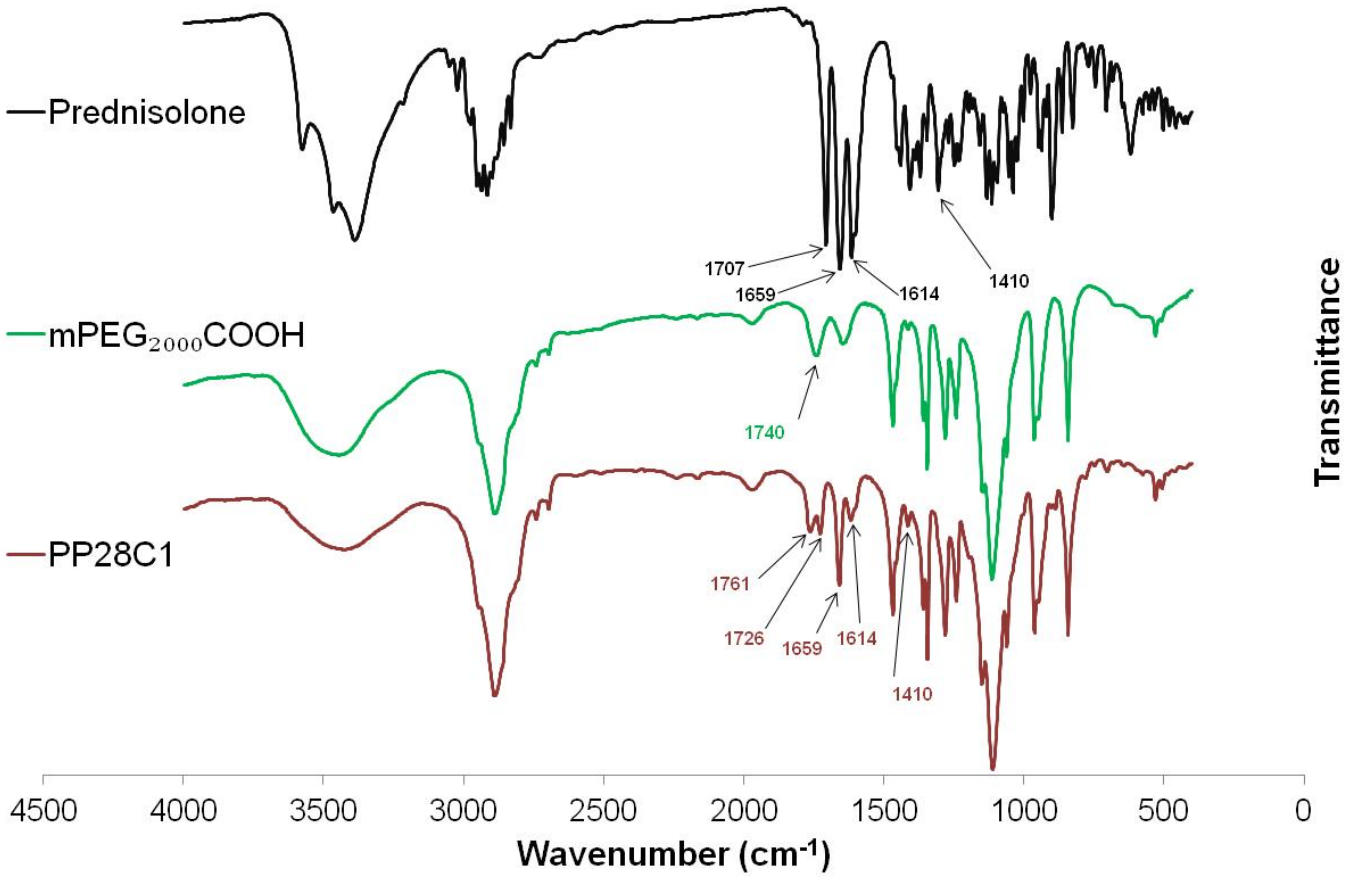

Fig.II.31. FTIR spectra of prednisolone, oxidised $mPEG_{2000}$, PP28C1
— Prednisolone, — $mPEG_{2000}COOH$, — PP28C1 ($mPEG_{2000}$-prednisolone)

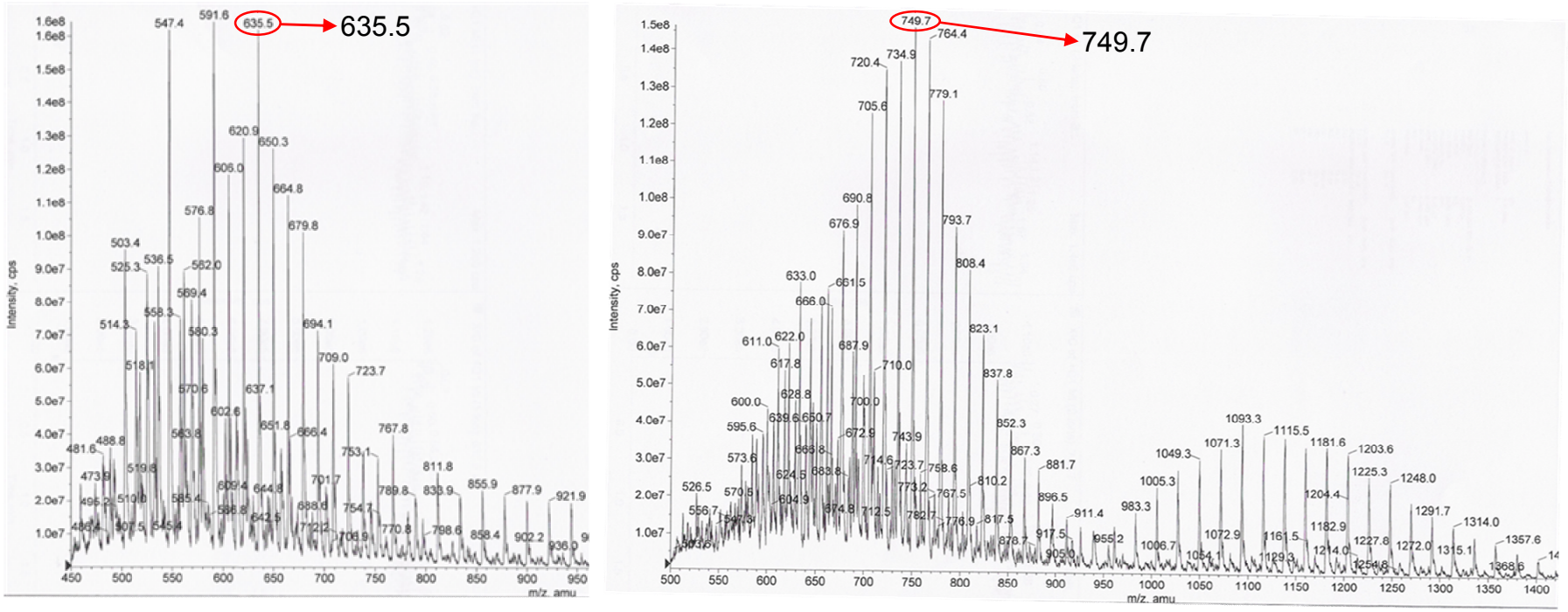

Fig.II.32. Mass spectra of $mPEG_{2000}COOH$ (left) and mPEG-prednisolone (right)

The maximum signal for triply charged mPEGCOOH was at 635.5 atomic mass units. Under the same ionisation conditions, the maximum triply charged signal for mPEG-prednisolone was 749.7 amu. The mass difference of the triply charged species was therefore 114.2 amu (749.7-635.5). Assuming the two compounds did ionise in the same way and produced the same ionic complexes, the mass difference between $mEG_{2000}COOH$ and mPEG-prednisolone was 342.6 Da (3×114.2) compared to the theoretical mass difference being 342.4 Da (addition of prednisolone at 360.4 Da and loss of water at 18 Da).

c. Production and purification of PEG-prednisolone esters of other molecular weights

Conjugates of oxidised PEG_{1000}, PEG_{2000} and PEG_{3400} were obtained and characterised in exactly the same manner as described above for the $mPEG_{2000}$ (PP28). FTIR spectra for all PEG-prednisolone ester conjugates are displayed in Fig.II.33. Table. II.14 sums up NMR, mass spectrometry results, elemental analyses and synthetic yields for PEG-prednisolone ester conjugates. Proton NMR of the purified products and detailed calculation of mass spectrometry analyses are available in Appendix 3, Fig.VI.35 to Fig.VI.40.

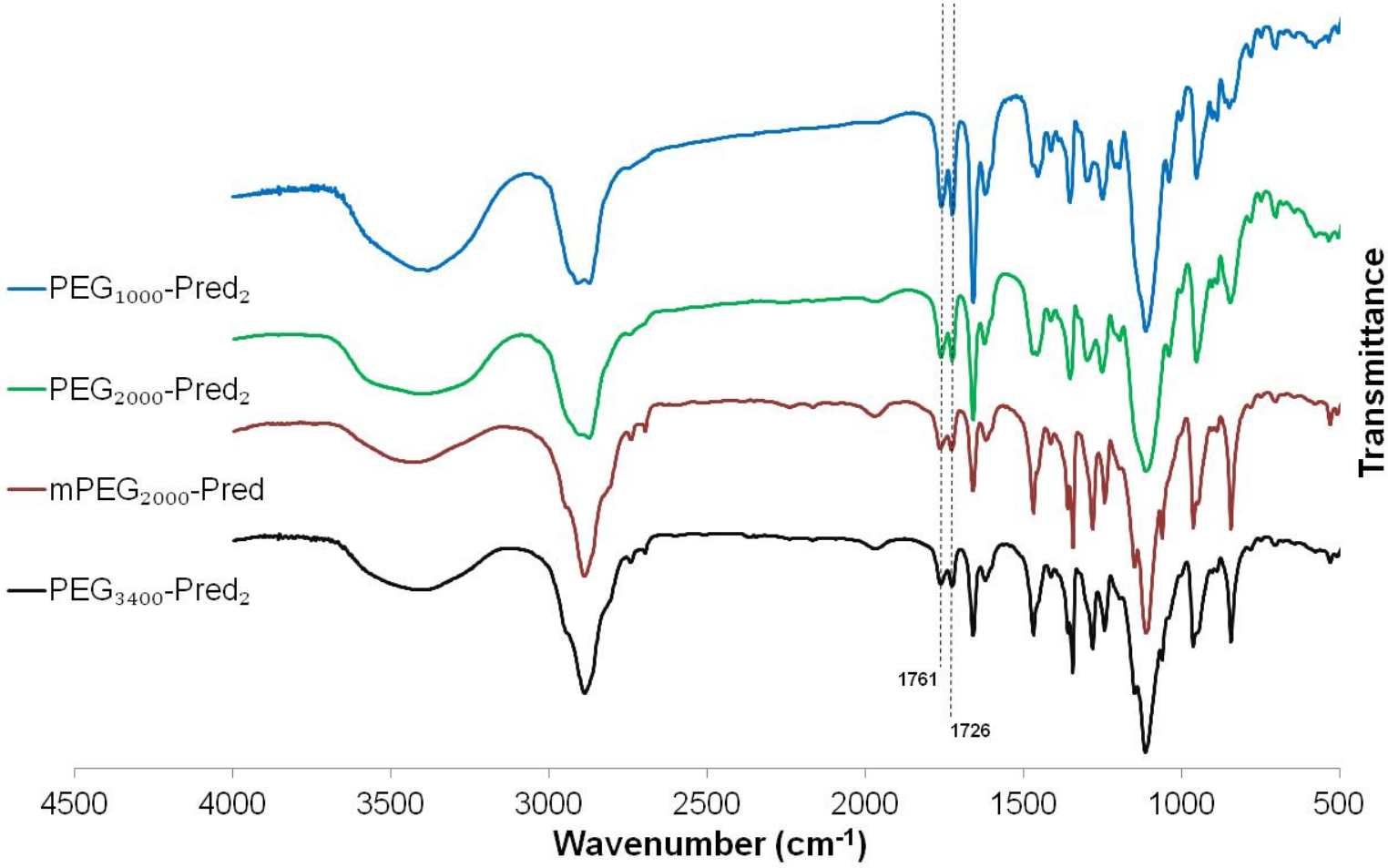

Fig.II.33. FTIR spectra of PEG-prednisolone conjugates
PEG_{1000}-$Pred_2$, PEG_{2000}-$Pred_2$, $mPEG_{2000}$-Pred, PEG_{3400}-$Pred_2$

Table. II.14. PEG-prednisolone ester conjugate analyses

Product	Type	Formula	Average MW Da	NMR mol of Pred / mol of PEG	Elemental analysis Measured %	Elemental analysis Theoretical %	Mass spectrometry Measured Δ_{mass} Da	Mass spectrometry Theoretical Δ_{mass} Da	Synthetic yield (II.4.2.2) %
PP33w3	PEG_{1000}-$Pred_2$	$C_{86}H_{138}O_{33}$	1700	1.91 (Fig.VI.35)	% C: 58.3 % H: 8.1 % N: -0.3	% C: 57.0 % H: 8.7 % N: 0	684.2 (Fig.VI.36)	684.9	69
PP32D	PEG_{2000}-$Pred_2$	$C_{136}H_{238}O_{58}$	2801	2.07 (Fig.VI.37)	% C: 57.1 % H: 8.0 % N: 0	% C: 58.3 % H: 8.5 % N: 0	685.5 (Fig.VI.38)	684.9	60
PP28C1	$mPEG_{2000}$-Pred	$C_{116}H_{216}O_{53}$	2459	0.99 (Fig.II.30)	% C: 56.3 % H: 8.8 % N: -0.1	% C: 56.5 % H: 8.8 % N: 0	342.6 (Fig.II.32)	342.4	58
PP31P2	PEG_{3400}-$Pred_2$	$C_{194}H_{354}O_{87}$	4079	1.94 (Fig.VI.39)	% C: 55.9 % H: 8.1 % N: 0.2	% C: 57.0 % H: 8.7 % N: 0	685.3 (Fig.VI.40)	684.9	75

Summary

Esters of oxidised PEG and prednisolone of different molecular weights were produced using a coupling reagent. They were then purified and characterised by 2D NMR, FTIR, elemental analysis and mass spectrometry. The synthetic yields varied upon the molecular weight and the subsequent purification procedure. PEG_{1000}-$Pred_2$ was an oily brown product, recovered in good yield (η=69%) by silica gel chromatography whereas PEG_{3400}-$Pred_2$ was an off white powder recrystallised from isopropanol, in good yield (η=75%). The two conjugates of 2000 Da possessed intermediate physical properties. $mPEG_{2000}$-Pred was a light-brown powder, recovered from crystallisation in isopropanol (η=58%) and PEG_{2000}-$Pred_2$ was a waxy paste, recovered by silica gel chromatography (η=60%). This method was an improvement compared to the acyl chloride route since the conversion rates were higher, there was no side reaction and the purifications required less steps, affording much better synthetic yields of the purified ester of PEG and prednisolone.

II.3.3. PEG-salbutamol

II.3.3.1. Modification of salbutamol

Salbutamol free base: the resulting powder was obtained in good yields (86%) and was confirmed (by NMR) to be a free base form of salbutamol. The solubility properties of salbutamol free base in organic solvents were improved compared to salbutamol sulphate since salbutamol free base was soluble in THF and dioxane whereas salbutamol sulfate was soluble in more polar solvents such as water, DMSO, alcohols. The precipitate recovered by filtration of the THF solution was confirmed to be sodium sulphate (Fig.II.35), extracted from salbutamol sulphate solution by sodium hydroxide, to give the free base form of salbutamol. Analysis of 2D NMR of salbutamol sulfate and salbutamol free base was conducted and the results are displayed in Table. II.15. Fig.II.34 illustrates the position numbering of salbutamol and dodecyl sulfonic acid.

Salbutamol dodecyl sulfate: the resulting powder was obtained in good yields (88%) and was confirmed to be salbutamol dodecyl sulfate (Fig.II.35). Solubility in organic solvents was maintained and the amine group was protonated since the signals in positions 8 and 9 were closer to those of salbutamol sulfate. The ratio dodecyl sulfonic acid/salbutamol was 1/1 (Table. II.15).

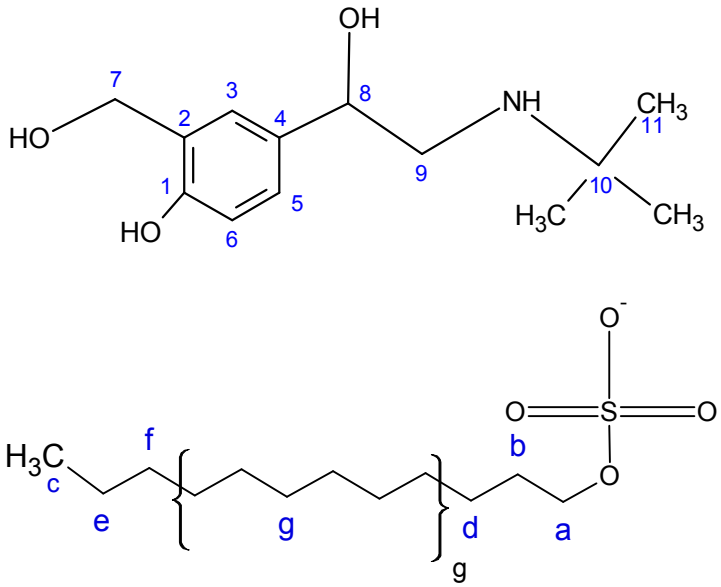

Fig.II.34. Position numbering of salbutamol and dodecyl sulfonic acid

The full assignments of 2D NMR spectra are available in Appendix 4, Fig.VI.41, Fig.VI.42, and Fig.VI.43 for respectively salbutamol sulfate, salbutamol free base and salbutamol dodecyl sulfate.

Table. II.15. NMR analysis of the different forms of salbutamol

Salbutamol sulfate					Salbutamol free base				Salbutamol dodecyl sulfate				
#	Type	H shift (ppm)	$\int H$	C shift (ppm)	Type	H shift (ppm)	$\int H$	C shift (ppm)	Type	H shift (ppm)	$\int H$	C shift (ppm)	#
11	s	1.19	9	26.48	s	1.01	9	29.10	s	1.29	9	25.18	11
10		NA		53.97		NA		49.48		NA		56.67	10
9	m	2.75	2	49.34	m	2.53	2	51.11	m	2.89	2	48.33	9
8	dd	4.68	1	70.19	dd	4.38	1	72.80	dd	4.75	1	69.54	8
7	s	4.47	2	58.45	s	4.47	2	59.10	d	4.50	2	58.45	7
6	d	6.73	1	114.55	d	6.66	1	114.55	d	6.77	1	114.88	6
5	dd	7.06	1	125.33	dd	6.96	1	125.32	dd	7.10	1	125.64	5
4		NA		133.19		NA		134.10		NA		132.28	4
3	s	7.31	1	125.65	d	7.22	1	125.33	d	7.36	1	125.65	3
2		NA		128.69		NA		128.24		NA		128.69	2
1				153.91				154.34				154.34	1
									t	3.67	2	65.95	a
									m	1.47	2	29.41	b
									t	0.87	3	14.09	c
												25.50	d
									s	1.24	18	22.53	e
												31.37	f
												29.15	g

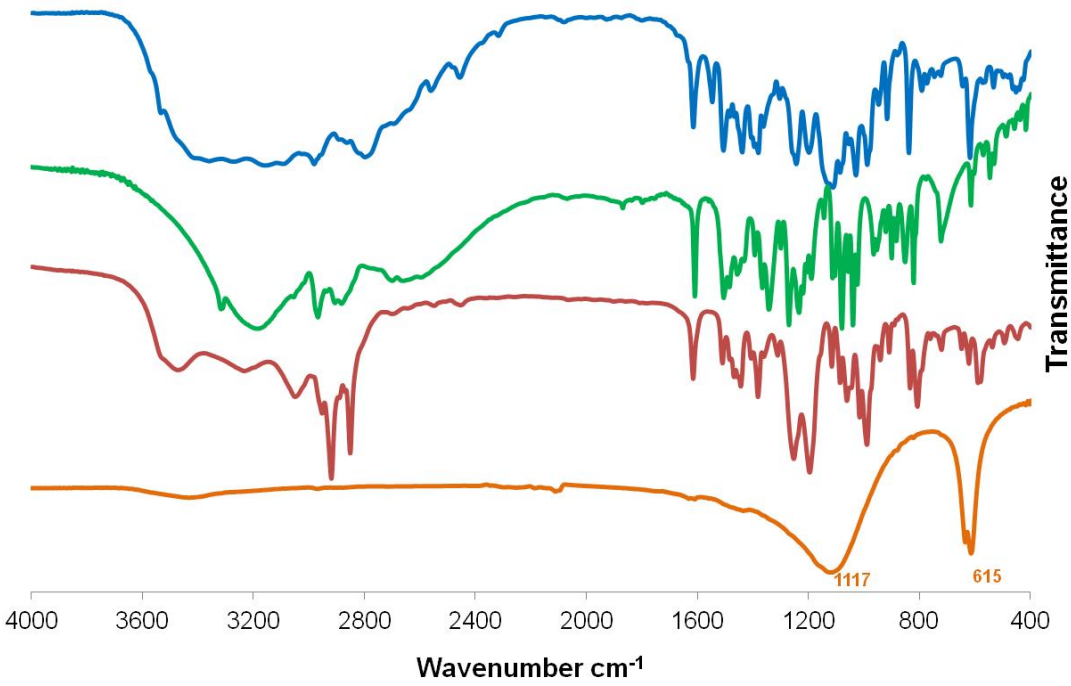

Fig.II.35. FTIR spectra of salbutamol sulfate, salbutamol free base, salbutamol dodecyl sulfate and sodium sulfate
— salbutamol sulfate, — salbutamol free base, — salbutamol dodecyl sulfate, — sodium sulfate

II.3.3.2. PEG-salbutamol esters

a. Esterification

The conjugation of oxidised PEG and salbutamol was the most efficient through the acyl chloride route and the use of salbutamol dodecyl sulfate. A relatively short reaction time was necessary since the product seemed to degrade if the reaction was prolonged for too long.

The choice of the tertiary amine base was therefore of primary importance since it needs to scavenge the hydrochloric acid formed upon conjugation and push the reaction toward completion (Scheme.II.8). Therefore, the higher the pKa of the base, the better. However, it was necessary that the tertiary amine base had a pKa lower that the pKa of the salbutamol amine group (pKa_2 = 10.37), in order to keep it protonated. Triethylamine has a pKa (10.72) [117] which is higher than salbutamol and therefore deprotonated the amine group of the drug. Pyridine and

2,6 lutidine have lower pKa values (5.17 and 6.71 respectively) [117] and some conjugation was obtained with both amine bases. The reaction kinetic seemed to be faster with 2,6 lutidine, probably because of its higher pKa. A compromise was found in 2,6 lutidine, a tertiary amine base with a pKa high enough to quickly precipitate HCl and low enough to leave salbutamol protonated.

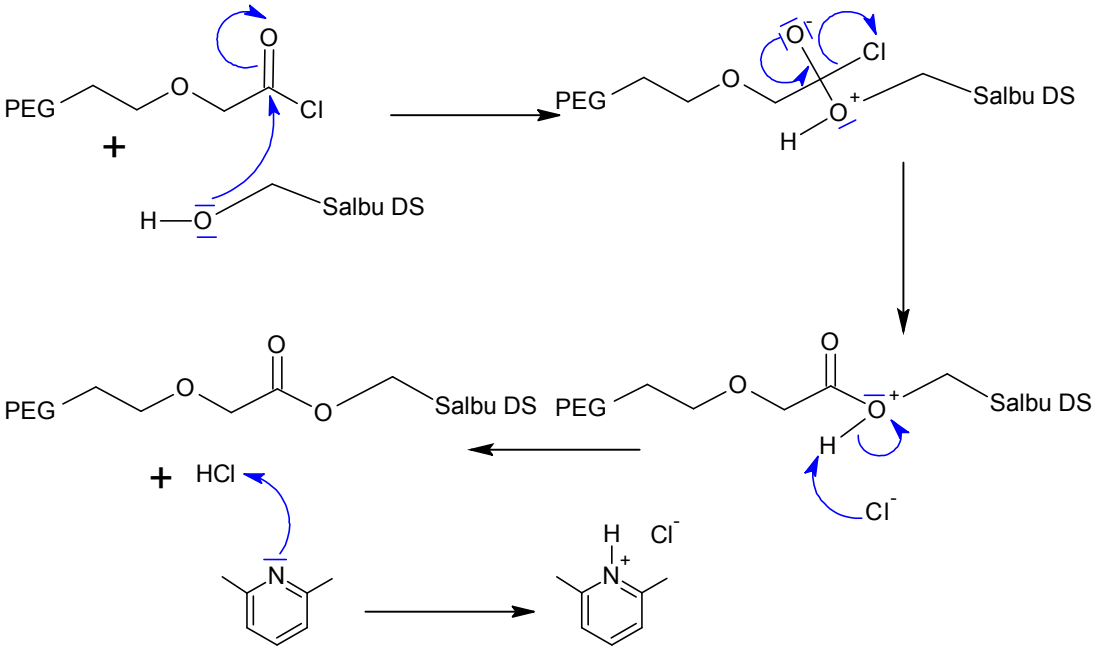

Scheme.II.8. Mechanism of PEG-salbutamol esterification via acyl chloride

b. Purification

The following paragraph illustrates the strategy employed to purify PS62 (PEG_{2000}–salbutamol ester). The same methodology was used to purify the two other conjugates (PEG_{3400}-salbutamol and $mPEG_{2000}$-salbutamol).

The crude product PS62S2 contained 2,6 lutidine, free salbutamol, and dodecyl sulfonate as contaminant (Appendix 4, Fig.VI.44). The first purification step consisted of anion exchange to replace the dodecyl sulfonate with chloride ions. After passage through the resin, 90% of the dodecyl sulfonate had been removed in the product PS62 IRACl1 (Appendix 4, Fig.VI.45), with salbutamol still conjugated

to PEG. The second purification step consisted in washing away the excess of salbutamol. A dilute solution of HCl was thoroughly mixed with a solution of the product solubilised in DCM/$CHCl_3$ and water-soluble salbutamol chloride was washed away in the aqueous phase. The product PS62X1 (Appendix 4, Fig.VI.46) was freed of solvent traces (DCM, $CHCl_3$, 2,6 lutidine) and traces of remaining dodecyl sulfonic acid by precipitation in diethyl ether to yield a yellow solid. Table. II.16 summarises the product composition throughout purification.

Table. II.16. PS62 contaminant composition throughout purification

Contaminant / Product	mol of contaminant / mol of PEG_{2000}		
	dodecyl sulfonate	**2,6 lutidine**	**free salbutamol**
PS62S2	5.0	8.8	2.8
PS62IRACI1	0.5	4.9	2.3
PS62X1	0.5	3.3	0
PS62Y1	0	0	0

The purified product PS62Y1 appeared to be composed of a mixture of PEG ester of salbutamol and unreacted carboxyl groups (NMR in MeOD). On average, for one mole of PEG_{2000} (-O-C$\underline{H}_2$-C$\underline{H}_2$-O-, δ 3.63, 192 H), there was 0.45 mol of unconjugated oxidised PEG (PEG-C$\underline{H}_2$-COO^-, δ 4.00, 0.90 H), 1.35 mol of PEG (PEG-C$\underline{H}_2$-CO-O-Salbu, δ 4.20, 2.31 H) conjugated to the primary hydroxyl group of salbutamol (Salbu-C$\underline{H}_2$-O-CO-PEG, δ 5.22, 2.34 H), 0.20 mol of which was conjugated to the secondary hydroxyl group of salbutamol as well (PEG-C$\underline{H}_2$-CO-O-Salbu, δ 4.17, 0.40 H and Salbu-C$\underline{H}$-O-CO-PEG, δ 4.98, 0.23 H). Two dimensional NMR confirmed the structure of PEG_{2000}-$Salbu_{1.35}$ (Appendix 4, Fig.VI.47).

The results obtained for PEG_{2000}, PEG_{3400} and $mPEG_{2000}$ salbutamol ester conjugates are displayed in Table. II.17 and illustrated in Fig.II.36. Proton NMR spectra of purified PEG_{3400}-salbutamol ester and mPEG-salbutamol ester are given in Appendix 4, respectively Fig.VI.48 and Fig.VI.49.

The average number of salbutamol per PEG was calculated as

(II.8) $$n = B - \frac{C}{2}$$

A general formula PEG-$Salbu_n$ was generated and used to calculate the average molecular weight and elemental mass composition.

Table. II.17. PEG-salbutamol ester conjugates characterised by NMR

Type	MW Da	average number of PEG unit ā	mol conjugated to		
			primary OH group B	secondary OH group C	free COOH D
PEG_{2000}-$Salbu_{1.25}$	2573	48	1.36	0.20	0.45
PEG_{3400}-$Salbu_{1.53}$	3987	78.5	1.62	0.17	0.20
$mPEG_{2000}$-$Salbu_{0.85}$	2336	46	0.88	0.05	0.16

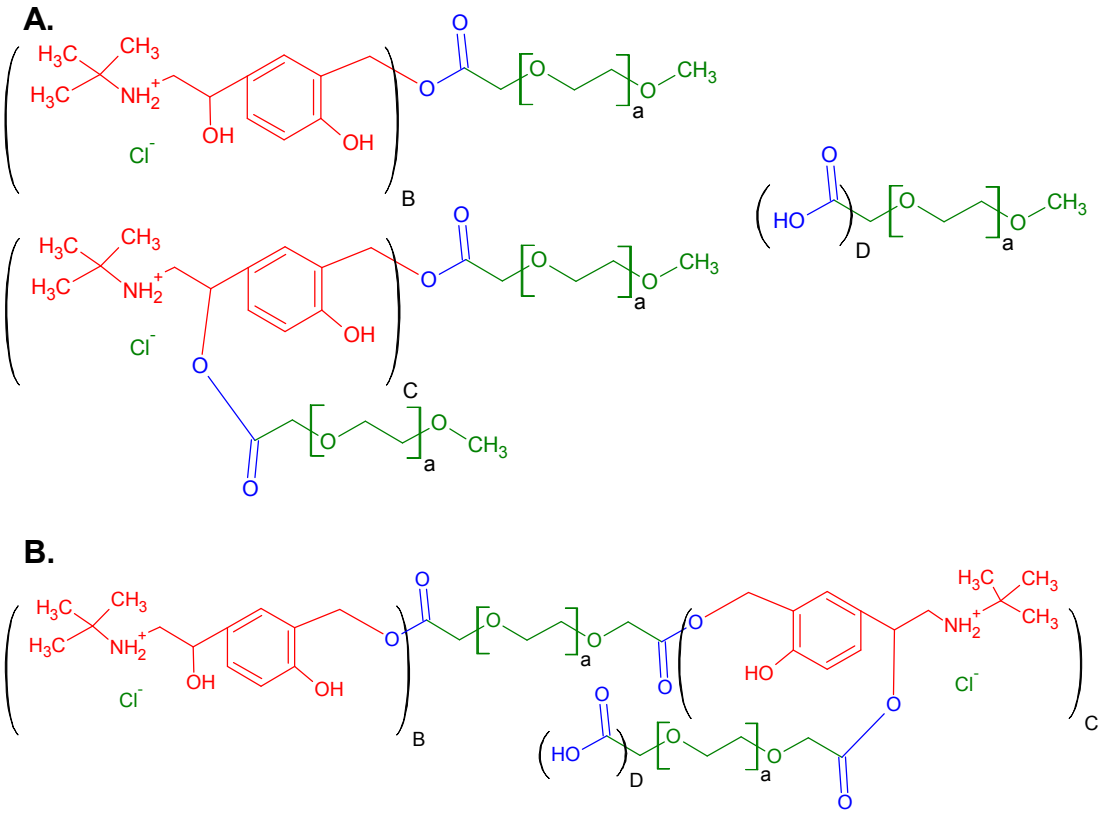

Fig.II.36. Schematic of PEG-salbutamol ester mixtures determined by NMR
A. mPEG-salbutamol ester conjugation mixture, **B.** PEG-salbutamol ester conjugation mixture

The purified products were analysed by FTIR (Fig.II.37) and presented spectra typical of oxidised PEG while the signal for the carbonyl stretch (ν(C=O)) was shifted to slightly higher wavenumbers from 1745cm^{-1} to 1747-1749 cm^{-1}. Two typical signals for salbutamol at 1616 and 1202 cm^{-1} (ν(C=C) and phenyl ring vibration, respectively [118]) were found in the conjugates but not in oxidised PEG, illustrating the presence of salbutamol in the conjugates.

Elemental analysis confirmed the presence of nitrogen (from salbutamol) in the right proportions (Table. II.18), further confirming the obtained product composition.

Table. II.18. Elemental analysis of PEG-salbutamol ester conjugates

Type	MW (Da)		Calculated %	Measured %
PEG_{2000}-$Salbu_{1.25}$	2573	C	54.31	53.7
		H	8.74	8.58
		N	0.68	1
PEG_{3400}-$Salbu_{1.53}$	3987	C	54.50	53.59
		H	8.86	8.74
		N	0.54	0.45
$mPEG_{2000}$-$Salbu_{0.85}$	2336	C	54.54	53.90
		H	8.93	8.78
		N	0.51	0.46

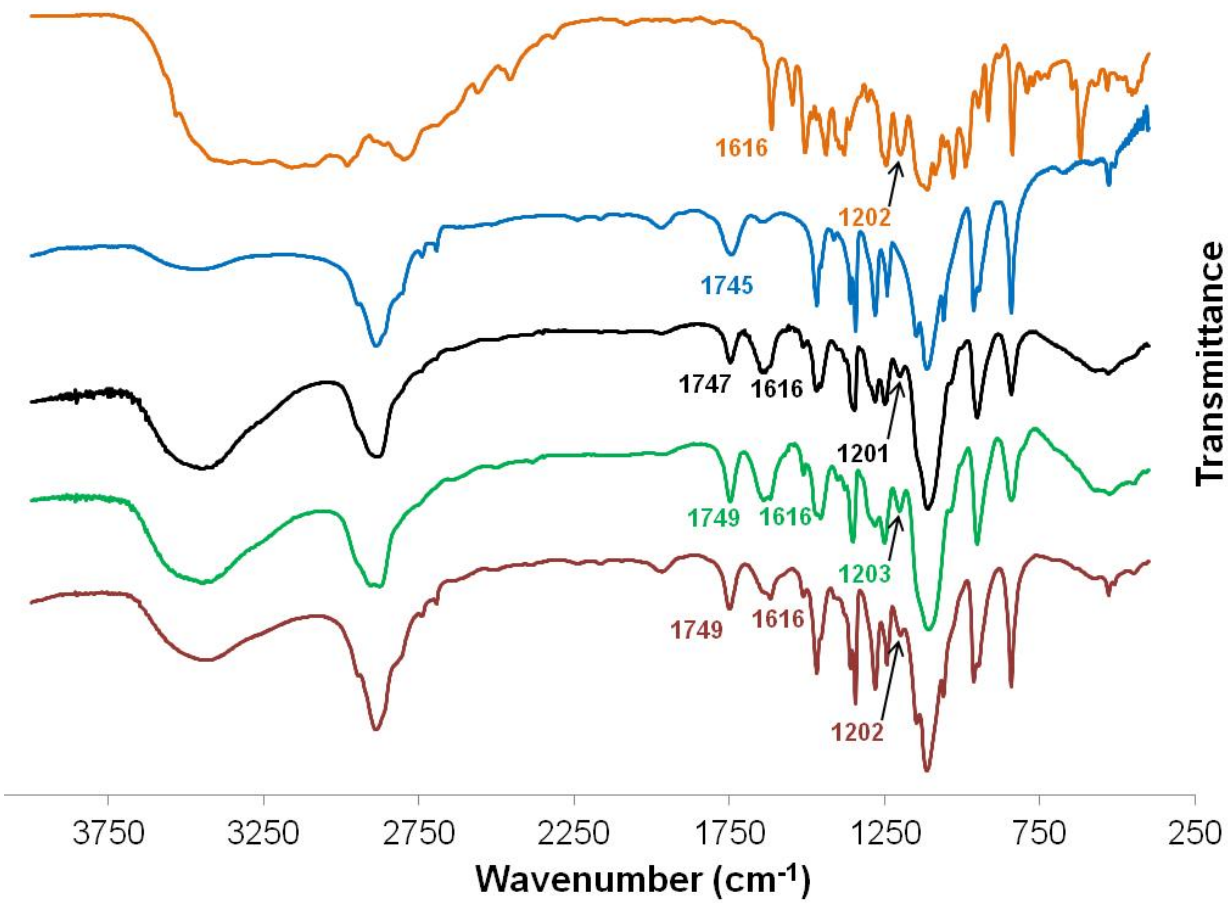

Fig.II.37. FTIR spectra of salbutamol sulfate, oxidised PEG, PEG-salbutamol conjugates
— Salbutamol sulfate, — PEGCOOH, — PEG_{1000}-$Salbu_2$, — PEG_{2000}-$Salbu_2$, — $mPEG_{2000}$-Salbu

Summary

Direct esterification of oxidised PEG and salbutamol sulfate was inefficient due to the poor drug solubility in organic solvents. Solubility was improved by producing a free base form of salbutamol, which was soluble in THF but the conjugation efficiency was not improved due to the salbutamol amine group competing with the primary hydroxyl group to potentially form undesirable amide bonds. The production of salbutamol dodecyl sulfate had the benefit to maintain organic solvent solubility with the fatty chain of dodecyl sulfonate (C_{12}) and the protonation of salbutamol amine group which was accordingly not nucleophilic. It was necessary to maintain the amine group protonated and the tertiary amine base used to accelerate the esterification was carefully selected. Esterification with Mukaiyama reagent, salbutamol dodecyl sulfate and 2,6-lutidine proceeded too slowly and there was a competition between esterification and hydrolysis of the product, resulting in partial esterifications (data not shown).

As a comparison, ester conjugates of oxidised PEG_{2000}, $mPEG_{2000}$ and PEG_{3400} were also produced via the acyl chloride route, purified by anion exchange and characterised by 2D NMR, FTIR and elemental analysis. There was no decarboxylation since the excess of thionyl chloride was limited to 6.3 (relative to PEG carboxylic acid groups). The reactions were less efficient (77.5-90% conjugation) than with prednisolone and some conjugation to the secondary hydroxyl group occurred. Nonetheless, products of sufficient purity were obtained in good yields (56-59%).

II.4. Experimental

II.4.1. TEMPO oxidation of Polyethylene glycols

PEG 1000, PEG 2000, PEG 3400, deuterated NMR solvents, spectroscopic grade potassium bromide and sodium hypochlorite solution were purchased from Sigma Aldrich, (MO, USA), mPEG 2000 was purchased from Alfa Aesar (Heysham, UK), TEMPO was a Fluka product (Buchs, Switzerland). Fisher scientific (Loughborough, UK) provided concentrated hydrochloric acid and sodium hydroxide. Sodium bromide was purchased from Riedel-de Haën (Sleeze, Germany). Unless stated otherwise, organic solvents were of laboratory grade, purchased from Fisher scientific.

PEG_{3400}: A TEMPO solution (37 mM) was freshly prepared by dissolving TEMPO (43.36 mg, 0.28 mmol) in warm deionised water (7.5 mL) and thoroughly mixing until complete dissolution. In a 250 mL beaker, PEG_{3400} (33.95 g, 10 mmol of PEG, 20 mmol of hydroxyl group) and sodium bromide (833.0 mg, 8.1 mmol) were dissolved in deionised water (150 mL). TEMPO solution (5.275 mL, 0.20 mmol) was then added to the mixture and the pH was adjusted to 10 with sodium hydroxide solution (0.5 M). The solution was then placed on an ice-water bath and the temperature dropped to 2°C and maintained at that temperature during the reaction. Cold aqueous sodium hypochlorite solution (35 mL, 13% available chlorine, pH adjusted to 10 with 2M HCl) was then slowly added in aliquots over more than 24 minutes whilst the pH was maintained at 10 by dropwise addition of cold NaOH (0.5 M) solution when required. The mixture was then left to complete the reaction for 300 min, and was subsequently slowly warmed up to 17°C. Excess sodium hypochlorite was quenched with ethanol (25 mL) and the pH was adjusted

to three with aqueous HCl (2 M). Oxidised PEG was then extracted with DCM, dried over $MgSO_4$, filtered and concentrated using a rotary evaporator. The product was then precipitated in diethyl ether, collected by vacuum filtration and dried to constant mass in a vacuum desiccator to yield 31.89 g of a white powder (η = 93%). IR (KBr disc): ν_{max} 530, 843, 962, 1122, 1242, 1281, 1344, 1468, 1745, 2897 cm^{-1}. ^{1}H-NMR (400 MHz, methanol-d_4) δ 4.12 (s, 4H, PEG-(C$\underline{H}_2$-COOH)$_2$), 3.64 (br. s., 299H, PEG backbone).

PEG_{1000}: The same procedure as for oxidation of PEG_{3400} was employed. Briefly, a fresh TEMPO solution (40 mM) was prepared by solubilising TEMPO (93.59 mg, 0.60 mmol) in warm deionised water (15 mL). PEG_{1000} (5 g, 10 mmol of OH) was oxidised using fresh TEMPO solution (2.5 mL, 0.10 mmol), NaBr (431.5 mg, 4.19 mmol) and 20 mL (35 mmol) of aqueous sodium hypochlorite solution (13% available chlorine, pH adjusted to 10 with 2M HCl). The mixture was left to react overnight and after acidification, oxidised PEG_{1000} was extracted three times with DCM (60 mL), concentrated and precipitated in n-hexane (200 mL). It was then left to dry to constant weight in a vacuum desiccator to yield 2.33 g of a white oily product (η = 45%). IR (KBr disc): ν_{max} 845, 955, 1103, 1248, 1348, 1462, 1743, 2874 cm^{-1}. ^{1}H NMR (400 MHz, chloroform-d) δ 4.16 (s, 4H, PEG-(C$\underline{H}_2$-COOH)$_2$), 3.65 (s, 81H, PEG backbone).

PEG_{2000}: The same procedure as for oxidation of PEG_{3400} was employed. Briefly, a fresh TEMPO solution (56 mM) was prepared by dissolving TEMPO (86.88 mg, 0.56 mmol) in warm deionised water (10 mL). PEG_{2000} (20 g, 20 mmol of OH) were oxidised using the freshly prepared TEMPO solution (3.5 mL, 0.2 mmol),

NaBr (829.7 mg, 8.1 mmol) and 35 mL (61 mmol) of aqueous sodium hypochlorite solution (13% available chlorine, pH adjusted to 10 with 2M HCl). The mixture was left to react overnight and after acidification, oxidised PEG_{2000} was extracted three times with DCM (75 mL), concentrated and precipitated in diethyl ether (800 mL). It was then left to dry to constant weight in a vacuum desiccator to yield 17.73 g of a white powder (η = 87%). IR (KBr disc): ν_{max} 528, 843, 962, 1107, 1242, 1279, 1342, 1468, 1743, 2879 cm^{-1}. ^1H NMR (400 MHz, chlorofom-d) δ 4.07 (s, 4H, PEG-(C$\underline{H}_2$-COOH)$_2$), 3.58 (br. s., 172H, PEG backbone).

$mPEG_{2000}$: The same procedure as for oxidation of PEG_{3400} was employed. Briefly, a fresh TEMPO solution (41 mM) was prepared by dissolving TEMPO (70.6 mg, 0.45 mmol) in warm deionised water (11 mL). Ten grams of $mPEG_{2000}$ (4.9 mmol of OH) were oxidised using fresh TEMPO solution (1.2 mL, 0.05 mmol), NaBr (239.4 mg, 2.3 mmol) and 14.4 mL (25 mmol) of aqueous sodium hypochlorite solution (13% available chlorine, pH adjusted to 10 with 2M HCl). The mixture was left to react overnight and after acidification, oxidised $mPEG_{2000}$ was extracted three times with DCM (75 mL), concentrated and precipitated in diethyl ether (300 mL). It was then left to dry to constant weight in a vacuum desiccator to yield 7.66 g of a white waxy powder (η = 76%). IR (KBr disc): ν_{max} 530, 843, 964, 1117, 1244, 1281, 1344, 1468, 1654, 1742, 2893 cm^{-1}. ^1H-NMR (400 MHz, chloroform-d) δ 4.08 (s, 2H, PEG-C$\underline{H}_2$-COOH), 3.58 (s, 178H, PEG backbone), 3.32 (s, 3H, terminal methoxy).

II.4.2. Esterification of PEG and prednisolone

For all esterification reactions, the glassware was dried by flame drying. Dry conditions were used to conduct the reactions. Solutions and suspensions were transferred with a cannula and transferred volumes replaced with Argon (supplied by BOC, UK). The solid reagents were stored in a vacuum desiccator and further dried prior to reaction by creating a high vacuum (less than 13 Pa) in the reaction vessel for at least 180 min. The liquid reagents were supplied dry and stored over molecular sieves.

Amberlite IRA 200 (C)Na^+ was purchased from Alfa Aesar, prednisolone, dry triethylamine were purchased from Sigma, thionyl chloride was a Fluka product. Dry DCM, dry THF were purchased from ACROS organics (Geel, Belgium).

Cation exchange resin preparation. The resin was washed in deionised water until the eluent was clear, and the beads were drained by vacuum filtration using a Venturi device.

Mukaiyama reagent was purchased from Fluka, dry pyridine was purchased from Acros organics.

II.4.2.1. Acyl chloride

PP11: Oxidised PEG_{3400} (8.56 g, 5.0 mmol of COOH) was placed in a two-neck 100 mL round bottom flask mounted with a condenser. The polymer was then solubilised in dry DCM (50 mL) and thionyl chloride (10 mL) was added with a glass pipette, under an argon flux. The reaction was stirred overnight at 40°C. The heating was stopped and solvent and excess of thionyl chloride were evaporated to dryness by vacuum distillation to yield an off-white solid. In a 250 mL round bottom flask, dry prednisolone (2522 mg, 7.0 mmol) was poured over a flow of

argon and dissolved in dry THF (75 mL). Triethylamine (1.8 mL, 13 mmol) was added to the prednisolone solution with a syringe. PEG acyl chloride was solubilised in dry DCM (40 mL) and slowly added to the stirred solution of prednisolone and triethylamine over 15 minutes at room temperature. The temperature was then set to 40°C. The reaction was stopped after 1200 minutes by switching the heating and stirring off. The solution was then filtered and the solvent was evaporated off. The crude product *PP11BS1* was analysed by NMR. A small fraction of the product was resuspended in DCM and mixed with silica gel and the solvent was removed by rotary evaporation. The dry silica gel was then transferred onto a paper filter and washed with ethyl acetate (fractions A to D) until no more fluorescence was detected in the eluent (checked by TLC). The silica was then washed with DCM/MeOH 90/10 v/v (fractions E to K) until no fluorescence was detected in the eluent. Fractions E to K were pooled together and evaporated to dryness for NMR analysis (*PP11SFEK*).

PP14: The reaction was carried out in the same way as for PP11. Briefly, oxidised PEG_{3400} (5.04 g, 2.9 mmol of COOH) was chlorinated overnight with thinoyl chloride (6.0 mL, 83 mmol) in DCM (20 mL). After drying, PEG acyl chloride dissolved in dry DCM (30 mL) was added to a solution of prednisolone (1.47 g, 4.1 mmol) and triethylamine (1 mL, 7.2 mmol) in dry THF (70 mL). The reaction was carried out for 1580 min at 40°C and after completion, the mixture was filtered and the solvent evaporated to dryness to give *PP14S1*, which was analysed by NMR. *PP14S1* was then solubilised in DCM (200 mL). Dry silica gel (24g) was added to half of the PP14S1 solution, thoroughly stirred to let the product to adsorb on silica, and the solvent was subsequently removed by rotary evaporation. The dry silica

was transferred onto a filter and washed with diethyl ether/ethyl acetate 50/50 v/v (fractions 1-3). THF/DCM 40/60 v/v was then used and 500 mL fractions were collected for NMR analysis (fractions 4-7). Finally, THF/DCM 50/50 v/v was used for the last two fractions (8 and 9). The fractions were concentrated and individually precipitated in diethyl ether. *PP14SF4P* was analysed by NMR. The precipitated fractions 4 to 9 were pooled together, solubilised in acetone (100 mL) and mixed overnight at 250 rpm with prepared cation exchange resin (57 g). The suspension was then filtered, the beads washed 3 times with acetone (100 mL), the solvent evaporated to dryness and the product *PP14SFDC1S* analysed by NMR.

PP08: The reaction was carried out in the same way as for PP11. Briefly, oxidised $mPEG_{2000}$ (3.5 g, 1.7 mmol of COOH) was chlorinated overnight with thionyl chloride (3.5 mL, 48.2 mmol) in DCM (30 mL). After drying, PEG acyl chloride in dry DCM (25 mL) was added to a solution of prednisolone (876.7 mg, 2.4 mmol) and triethylamine (650 µL, 4.7 mmol) in dry THF (25 mL). The reaction was carried out for 1260 min at 40°C and after completion, the mixture was filtered and the solvent evaporated to dryness. The product was then resuspended in DCM (13 mL) and precipitated in diethyl ether (200 mL) to give 3781 mg of *PP08P2*, analysed by NMR. A small fraction of PP08P2 (255 mg) was then solubilised in DCM (8 mL) and the flask washed with two times six millilitres of THF. To this stirred solution was added the prepared cation exchange resin (1.80 g), previously washed twice with 50 mL of THF/DCM (60/40 v/v) and left overnight. The suspension was filtered, washed with DCM and the solvents were evaporated. The product *PP08DC2* was analysed by NMR and then solubilised in DCM (8 mL) and precipitated in cyclohexane (80 mL) to yield 106 mg of precipitated product that

was then solubilised again in DCM (15 mL) and adsorbed on dry silica (454.5 mg). The solvent was then removed by rotary evaporation. The silica was transferred onto a paper filter and washed with 100 mL of diethyl ether/ethyl acetate (90/10 v/v) (fraction 1) and 100 mL of DCM/MeOH (80/20 v/v) (fraction 2). The second fraction was evaporated to dryness to give *PP08DC2DF1B*, analysed by NMR.

PP16: The reaction was carried out in the same way as for PP11. Briefly, oxidised PEG_{2000} (3.05 g, 3.0 mmol of COOH) was chlorinated overnight with thinoyl chloride (10.0 mL, 140 mmol) in DCM (10 mL). After drying, PEG acyl chloride dissolved in dry DCM (40 mL) was added to a solution of prednisolone (1.59 g, 4.4 mmol) and triethylamine (1.3 mL, 9.3 mmol) in dry THF (60 mL). The reaction was carried out for 1105 min at 45°C and after completion, the mixture was filtered and the solvent evaporated to dryness to give *PP16S1*, analysed by NMR. *PP14S1* was solubilised in DCM (50 mL) and washed with 15 mL of 0.5 M HCl. The organic phase was collected and dried over $MgSO_4$. The solvent was evaporated to dryness and *PP16HCl* analysed by NMR. *PP16HCl* was solubilised in DCM (50 mL), adsorbed on dry silica (5.1 g) and DCM was removed by rotary evaporation. The silica was transferred onto a paper filter and washed with one litre of diethyl ether/ethyl acetate (50/50 v/v). A silica gel chromatography column was loaded with the treated silica (bed height 17 cm, 120 mL) and THF/ethyl acetate (50/50 v/v). The column was subsequently washed with 200 mL of the packing solvent mixture, then 160 mL of THF. The *PP16SGA* fraction was collected, evaporated to dryness, solubilised in DCM (15 mL), and precipitated in diethyl ether (200 mL) to yield an off white paste (*PP16SGAp*), analysed by NMR.

PP13: The reaction was carried out in the same way as for PP11. Briefly, oxidised PEG_{1000} (1.57 g, 3.1 mmol of COOH) was chlorinated overnight with thinoyl chloride (5.0 mL, 69 mmol) in DCM (30 mL). After drying, PEG acyl chloride dissolved in dry DCM (25 mL) was added to a solution of prednisolone (1.51 g, 4.2 mmol) and triethylamine (1.1 mL, 7.9 mmol) in dry THF (40 mL). The reaction was carried out for 1600 min at 40°C and after completion, the mixture was filtered and the solvent evaporated off to dryness to give *PP13S1*, analysed by NMR. The product was solubilised in acetone (100 mL) and mixed with prepared cation exchange resin (19 g), and washed with acetone (250 mL). The ion exchange was carried out overnight over gentle mixing. The suspension was filtered, the resin rinsed six times with DCM (25 mL), the solvents evaporated to dryness to give an oily product *PP13DC1*. The product was then solubilised in DCM (50 mL) and cation exchanged with 10 g of prepared resin (washed with 300 mL of acetone and 25 mL of DCM) for 120 min. The suspension was filtered, the resin washed with DCM (100 mL) and the solvent evaporated to dryness to give 1.22 g of *PP13DC2* (analysed by NMR). The product was suspended in DCM (70 mL), adsorbed on dry silica (6 g), the solvent removed and the silica transferred onto a paper filter. The silica was washed with 4 times 350 mL of ethyl acetate/diethyl ether (10/90 v/v) to give fraction A, then 350 mL of DCM/MeOH (80/20 v/v) were used to give fraction B. The solvents were removed by rotary evaporation to yield 699.2 g of dry product *PP13DC2DFB*, analysed by NMR (η = 28%).

PP17: Dry $PEG_{3400}COOH$ (2.04 g, 1.2 mmol of COOH) was poured into a two-necked 100 mL round bottom flask, mounted with a condenser, flushed with argon and solubilised in DCM (15 mL). Thionyl chloride (3.0 mL, 41 mmol) was added

and the temperature was increased to 45°C. After 240 min, the solvent and excess of thionyl chloride were removed by vacuum distillation to yield a white solid. In a two-necked 100 mL round bottom flask, mounted with a condenser, prednisolone (764.0 mg, 2.1 mmol) was added to THF (20 mL). Dry pyridine (1.1 mL, 13.7 mmol) was added in the stirred solution of prednisolone. PEG acyl chloride was solubilised in DCM (20 mL) and slowly transferred into the prednisolone/pyridine solution over seven minutes. The temperature was increased to 45°C and the reaction was carried out for 1010 minutes. *PP17S2* was obtained by evaporation of solvents.

PP22/PP23: Oxidised PEG_{3400} (2.04 g, 0.6 mmol PEG, 1.2 mmol of carboxylic acid) were poured, under Argon, into a two-necked 100 mL round bottom flask mounted with a condenser. After drying, the polymer was solubilised in dry DCM (15 mL). Thionyl chloride (6.0 mL, 83 mmol) was then added with a syringe and the temperature was increased and maintained at 45°C under stirring. The mixture was left to react for 215 min. The solvents were then evaporated off by vacuum distillation and a yellowish solid was obtained. The solid was resuspended in dry DCM (16 mL) and transferred into a sealed 50 mL measuring cylinder, flushed with Argon beforehand. The flask was further washed with dry THF (10 mL) and the solution added into the measuring cylinder.

PP22: prednisolone (448.6 mg, 1.24 mmol) was poured into a two necked 50 mL round bottom flask mounted with a condenser and flushed with Argon for more than 15 minutes after drying. Prednisolone was solubilised in exactly 10 mL of dry THF and stirred. Dry pyridine (600 µL, 7.46 mmol) was added with a syringe under

argon. Thirteen millilitres of the PEG acyl chloride solution (0.3 mmol of PEG, 0.15 mmol of acyl chloride) were then slowly added into the prednisolone/pyridine solution over 5 minutes. The temperature was then increased and maintained at 50°C under constant stirring. After 120 min, a sample (500 µL) was taken under argon, the solvent evaporated, the crude product resuspended in deuterated methanol and analysed by NMR (*PP22S1*) and the reaction was continued for 1000 min. The solvents were then evaporated off by rotary evaporation and the product *PP22S2* analysed by NMR.

PP23: prednisolone (216.7 mg, 0.63 mmol) was used following the same procedure as for PP22.

PP20/PP21: PEG_{3400} acyl chloride was produced according to the same procedure as for *PP22/PP23*. Briefly, PEG_{3400} diacid (2.03 g, 0.59 mmol of PEG, 1.18 mmol of carboxylic acid) was reacted with thionyl chloride (6.0 mL, 83 mmol) for 240 min at 45°C. The product was then solubilised in dry DCM (45 mL).

PP20: prednisolone (314.0 mg, 0.87 mmol) was solubilised in dry THF (15 mL). Dry pyridine (100 µL, 1.24 mmol) was added and 22.5 mL of PEG acyl chloride solution (0.30 mmol of PEG, 0.59 mmol of acyl chloride) was then slowly added to the mixture over 40 minutes, under stirring. The temperature was subsequently increased and maintained at 45°C. After 30 minutes, a sample was taken and analysed by NMR (*PP20S1*) and the reaction was continued for 1410 min when the solvents were evaporated to dryness to give *PP20S2*, analysed by NMR.

PP21: prednisolone (309.3 mg, 0.86 mmol) was solubilised in dry THF (20 mL), and 22.5 mL of PEG acyl chloride solution (0.30 mmol of PEG, 0.59 mmol of acyl chloride) added all at once. Dry pyridine (100μL) was mixed with dry DCM and slowly added to the mixture over 40 minutes while stirring. The temperature was then increased and maintained at 45°C. After 45 minutes, a sample was taken and analysed by NMR (*PP21S1*) and the reaction was continued for an additional 1380 min when the solvents were evaporated to dryness to give *PP21S2* and analysed by NMR.

PP25/PP26: PEG_{3400} acyl chloride was produced according to the same procedure as for *PP22/PP23*. Briefly, PEG_{3400} diacid (2.02 g, 0.59 mmol of PEG, 1.18 mmol of carboxylic acid) was reacted with thionyl chloride (900 μL, 12.4 mmol) for 180 min at 30°C. The product was then solubilised in dry DCM (30 mL).

PP25: prednisolone (221.4 mg, 0.62 mmol) was solubilised in dry THF (15 mL). Dry pyridine (900 μL, 11.2 mmol) was added, followed by 15 mL of PEG acyl chloride solution (0.30 mmol of PEG, 0.59 mmol of acyl chloride), under stirring, over 10 minutes. The temperature was then increased and maintained at 40°C for 1245 min. The solvents were evaporated by rotary evaporation and *PP25S1* analysed by NMR.

PP26: prednisolone (441.7 mg, 1.23 mmol) was solubilised in dry THF (15 mL). Dry pyridine (900 μL, 11.2 mmol) was added, followed by 15 mL of PEG acyl chloride solution (0.30 mmol of PEG, 0.59 mmol of acyl chloride) under stirring and over 10 minutes. The temperature was then increased and maintained at 40°C

for 1185 min. The solvents were evaporated by rotary evaporation and *PP26S1* analysed by NMR.

II.4.2.2. Mukaiyama reagent

PP04: prednisolone (112.5 mg, 0.31 mmol) and Mukaiyama reagent (82.85 mg, 0.32 mmol) were added in a 100 mL two necked round bottom flask mounted with a condenser. The flask was flushed with argon after drying and the products suspended in dry DCM (40 mL), under stirring. In a two necked 50 mL round bottom flask, oxidised $mPEG_{2000}$ (501.2 mg, 0.24 mmol of carboxylic acid) was solubilised in dry DCM (20 mL). The PEG solution was then transferred under argon to the stirred suspension of prednisolone and Mukaiyama reagent at room temperature, over 5 minutes. Triethylamine (125 µL, 0.86 mmol) was added with a syringe. The temperature was then increased and maintained at 40°C. A first sample (PP04S1) was withdrawn after 250 min, the solvent evaporated off and analysed by NMR. The reaction was stopped after 1310 min (PP02S2).

PP01: oxidised PEG_{3400} (700.3 mg, 0.20 mmol of PEG, 0.41 mmol of carboxylic acid) and prednisolone (180.7 mg, 0.50 mmol) were poured in a two necked 100 mL round bottom flask mounted with a condenser. After drying, dry THF (60 mL) was added under stirring and the temperature was increased to 40°C. Dry triethylamine (150 µL, 1.08 mmol) was then added with a syringe. Mukaiyama reagent was placed in a two necked 50 mL round bottom flask and suspended in dry THF (10 mL). Mukaiyama suspension was then transferred into the PEG/prednisolone/triethylamine suspension and the temperature was increased and maintained at 50°C. A first sample was taken after 1270 min (PP01S1) and a second sample after 2440 min (PP1S2).

PP24: prednisolone (309.2 mg, 0.86 mmol) and Mukaiyama reagent (226.1 mg, 0.88 mmol) were added in a 100 mL argon-flushed two necked round bottom flask mounted with a condenser. The products were suspended in dry THF (10 mL) and dry DCM (10 mL), under stirring and 350 µL of dry triethylamine (2.5 mmol) were added with a syringe. In a 2 neck 50 mL round bottom flask, 1009 mg of oxidised PEG_{3400} (0.29 mmol of PEG, 0.59 mmol of carboxylic acid) were solubilised in 20 mL of dry DCM. PEG solution was slowly added to Mukaiyama reagent/prednisolone/triethylamine solution over 12 min and the temperature was increased to 50°C. A sample was taken after 60 min (PS24S1) and the reaction was continued for 1250 min (PS24S2).

PP27: The procedure used for PP24 was employed. Briefly, prednisolone (318.7 mg, 0.88 mmol), Mukaiyama reagent (451.9 mg, 1.77 mmol) and 500 µL of dry triethylamine (3.59 mmol) were suspended in a mixture of dry DCM (12 mL) and dry THF (12 mL). PEG solution (1001 mg, 0.59 mmol of carboxylic acid) was slowly added to the mixture. A first sample was withdrawn after 1000 min (PP27S1) and the reaction carried out for a total of 2460 min (PP27S2) at 50°C.

PP33: oxidised PEG_{1000} (2050 mg , 3.99 mmol of carboxylic acid) was placed in a two necked 100 mL round bottom flask under high vacuum (less than 13 Pa) for more than 300 min. Dry Mukaiyama reagent (3035 mg, 11.88 mmol) and dry prednisolone (1983 mg , 5.50 mmol) were poured in a two necked 100 mL round bottom flask mounted with a condenser and the flask was then maintained under high vacuum (less than 13 Pa) for more than 300 min. Oxidised PEG was solubilised in dry DCM (15 mL). Prednisolone and Mukaiyama reagent were

suspended in dry THF (50 mL) and dry triethylamine (3.3 mL, 24 mmol) was added. PEG solution was slowly transferred to the suspension at room temperature over 10 minutes under stirring. The flask that contained PEG was rinsed with dry DCM (5 mL) and transferred to the reaction mixture. Temperature was then maintained at 40°C for 4320 min. Heating and stirring were stopped, the solution filtered and solvents evaporated to dryness.

The dry residue was solubilised in acetonitrile (12 mL) and loaded into a chromatography column packed with silica gel in acetonitrile (25 cm bed height, 200 mL). The column was washed with 5 column volumes of acetonitrile until no more product was visibly coming out of the column (TLC plate revealed by UV light). Tetrahydrofuran was then used to recover the ester conjugate (2 column volumes). After evaporation of THF, the product was resuspended in DCM (15 mL) and precipitated in diethyl ether (200 mL) to yield a viscous dark yellow syrup that stuck to the beaker walls (PP33w1). The product was then taken up in DCM (15 mL) and precipitated in 200 mL of pentane (PP33w2). A third precipitation in diethyl ether afforded a yellow paste that was resuspended in a minimum amount of methanol, transferred to a glass vial and dried until constant weight (PP33w3) to afford 2330 mg of pure product (η = 69%). Elemental analysis: measured C 58.3% H 8.1% N -0.3%, calculated C 57%, H 8.7%, N 0%. IR (KBr disc): ν_{max} 847, 949, 1113, 1246, 1292, 1350, 1450, 1659, 1724, 1761, 2870 cm^{-1}. Selection of significant ^{1}H-NMR signals (400 MHz, methanol-d_4) δ 7.50 (d, *J* = 9.90 Hz, 1H), 6.28 (dd, *J* = 1.90, 10.00 Hz, 1H), 6.03 (s, 2H), prednisolone alkene protons, 4.94 - 5.21 (m, 4H), prednisolone-C=O-C$\underline{H}_2$-O-C=O-PEG), 4.33 (s, 4H), PEG-C$\underline{H}_2$-C=O-O-Pred, 3.66 (s, 81H), PEG backbone.

PP28: the same production procedure as for PP33 was employed. Briefly, oxidised $mPEG_{2000}$ (4007 mg , 1.95 mmol of carboxylic acid) dissolved in dry DCM (20 mL) was slowly added to a suspension of prednisolone (1001 mg, 2.78 mmol), Mukaiyama reagent (1557 mg, 6.10 mmol) and triethylamine (1.7 mL, 12 mmol) in dry THF (20 mL). The mixture was allowed to react for 4110 min at 40°C. Heating and stirring were stopped, the solution filtered and solvents evaporated to dryness. The dry residue was solubilised in warm propan-2-ol and left to crystallise overnight to afford yellow crystals. The crystals were then filtered and washed with diethyl ether/propan-2-ol (75/25 v/v) and cold diethyl ether. The crystals were then dried until constant weight in a vacuum desiccator and afforded 2816 mg of pure product (η = 58%). Elemental analysis: measured C 56.3% H 8.8% N -0.1%, calculated C 56.5%, H 8.8%, N 0%. IR (KBr disc): ν_{max} 843, 962, 1113, 1242, 1283, 1344, 1468, 1659, 1761, 2893 cm^{-1}. Selection of significant ^{1}H-NMR signals (500 MHz, methanol-d_4) δ 7.48 (d, J = 9.93 Hz, 1H), 6.26 (dd, J = 1.89, 10.09 Hz, 1H), 6.01 (s, 1H), prednisolone alkene protons, 4.99-5.12 (m, 2H), prednisolone-C=O-C$\underline{H}_2$-O-C=O-PEG), 4.31 (s, 2H), PEG-C$\underline{H}_2$-C=O-O-Pred, 3.63 (s, 184H), PEG backbone, 3.36 (s, 3H), methoxy PEG.

PP32: the same production procedure as for PP33 was employed. Briefly, oxidised PEG_{2000} (2013 mg , 2.0 mmol of carboxylic acid) dissolved in dry DCM (20 mL) were slowly added to a suspension of prednisolone (997.4 mg, 2.77 mmol), Mukaiyama reagent (1512 mg, 5.92 mmol) and triethylamine (1.7 mL, 12 mmol) in dry THF (20 mL). The mixture was allowed to react for 4245 min. Heating and stirring were stopped, the solution filtered and solvents evaporated to dryness.

The dry residue was solubilised in acetonitrile (10 mL) and loaded into a chromatography column packed with silica gel in acetonitrile (24 cm bed height, 170 mL). The column was washed with 4 column volumes of acetonitrile until no more product was visibly coming out of the column (TLC plate revealed by UV light). Tetrahydrofuran was then used to recover the ester conjugate (6 column volumes). After evaporation of THF, the product was resuspended in DCM (12 mL) and precipitated in ice cold diethyl ether (200 mL), washed with ice cold diethyl ether, and filtered to yield a pale yellow solid that melted rapidly at room temperature. The product was transferred to a glass vial and dried until constant weight (PP32C2) and afforded 1699 mg of pure PEG-prednisolone (η = 60%). Elemental analysis: measured C 57.1% H 8.0% N 0%, calculated C 58.3%, H 8.5%, N 0%. IR (KBr disc): ν_{max} 849, 953, 1117, 1253, 1302, 1354, 1471, 1659, 1726, 1761, 2883 cm^{-1}. Selection of significant ^{1}H-NMR signals (400 MHz, methanol-d_4) δ 7.48 (d, *J* = 9.90 Hz, 2H), 6.25 (dd, *J* = 1.90, 10.10 Hz, 2H), 6.01 (s, 2H), prednisolone alkene protons, 4.91 - 5.21 (m, 4H), prednisolone-C=O-C$\underline{H}_2$-O-C=O-PEG), 4.30 (s, 4H), PEG-C$\underline{H}_2$-C=O-O-Pred, 3.63 (s, 180H), PEG backbone.

PP31: the same production procedure as for PP33 was employed. Briefly, oxidised PEG_{3400} (3405 mg, 2.0 mmol of carboxylic acid) dissolved in dry DCM (30 mL) were slowly added to a suspension of prednisolone (1002 mg, 2.78 mmol), Mukaiyama reagent (1561 mg, 6.11 mmol) and triethylamine (1.7 mL, 12 mmol) in dry THF (20 mL). The mixture was allowed to react for 4380 min. Heating and stirring were stopped, the solution filtered and solvents evaporated to dryness.

The dry residue was solubilised in warm propan-2-ol and left to crystallise overnight to afford off-white crystals. The crystals were then filtered and washed

with diethyl ether/propan-2-ol (75/25 v/v) and solubilised in DCM (14 mL) to be precipitated in diethyl ether (200 mL). The crystals were then filtered by vacuum filtration on a filter paper, collected and dried in a vacuum desiccator until constant weight. The reaction afforded 3030 mg of pure product (η = 75%). Elemental analysis: measured C 55.9% H 8.1% N 0.2%, calculated C 57.0%, H 8.7%, N 0%. IR (KBr disc): ν_{max} 843, 964, 1116, 1242, 1282, 1344, 1468, 1661, 1728, 1765, 2891 cm^{-1}. Selection of significant ^{1}H-NMR signals (500 MHz, methanol-d_4) δ 7.48 (d, *J* = 10.09 Hz, 2H), 6.26 (dd, *J* = 1.89, 10.09 Hz, 2H), 6.01 (s, 2H), prednisolone alkene protons, 4.93 - 5.18 (m, 4H), prednisolone-C=O-C$\underline{H}_2$-O-C=O-PEG), 4.31 (s, 4H), PEG-C$\underline{H}_2$-C=O-O-Pred, 3.63 (s, 299H), PEG backbone.

II.4.3. Esterification of PEG and salbutamol

Salbutamol sulfate and Amberlite IRA Cl^- were purchased from Alfa Aesar, dry 2,6-lutidine was an Aldrich product, sodium dodecyl sulfate was purchased from Melford (Ipswich, UK).

Salbutamol FB: salbutamol sulfate (2192 mg, 7.6 mmol) was dissolved in deionised water (75 mL). The pH was adjusted to 9.72 using sodium hydroxide solution (2.5 M). Water was evaporated off in a rotary evaporator set at 60°C, mounted with a splash guard to avoid condensing water refluxing back in the flask. The residue was resuspended in THF (50 mL), the solution filtered, the filtrant resuspended twice more in THF (50 mL) and subsequently filtered. The organic solution was concentrated to 30 mL and salbutamol free base was precipitated in n-hexane (200 mL) as a white crystalline powder. The precipitate was recovered by gravitation filtration and left to dry in a vacuum oven until constant weight (1572 mg, η = 86%). ^{1}H NMR (400 MHz, METHANOL-d_4) δ 7.24 (d, J = 2.26 Hz, 1H), 7.05 - 7.12 (m, 1H), 6.73 (d, J = 8.03 Hz, 1H), 4.65 (s, 2H), 4.58 - 4.63 (m, 1H), 2.55 - 2.89 (m, 2H), 1.11 (s, 9H). IR (KBr disc): ν_{max} 613, 719, 819, 1038, 1078, 1269, 1338, 1502, 1606, 2964 cm^{-1}.

Salbutamol dodecyl sulfate: salbutamol free base (1335 mg, 5.58 mmol) was dissolved in deionised water (125 mL), and 36.43 mL (5.58 mmol) of dodecyl sulfonic acid solution at 0.1531 M (3091 mg of sodium dodecyl sulfate (SDS) (10.72 mmol) adjusted to pH 1.5 in 70 mL) were added under stirring. The solution lost its pale yellow colour and a white precipitate rapidly appeared. The solution

was filtered through a paper filter using a Ventrui vacuum system and the precipitate was dried using high vacuum until constant weight (2483 mg, η = 88%). ^{1}H NMR (400 MHz, DMSO-d_6) δ 7.22 (d, *J* = 1.76 Hz, 1H), 6.96 (dd, *J* = 2.13, 8.16 Hz, 1H), 6.66 (d, *J* = 8.28 Hz, 1H), 4.47 (s, 2H), 4.38 (dd, *J* = 5.27, 7.28 Hz, 1H), 2.52 - 2.58 (m, 2H), 1.01 (s, 9H). IR (KBr disc): ν_{max} 594, 812, 993, 1202, 1258, 1385, 1618, 2853, 2922 cm^{-1}.

PS62: oxidised PEG_{2000} (1309 mg, 1.29 mmol of COOH) was poured in a 100 mL two necked round bottom flask. Salbutamol dodecyl sulfate (1406 mg, 2.78 mmol) was placed in a 100 mL two necked bottom flask mounted with a condenser. Both flasks were connected to high vacuum (less than 13 Pa) overnight to dry the products. PEG was solubilised in dry DCM (20 mL) under stirring and thionyl chloride (500 µL, 6.88 mmol) was injected with a syringe. The reaction was allowed to proceed for 240 min. Heating was stopped and after cooling down, the solvent and excess thionyl chloride were evaporated off. Salbutamol dodecyl sulfate was solubilised in dry THF (44 mL) and heated to 50°C, under stirring. Dry 2,6 lutidine (780 µL, 6.70 mmol) was added with a syringe. PEG acyl chloride was solubilised in dry DCM (20 mL) and added in aliquots to the salbutamol/lutidine solution. After 45 min, heating and stirring were stopped, the solvent evaporated to dryness and the dry residue analysed by NMR (PS62S2). The product was suspended in 20 mL of MeOH and passed through an anion exchange column (resin: IRA Cl^- equilibrated in MeOH, column 25.5 cm length by 24 mm internal diameter (ID)). The solvent was evaporated using a rotary evaporator at 40°C, the dry residue PS62IRACl1 analysed by NMR. The product was solubilised in DCM (80 mL) and chloroform (20 mL) and washed with 20 mL of dilute HCl solution (1

drop of 0.02 M HCl in one litre of deionised water). The organic layer was recovered and dried over $MgSO_4$, filtered and the solvents evaporated off (PS62X1). The product was finally solubilised in 10 mL, then another 3 mL of DCM and precipitated in a mixture of 150 mL of diethyl ether and 15 mL of n-hexane. The purified product was filtered using a Ventrui vacuum system and washed with diethyl ether/propan-2-ol (50/50 v/v) to yield a white powder that melted rapidly at room temperature. PS62Y1 was left to dry until constant weight in a vacuum oven (943 mg, η = 57%). Elemental analysis: measured C 53.70%, 8.58H %, N 1%, calculated C 54.31%, H 8.74%, N 0.68%. IR (KBr disc): ν_{max} 837, 951, 1097, 1250, 1350, 1454, 1616, 1749, 2870 cm^{-1}.

PS57: the same methodology as for PS 62 was used to produce an ester of oxidised $mPEG_{2000}$ and salbutamol. Briefly, oxidised $mPEG_{2000}$ (1264 mg, 0.62 mmol) was reacted with thionyl chloride (280 µL, 3.86 mmol). PEG acyl chloride was then reacted with a mixture of salbutamol dodecyl sulfate (742.5 mg, 1.47 mmol) and 2,6 lutidine (400 µL, 3.43 mmol) for 44 min at 50°C. The crude product PS57S2 was purified by anion exchange ($IRACl^-$ in MeOH, 21 cm length, 24 mm ID), followed by a dilute HCl wash, and precipitation in diethyl ether to yield a brown powder (η = 59%). Elemental analysis: measured C 53.90%, 8.78H %, N 0.46%, calculated C 54.54%, H 8.93%, N 0.51%. IR (KBr disc): ν_{max} 843, 964, 1117, 1282, 1344, 1467, 1616, 1749, 2893 cm^{-1}.

PS60: The same methodology as for PS62 was used to produce an ester of oxidised PEG_{3400} and salbutamol. Briefly, oxidised PEG_{3400} (2138 mg, 1.25 mmol of COOH) was reacted with thionyl chloride (500 µL, 6.88 mmol). PEG acyl chloride

was then reacted with a mixture of salbutamol dodecyl sulfate (1424 mg, 2.82 mmol) and 2,6 lutidine (780 μL, 6.70 mmol) for 37 min at 50°C. The crude product PS60S2 was purified by anion exchange ($IRACl^-$ in MeOH, 21 cm length, 24 mm ID), followed by a dilute HCl wash, and precipitation in diethyl ether to yield a white powder (η = 56%). Elemental analysis: measured C 53.59%, 8.74H %, N 0.45%, calculated C 54.50%, H 8.86%, N 0.54%. IR (KBr disc): ν_{max} 841, 951, 1103, 1248, 1346, 1466, 1616, 1747, 2874 cm^{-1}.

II.5. Conclusion

PEG of various molecular weights (1000, 2000, 3400 Da) and end groups (mPEG of PEG) were quantitatively oxidised and the primary hydroxyl groups turned into carboxylic acids. Esters of oxidised PEG and prednisolone and salbutamol were produced, purified and characterised. Overall, four prednisolone conjugates were produced (PEG_{1000}-$Pred_2$, PEG_{2000}-$Pred_2$, $mPEG_{2000}$-Pred, PEG_{3400}-$Pred_2$) and three salbutamol conjugates (PEG_{2000}-$Salbu_{1.25}$, $mPEG_{2000}$-$Salbu_{0.85}$, PEG_{3400}-$Salbu_{1.53}$). The synthesis of PEG-prednisolone ester conjugates produced fully conjugated polymeric prodrugs whereas PEG-salbutamol was more troublesome and only partial conjugations were achieved. The two conjugation and purification methods were highly reproducible and were repeated for several PEG molecular weights. The conjugates were obtained in high purity and sufficient amounts (gram scale) were produced for *in vitro* and *ex vivo* testing.

Chapter III. In vitro testing

III.1. Introduction

In vitro testing of pharmaceutics has always played a critical role in the drug development process but with pressure from authorities to reduce the use of animals, *in vitro* testing has become increasingly important and new models of tissue, organ, or disease are published regularly [119]. The conjugates were therefore tested *in vitro* to evaluate their aqueous stability and cytotoxicity. The aim of this chapter is to evaluate the behaviour of the conjugates *in vitro*, in systems of increasing complexity.

Firstly, aqueous stability of the conjugates was assessed in buffers at different pHs. The pH range was biologically relevant and covered the naturally occurring pH in the lung, according to published literature. The pH of exhaled breath condensate of healthy non smokers was measured at 7.43, 7.41 for asthmatic non smokers and 6.91 for asthmatic smokers [120], the pH was also lower (7.16) in patient with COPD [121]. In another study, exhaled breath condensates of healthy subjects had a pH of 6.08 [122]. Hunt measured the pH of exhaled airway vapours and obtained values of 7.65 and 5.23 for healthy subjects or individuals admitted to the hospital with acute asthma respectively [123]. In a fifth study, exhaled breath condensate of healthy individuals exhibited a pH of 8.27 and no difference was observed with patients suffering from COPD or asthma. Subjects with a cold, however, had a significantly lower pH value of exhaled breath condensate (7.56) [124]. Overall, there is a great variability in published pH values for exhaled breath condensate. Since there is no consensus on the pH value of lung fluids, a pH range (6.2 to 8.0)

rather than the usual *in vitro* assessment at pH 7.4 (blood pH) was chosen in this study to account for this variability.

The human bronchial epithelial cell line Calu-3 is a well established model of the human airways [72, 125]. The cells can be cultured in submerged conditions or at an air-liquid interface and both conditions are suitable models for the human airway epithelium [126] despite small morphological differences [77] [127]. Calu-3 cells have been used to study the transepithelial transport of drugs [128] [129], to characterise aerosols in the airways [130] or to measure local pharmacokinetic and metabolism of drugs [131] [132]. The Calu-3 cell line was therefore used as an *in vitro* model of the human airway epithelium in this study.

Cytotoxicity of the conjugates was then assessed using a measure of Lactate Dehydrogenase release from cells. Cell metabolism or cell membrane integrity are commonly used to assess cytotoxicity of a compound [133]. In the case of lung delivery, cell membrane integrity appeared to be of primary interest since the lung epithelium plays the role of a barrier and any variation in cell permeability would dramatically modify the epithelium absorption properties. The choice was also based on previous experiences in the laboratory and the ease of experimental procedure.

III.2. Material and methods

III.2.1. HPLC methodologies

For both drugs, the High Performance Liquid Chromatography (HPLC) system used for quantitative analyses was an Agilent 1050 series, equipped with a 21-position autosampler rack and an on-line degasser (Waldbronn, Germany), controlled by Chemstation software (rev A 08.03, Agilent). Ultrapure water was used throughout the analyses (18.2 $M\Omega.cm^{-1}$ at 25°C, delivered by a PureLab type of water purifier from ELGA, Marlow, UK). HPLC grade methanol, SDS, and analytical grade 85% phosphoric acid were purchased from Fisher scientific, prednisolone and triethylamine were purchased from Sigma and salbutamol sulfate was purchased from Alfa Aesar.

Stock solutions of drugs and conjugates were prepared in methanol. These solutions were serially diluted in methanol using positive displacement pipettes and analysed by HPLC. The peak area *vs* concentration was plotted and linear regression performed to assess the limits of quantification for each molecule. Known amounts of compounds were dissolved in buffers and analysed by HPLC to validate the method. Stock solutions and calibration solutions were stored for up to 2 months at -20°C.

III.2.1.1. Prednisolone

Prednisolone and prednisolone conjugates were analysed using a Gemini reverse phase C_{18} stationary phase (Phenomenex, Macclesfield, UK), 100 × 3 mm, 3 µm particle size. The mobile phase was a gradient of methanol in water from 65 to 90% organic in aqueous (Fig.III.1) at 0.5 $mL.min^{-1}$ and 10 µL of sample were injected. The column was maintained at 40°C and the detector set at 242 nm.

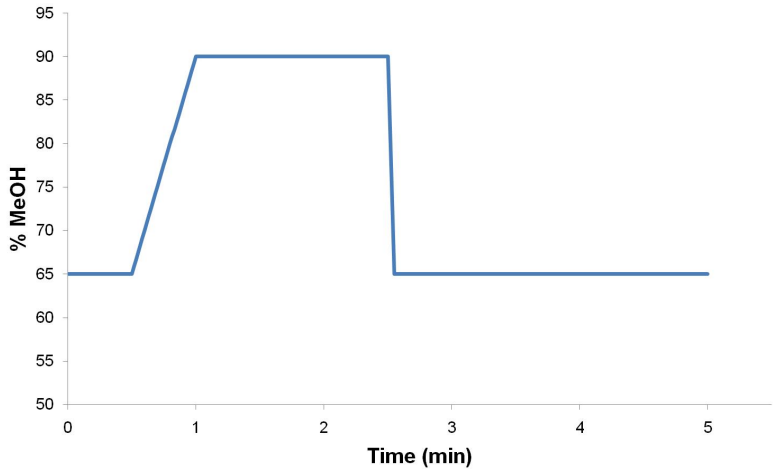

Fig.III.1. Gradient for HPLC analyses of prednisolone and prednisolone conjugates

Calibration solutions were prepared as a mixture of conjugate and prednisolone and the correlation between signal peak area for the two molecules and corresponding concentration was used to determine the calibration curve. Stock solutions of the conjugates and of prednisolone were prepared in methanol, according to Table. III.1. An example of solutions preparation for calibration of PP33 (PEG_{1000}-$Pred_2$) is given in Table. III.2, the solution preparation tables for the other conjugates are in Appendix 5, Table. VI.1 to Table. VI.3. Briefly, 64 µL of stock solutions of prednisolone and of the conjugate were mixed together with 172 µL of methanol to make up solution TA. Solution T1 was produced by diluting TA (32 µL) in methanol (168 µL). Two fold dilutions in methanol were then serially prepared (solutions R2 to R9).

Table. III.1. Stock solutions of prednisolone and prednisolone conjugates

Compound	Type	MW	Weight	Volume of MeOH	[Conjugate]	[Pred]
		Da	mg	µL	mM	mM
prednisolone	free drug	360.45	9.32	862	NA	29.9
PP33	PEG_{1000}-$Pred_2$	1700	19.76	775	15.0	30.0
PP28	$mPEG_{2000}$-$Pred_1$	2459	37.74	477	32.2	32.2
PP29	PEG_{2000}-$Pred_2$	2801	35.68	849	15.0	30.0
PP31	PEG_{3400}-$Pred_2$	4079	29.18	477	15.0	30.0

Table. III.2. Calibration solution preparation for P33

Solution	Volume of Pred stock	Volume of PP33 stock	Volume of methanol	[Conjugate]	[Prednisolone]
	µL	µL	µL	mM	mM
Pred-PP33 TA	64	64	172	3.20	6.40

Solution	Volume of Pred-PP28 TA	Volume of methanol	[conjugate]	[prednisolone]
	µL	µL	mM	mM
Pred-PP33 T1	32	168	0.51	1.02

Solution	Volume of standard	Volume of methanol	[Conjugate]	[Prednisolone]
	µL	µL	µM	µM
Pred-PP33 R2	200 µL of R1	200	255.97	511.94
Pred-PP33 R3	200 µL of R2	200	127.98	255.97
Pred-PP33 R4	200 µL of R3	200	63.99	127.98
Pred-PP33 R5	200 µL of R4	200	32.00	63.99
Pred-PP33 R6	200 µL of R5	200	16.00	32.00
Pred-PP33 R7	200 µL of R6	200	8.00	16.00
Pred-PP33 R8	200 µL of R7	200	4.00	8.00
Pred-PP33 R9	200 µL of R8	200	2.00	4.00

III.2.1.2. Salbutamol

Salbutamol and salbutamol conjugates were analysed using a Supelcosil reverse phase C_{18} stationary phase (Sigma), 150 × 4.6 mm, 5 µm particle size, monitored at 225 nm. The mobile phase was a gradient of methanol in aqueous buffer from 60 to 90% organic in aqueous (Fig.III.2) at 2 $mL.min^{-1}$ and 20 µL of sample were injected. The column was maintained at 40°C. To prepare 1L of buffer, 1.44 g of SDS were dissolved in 980 mL of ultrapure water, 8 mL of phosphoric acid (85%) were added and the mobile phase pH was adjusted to 2.5 with triethylamine (11 mL).

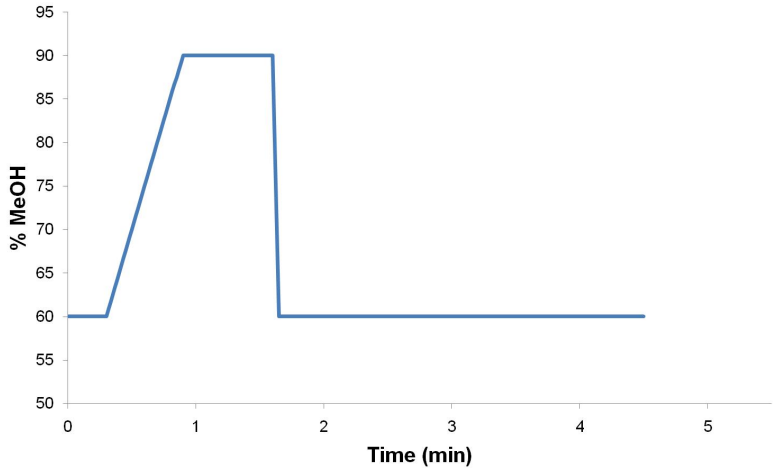

Fig.III.2. Gradient for HPLC analyses of salbutamol and salbutamol conjugates

Stock solutions were prepared in methanol according to Table. III.3, and calibration solutions were prepared by serially diluting the stock solutions in methanol (Appendix 6, Table. VI.4, Table. VI.5, Table. VI.6). After HPLC analysis, the correlation between signal peak area and concentration was used to determine the calibration curve.

Table. III.3. Stock solutions of salbutamol and salbutamol conjugates

Compound	Type	MW	Weight	Volume of MeOH	[conjugate]	[Salbu]
		Da	mg	µL	mM	mM
Salbutamol sulfate	free drug	576.71	3.94	455	NA	30.0
PS57	$mPEG_{2000}$-$Pred_1$	2336	76.74	930	35.3	30.0
PS60	PEG_{3400}-$Pred_2$	3987	44.11	590	18.8	28.7

III.2.2. Hydrolysis in simple buffers

III.2.2.1. Buffer preparation

Sodium phosphate salts were purchased from Sigma, other salts from Fisher Scientific.

Buffers were prepared at pH 6.2, 7.4, 8.0 and 9.0. Mc Ilvaine buffers [134] covered the range 6.2 to 7.4 and phosphate buffers covered the range 7.4 to 9.0. KCl was used to maintain a constant ionic strength of 0.5.

McIlvaine buffers of 0.5 ionic strength were prepared according to published literature [135]. Briefly, a solution of 0.2 M Na_2HPO_4 was prepared by dissolving 1.42 g of dry disodium hydrogen phosphate in 50 mL of deionised water. A solution of citric acid at 0.1 M was prepared by dissolving 10.51 g of dry citric acid in 500 mL of deionised water. Appropriate volume of citric acid and disodium hydrogen phosphate solutions were then mixed and KCl added to adjust ionic strength to 0.5 (Table. III.4). The pH was then adjusted with drops of HCl or NaOH 2 M.

Table. III.4. Recipe for Mc Ilvaine buffers

pH	0.2 M Na_2HPO_4	0.1 M citric acid	Total volume	KCl to get µ = 0.5
	mL	mL	mL	mg
6.2	33.05	16.95	50	530
7.4	45.425	4.575	50	24

Phosphate buffers at pH 7.4, 8.0 and 9.0 were prepared according to equation (III.1), using a pKa value of 7.21 for phosphate [136]. The complete recipe for phosphate buffer preparation is displayed in Table. III.5, the calculations were based on acid base reaction for phosphate:

(III.1) $pH = pKa + log\frac{[Na_2HPO_4]}{[NaH_2PO_4]}$

A solution of 0.1 M NaH_2PO_4 was prepared by dissolving 2.84 g of salt in 200 mL of deionised water. 0.1 M Na_2HPO_4 solution was prepared by dissolving 600 mg of salt in 50 mL of deionised water. Appropriate volumes of the two buffers were mixed together, required amount of KCl added and pH adjusted with drops of HCl 2M or NaOH 2M. The ionic strength, μ was calculated as follows:

(III.2) $\mu = \frac{1}{2}\sum_{i=1}^{n} c_i z_i^2$

Where c_i is the molar concentration of an ion of charge z_i.

e.g. For phosphate buffer at pH 7.4:

$\mu = \frac{1}{2}$ ([NaH_2PO_4]×(+1)^2 + [NaH_2PO_4]×(-1)^2 + 2 [Na_2HPO_4]×(+1)^2 + [Na_2HPO_4]×(-2)^2)

$\mu = \frac{1}{2}$ ($\frac{19.62mL \times 0.1M}{50mL}$×(1+1)+ $\frac{30.38mL \times 0.1M}{50mL}$×(2×1+4))

$\mu = \frac{1}{2}$ (0.03924×2 + 0.06076×6)

μ = 0.22152

The ionic strength was adjusted by adding KCl, which contribution was calculated as $\mu_{KCl} = \frac{1}{2}$ ([KCl]×(-1)^2 + [KCl]×(+1)^2)

μ_{KCl} = [KCl]

The required concentration of KCl needed for e.g. phosphate buffer at pH 7.4 is therefore 0.5 – 0.22 = 0.28 M. The number of moles of KCl in 50 mL of buffer is 0.05×0.28 = 0.014 moles (1.04 g).

Table. III.5. Recipe for Phosphate buffers

pH	NaH_2PO_4 0.1 M	Na_2HPO_4 0.1 M	V	μ	KCl to get μ = 0.5	
	mL	mL	mL		M	g
7.4	19.62	30.38	50	0.22	0.28	1.04
8	6.98	43.02	50	0.27	0.23	0.85
9	0.80	49.20	50	0.30	0.20	0.76

The buffers were filtered through 0.2 μm polyethersulfone filter (Sartorius), stored in the fridge and used within a month. Several batches of buffers were prepared during the course of the studies.

III.2.2.2. PEG-prednisolone

For practical reasons due to the different hydrolysis rates, three protocols were employed for hydrolysis studies. The general procedure consisted of preparing a concentrated stock solution (Table. III.7) of conjugate in MeOH (30 mM in prednisolone) and at time 0, adding a small amount of methanolic stock solution to pre-warmed buffer at 37°C. A 70 μL sample was taken at predetermined intervals and directly analysed by HPLC. Each study was done in triplicate. PP29 (PEG_{2000}-$Pred_2$) hydrolysis was used to test the continuity of the buffer range and hydrolysis was measured at pH 7.4 with the two buffer types.

- Protocol 1: In a glass vial with a magnetic stirrer, placed in a temperature-controlled oil bath, 3.5 mL of buffer was thermally equilibrated for more than 15 min. At time 0, 50 μL of stock solution in MeOH was added and samples were withdrawn regularly and directly analysed by HPLC. This protocol was followed for the first trials but the heating system (oil bath) was a bit messy and was later replaced by the use of a heat block.

- Protocol 2: One mL of buffer was transferred in a 1.5 mL centrifugation tube and placed to warm up at 37°C on a heat block for at least 15 min. To this solution was added 14.3 µL of conjugate stock solution in MeOH at time 0 (working concentration 423 µM in prednisolone). The tube was vortexed and left with no more agitation at 37°C. A 70 µL sample was regularly taken and directly analysed by HPLC. This protocol was used for hydrolyses at pH 7.4, 8.0 and 9.0.
- Protocol 3: At time 0, 14.3 µL of methanolic stock solution was added to 1 mL of pre-heated McIlvaine buffer at pH 6.2. The solution was then rapidly aliquoted in 70 µL individual scintillation vials, and placed in a temperature-controlled cabinet, at 37°C, 5% CO_2. The vials were then frozen at -80°C at regular intervals. They were all directly analysed by HPLC at once upon thawing. This protocol was used for hydrolysis studies at pH 6.2.

The following design of experiment (DoE) was used to measure the hydrolysis rates of PEG-prednisolone conjugates in simple buffers, each condition was performed in triplicates (Table. III.6):

Table. III.6. DoE for PEG-Pred hydrolysis study

Conjugate	Type	pH 6.2*	pH 7.4*	pH 7.4**	pH 8.0**	pH 9.0**
PP33	PEG_{1000}-$Pred_2$	P3	P2	-	P2	-
PP28	mPEG-Pred	P3	P2	-	P2	-
PP29	PEG_{2000}-$Pred_2$	P1 P3	P2	P2	P2	P1 P2
PP31	PEG_{3400}-$Pred_2$	P3	P2	-	P2	-

** Mc Ilvaine buffer, µ=0.5. ** Phosphate buffer, µ=0.5. P1/2/3: Protocol 1/2/3*

Table. III.7. Stock solutions for PEG-prednisolone hydrolysis studies

Conjugate	MW Da	Mass of conjugate mg	Volume of methanol µL	[Conjugate] mM	Corresponding [prednisolone] mM
PP33	1700	35.68	849	15	30
PP28	2459	37.74	509	30	30
PP29	2801	19.76	775	15	30
PP31	1700	29.18	477	15	30

III.2.2.3. PEG-salbutamol

Protocol 2 was used to assess the stability of PEG-salbutamol conjugates in buffers: the hydrolysis was conducted at different temperatures (in the fridge at 8°C, at room temperature, or 37°C). Samples were directly analysed by HPLC.

III.2.3. Cytotoxicity assay with Calu-3 cells

III.2.3.1. Cell culture

Human bronchial epithelial cells Calu-3 obtained from the American Type Culture Collection were maintained in Dulbecco's Modified Eagle's medium: nutrient mixture F-12 Ham (1:1) (Sigma) supplemented with 10% Foetal Bovine Serum (FBS), 100 UI.mL^{-1} penicillin and 100 µg.mL^{-1} streptomycin (Invitrogen), 2 mM glutamine (Invitrogen) and 1% v/v non-essential amino acids (100×, Invitrogen) at 37°C in a 5% CO_2 atmosphere. The cells were used between passage 20 and 40. When reaching approximately 90% confluence, the cells were split and 1/3 was used to seed a new 75 cm^2 cell culture flask.

For cytotoxicity experiments, Calu-3 cells were seeded on a 96 well plate (Corning Costar) at 1×10^5 cells.cm^{-2} and grown for 24 hours in maintenance medium until confluence.

III.2.3.2. Solution preparation

A stock solution of prednisolone in ethanol was prepared by dissolving 5.28 mg of prednisolone in 293 µL of ethanol (50 mM). This stock solution was then diluted (1/2) in serum free medium (Pred CA). Solution Pred CB was obtained by diluting Pred CA 50 fold in serum-free medium and the next dilutions were performed in serum-free medium containing 1 % ethanol, according to Table. III.8, so that the concentration in ethanol was maintained at 1% in the working solutions.

Table. III.8. Solution preparation for prednisolone cytotoxicity assay

Solution	Volume of standard µL	Volume of medium µL	[Prednisolone] µM	% EtOH
Pred CA	100 µL of stock	100 µL of medium	25000	50
Pred CB	80 µL of CA	3920 µL of medium	500	1
Pred CC	1700 µL of CB	1700 µL of medium*	250	1
Pred CD	1300 µL of CB	1950 µL of medium*	100	1
Pred CE	1250 µL of CB	1250 µL of medium*	50	1
Pred CF	450 µL of CB	1800 µL of medium*	10	1
Pred CG	220 µL of CB	1980 µL of medium*	10	1
Pred CH	200 µL of CB	1800 µL of medium*	0.1	1

** Medium contained 1 % EtOH*

Stock solutions containing the conjugates were prepared in ethanol at 0.1 M in prednisolone, according to Table. III.9.

Table. III.9. Stock solution preparation of PEG-prednisolone conjugates for cytotoxicity assays

Prednisolone conjugate	MW Da	Number of prednisolone per molecule of PEG	Mass for stock solution mg	Volume of EtOH for 0.1 M solution µL
PP28	2459	1	13.32	54
PP29	2801	2	15.27	109
PP31	4079	2	10.87	53
PP33	1700	2	8.10	95

The solutions were serially diluted (1/10) in ethanol (solution CA to CG). Each working solution was freshly prepared by adding 10 µL of ethanol solution (CA to CG) in 990 µL of serum free medium, so that the final ethanol concentration in all working solutions was 1%. The equivalent prednisolone concentrations tested ranged from 1000 µM to 0.0001 µM (8 solutions), according to Table. III.10.

Table. III.10. Dilutions for conjugate solution preparation for cytotoxicity assay

Solution	Volume of standard (µL)	Volume of ethanol (µL)	[Prednisolone] (mM) in ethanol	Actual [prednisolone] (µM) in medium
Conjugate Stock	NA	NA	100	1000
Conjugate CA	20 µL of Stock	180	10	100
Conjugate CB	20 µL of CA	180	1	10
Conjugate CC	20 µL of CB	180	0.1	1
Conjugate CD	20 µL of CC	180	0.01	0.1
Conjugate CE	20 µL of CD	180	0.001	0.01
Conjugate CF	20 µL of CE	180	0.0001	0.001
Conjugate CG	20 µL of CF	180	0.00001	0.0001

III.2.3.3. Lactate Dehydrogenase assay

A commercially available membrane integrity test was used (CytoTox-ONE, ref G7891, Promega). The principle of the test is based on measuring the release of Lactate Dehydrogenase (LDH) from Calu-3 cells (Scheme.III.1). LDH is a cytosolic enzyme that can leak out of damaged cells. The kit solutions provide lactate that is transformed into pyruvate by LDH, producing reduced Nicotinamide adenine dinucleotide (NADH) out of NAD^+ (supplied). Resazurin (supplied) is then transformed into resorufin (fluorescent) by diaphorase (provided), oxidising NADH, H^+ back to NAD^+.

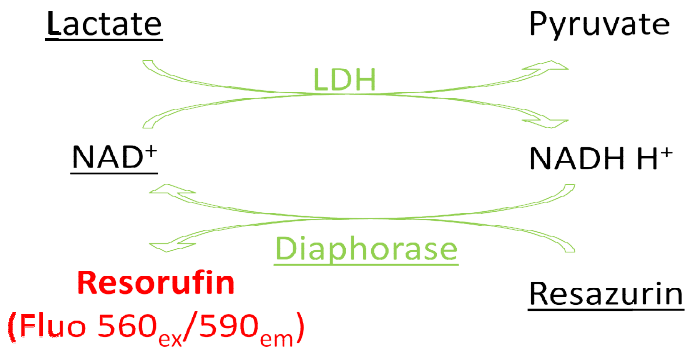

Scheme.III.1. LDH measure with CytoTox-ONE kit assay

The maintenance medium in each well was removed and the cells washed with 200 µL of Phosphate Buffered Saline (PBS) solution. At time 0, Calu-3 cells were incubated in 100 µL of the prednisolone or conjugate working solution at different concentration for 20 h at 37°C, 5% CO_2. The cell culture plate was then removed from the incubator and left to equilibrate at room temperature. For measuring the maximum release of LDH, 6 wells containing Calu-3 were exposed to 2 µL of lysis solution (9% (w/v) solution of Triton X-100 in water) for 5 min. In a black 96 well plate, 50 µL of medium was sampled from each well and 50 µL of substrate mix (containing lactate, NAD+ and resazurin) was then added and incubated at room

temperature for 10 min, shielded from light. Twenty-five microlitres of stop solution were then added and the fluorescence measured within an hour, after 10 s of shaking (excitation wavelength of 560 nm and emission wavelength of 590 nm) on an Infinite plate reader (Tecan).

Percentage of LDH release for a particular condition was calculated according to the manufacturer's instructions using the following formula (III.3):

(III.3) $$\% LDH = 100 \times \frac{Fluo_{exp} - \overline{Fluo_{back}}}{\overline{Fluo_{max}} - \overline{Fluo_{back}}}$$

Where:
$Fluo_{exp}$ is the experimental fluorescence measured for a particular well
$\overline{Fluo_{back}}$ is the average (n=6) fluorescence signal measured for cell culture medium background
$\overline{Fluo_{max}}$ is the average (n=6) fluorescence signal measured for cells exposed to lysis buffer (100% LDH release)

III.2.4. Hydrolysis in presence of Calu-3 cells

Calu-3 cells were seeded at a density of 74 000 cells.cm^{-2} on 3 wells of a 6-well cell culture plate and allowed to grow at 37°C, 5% CO_2 for 5 days until confluence in 2.9 mL of maintenance medium that was changed once during growth. The medium was then removed, the cells rinsed with warm PBS and 3 mL of warm serum-free medium added in all the wells. The correct volume of medium was removed from each well and replaced by the conjugate stock solution in ethanol (Table. III.11) so that the actual concentration of prednisolone was 700 µM for all experiment (700 µM of PP28 and 350 µM of PP29 and PP33).

Table. III.11. Conjugate stock solutions in ethanol for Calu-3 hydrolysis

Conjugate	MW Da	Mass of conjugate mg	Volume of ethanol µL	[Conjugate] mM	Corresponding [prednisolone] mM	Volume of ethanol solution µL
PP29	2801	38.42	392	35	70	30
PP28	2459	35.62	413.8	35	35	60
PP33	1700	26.7	449	35	70	30

The cell culture plates were then placed on a Stuart rocker and incubated at 37°C, 5% CO_2, under gentle see-saw waving (max angle 7°) and samples were withdrawn at specific time points. The sampling procedure was as follow: 30 µL of medium were mixed with 90 µL of cold methanol (prepared centrifuge tubes were stored at -20´C), vortexed and stored at -80°C before being centrifuged at 13,000 g, 4°C, upon thawing. Then the supernatant was collected and analysed using the previously established HPLC-UV methods (III.2.1 p.125).

III.2.5. Hydrolysis rate calculations and kinetic simulations

This section illustrates the methodology used to analyse the data collected during the two hydrolysis experiments: in buffers and in the presence of Calu-3 cells.

III.2.5.1. Simple case of mPEG-Pred

One mole of PP28 (mPEG-Pred) gave one mole of prednisolone and one mole of oxidised PEG (Scheme.III.2). The starting material and prednisolone concentrations were measured by previously established HPLC-UV methods. PEG was not monitored.

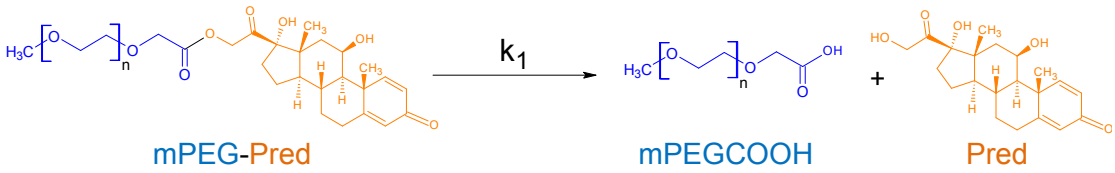

Scheme.III.2. Hydrolysis of PP28

Hydrolysis of esters in aqueous medium follows a pseudo-first order kinetics [137] and the rate law followed by the reactant PP28 was therefore

(III.4) $\frac{d[PP28]}{dt} = -k_1[PP28]$

Once integrated, the rate law for a first order kinetic expression became

(III.5) $[PP28]_t = [PP28]_0 e^{-k_1 t}$

$$ln[PP28]_t = ln[PP28]_0 - k_1 t$$

The pseudo-first order kinetic constant k_1 was calculated as the slope of the plot ln[PP28]=f(t). The logarithm transformation and linear regression were performed using Excel.

The half-life was defined as the time needed to degrade half of the starting concentration of PP28 and therefore

$$\ln [PP28]_{t_{1/2}} - \ln [PP28]_0 = -k_1 . t_{1/2}$$

$$t_{1/2} = -\frac{1}{k_1} \ln \left(\frac{1}{2}\right)$$

(III.6) $t_{1/2} = \frac{ln2}{k_1}$

III.2.5.2. Case of PEG-Pred$_2$

PEG-Pred$_2$ conjugates degraded in two steps in aqueous buffers, the first step generating one molecule of prednisolone and one molecule of an intermediate PEG-Pred$_1$. This intermediate further hydrolysed to give oxidised PEG and a second

molecule of prednisolone (Scheme.III.3). The starting material and prednisolone concentrations were measured by previously established HPLC–UV methods. The intermediate PEG-Pred$_1$ was visible by HPLC-UV but not quantifiable and PEG was not monitored.

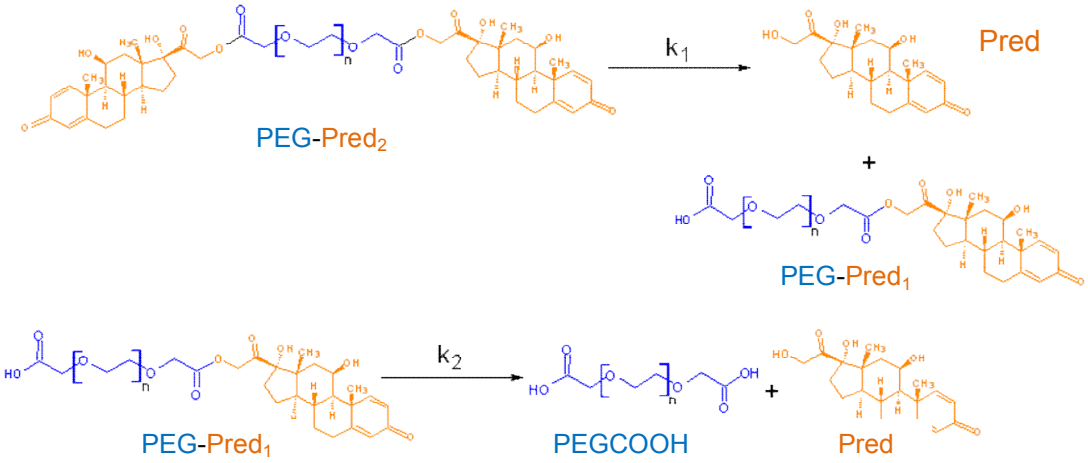

Scheme.III.3. Hydrolysis of PEG-Pred$_2$
Pred: prednisolone

The rate law for reaction 1 was $RXN1 = k_1[PEGPred_2]$ and $RXN2 = k_2[PEGPred_1]$ for reaction 2. PEG-Pred$_2$ was consumed in the reaction 1, prednisolone produced in reaction 1 and in reaction 2, PEG-Pred$_1$ was produced in reaction 1 and consumed in reaction 2 and oxidised PEG was produced in reaction 2. Therefore the rate laws for the four reactants were described by equation (III.7).

(III.7)

$$\begin{cases} \frac{d[PEGPred_2]}{dt} = -k_1[PEGPred_2] \\ \frac{d[Pred]}{dt} = k_2[PEGPred_1] + k_1[PEGPred_2] \\ \frac{d[PEGPred_1]}{dt} = k_1[PEGPred_2] - k_2[PEGPred_1] \\ \frac{d[PEG]}{dt} = k_2[PEGPred_1] \end{cases}$$

The constant k_1 was determined with Excel software in the manner described in III.2.5.1 (p. 138).

In the system of differential equations (III.7), PEG-$Pred_2$ and prednisolone were known (measured by HPLC-UV) and by solving this system, it was possible to simulate the concentrations of PEG and PEG-$Pred_1$ with time and calculated k_2. Berkeley Madonna software (v.8.3.18, the University of California, Berkeley, CA, USA), a solver of differential equations, was used to solve the system (III.7). The method used to determine the order of magnitude of k_2 and to simulate the concentrations of the intermediate PEG-$Pred_1$ and oxidised PEG was the following:

- The system of differential equations was written in the software
- The concentrations of prednisolone and PEG-$Pred_2$ were used as input (three sets of data for PEG-Pred concentrations with time (the three replicates) and three sets of data for prednisolone concentrations with time (the three corresponding replicates)
- The software was set to solve the equations and determine k_1, k_2 and the initial concentration of PEG-$Pred_2$.

The values calculated by the Berkeley-Madonna software for k_1 and initial concentration of PEG-$Pred_2$ were compared with respectively the value calculated for k_1 (using Excel) and with the theoretical value for the initial concentration of PEG-$Pred_2$ ($\frac{423}{2} = 211.5$ µM, III.2.2.2).

III.2.6. Statistical significance

Statistical tests were not systematically performed as the size of the data set generated was often too small to give meaningful statistically significant results compared to the number of tests to be performed. The relatively high number of groups and conditions tested meant a high probability of obtaining false positives due to the number of tests one could perform. Rather, the analysis was conducted using common sense and a careful examination of trends in the data. Nevertheless, where applicable, tests for equal means (null hypothesis H_0: $\mu_1 = \mu_2$) were applied when the data sets were normally distributed, with equal variance. One tailed Student's t-tests were used to statistically determine the significance (H_0 rejected if p-value < 0.05) of the difference between two sets of values.

III.3. Results and discussions

III.3.1. HPLC calibration

The linearity range for prednisolone compounds was 1 to 1000 µM (Table. III.12), and 5 to 500 µM for salbutamol compounds (Table. III.13). These results were sufficient for the purpose of *in vitro* testing where concentrations of drugs were artificially high compared to *in vivo* biologically relevant experiments. The standard solutions were used regularly to calibrate the system.

Table. III.12. HPLC characteristics of prednisolone and PEG-prednisolone conjugates

Compound	Retention time min	LLOQ µM	ULOQ µM
prednisolone	2.1	0.06	1024
PP33	4.4	2.00	256
PP28	4.0	1.07	1092
PP29	4.4	0.25	512
PP31	4.4	7.84	502

LLOQ: Lower Limit Of Quantification, ULOQ: Upper Limit Of Quantification

Table. III.13. HPLC characteristics of salbutamol and PEG-salbutamol conjugates

Compound	Retention time min	LLOQ µM	ULOQ µM
Salbutamol sulfate	1.11	4.7	601
PS60	2.40	7.3	469
PS57	2.16	5.5	707

LLOQ: Lower Limit Of Quantification, ULOQ: Upper Limit Of Quantification

III.3.2. Hydrolysis in simple buffers

This section illustrates the results obtained for hydrolysis studies in simple buffers for prednisolone and salbutamol ester conjugates.

III.3.2.1. PEG-prednisolone

a. Simple case of PP28

Fig.III.3 illustrates the degradation and appearance profiles of PP28 (▲) and prednisolone (▲) respectively, in McIlvaine buffer at pH 7.4 and 37°C. The degradations of the conjugate in buffers at different pH values and 37°C gave typical pseudo-first rate kinetic degradation profiles. Other examples of hydrolysis profiles at pH 6.2 and 8.0 are exhibited in appendices (Appendix 7, Fig.VI.50, Fig.VI.51).

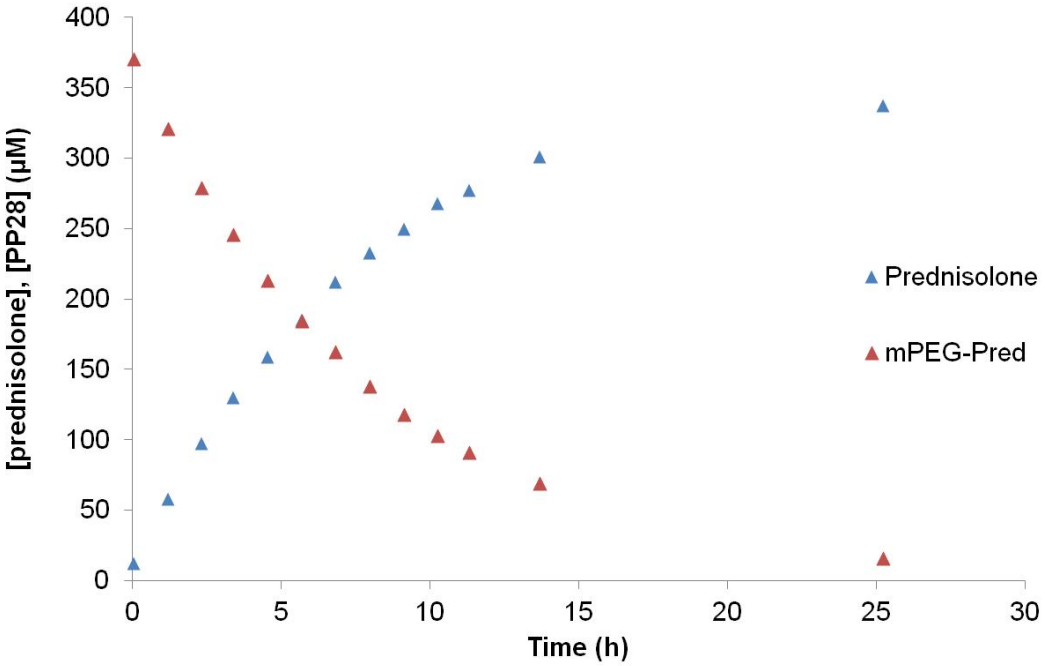

Fig.III.3. Hydrolysis profile of PP28 ($mPEG_{2000}$-Pred) in McIlvaine buffer at pH 7.4

The plot of ln(PP28) *vs* time gave a straight line (Fig.III.4), confirming that the degradation followed pseudo-first order kinetics and the slope of ln[PP28] = f(time) gave the first order degradation constant k_1.

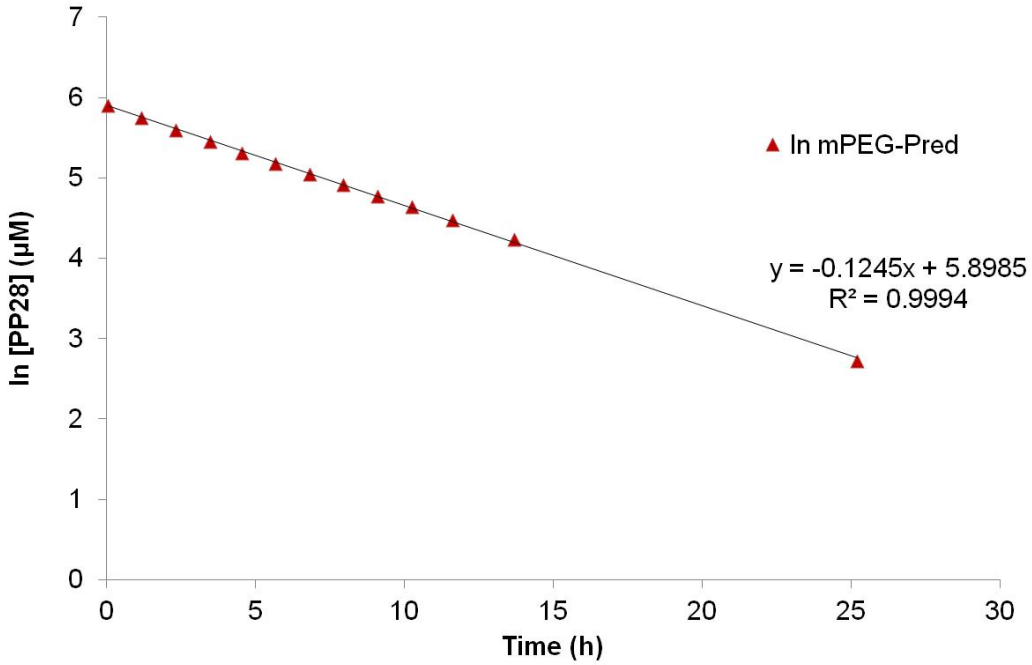

Fig.III.4. Plot of ln[PP28] vs time at pH 7.4
Logarithmic transformation and linear regression performed using Excel

Using equation (III.5), the first order degradation constant for PP28 at pH 7.4 and 37°C was determined as **0.1245 h^{-1}**. The corresponding half-life was then calculated as $t_{1/2} = \frac{ln2}{0,1245}$ (III.6)

$$t_{1/2} = 5.57 \text{ h}$$

The same methodology was repeated for all three replicates for all three pHs. The values for calculated half-lives are consigned in Table. III.14.

b. Cases of the disubstituted PEG-Pred$_2$

An example of a typical hydrolysis profile for PP29 (PEG_{2000}-$Pred_2$) at pH 7.4 and 37°C is illustrated in Fig.III.5. Similarly to PP28, a first order kinetic was deduced from the plots of ln [PP29] = f(time) (Appendix 7, Fig.VI.52). Other degradation profiles are displayed in Appendix 7. Half-lives were calculated according to equation (III.6). The results for the calculated half-lives for all conjugates are combined in Table. III.14 and illustrated in Fig.III.6

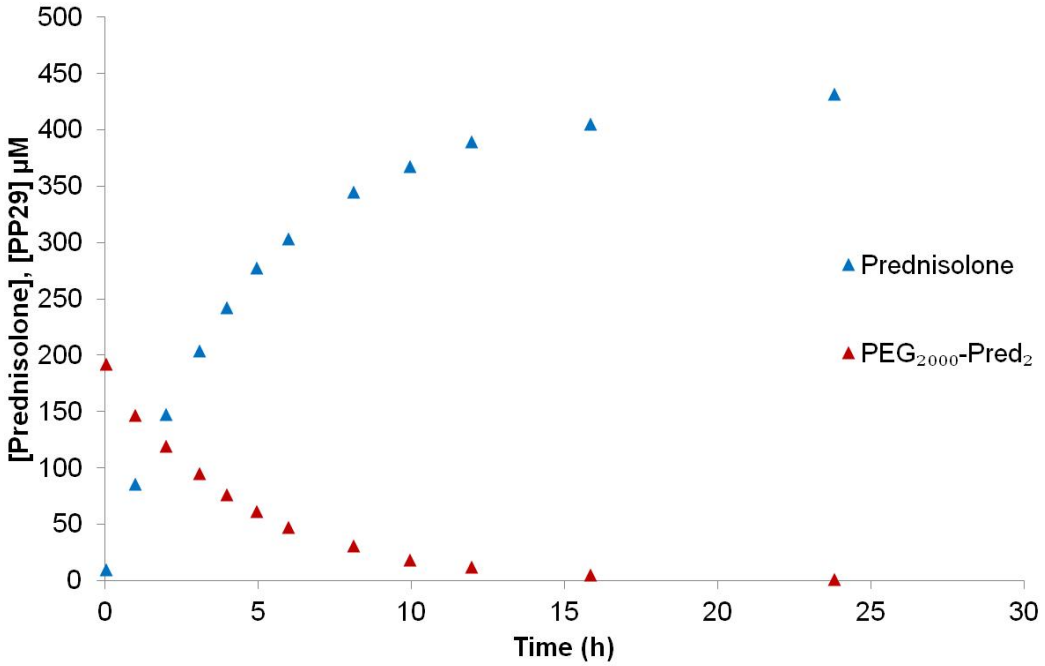

Fig.III.5. Hydrolysis profile of PP29 (PEG_{2000}-$Pred_2$) in McIlvaine buffer at pH 7.4

Table. III.14. Calculated half-lives, in hour, for PEG-prednisolone conjugates in buffers of various pHs

Conjugate	Type	pH 6.2*	pH 7.4	pH 8.0**	pH 9.0**
PP33	PEG_{1000}-$Pred_2$	38.37 ±1.38	2.84 ±0.05*	0.91 ±0.01	
PP28	$mPEG_{2000}$-Pred	73.28 ±0.17	5.58 ±0.03*	2.01 ±0.03	
PP29	PEG_{2000}-$Pred_2$	33.94 ±0.20^{P2} 32.30 ±0.23^{P1}	2.97 ±0.01* 3.35 ±0.005**	1.00 ±0.02	0.18 ±0.005$^{P1/2}$
PP31	PEG_{3400}-$Pred_2$	40.12 ±0.60	3.02 ±0.02*	0.94 ±0.001	

** Mc Ilvaine buffer, µ=0.5. ** Phosphate buffer, µ=0.5. P1/2: Protocol 1 and protocol 2 were used. Average of n=3±SD*

The hydrolysis of PP29, in McIlvaine and phosphate buffer at pH 7.4, gave half-life values of respectively 2.97 (±0.01) and 3.35 (±0.005) h. Although statistically significantly different, these two values were within 13% of each other and therefore the two buffer systems provided a continuous range of pH to study the conjugates aqueous stability. Nevertheless, this difference illustrated the limitations of such in vitro studies where the type of buffering agent might play a role in the hydrolysis rate.

The comparison of the two experiments for PP29 hydrolysis at pH 6.2, reveals that stirring the solution during hydrolysis (protocol 1) statistically significantly increased the hydrolysis rate by 5% (32.30±0.23 h with stirring and 33.94±0.20 h in static conditions).

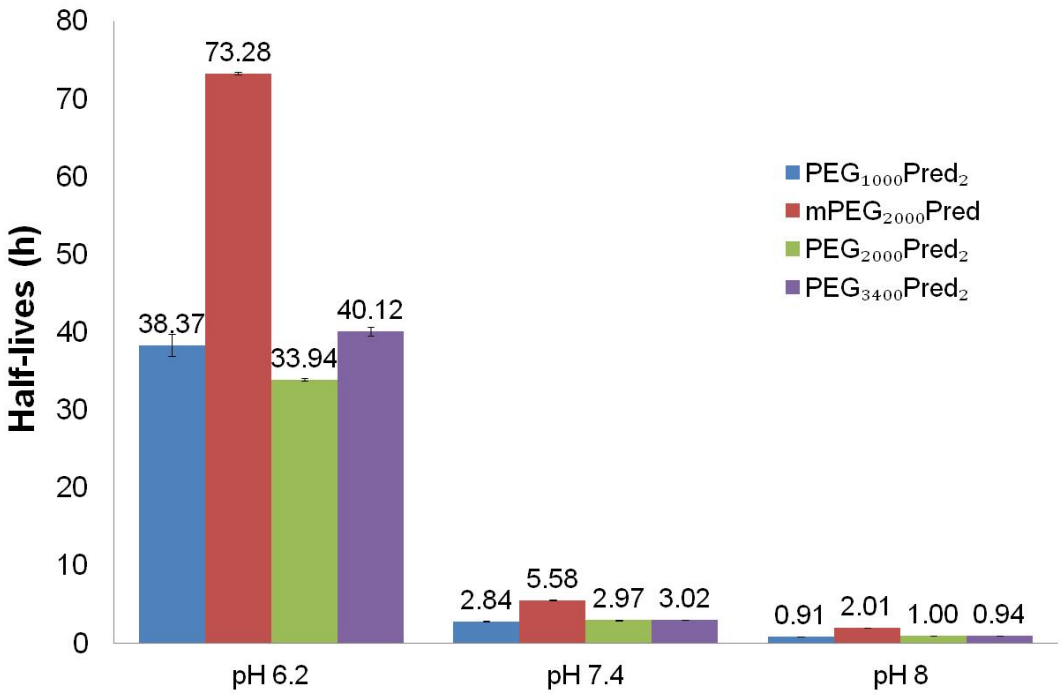

Fig.III.6. Half-lives of PEG-prednisolone conjugate hydrolysis in buffers at pH 6.2, 7.4 and 8.0
Data are mean of 3 ± SD

This study also revealed that the hydrolysis rate was pH dependent. Fig.III.7 illustrates the free-energy relationship between the logarithm of hydrolysis rate (log(k)) and the logarithm of proton concentration (-pH) for PP29, over the pH range 6.2 to 9.0.

For each pH, the aqueous stability of the three disubstituted conjugates (PEG-$Pred_2$) were similar. For example at pH 7.4, the hydrolysis half-lives of PP33, PP29 and PP31 (respectively PEG_{1000}, PEG_{2000} and PEG_{3400}-$Pred_2$) were between 6% of each other (Table. III.14). The same was true at pH 6.2 and 8.0 where values were respectively within 18% and 10% range (Table. III.14).

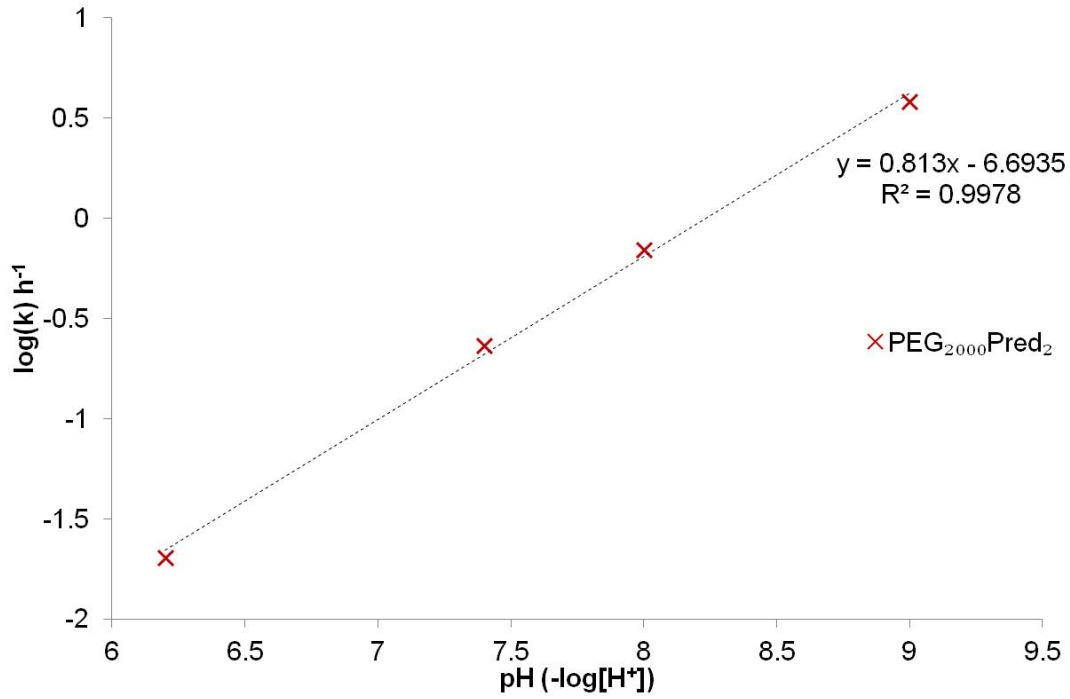

Fig.III.7. Free-energy linear relationship between log(k) and log[H^+] for PP29 hydrolysis
Logarithm transformation and regressions performed using Excel

Finally, the half-life of hydrolysis for $mPEG_{2000}$-Pred (PP28) was twice the value of those of $PEG\text{-}Pred_2$, at pH 6.2, 7.4 and 8.0. Therefore, mPEG-Pred was twice as stable as $PEG\text{-}Pred_2$, over the polymer molecular weight and pH range studied.

The intermediate $PEG\text{-}Pred_1$ was not isolated neither was it specifically produced to measure its degradation kinetics using a HPLC-UV method. However, a low trace signal of this intermediate compound was visible with HPLC-UV (but not quantifiable) at a retention time similar to this of $mPEG\text{-}Pred_1$ (4.05 min). The release profile of prednisolone in the buffer was used to determine the value of k_2, hydrolysis rate constant of $PEG\text{-}Pred_1$.

Fig.III.8 illustrates a comparison between a simulated and a calculated degradation profile for $PEG_{2000}\text{-}Pred_2$ (PP29) at pH 7.4 and 37°C, obtained using Berkeley-Madonna software. The simulated profile (dotted lines) was calculated under the assumption that the hydrolysis rate constant of $PEG\text{-}Pred_1$ would be similar to that of $mPEG\text{-}Pred_1$ (PP28) at pH 7.4 ($t_{1/2}$ = 5.58 h, k = 0.124 h^{-1}). The calculated profile (plain lines) was obtained by fitting the experimental data of PP29 hydrolysis at pH 7.4.

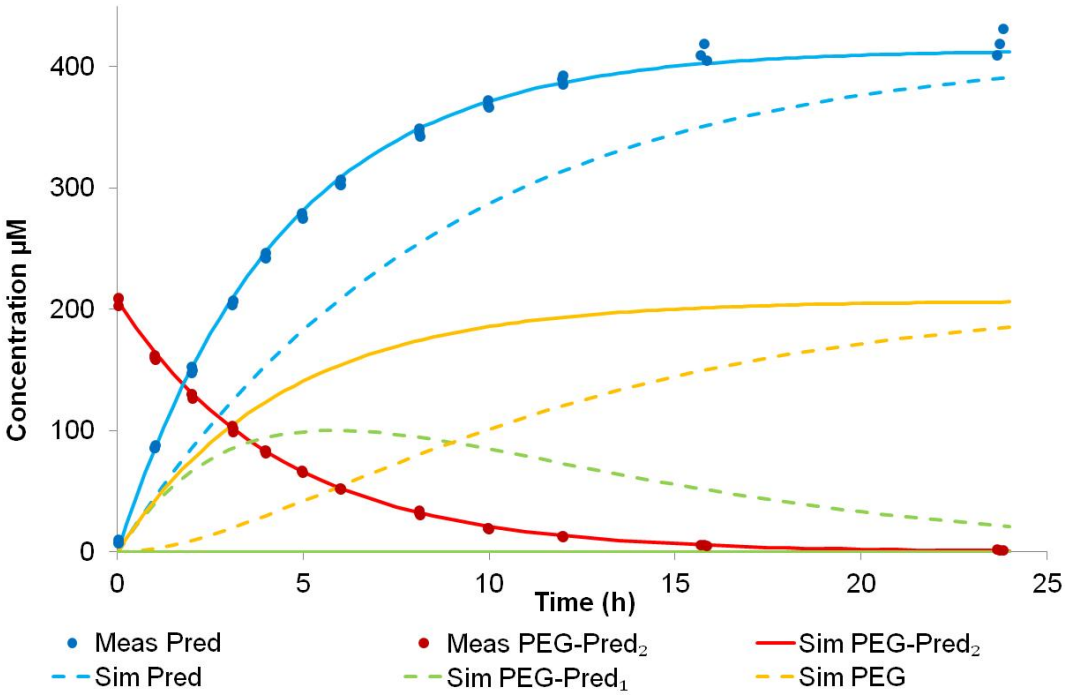

Fig.III.8. Degradation profile of PEG_{2000}-$Pred_2$ at pH 7.4 and simulation using mPEG-$Pred_1$ rate constant

Meas: Measured values, Sim, plain lines: Simulated values obtained after solving the system differential equation (III.7) using Berkeley Madonna software. Calculated k_1 = 0.228651 h^{-1}, k_2 = 10.9662 h^{-1}, initial PEG_{2000}-$Pred_2$ = 207 µM, Sim, dotted lines: Simulated values obtained using k_1 = 0.228651 h^{-1}, k_2 = 0.124323 h^{-1}, initial PEG_{2000}-$Pred_2$ = 207 µM

By setting the value of k_2 equal to that of mPEG-Pred hydrolysis rate constant, a delay in prednisolone appearance (- - -) was observed as compared to the real, fitted prednisolone (—) profile. The hydrolysis profile of PEG-$Pred_2$ remained obviously unchanged since it was only described by k_1. Under this assumption, the concentration of the intermediate PEG-$Pred_1$ (- - -) was not negligible since it went up to 100 µM in this example. In this case, the calculated value for k_2 was found to be 88 times that of mPEG-Pred hydrolysis rate constant.

These simulations were repeated for all experiments (the four conjugates and the three different pH) and the values obtained for the constants k_2 were consistently much higher than the hydrolysis rate constant of mPEG-Pred and much higher than

k_1. This meant that the concentration of PEG-$Pred_1$ could be neglected and the hydrolysis simplified to

$$PEGPred_2 \xrightarrow{k_1} 2Pred + PEG$$

An example of a simulation obtained for PP29 (PEG_{2000}-$Pred_2$) hydrolysis at pH 6.2 is displayed in Fig.III.9. The concentration of PEG-$Pred_1$ remained always below 14 µM, which is negligible in comparison to the concentration of the other entities.

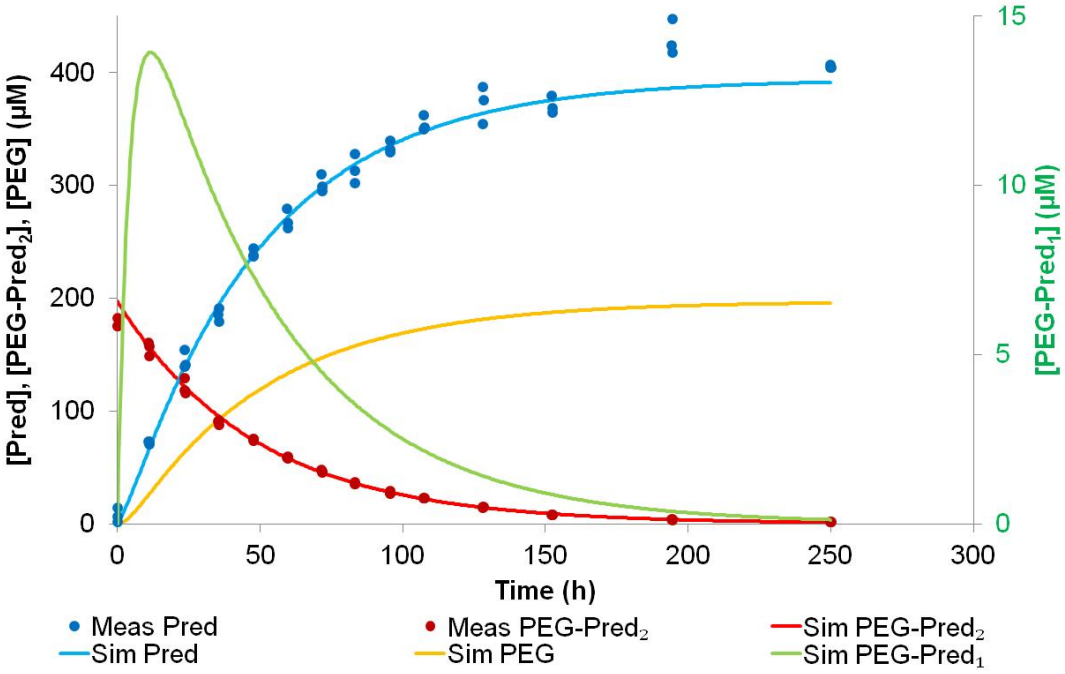

Fig.III.9. Simulation for PP29 hydrolysis at pH 6.2
Meas: Measured values, Sim: Simulated values obtained after solving the system differential equation (III.7) using Berkeley Madonna software. Calculated k_1 = 0.020455 h^{-1}, k_2 = 0.228221 h^{-1}, initial PEG_{2000}-$Pred_2$ = 197 µM.

Overall, the simulations gave meaningful results since the calculated initial concentrations of the conjugates were those expected. Berkeley Madonna used the degradation profile of PEG-$Pred_2$ and the appearance profile of prednisolone to estimate k_1, k_2 and the initial conjugate concentration. Whereas the simple excel regression used only the PEG-$Pred_2$ degradation profile to estimate k_1. Berkeley Madonna software was mainly used to determine the instability of the intermediate

compound PEG-Pred$_1$ and reliable simulations required good mass balance regarding the total amount of prednisolone measured in the system. Nevertheless, the fitted hydrolysis rate constants using both methods (excel and Berkeley Madonna) were very close. For example, k_1 for PP29 at pH 6.2 was calculated as 0.20455 h^{-1} with Berkeley Madonna software and 0.020423 h^{-1} using excel regression.

III.3.2.2. PEG-salbutamol

The hydrolysis of PEG-salbutamol conjugates was extremely fast compared to that of PEG-prednisolone conjugates. The optimal conditions for approximating hydrolysis rates were found to be room temperature for pH 6.2 and 8°C for pH 7.4. At pH 8.0, the hydrolysis was so fast, even at 8°C, that no reliable result was obtained. Approximate values for hydrolysis half-lives were calculated using Berkeley Madonna software, and the following equations were used to simulate PEG-salbutamol hydrolysis rates:

(III.8) $$mPEGSalbu_1 \xrightarrow{k_1} Salbu + mPEG$$

$$PEGSalbu_2 \xrightarrow{k_1} Salbu + PEGSalbu$$

$$PEGSalbu \xrightarrow{k_2} Salbu + PEG$$

Table. III.15 summarises the calculated hydrolysis rates for PEG-salbutamol conjugates:

Table. III.15. Hydrolysis rate constants and corresponding half lives for PEG-salbutamol at pH 6.2 and 7.4

pH	T	Type	Order	k_1	$t_{1/2}$ min	k_2	$t_{1/2}$ min
6.2	RT	$mPEG_{2000}$-Salbu	First	1.53 h^{-1}	27.2		
7.4	8°C		Second	22.36 $h.L.nmol^{-1}$	6.9[a]		
6.2	RT	PEG_{3400}-$Salbu_2$	First	3.21 h^{-1}	12.9	2.72 h^{-1}	15.3[b]
7.4	8°C		Second	91.74 $h.L.nmol^{-1}$	2.7[b]	57.19 $h.L.nmol^{-1}$	16.1[c]

[a]*Calculated using initial [mPS_1] = 389 µM,* [b]*Calculated using initial [PS_2] = 240.18 µM,* [c]*Calculated using initial [PS_1] = 65.14 µM, RT: Room Temperature*

Once again, the hydrolysis rate of the disubstituted conjugate PS60 was approximately twice as fast as that of the monosubstituted conjugate PS57 (Table. III.15). The intermediate PEG-$Salbu_1$ had half-lives of 15-16 min at pH 6.2 and 7.4.

III.3.2.3. Discussion

Ester hydrolysis in aqueous solutions was described in depth by Erkki K. Euranto [137] and is driven by three mechanisms: acid, neutral and base catalysed hydrolyses.

The actual overall rate is described by

(III.9) $$\frac{d[ester]}{dt} = -(k_{\mathrm{OH}}[HO^-] + \mathrm{k_0} + \mathrm{k_H}[H_3O^+])[ester]$$

Where k_{OH} and k_H are the rate coefficients of respectively hydroxide-ion and hydrogen-ion catalysed hydrolysis (in $mol.L^{-1}.h^{-1}$), [HO^-] and [H_3O^+] are respectively the concentrations of hydroxide and hydrogen ions, and k_0 is the neutral hydrolysis rate constant (in h^{-1}).

At any given pH, one of the three mechanisms dominates and the overall rate of hydrolysis is considered to be pseudo first order kinetics, and is described as:

(III.10) $$\frac{d[ester]}{dt} = -k_t[ester]$$

Where k_t is the pseudo first order observed rate constant, [ester] is the concentration in ester

For most ester compounds, $k_{OH} > k_{H}^{+}$ and therefore the minimum hydrolysis rate is obtained at acidic pH and the reaction is driven by a base-catalysed mechanism. Nowadays, an addition-elimination mechanism is used to describe the base-catalysed ester hydrolysis [137] as shown in Scheme.III.4:

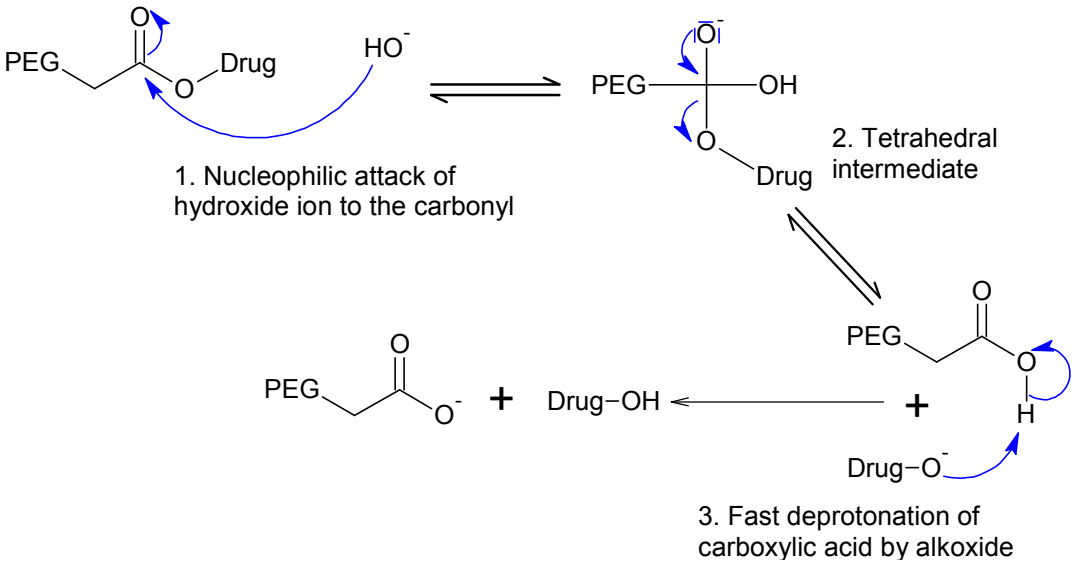

Scheme.III.4. Base-catalysed ester hydrolysis

The slower hydrolysis rate of mPEG-Pred$_1$ compared to PEG-Pred$_2$ can be explained by the formation of micelles. It can indeed be hypothesised that in aqueous buffers, the monosubstituted conjugate can easily self-assemble into micelles, the terminal prednisolone playing the role of a lypophilic head and the PEG chain a hydrophilic tail (Fig.III.10). On the other hand, it may be more difficult for the the disubstituted conjugates to form micelles due to the relatively short polymer length, and despite the polymer chain flexibility. Micelles of methoxy-PEG$_{3500}$-succinyl-(Embelin)$_2$ were produced by Y. Huang with a diameter of about 20 nm [138]. The protocol used to study the hydrolysis kinetics of PEG-drug conjugates may be suitable for the formation of micelles, since it bears some similitude with the interfacial deposition method [139] of producing nanoparticles,

where ethanol is used as organic solvent. The ester link could therefore be protected from hydrolysis, being isolated from hydroxyl (HO^-) and hydroxonium (H_3O^+) ions in the lypophilic core of the micelles.

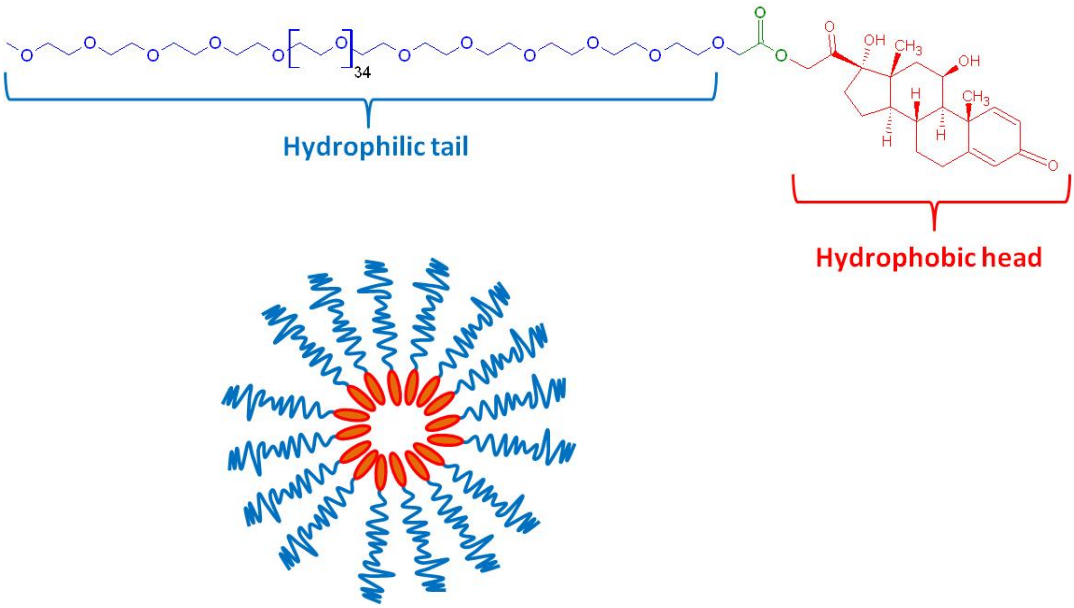

Fig.III.10. Possible micelle formation with mPEG-Pred

The hydrolysis of PEG-$Pred_2$ gives a molecule of prednisolone and PEG-$Pred_1$ which differs from mPEG-$Pred_1$ only by the terminal group. The former possesses a carboxylate where the later is end-capped by an unreactive methyl group.

As demonstrated in III.3.2.1 (p.151), $^-$OOC-PEG-$Pred_1$ is very unstable in aqueous buffers, whereas mPEG-$Pred_1$ is stable. This difference of stability may be explained by the neighbouring group participation [140] of the carboxylate. This group potentially catalyses the ester hydrolysis by intramolecular nucleophilic or base catalysis (Scheme.III.5). The hydrolysis of acetyl salicylic acid [141] [142] and other acyl esters of salicylic acids has been extensively studied [143] and it was concluded that hydrolysis is mostly driven by intramolecular base catalysis [144] [145] [146], whereas the hydrolysis of 3,5-dinitroaspirin carboxylate anion and of

monophenyl esters of dibasic acids were catalysed by intramolecular nucleophilic processes [147, 148]. Other mechanisms have been proposed to describe neighbouring influence of carboxylic acids/carboxylate on the hydrolysis rate of ester hydrolysis, such as electrophilic participation and bifunctional catalysis [137].

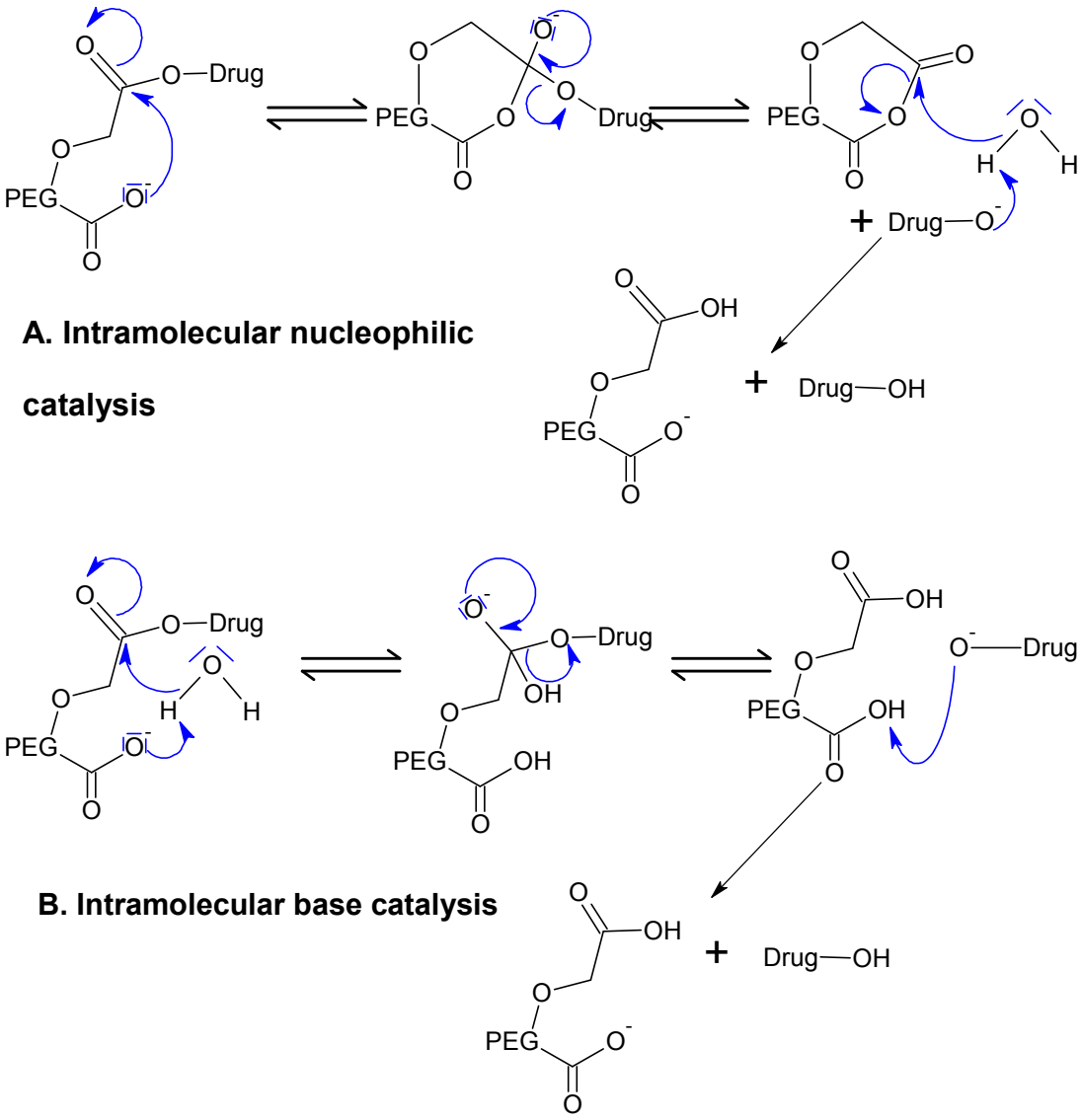

Scheme.III.5. Intramolecular nucleophilic (**A**) and intramolecular base (**B**) catalysed hydrolysis of PEG-Pred$_1$ by carboxylate

PEG-salbutamol hydrolysis rates were much faster than those of PEG-prednisolone and they differed from those of published experiments with prodrugs of salbutamol. In 1994, it was reported [149] that triesters of salbutamol (acetyl, isobutyl and pivalyl) hydrolysed at a rate of 0.2 to 0.5 $days^{-1}$ at pH 7.4. The difference observed could be explained by the fact that these esters are highly lipophilic compared to PEG-salbutamol. Also, the three hydroxyl groups of salbutamol were conjugated and the ester links of the resulting prodrugs were more hindered than in □□□□□=1721.8 □□□□−□□1

same conclusions could be drawn from another study published in 2000, where triesters of butyryl-salbutamol hydrolysed slowly in approximately 45 minutes in lung homogenate, despite the possible presence of esterases [150]. Those two publications lacked a kinetic study and the analytical methods did not allow any quantification of the intermediates (diester and monoester) that led to the release of salbutamol, a conjugate possessing a secondary amine group whereas prednisolone conjugates do not. Inter or intramolecular catalysis could easily explain the fast hydrolysis rate for salbutamol derived compounds. It has previously been reported that intramolecular catalysis of ester hydrolysis by nitrogen containing groups such as imidazole [151], amide [152], but more importantly by protonated amino groups [153-157] can dramatically increase the hydrolysis rate (Scheme.III.6). The later cooperative neighbouring effect is thought to be driven by an intermolecular acid-catalysed mechanism, and then attack of a hydroxide ion, potentially involving a hydrogen bonding with the protonated amino group and the double bonded oxygen of the ester link [158]. The deprotonated amine group could also be involved in an intramolecular base catalysis similar to that of carboxylate (Scheme.III.7).

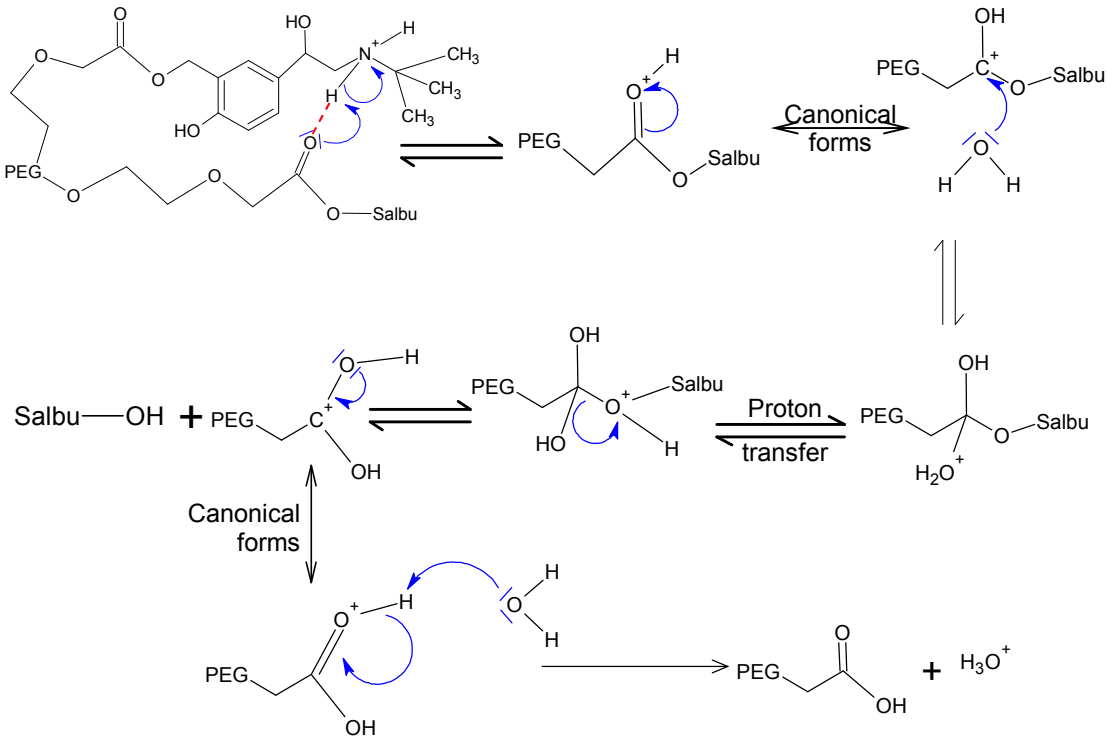

Scheme.III.6. PEG-salbutamol intramolecular acid catalysis with protonated amine

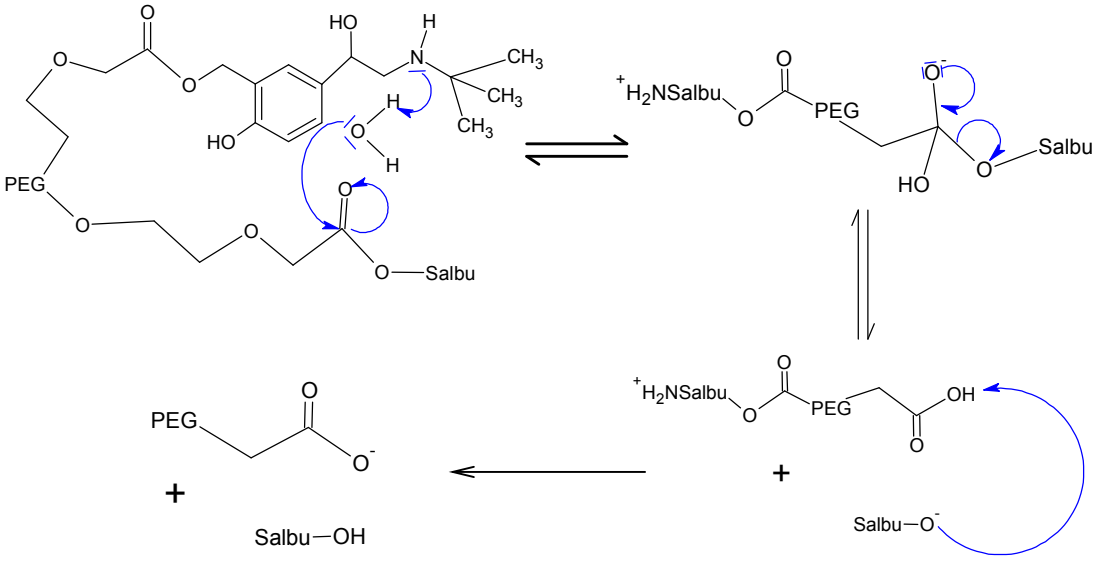

Scheme.III.7. PEG-salbutamol intramolecular base catalysis with deprotonated amine

In the pH range studied, the salbutamol amino group is mostly protonated, since the pKa for salbutamol amine group is 9.22 [111] and therefore the acid catalysed mechanism (Scheme.III.6) is more likely. This intramolecular acid catalysis of alkaline hydrolysis has previously been described by Deng et al. [159, 160] for cocaine. The amine group from another conjugate molecule could potentially catalyse the hydrolysis via intermolecular catalysis; therefore, the hydrolysis of PEG-salbutamol was probably catalysed by both intra- and intermolecular processes (Scheme.III.8).

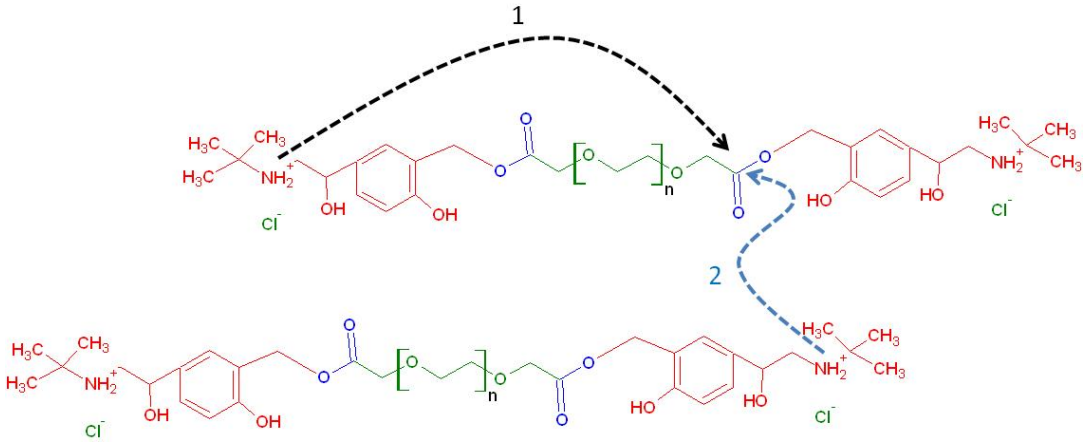

Scheme.III.8. Intra (1) and intermolecular (2) catalysis of PEG-salbutamol hydrolysis

III.3.3. Cytotoxicity assays

This section presents the cytotoxicity study conducted with PEG-prednisolone conjugates on the human airway epithelial cell line Calu-3. Cytotoxicity was assessed using LDH release from the cells.

III.3.3.1. Results

Spontaneous LDH release from Calu-3 cells was used as an internal standard for interpretation of the values obtained. The following graphs display the average % of LDH release from Calu-3 after 20 h incubation with prednisolone and PEG-prednisolone conjugates.

A. Prednisolone

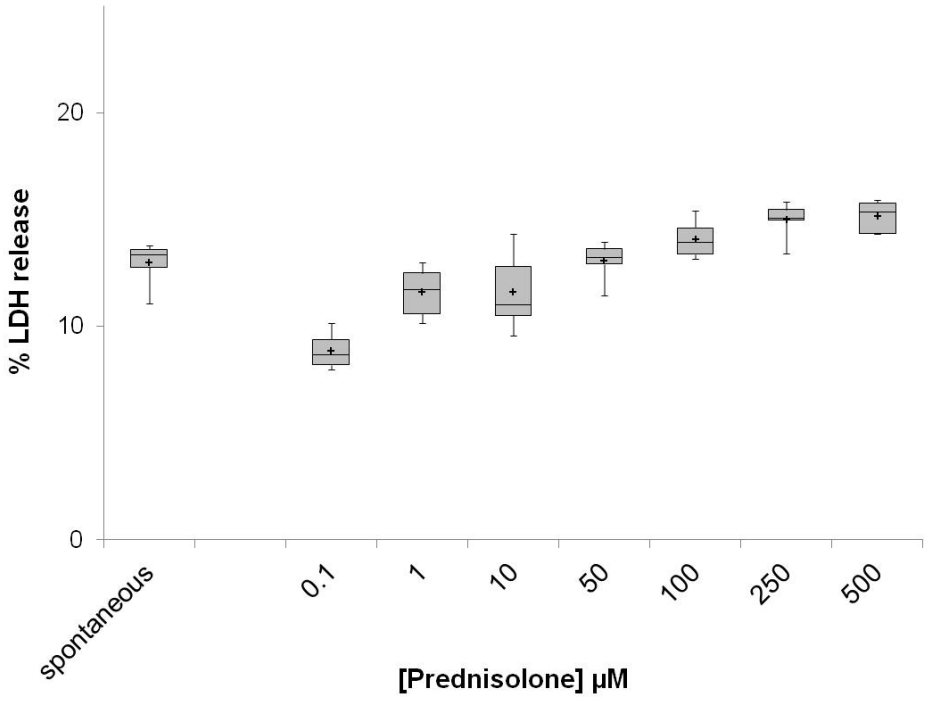

B. PEG_{1000}-$Pred_2$ (PP33)

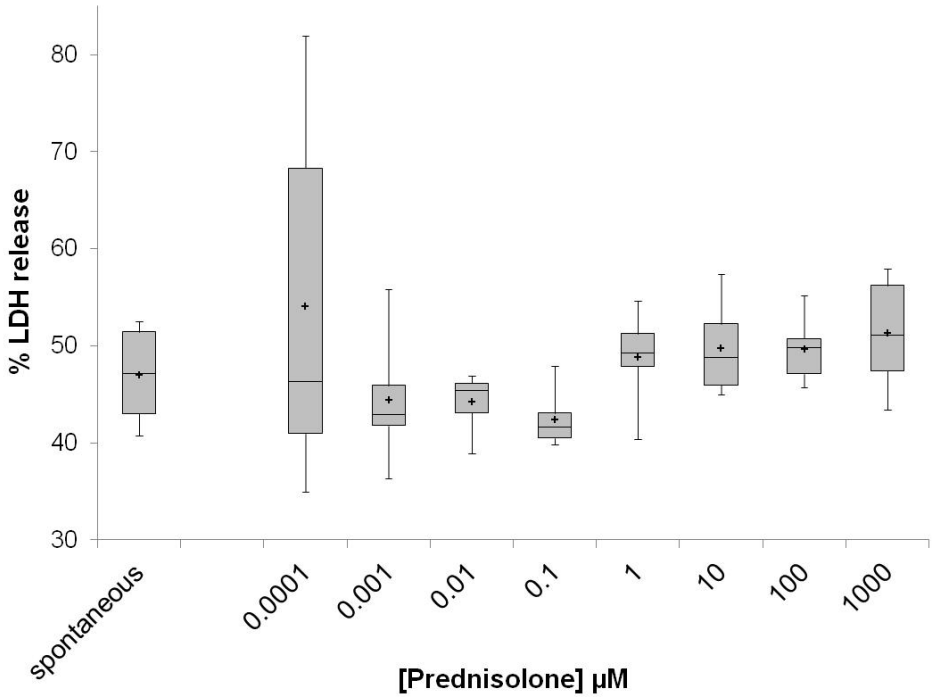

C. $mPEG_{2000}$-$Pred_1$ (PP28)

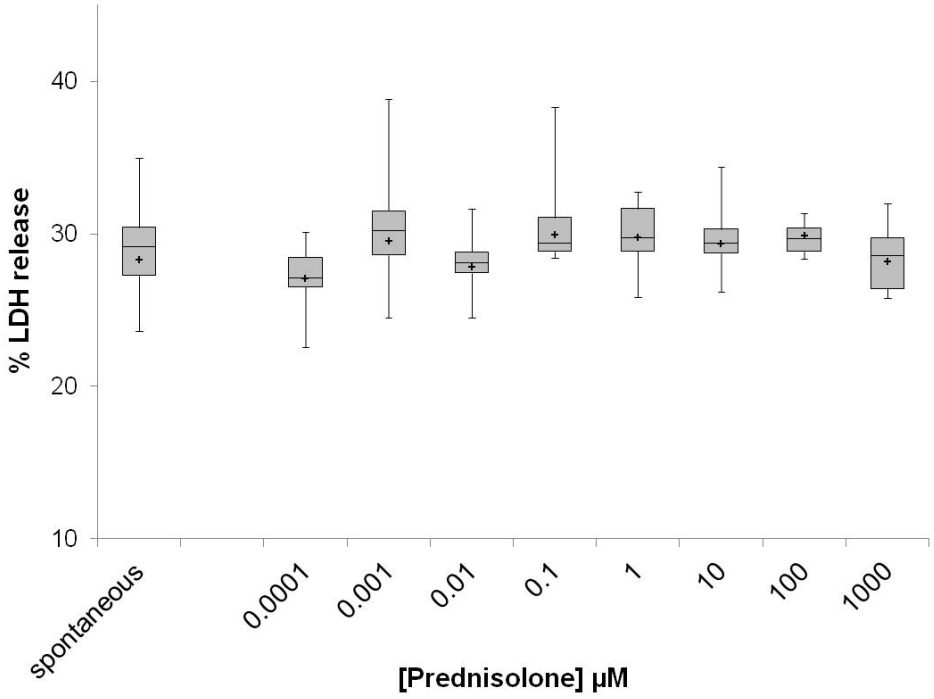

D. PEG_{2000}-$Pred_2$ (PP29)

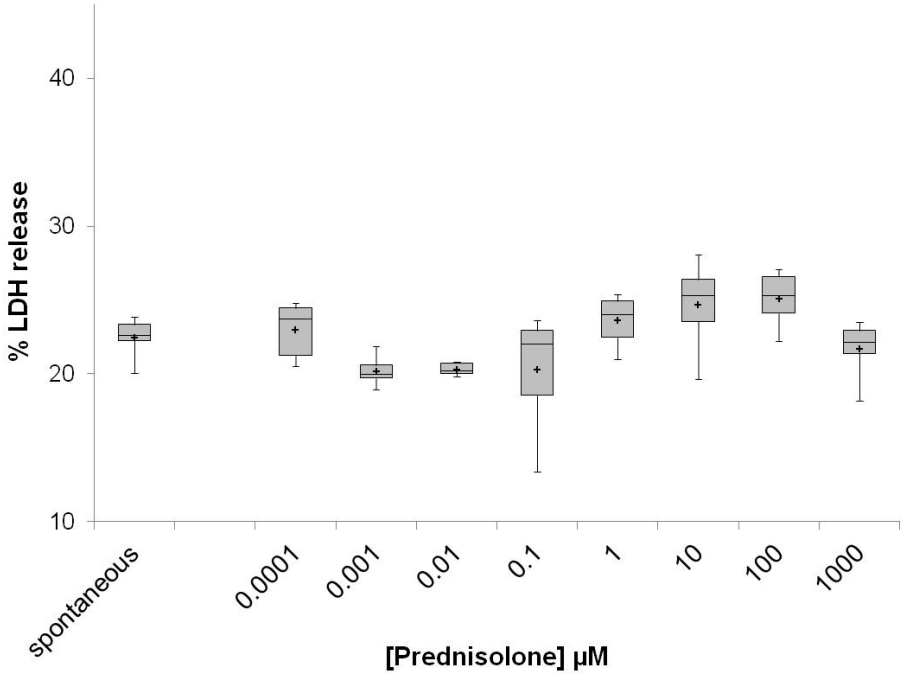

E. PEG_{3400}-$Pred_2$ (PP31)

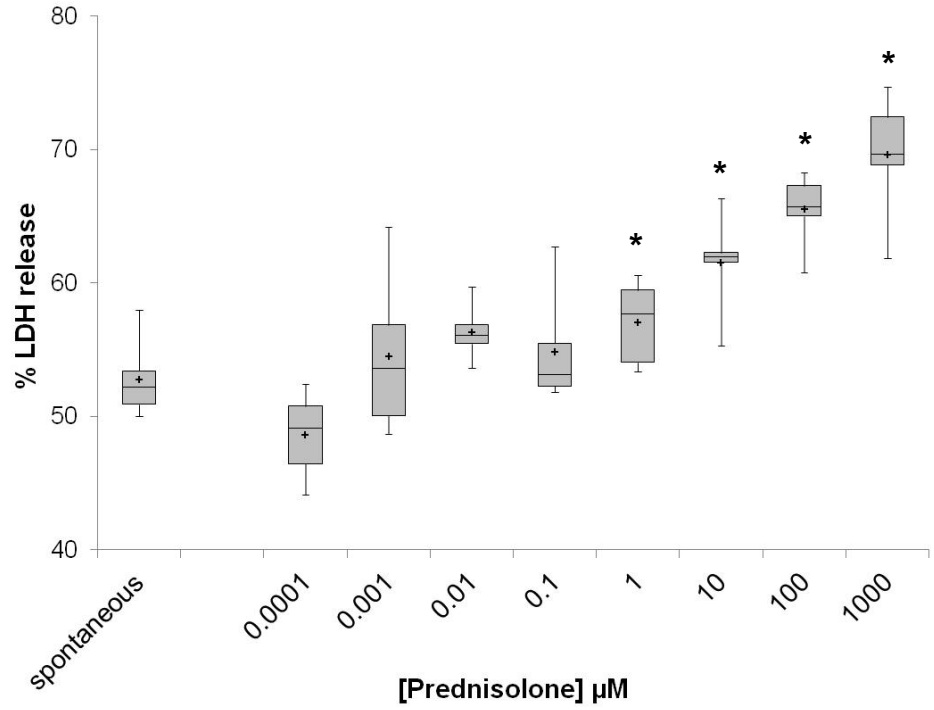

Fig.III.11. Cytotoxicity profiles of prednisolone and PEG-prednisolone conjugates % LDH released by Calu-3 cells, after 20h incubation with the different compounds. Spontaneous indicates the LDH released by untreated cells. Box Plots represent the five-number experiments summary: maximum measured value, upper quartile, median, lower quartile, minimum measured value. The mean is also represented (+). n=6 replicate. * $p<0.05$ (one tailed t-test, equal variances, H_0: $\mu_{[conjugate]} = \mu_{spontaneous}$).

The percentage of LDH released after incubation with prednisolone, PEG_{1000}-$Pred_2$ (PP33), $mPEG_{2000}$-$Pred_1$ (PP28) and PEG_{2000}-$Pred_2$ (PP29) did not exceed the naturally occurring LDH leakage from untreated cells (spontaneous LDH release), up to 500 and 1000 µM in prednisolone when using respectively prednisolone and the conjugates. Therefore both the conjugates and prednisolone were considered not cytotoxic in the assay up to 1000 and 500 µM respectively.

For PEG_{3400}-$Pred_2$ (PP31), the calculated LDH release values in the presence of 1 to 1000 µM in drug were statistically significantly higher than the spontaneous values (one tailed t-test, equal variances). PEG_{3400}-$Pred_2$ was therefore considered cytotoxic at concentrations above 1 µM.

III.3.3.2. Discussion

LDH assays were conducted in order to get a feel for the toxicity induced by the conjugates and the release of oxidised PEG. The compounds to be studied did not have a noticeable effect on Calu-3 membrane integrity apart for PEG_{3400}-$Pred_2$ which was not subsequently used for hydrolysis test with Calu-3 (III.3.4). It is worth noting that this conjugate was only cytotoxic at concentrations above 1 µM, way above any biologically relevant lung concentration.

In a standard inhaled administration of 200 µg of budesonide (MW 430.5 Da) with Pulmicort Turbohaler® 200 mcg, the delivery efficiency is usually of about 15-35 % [161] [162], and more than 90% of budesonide is made of particles of less than 4 µm [163]. The dose reaching the lungs is therefore approximately 70 - 160 nmol. Assuming the dose is evenly distributed through the lungs (approximately 70 m^2), the ratio dose/epithelium surface area is clinically in the region of 1 - 2.3 $nmol.m^{-2}$.

For the cell culture cytotoxicity tests, the epithelium was grown on 0.32 cm^2 (manufacturer's specifications) and the lowest significant cytotoxic dose was 0.1 nmol (100 µL at 1 µM), giving a ratio of 3125 $nmol.m^{-2}$, more than a thousand times more concentrated than clinically possible.

It is known however that inhaled particles are not evenly distributed in the lung. In a study published by Kim et al. in 1996 [164], the deposition pattern of inhaled particles of 1, 3 and 5 µm was defined as a function of inhalation flow rate (150, 250 and 500 $mL.s^{-1}$), in 11 healthy men. The surface dose was calculated as the ratio between the local deposition fraction and the surface area. The highest value for 3 µm particles (relevant particle size) in the airway, was $3.33\times10^{-5}.cm^{-2}$, obtained for the lowest flow rate. In this study, the total deposition fraction (for 3 µm particles) was 37 to 59%, slightly higher than the delivery efficiency of Turbohaler®. Let's apply this maximum experimental surface dose to budesonide. The maximum surface dose would be 155 $nmol.m^{-2}$ according to equation (III.11), twenty times less than the highest non toxic concentration for PP31.

(III.11) $3.33.10^{-5} \times \frac{200.10^{-6}}{430.5} = 1.55.10^{-11} mol.cm^{-2} = 155\, nmol.m^{-2}$

In conclusion, the cytotoxicity observed for one conjugate was not biologically relevant as it concerned a very high dose of compound. However, the shape of the cytotoxicity profile observed for PEG_{3400}-$Pred_2$ (Fig.III.11.E) shows a relationship between cytotoxicity and concentration above 0.1 µM and proves the reliability of the assay. The other conjugates were definitely not cytotoxic.

Although some literature is available for PEG toxicity, the route of administration is often oral, seldom intravenous, subcutaneous or intra peritoneal, but hardly ever inhaled. In any case, the studies are mostly concerned by the toxicity of native PEG and in the present work, monomethoxy-monocarboxy-PEG (mPEG-COOH) or dicarboxy-PEG (PEG-$COOH_2$) were released from the conjugates. According to the review by R. Webster et al. [95] native PEG is not toxic at the doses used in drug-conjugate technologies. PEG has been used to decrease the cytotoxicity of drugs [104] [98] [99] [165] [166] and it has been observed that PEG-conjugates did not have obvious cytotoxicity [167] [168]. In their reviews, both Zalipsky [169] and Greenwald [92] described PEG-conjugates as non toxic.

III.3.4. Hydrolysis in the presence of Calu-3 cells

The conjugates PEG_{1000}-$Pred_2$, PEG_{2000}-$Pred_2$ and $mPEG_{2000}$-Pred were stable in buffers of biologically relevant pH (III.3.2), and were not cytotoxic towards Calu-3 cells (III.3.3). This section illustrates the last step of in vitro testing: stability of the conjugates in the presence of human bronchial epithelial tissue.

III.3.4.1. Results

Hydrolysis of $mPEG_{2000}$-$Pred_1$ (PP28) in serum-free medium followed a first order degradation profile with a half life of 13.47 ±0.10 h (Fig.III.12). In the presence of cells, the degradation was slower and the apparent half-life increased to 15.85 ±0.02 h (Fig.III.12). These values are in the same order of magnitude as the degradation rates obtained in the MacIlvaine and phosphate buffers (III.3.2.1).

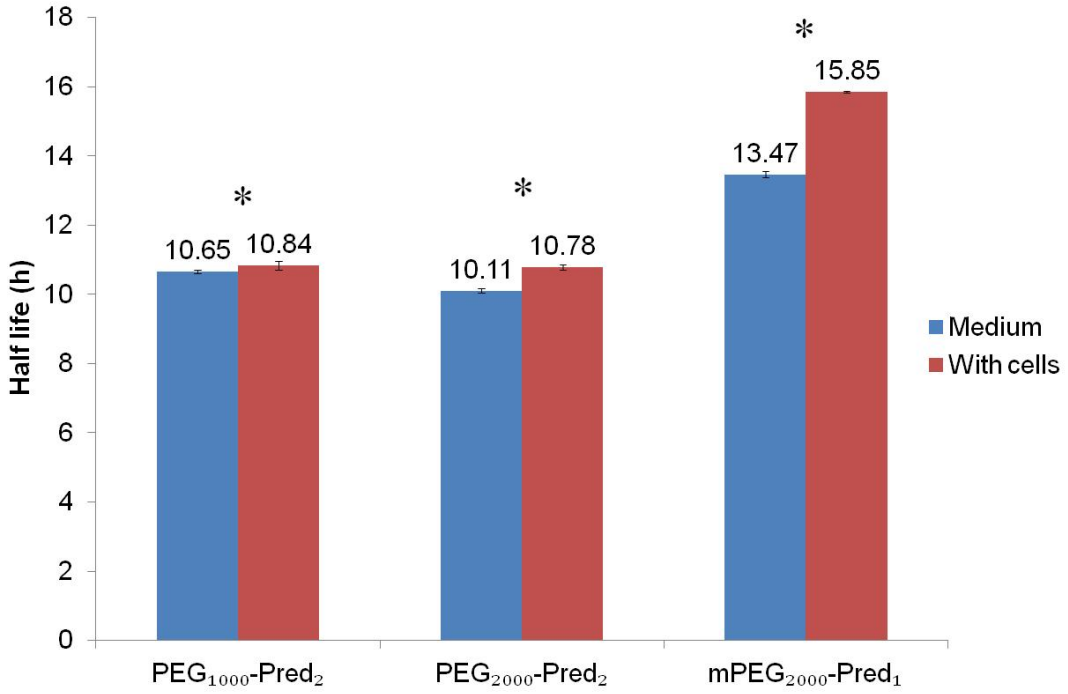

Fig.III.12. Hydrolysis half-lives of the conjugates in cell culture medium and in the presence of Calu-3 cells

*Half lives in medium and with cells were statistically significantly different (unpaired, one tailed Student's t-test, equal variances)

The hydrolysis rate constant of the disubstituted conjugates PEG_{2000}-$Pred_2$ (PP29) and PEG_{1000}-$Pred_2$ (PP33) were also lower in the presence of Calu-3 than in serum-free cell culture medium (Table. III.16). Using the same simulations as in the hydrolysis in simple buffers (III.3.2), the calculated values for the hydrolysis rate of the intermediate PEG-$Pred_1$ (for PP29 and PP33 hydrolysis studies), k_2 were higher than the rate of PEG-$Pred_2$ hydrolysis (k_1), but not as high as in the simple buffers (III.3.2.1).

Table. III.16. Spontaneous hydrolysis rate constants of the PEG-prednisolone conjugates in cell culture medium with and without Calu-3 cells

Compound	Medium	k_1 h^{-1}	SD %	k_2 h^{-1}	SD %
$mPEG_{2000}$-$Pred_1$	No cell	0.0515	± 0.71	NA	
	With Calu-3	0.0437	± 0.14		
PEG_{1000}-$Pred_2$	No cell	0.0651	± 0.55	0.1433	± 0.33
	With Calu-3	0.0639	± 1.22	0.1538	± 2.39
PEG_{2000}-$Pred_2$	No cell	0.0686	± 0.68	0.2102	± 4.05
	With Calu-3	0.0643	± 0.57	0.2157	± 2.21

Mean of 3 measurements

III.3.4.2. Discussion

These observations ruled out any significant influence of enzymes in the system since one would expect a much faster hydrolysis rate with significant enzymatic activity. The overall hydrolysis rate was mainly controlled by spontaneous hydrolysis, explaining the slower apparent hydrolysis rate with cells. The pH indicator phenol red, had turned orange in the culture medium with the cells at the end of the experiments, indicating a lower pH due to cell metabolism (Appendix 8, Fig.VI.53).

The hydrolysis rates were faster in cell culture medium than in buffers at pH 7.4, and salt effect may explain this result. Positive salt effects for acid catalysis of ethyl acetate have been described [170]. Positive salt effect has also been described by Hoppé and Prue [171] for the hydrolysis of half ester of dicarboxylic acids. Particularly K^+ and Na^+ ions had a positive effect on the hydrolysis rates of potassium ethyl adipate, through the formation of a chelate complex.

A similar complex (Fig.III.13) may form during hydrolysis in simple buffers and partially explain the faster hydrolysis rate observed in cell culture medium compared to simple buffers, by stabilising the transition state:

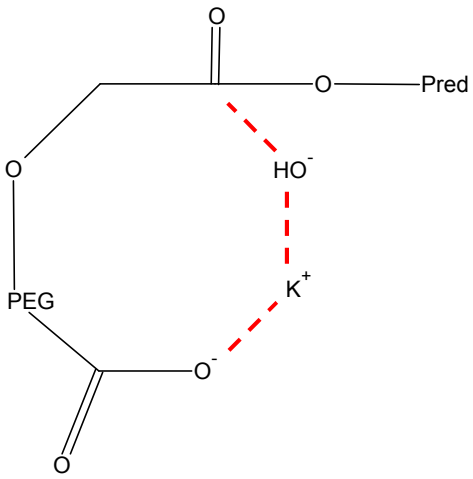

Fig.III.13. Chelate complex for $^{-}$OOC-PEG-Pred$_1$ hydrolysis in buffer

The ionic strength used in the buffers was fixed at 0.5, which is higher than the physiologic ionic strength (saline is 9 g.L^{-1} NaCl, μ = 0.154) used in cell culture medium. An estimated ionic strength for the cell culture medium was calculated at 0.14 from the more concentrated ions (NaCl, KCl, $NaHCO_3$), using the manufacturer product information sheet and equation (III.2). In cell culture medium, the concentration of K^+ and Na^+ ions were lower than in the buffers and because of positive salt effects, the intermediate $^{-}$OOC-PEG-Pred$_1$ was less stable in cell culture medium. However, PEG terminal carboxylate group may still be playing an important catalytic role as the intermediate $^{-}$OOC-PEG-Pred$_1$ was less stable than mPEG-Pred$_1$.

III.4. Conclusion

In this chapter, the stability of the conjugates in aqueous solutions at pH 6.2, 7.4 and 8.0 was evaluated, some cytotoxicity tests were performed and the influence of cells on the hydrolysis rate was tested. The main findings of *in vitro* testing were the following:

- PEG-salbutamol conjugates were unstable under physiological pH and their study was not pursued any further, these conjugates were clearly inappropriate for sustained delivery of drugs to the lung.
- PEG-prednisolone conjugates achieved a sustained release of prednisolone *in vitro*. Under biologically relevant pH, the conjugates hydrolysis rates were pH dependent. mPEG-$Pred_1$ was twice as stable as PEG-$Pred_2$ (half lives of 3 to 6 hours at pH 7.4, 35 to 70 hours at pH 6.2) and between pH 6.2 to 8.0, the hydrolysis rates changed by a factor 40. Such hydrolysis rates were promising and justified further study.
- Conjugates of molecular weights 1000 and 2000 Da were not cytotoxic to human lung tissue (Calu-3 cells) according to the membrane integrity test based on LDH release. Therefore, the three conjugates PEG_{1000}-$Pred_2$, PEG_{2000}-$Pred_2$ and $mPEG_{2000}$-Pred were safe to use with human bronchial airway epithelial cells Calu-3, a more biologically relevant *in vitro* system. However, since PEG_{3400}-$Pred_2$ exhibited significant cell membrane damage between 1 to 1000 µM, this conjugate was not used in the next studies.
- Finally, Calu-3 cells did only marginally affect the hydrolysis rates and no influence of Calu-3 esterases [172] was observed. These findings further confirmed the potential suitability of the selected ester conjugates of PEG and prednisolone for sustained drug delivery to the lungs.

- After *in vitro* studies, out of the seven ester conjugates tested, three candidates remained. Their stability under physiological conditions and in the presence of Calu-3 cells along with their non-cytotoxic profiles made them suitable candidates for an even more physiologically relevant *ex vivo* model: the Isolated and Perfused Rat Lung.

Chapter IV. *Ex vivo* testing

IV.1. Introduction

After successful evaluation of the drug action *in vitro*, the next stage in the drug development journey requires validations *in vivo*, in animal models. In the case of respiratory medicines, rats are often used and the drug pharmacokinetics studied. In the pharmaceutical industry, the accepted ethical rule for such tests is the 3Rs – Replacement, Refinement and Reduction – as first described in 1959 by Russel and Burch [173]. Hence, researchers have to replace the use of living vertebrates where possible, refine their experiments to limit animal pain and reduce the number of animals used to gain comparable levels of information [174] [175]. *Ex vivo* models have been developed to provide an intermediate between *in vitro* and *in vivo* experiments. In respiratory work, the use of an isolated and perfused rat lung prior to any *in vivo* evaluation is in line with the 3Rs guidelines.

The Isolated and Perfused Rat Lung model [176] is a useful tool to directly assess the absorption rate of drugs in the lung [177]. Despite some limitations, mostly around the technical difficulty, the time required to perform the procedure and the relatively short viability (2-3 h), the IPRL has been shown to give good *ex vivo*/*in vivo* correlation in regards to absorption half lives [178]. The IPRL, and especially the single pass method [73], although more expensive than the recirculation method, is therefore useful to predict *in vivo* pharmacokinetic profiles. It has been used to study lung absorption properties of inhaled drugs administered by forced instillation [179] [180], nebulisation [181] or as dry powders [182] [183] [184]. The set up used in the experiments presented in this chapter was designed to

specifically study the influence of hydrolysis rate in the apparent absorption rate of prednisolone from the lung. Therefore, the choice was made to administer the compounds as nebulised solutions. Thus, any observed variation in absorption rate would be due to hydrolysis and not dissolution rate differences between the compounds, since the drug and conjugates were already solubilised when reaching the lung. Out of the three remaining potential candidates, the choice was made to use PEG_{2000}-$Pred_2$ and $mPEG_{2000}$-Pred for this study. The rationale behind this decision was based on economical and scientific reasons:

- the IPRL set up was quite expensive and time consuming and
- PEG_{1000}-$Pred_2$ was the more likely to be absorbed by the epithelium, PEG_{3400}-$Pred_2$ may have been cytotoxic, and the comparison between the two selected conjugates would be made easier since they have the same molecular weight.

Tandem mass spectrometry was used to measure the concentration of the compounds in biological media and lung. This technique presents the advantage of being sensitive and specific compared to HPLC-UV. Methods to measure prednisolone by tandem mass spectrometry in cosmetic products [185] and in human serum [186] have already been published. PEG prodrugs of resveratrol were also studied by LC/MS [187]. The specificity of the technique ensured that the release of native (and therefore biologically active) prednisolone was measured. The sensitivity of the measurements allowed working with clinically relevant drug concentrations associated with *ex-vivo* experiments.

The Berkeley Madonna software was used to calculate hydrolysis rates in the lung that were not directly measurable. The profile of drug retention in the lung, unavailable with IPRL experiments, was also simulated with the software.

IV.2. Materials and Methods

IV.2.1. Analytical techniques

Prednisolone, PEG_{2000}-$Pred_2$, $mPEG_{2000}$-Pred, $mPEG_{2000}COOH$ and $PEG_{2000}COOH_2$ were analysed in perfusate and in lung tissue. Dexamethasone was used as the internal standard. The compounds were detected by Multiple Reaction Monitoring (MRM) as it allowed to specifically monitor a particular chemical entity and could differentiate between two metabolites of the same compound.

IV.2.1.1. LC-MS/MS method

a. Equipment and material

For *ex vivo* analysis, the analytical system consisted of an HPLC (Agilent 1100 series) coupled with a CTC analytic HTC-xt autosampler robot. The mass spectrometer was an API 4000 (Applied Biosystems), and the analysis was performed with Analyst software (v. 1.4.2., ABSCIEX, Framingham, MA, USA). Infusion experiments were performed using a syringe pump "Model 22" (Harvard apparatus, Edenbridge, UK) equipped with a 500 µL precision glass syringe (Hamilton, Bonaduz, Switzerland). HPLC grade methanol, acetonitrile and dichloromethane were purchased from Rathburn (Walkerburn, Scotland), analytical grade formic acid was purchased from Riedel-de Haën, Absolute ethanol (99.5%) was purchased from Kemetyl AB (Haninge, Sweden). Deionised and ultrapure (18.2 $M\Omega.cm^{-1}$ at 25°C) water were produced in-house by reverse osmosis, with respectively Purelab Prima and Maxima systems (ELGA). Analytical grade dexamethasone was purchased from Riedel-de Haën and prednisolone from Sigma. Acetate buffer at pH 5.0 was prepared to resuspend the lung homogenates. The low buffer pH was used to reduce the level of spontaneous hydrolysis rate of the conjugates once extracted from the lungs. Two hundred mL of acetate buffer was

prepared by mixing 129 mL of sodium acetate solution (0.1 M, 2.72 g of sodium acetate in up to 200 mL of deionised water) and 71 mL of acetic acid (0.1 M, 572 µL of acetic acid in up to 100 mL of deionised water). The pH was adjusted with a few extra drops of acetic acid solution.

b. HPLC conditions

Two solvent mixtures were used as mobile phases:

- Mobile phase A (aqueous): 5% acetonitrile (v/v), 0.1% (v/v) formic acid in ultrapure water.
- Mobile phase B (organic): 4.9% ultrapure water (v/v), 0.1% formic acid in acetonitrile.

The stationary phase was a Hypurity C_{18} reverse phase column (ref 22105-102130, Thermo), 100 × 2.1 mm, 5 µM particle size. The flow rate was set at 825 µL.min^{-1}, the injection volume was 5 µL and the runtime was 3 minutes. The following gradient was used (Fig.IV.1):

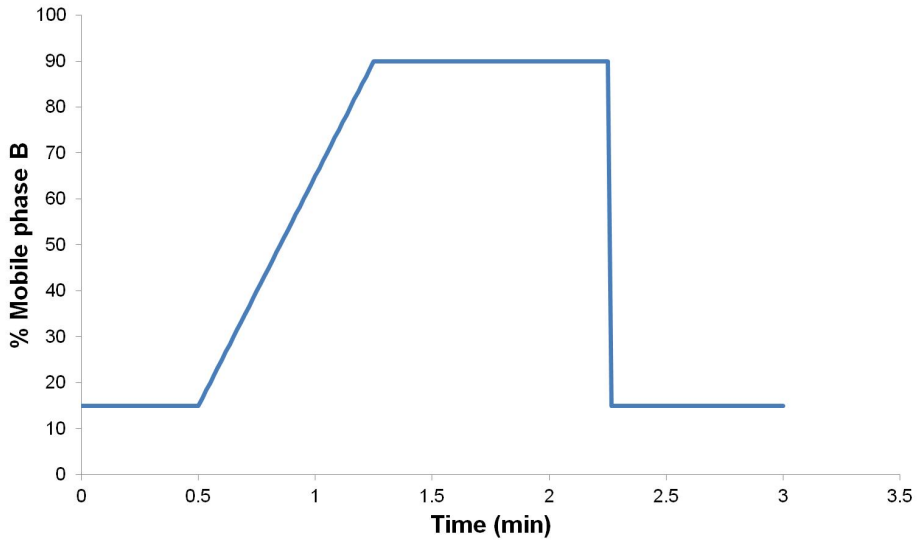

Fig.IV.1. Gradient for LC-MS/MS analyses

A valco valve protected the ionisation source and the liquid chromatography system was actually connected to the mass spectrometer between time 1.6 and 2 minutes. The eluent was directed to waste for the remainder of the run.

c. Mass spectrometry conditions

Solutions of analytes at 1 µM were prepared in a mixture of mobile phases A/B (50/50 v/v) and infused in the mass spectrometer at 10 $\mu L.min^{-1}$ with the LC system set at 825 $\mu L.min^{-1}$, 50/50 A/B (v/v). A full scan for primary ions (Q1) was obtained between 300 and 3000 m/z for 2 minutes in positive mode. The stability of the maximum ion was assessed in Q1M1 mode for 2 minutes. Identification and parameter optimisation of a unique precursor ion was performed in quantitative optimisation mode for each individual compound.

d. Calibrations

Concentrated stock solutions of the compounds were freshly prepared in methanol and the following sets of calibration solutions were prepared:

- Prednisolone and dexamethasone: the stock solutions were prepared in methanol at 80 µM of each compound. The first calibration solution was prepared by diluting by 100 fold the stock solution (methanol solution) in perfusate or lung homogenate suspension and further diluting 2 fold sequentially up to 10 points (800, 400, 200, ... to 1.5625 nM).
- PP28 and dexamethasone: stock solutions were prepared in a similar way but the serial dilution was 3 fold between each solution and 8 solutions were prepared on ice (800, 267, ... to 0.3657 nM).
- The same procedure was repeated for PP32, $mPEG_{2000}COOH$ and $PEG_{2000}COOH_2$.

The compounds were then extracted and resuspended in a mobile phases A/B (50/50) according to the extraction procedures described in IV.2.1.2.

Quadratic regressions with 1/(analyte concentration)^2 weighting were performed with Analyst software, and a new set of calibration solutions was prepared fresh for each batch of samples. The calibrations were validated as follow: the calculated concentration of each standard had to fall within 15% of the actual standard concentration, otherwise the invalid point was discarded and the regression performed again. At least two thirds of the standards had to fall within 15% of their nominal value (e.g. at least 6 over an 8 point calibration curve or 7 over a 10 point calibration curve) otherwise the calibration was repeated. Standards were randomly analysed throughout the batch of injections.

IV.2.1.2. Sample work up

a. Samples from perfusate

At the end of the experiment, 430 µL of perfusate from selected collection tubes, was sampled and added to 20 µL of spiked solution of perfusate containing 1126.5 µM of dexamethasone in 2 mL centrifugation tubes. For prednisolone experiments, the samples collected at time points around the maximum perfusate concentration (C_{max}) were diluted 3 fold in perfusate prior to mixing with dexamethasone spike. The samples were stored at -20°C for up to a week before being thawed on ice and extracted twice with 900 µL of HPLC grade dichloromethane, the solvent was then dried under nitrogen. The samples were then resuspended in 450 µL of mobile phases A/B (50/50, v/v), centrifuged at 15,000 g, 4°C and 150 µL of the supernatant transferred to a 96 well microplate (Nunc) for LC-MS/MS analysis.

b. Samples from lungs

To measure the amount of drug remaining in the lungs at the end of the absorption studies, the tissues were firstly frozen in liquid nitrogen and homogenised with a tissue tube impactor (Covaris), the operation was repeated three times. The resulting crushed lungs were resuspended in 4 mL of acetate buffer at pH 5 and homogenised for three minutes at 37°C in a focused ultrasonicator (Covaris). A 200 µL sample of the resulting homogenate was then mixed with 250 µL of buffer containing 9×10^{-8} M of dexamethasone. This solution was extracted twice with 900 µL of HPLC grade dichloromethane, and the solvent dried under nitrogen. The samples were resuspended in 450 µL of mobile phases A/B (50/50), vortexed and centrifuged at 15,000 g for 10 min at 4°C. A 150 µL sample of the supernatant was transferred in a 96 microplate and 5 µL analysed by the LC-MS/MS method previously established (IV.2.1).

IV.2.2. Isolated Perfused Rat Lung

IV.2.2.1. Solution preparation and administration to the IPRL

Solutions of prednisolone and PEG-prednisolone conjugates in 25% ethanol for nebulisation were prepared at a final concentration of 2 $mg.mL^{-1}$ in prednisolone, according to Table. IV.1. To maintain similar osmotic properties, the prednisolone solutions were complemented with the same amount of PEG used for the conjugates. In detail, prednisolone was dissolved in ethanol to reach a concentration of 8 $mg.mL^{-1}$ and then diluted four fold in a PEG_{2000} (7.4 $g.L^{-1}$) water solution. The conjugate solutions were prepared by dissolving the compounds in ethanol at 8 $mg.mL^{-1}$ in prednisolone and then, just before nebulisation, diluting four fold in water.

Table. IV.1.Composition of the solutions for nebulisation

Compound	V EtOH solution	V water / PEG solution	[Prednisolone]		[PEG]
	mL	mL	mg.mL^{-1}	mM	mM
prednisolone	0.75	2.25	2	5.55	2.77
mPEG$_{2000}$-Pred (PP28)	0.3	0.9	2	5.55	5.55
PEG$_{2000}$-Pred$_2$ (PP32)	0.3	0.9	2	5.55	2.77

IV.2.2.2. Nebulisation to the IPRL

a. IPRL set-up

The isolated and perfused rat lung is a well established model used to study pharmacokinetic properties of inhaled drugs and is routinely used at AstraZeneca, Mölndal. Dr Pär Ewing kindly conducted the surgery and IPRL set up (Fig.IV.2), the experiments were approved by the local ethics committee. The procedure has been described in details elsewhere [188]. Briefly, male Wistar rats were administered an overdose of sodium pentobarbital (0.8 mL at 100 mg.mL^{-1}, intraperitoneal). The animal were bled to death and heparin was injected in the heart. The pulmonary artery was cannulated and the lung perfused at approximately 20 mL.min^{-1} with Krebs-Ringer buffer (4% Bovine Serum Albumin w/v) [188] (Appendix 9, Table. VI.7), maintained at 37°C and pH 7.4 by bubbling CO_2. The pulmonary vein was cannulated and the silicon tubing exiting the apex of the heart was connected to an autosampler. Finally, the trachea was also cannulated and the isolated lung and heart were placed in an artificial thorax with a negative pressure of -0.4 kPa and maintained at 37°C. The lung was ventilated using a rodent ventilator at a tidal volume of 2 mL and 75 rpm. A single-pass perfusion method was used and the perfusate was initially directed to waste. Pulmonary resistance, dynamic compliance and examination for oedema were used to assess the lung

integrity for 15 minutes before the experiment started. Only IPRL that met our preset criteria were proceeded to the next step.

b. Inhalation to IPRL

For each experiment, 1 mL of solution for inhalation was transferred to an Aeroneb Lab nebuliser (control module AG-AL7000, 2.5-4.0 μm mesh size, nebuliser head AG-AL 1100) and nebulised into a 500 mL polyethylene terephthalate spacer. The nebuliser was left running for approximately 2-3 minutes to prime the spacer. The spacer was connected upstream to the exposure line. The exposure line was comprised by a flow-split which was connected to the tracheal cannula of the IPRL and to an upstream vacuum source operating at a constant negative pressure, resulting in a flow rate of 0.4 $L.min^{-1}$. The exposure cycle of the IPRL was initiated by manually opening a valve between the spacer and the exposure line and the produced aerosol was pulled through the exposure line using the negative pressure produced by the ventilator and the upstream vacuum source. Using this approach, at an average negative aerosol flow rate of approximately 0.4 $L.min^{-1}$, it took between 7 to 10 minutes to nebulise 1 mL of solution and empty the spacer. Hence, with the default respiratory rates and applied vacuum, during inspiration one third of total flow rate was inspired. The exposure cycle and perfusate sampling were started simultaneously (the autosampler changed tube every 30 s), the nebulisation apparatus was removed when the reservoir was empty. The perfusion and ventilation of the IPRL were allowed to continue for one hour. After that, the experiment was finished, the lung was removed from the chamber, collected and placed in an individual tissue tube (Covaris). The tissues were immediately frozen and stored at -80°C.

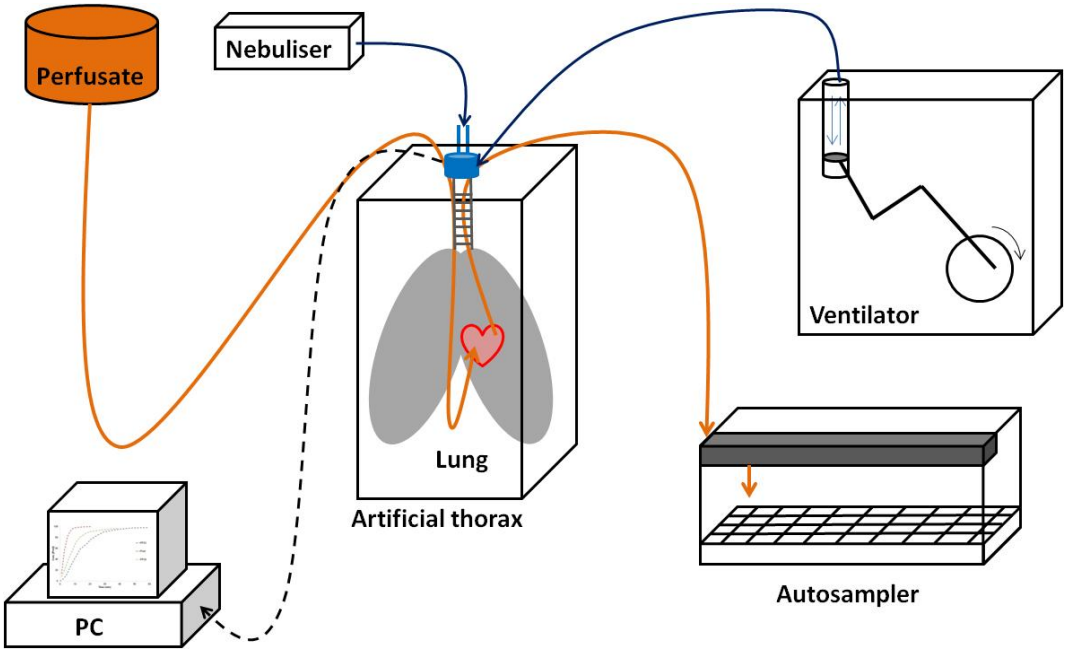

Fig.IV.2. Schematic of the IPRL set up

IV.2.3. Pharmacokinetic calculations

The cumulative amount of prednisolone that had been absorbed across the air blood barrier was calculated according to the method described below, inspired from Euler's method of estimating the area under the curve:

At anytime, *n(t)* was the sum of the amount of prednisolone recovered in all the fractions between time 0 and t:

(IV.1) $$n(t) = \sum_{i=0}^{i=t} n_i$$

The amount of prednisolone in a fraction i was calculated as the product of the concentration in prednisolone (c_i), determined by LC-MS/MS, multiplied by the corresponding volume of perfusate, determined by the measured perfusion rate ($\dot{V}_i$) and the time elapsed between two consecutive measurements (Δt) (Fig.IV.3). At any time i:

(IV.2) $$n_i = c_i . \Delta t . \dot{V}_l$$

The total administered dose was calculated using equation (IV.3), as the sum of prednisolone remaining in the lungs (N_{lung}) and the total amount of prednisolone recovered in the perfusate ($\sum_{i=0}^{\infty} n_i$).

(IV.3) $$Dose = N_{lung} + \sum_{i=0}^{\infty} n_i$$

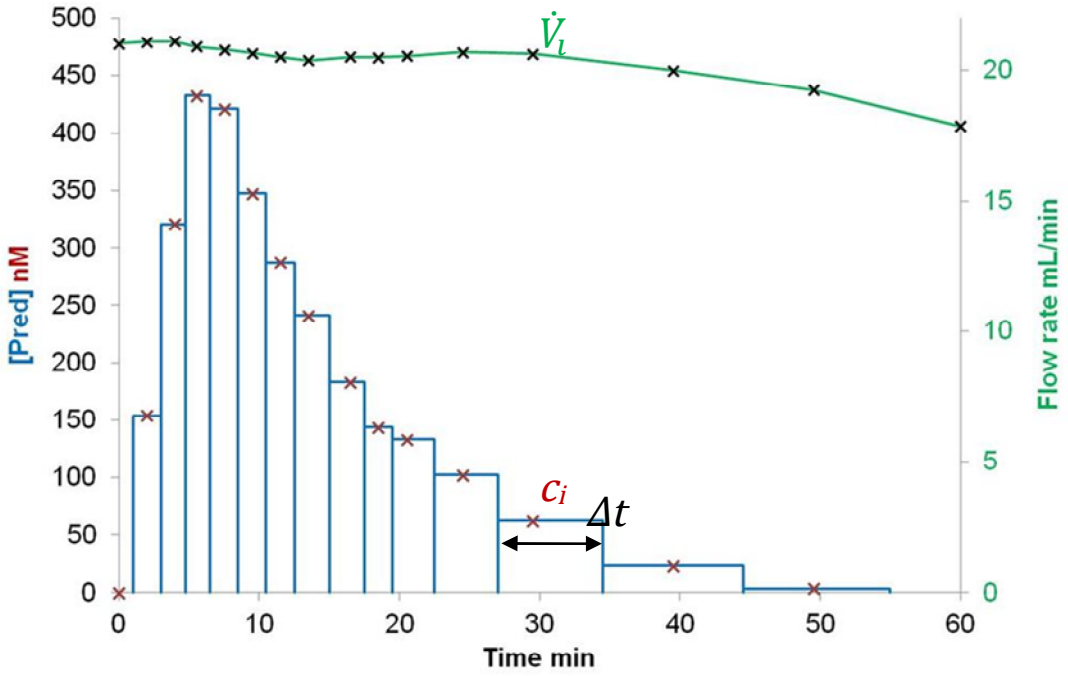

Fig.IV.3. Calculation of the total dose recovered in perfusate
The flow rate $\dot{V}_l$ was measured on line, c_i was determined by LC-MS/MS analysis, the blue histograms represent the Area Under the Curve [Pred] = f(t)

The normalised pharmacokinetic profiles were obtained by dividing the concentration of prednisolone in perfusate (c_i) by the total dose delivered.

The apparent lung absorption rate k was calculated as the slope of the straight line obtained when plotting ln c_i = f(t), assuming an apparent first order absorption. The half life was calculated as $t_{1/2} = \frac{ln2}{k}$.

IV.2.4.Pharmacokinetic simulations

The model described in Fig.IV.4 was used to simulate the fate of the compounds after administration to the IPRL.

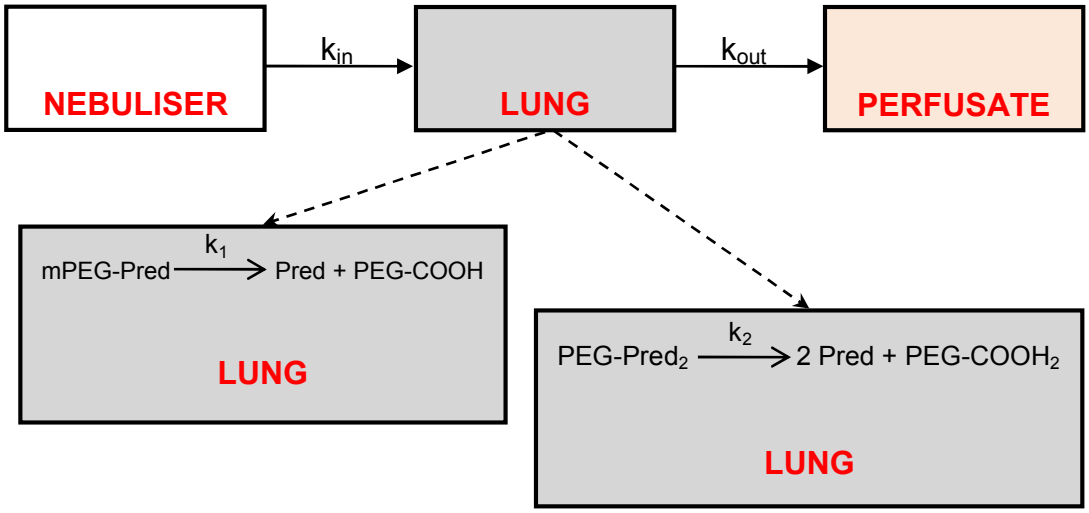

Fig.IV.4. Model of Isolated Perfused Rat Lung experiments
k_{in}: 0 order rate constant of drug administration, k_{out}: 1st order permeation rate constant of prednisolone from the lung, k_1: pseudo first order hydrolysis rate constant of mPEG-Pred, k_2: pseudo first order hydrolysis rate constant of $PEG\text{-}Pred_2$

The methodology used was to fit the cumulative amount of prednisolone recovered in perfusate with the model. The experiments conducted with prednisolone were used to determine k_{out}. Berkeley-Madonna software calculated the duration of administration and k_{out}, being given the total dose as input. This was repeated for the three replicates. The average value for the permeation rate of prednisolone from the lung, k_{out} was then used as fixed input to determine the hydrolysis rates in the lung for the conjugates, assuming a pseudo or apparent first order hydrolysis rate.

Thus, the cumulative amount of prednisolone in perfusate (obtained experimentally for each conjugate) was kinetically fitted, with k_{out} and the total dose as fixed input in the system, and the administration time and k_1 or k_2 calculated. The equations used are in Appendix 9, (VI.1).

IV.2.5. Statistical analysis

Where applicable, tests for equal means (null hypothesis H_0: $\mu_1 = \mu_2$) were applied when the data sets were normally distributed, with equal variance. One tailed Student's t-tests were used to statistically determine the significance (H_0 rejected if p-value < 0.05) of the difference between two sets of values.

IV.3. Results and discussions

IV.3.1. Analytical method

Table. IV.2 illustrates the retention times and the different optimised conditions for all the compounds used in the *ex-vivo* study, the entrance potential was 10 V (Appendix 10, Fig.VI.54).

Table. IV.2.Parameters for MRM and turbo spray ionisation

Compound	Retention time (min)	Q1 (m/z)	Q3 (m/z)	DP (V)	CE (V)	CXP (V)
prednisolone	1.70	361.3	147.1	41	29	10
dexamethasone	1.77	393.1	373.1	41	13	12
$mPEG_{2000}COOH$	1.72	635.4	103	61	47	6
$PEG_{2000}COOH_2$	1.70					
PP28	1.81	749.5	147.1	46	41	10
PP32	1.87	892.9	147.1	51	77	10

Q1: precursor ion, Q3: product ion, DP: Declustering Potential, CE: Collision Energy, CXP: Collision Cell exit Potential.

The system was calibrated over the concentration range 1.6-200 nM for prednisolone and dexamethasone and 0.37-89 nM for polymer based compounds.

IV.3.2. Prednisolone absorption profile in the IPRL

IV.3.2.1. Nebulisation, doses delivered and fraction remaining in the lungs

The nebulisation procedure was similar for all the tested compounds. However, it was difficult to initiate the nebuliser with the conjugates, but this was not the case for prednisolone. The dose precision and accuracy of nebulisers are dependent upon many interrelated factors beyond the scope of this thesis (e.g. compound physico-chemical properties, ambient conditions, compound concentration, physiological profile) [189]. This variability didn't have a significant impact on the interpretation of the experiments since the measurements were normalised to the actual dose delivered to the lung. Table. IV.3 illustrates the doses delivered and remaining fractions in the lungs for the IPRL experiments conducted.

Table. IV.3.Doses of prednisolone delivered to the lungs and remaining in the tissue at the end of the experiments

Experiment	Compounds	Total dose nmol	Total remaining in lungs %	Conjugate* in lungs %	% delivered**
PredRA	prednisolone	154.0	0.35	NA	2.8
PredRB	prednisolone	94.2	0.42	NA	1.7
PredRC	prednisolone	72.1	0.08	NA	1.3
PP28RA	mPEG-$Pred_1$	11.9	0.62	0.30	0.2
PP28RB[2]	mPEG-$Pred_1$		Too low		
PP28RC[1]	mPEG-$Pred_1$	46.4	5.96	1.69	0.8
PP28RD	mPEG-$Pred_1$	10.1	3.25	0.93	0.2
PP28RE	mPEG-$Pred_1$	10.1	0.76	0.27	0.2
PP32RA	PEG-$Pred_2$	141.4	2.21	0.37	2.5
PP32RB	PEG-$Pred_2$	93.6	2.01	0.39	1.7
PP32RC	PEG-$Pred_2$	36.6	1.90	0.26	0.7

**PEG-$Pred_1$, **amount of prednisolone nebulised was 5.55 µmol, [1]the lung integrity was compromised as it was the only experiment where some polymeric products (mPEG-$Pred_1$ and mPEGCOOH) were measured in the perfusate, [2]the dose delivered was too low to give exploitable readings*

For prednisolone experiments, less than 0.5% of the administered dose was detected in the lungs at the end of the experiment (Table. IV.3), about 2% for the disubstituted conjugate PEG-$Pred_2$ and less than 1% for the monosubstituted conjugate mPEG-$Pred_1$, with the exception of experiments PP28RC and PP28RD, for which 5.96 and 3.25 % of drug remained in the lungs respectively. No PEG-$Pred_2$ was recovered in the lungs, and the calibration for mPEG-$Pred_1$ was used to quantify the remaining intermediate PEG-$Pred_1$, which was always less than 1% of the delivered dose (Table. IV.3).

IV.3.2.2. Normalised pharmacokinetic profiles and outliers

The normalised, averaged pharmacokinetic profiles obtained for the free drug and the conjugates are presented in Fig.IV.5, the individual normalised plots are in Appendix 10, Fig.VI.55.

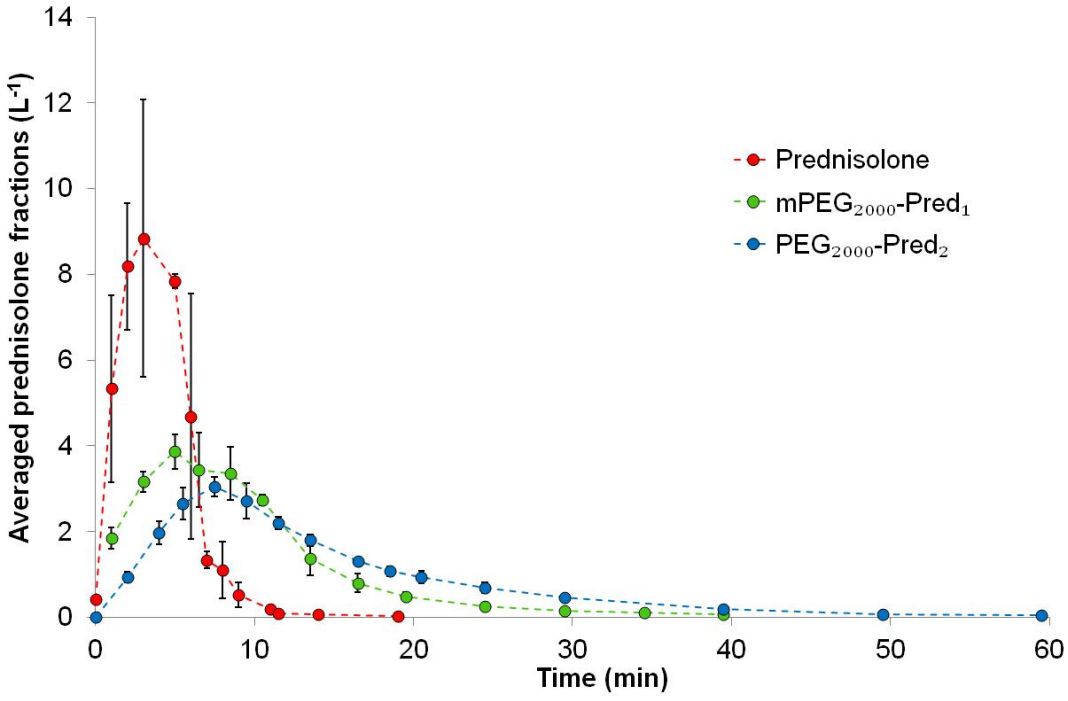

Fig.IV.5. Normalised absorption profiles of prednisolone in the IPRL obtained with prednisolone alone, mPEG-$Pred_1$ and PEG-$Pred_2$
Each individual measured concentration (nmol.L^{-1}) was divided by the total dose administered during the experiment (nmol) to give relative fractions of prednisolone in perfusate (L^{-1}). Data are presented as average of n=3 ±SD.

For all the experiments, there was an initial infusion period of about 7-10 minutes corresponding to the administration of the drug. After administration, the concentration of prednisolone in perfusate decreased instantly when using only prednisolone (•), and the drug was not detected in the perfusate after 20 minutes of experiment. With the conjugates, prednisolone was still detected in the perfusate after 40 minutes (•,•). There was neither PEG nor conjugate recovered in the perfusate that could be quantified during the experiments except for PP28RC.

PP28RC displayed a completely different pattern (Appendix 10, Fig.VI.55.) as 21.8% of the total dose was recovered in the form of the intact conjugate in the perfusate and 1.70% in the lung, the lung was probably leaky. This experiment was not considered further in the next analysis as it clearly was an outlier. The delivery efficiency during PP28RB experiment was not sufficient to obtain a concentration high enough in the perfusate to give exploitable results.

IV.3.2.3. Effect of PEG conjugation on C_{max} and t_{max}

The maximum concentration of prednisolone in perfusate divided by the total administered dose, relative C_{max} (maximum fraction of prednisolone in perfusate), was 9.13 ±1.37 L^{-1} for prednisolone, 4.22 ±0.20 L^{-1} for mPEG-$Pred_1$ (PP28) and 3.08 ±0.22 L^{-1} for PEG-$Pred_2$ (PP32). The relative C_{max} was statistically significantly lower for the conjugates and statistically significantly lower for PEG-$Pred_2$ than for mPEG-$Pred_1$ (one tail Student's t-test assuming equal variances, $p<0.05$).

The conjugates clearly reduced the relative C_{max} by 2.2 and 3.0 for respectively mPEG-$Pred_1$ (PP28) and PEG-$Pred_2$ (PP32).

The time to reach C_{max}, so called t_{max}, was difficult to measure with precision due to the variability in administration times (7 to 10 minutes) and therefore t_{max} was not visibly modified by the use of conjugates.

IV.3.2.4. Effect of PEG conjugation on the apparent lung absorption rate

The apparent rate of prednisolone absorption from the lungs was calculated as described in IV.2.3. The fitted datasets are available in Fig.IV.6. The conjugates also decreased the absorption rates in the IPRL, and the differences were statistically significant (one tail Student's t-test assuming equal variances, $p<0.05$). Absorption half lives were found to be 1.02 ± 0.17 min for prednisolone, 4.30 ± 0.70 min for mPEG-$Pred_1$ and 7.81 ± 0.88 min for PEG-$Pred_2$ (Table. IV.4). The drug residence time was therefore 4.2 times longer with mPEG-$Pred_1$ than with prednisolone alone and 7.7 times longer with PEG-$Pred_2$ than with prednisolone.

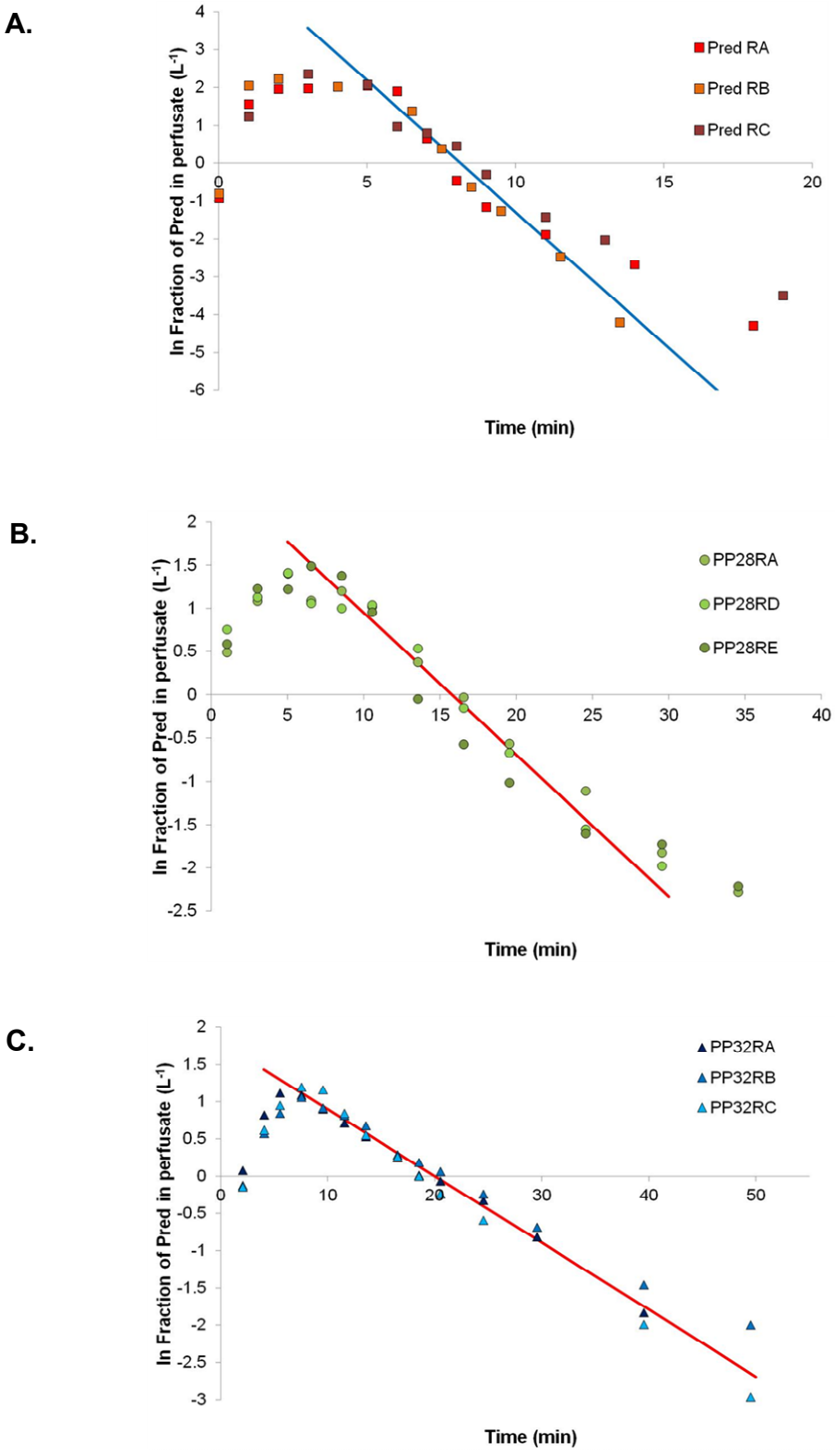

Fig.IV.6. Plots of ln (prednisolone fraction) as a function of time for prednisolone (**A**), PP28 (**B**) and PP32 (**C**) and fitted absorption rates for IPRL experiments
The slopes were individually calculated with a linear regression for ln (Pred)=f(t), using Excel. The straight lines represent the average absorption rate for (A) prednisolone, (B) mPEG-Pred$_1$ and (C) PEG-Pred$_2$ IPRL experiments, after the initial administration period.

Table. IV.4.Observed pharmacokinetic parameters for prednisolone, mPEG-Pred$_1$ and PEG-Pred$_2$

Compound	Experiment	Relative Cmax	Average Cmax (±SD) L^{-1}	Absorption rate min^{-1}	$t_{1/2}$ (±SD) min
prednisolone	PredRA	7.22	9.13 (±1.37)	0.7476	1.02 (± 0.17)
	PredRB	9.22		0.7646	
	PredRC	10.45		0.5705	
mPEG-Pred$_1$	PP28RA	4.08	4.22 (± 0.20)	0.1376	4.30 (± 0.70)
	PP28RD	4.11		0.1643	
	PP28RE	4.44		0.1897	
PEG-Pred$_2$	PP32RA	5.5	3.08 (± 0.22)	0.0888	7.81 (± 0.88)
	PP32RB	7.5		0.0798	
	PP32RC	7.5		0.1001	

IV.3.2.5. Discussion

Results in this section demonstrated clearly that the conjugation of PEG to prednisolone increased the pulmonary residence time. Since prednisolone was rapidly absorbed by the epithelium, a sustained delivery of the drug was achieved by a controlled hydrolysis of the PEG-conjugates. Consequently, the relative C_{max} was also decreased when using the conjugates compared to prednisolone.

Apart from one outlier experiment (PP28RC), PEG was not detected in the perfusate. This is consistent with the findings published in 2009 by Nektar Therapeutics [97]. In this study, the authors covalently conjugated PEG (0.55-20 kDa) to fluorescein isothiocyanate via a non hydrolysable linker. Fluorescent PEG was administered by intratracheal instillation to rats and the elimination rate from bronchoalveolar lavages was followed over time. The elimination rate of the conjugated PEG_{2000} was 0.097 h^{-1}. In other words, it took 1 h ($t_{10} = -\frac{1}{0.097} \times \ln(\frac{9}{10})$) to eliminate 10% of the administered PEG. In our study, the conjugates

may have crossed the epithelium but because the absorption rates of the polymers were certainly so much lower than that of prednisolone, we did not detect any polymer in the perfusate.

The observed half lives of the conjugates in buffers at pH 7.4 were 3.0 and 5.6 hours for respectively PEG_{2000}-$Pred_2$ and $mPEG_{2000}$-$Pred_1$ (III.3.2.1). In the IPRL model, the apparent absorption half lives measured were between 4 and 8 minutes. A spontaneous hydrolysis could not explain such rapid degradations in physiological conditions. The scale of the hydrolysis rate was different here and could only be justified by enzymatic activity. There were distinct activities of the enzymes towards mPEG-$Pred_1$ and PEG-$Pred_2$, since the apparent half life was twice as long for the latter.

IV.3.3. Pharmacokinetic modelling and simulations

IV.3.3.1. Prednisolone permeation rate from the lung

The permeation rate of prednisolone from the lung, k_{out} was estimated at 0.485 (±11% SD) min^{-1} using Berkeley Madonna software (Appendix 10, Table. VI.8).

IV.3.3.2. Hydrolysis rates in the lung

As suggested in IV.3.2.4, the conjugates were most probably substrates of lung esterases. To further illustrate the role of enzymatic degradation of the conjugates, the following simulations based on Michaelis-Menten kinetics, were performed.

In 1913, Michaelis and Menten [190] published a now classic paper, modelling the enzymatic activity of invertase, their findings were refined by Briggs and Haldane [191] when they introduced the steady state approximation.

Nowadays, under the assumption that the concentration of substrate is greater than that of enzymes, the rate of product formation is defined as:

(IV.4) $$\frac{d[P]}{dt} = \frac{V_{max}.[S]}{K_m + [S]}$$

In the present study, the rate of absorption of prednisolone from the lungs was fast and the limiting step was most likely the hydrolysis rate. Since the log plots of the concentration of prednisolone in perfusate with time obtained with the two conjugates were straight lines (Fig.IV.6), then the hydrolysis rate was independent of concentration of substrate. Therefore one could assume that the concentration of conjugate (substrate) was much lower than the Michaelis constant K_m. In this case, the hydrolysis rate followed an apparent first order kinetic, since equation (IV.4) could be simplified to:

(IV.5) $$\frac{d[P]}{dt} = \frac{V_{max}}{K_m}.[S]$$

Rate of product formation of a Michaelis-Menten kinetic, when $[S] << K_m$

Berkeley Madonna software was used to calculate the hydrolysis rate of the conjugates in lung, using the cumulative plots of prednisolone appearance in perfusate (Appendix 10, Fig.VI.56), and the value obtained in IV.3.3.1 for the permeability rate of prednisolone from the lung, k_{out} (Fig.IV.4). mPEG-Pred was found to hydrolyse at a rate constant of $k_1 = 0.157$ (± 1.5%) min^{-1} and $PEG\text{-}Pred_2$ at a rate constant of $k_2 = 0.101$ (± 13.3%) min^{-1}.

IV.3.3.3. Simulation using the fitted degradation and permeation rates

Simulations were performed with Berkeley Madonna, using the model illustrated in IV.2.4 and the calculated dissociation (k_1 = 0.157 min^{-1}, k_2 = 0.101 min^{-1}) and permeation (k_{out} = 0.485 min^{-1}) rate constants. An administration of 100 nmol of prednisolone (or equivalent with the conjugates) in 5 minutes was used to generate the simulations presented in Fig.IV.7.

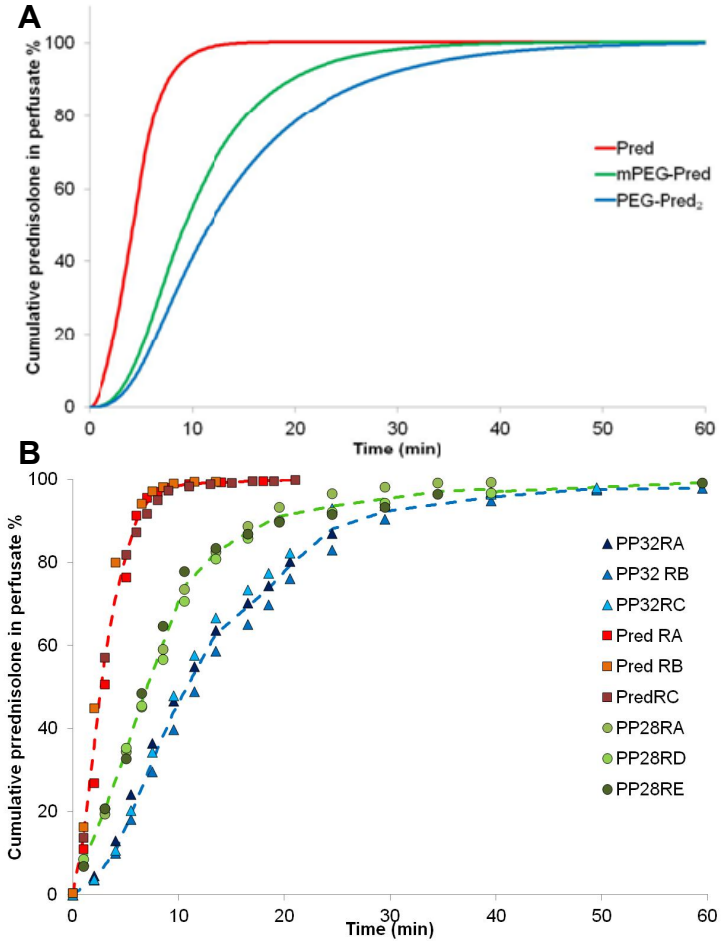

Fig.IV.7. Simulated and measured cumulative amount of prednisolone in perfusate

A. Simulations of cumulative prednisolone appearance in perfusate, following a 5 minutes administration time of 100 nmol of prednisolone or equivalent with the conjugates, using a prednisolone permeation rate constant of 0.485 min^{-1} and dissociation rate constants of k_1 = 0.157 min^{-1} for PP28 and k_2 = 0.101 min^{-1} for PP32. **B.** Experimental cumulative prednisolone appearance in perfusate obtained with prednisolone, PP28 and PP32.

The fitted model (**A**) described very closely the experimental data (**B**) obtained with IPRL for the three compounds despite the experimental variability in administration times (Fig.IV.7).

The corresponding prednisolone profile in lung is displayed in Fig.IV.8. This graph looks very similar to the normalised prednisolone concentration in perfusate profile (Fig.IV.5) since prednisolone permeation rate from the lung is very high. This visualisation is very useful to get an estimate of the actual amount of drug at the site of action: the lung. The sustained retention of prednisolone in lungs obtained with the conjugates is clear.

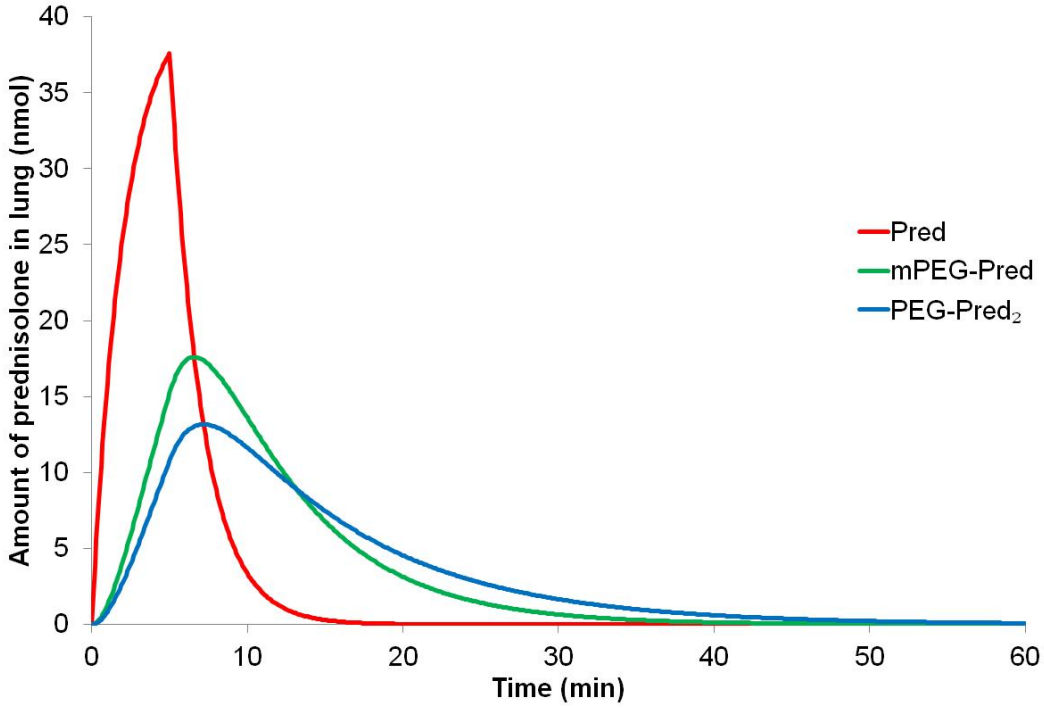

Fig.IV.8. Simulated profile of prednisolone amount in lung

Simulations of the amount of prednisolone in lung tissue, following a 5 minutes administration time of 100 nmol of prednisolone or equivalent with the conjugates, using a prednisolone permeation rate constant of 0.485 min^{-1} and dissociation rate constants of k_1 = 0.157 min^{-1} for PP28 and k_2 = 0.101 min^{-1} for PP32.

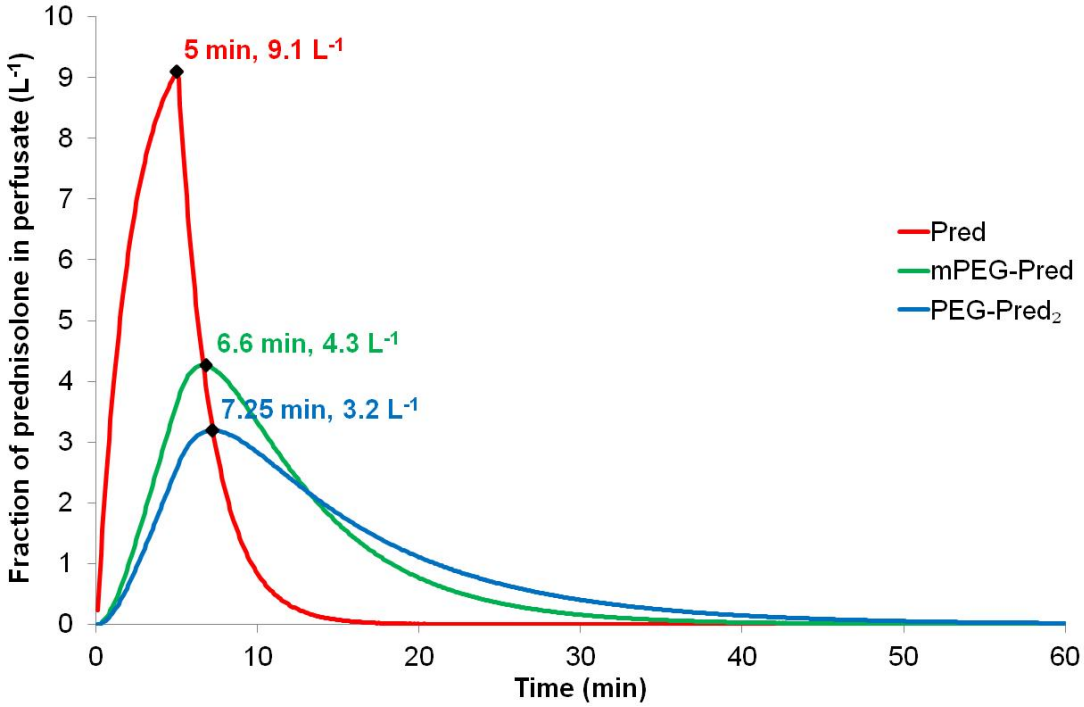

Fig.IV.9. Simulated profile of the fraction of prednisolone in perfusate

Simulations of the fraction of prednisolone in perfusate (concentration of prednisolone divided by total dose), following a 5 minutes administration time of 100 nmol of prednisolone or equivalent with the conjugates, using a prednisolone permeation rate constant of 0.485 min^{-1} and dissociation rate constants of k_1 = 0.157 min^{-1} for PP28 and k_2 = 0.101 min^{-1} for PP32.

The simulation confirmed that the relative C_{max} was lowered when using the conjugates and providing that the administration time was the same for all compounds, the t_{max} was also theoretically increased with the conjugates: from 5 min with the drug alone to 6.6 min with mPEG-$Pred_1$ and 7.25 min with PEG-$Pred_2$.

IV.3.3.4. Discussion

This section confirmed that the use of ester conjugates of PEG and prednisolone successfully improved the prednisolone pharmacokinetic profile in the IPRL model. Compared to prednisolone alone, C_{max} was decreased by a factor 2.8 and 2.1 and t_{max} was increased by 45 and 32% with PEG-$Pred_2$ and mPEG-Pred respectively. The lung esterase activity towards PEG-prednisolone conjugates, observed in the IPRL was also confirmed. The simulations clearly identified distinct enzymatic activities towards the mono and disubstituted conjugates: esterase activity towards mPEG-Pred ($t_{1/2}$=4.30 min) was superior compared to the activity towards PEG-$Pred_2$ ($t_{1/2}$=7.81 min). This could be explained by a lower affinity of the esterases towards the disubstituted PEG-$Pred_2$ compared to the monosubstituted mPEG-Pred. This esterase activity of the lungs has previously been reported in rabbit [192], mouse [193], rat [194], human [80] and is known to play a key role in the metabolism and activity of inhaled corticosteroids such as budesonide [195], beclomethasone [196] [197] or ciclesonide [198] [199], the latter two being administered as fatty acid ester prodrugs and then metabolised in the lung tissue to release the active drugs. Budesonide is converted into fatty acid ester and hydrolysed back to active drugs, in tissues and lung.

It was previously reported that ester prodrugs of inhaled corticosteroid and fatty acid could generate a sustained release of the drug to the peripheral parts of the lungs. The strategy employed was to reduce the drug aqueous solubility (with fatty acid chain) to achieve a longer lung residence time [55].

The model used for simulating IPRL experiments was simple and yet, allowed to generate normalised prednisolone profiles in perfusate that were very close to the experimental ones. Simulated relative C_{max} were within 4% of the average experimental values (Table. IV.4, Fig.IV.9). The model also provided a clear determination of t_{max}, which was impossible with the experimental data due to variability in administration times.

One limitation of the isolated and perfused rat lung is the difference between human and rat metabolic activities [81]. Liver and blood esterase activities towards fluazifop-butyl, paraoxon and phenylacetate were different in human liver and blood, and overall lower in human than rat tissues [200]. Paranitrophenyl acetate and ester prodrugs of propanolol were found to hydrolyse quicker in the cytosol of intestinal mucosal cells from rats than that of humans but slower in microsomes of rat intestinal mucosa as compared to humans [201]. Plasma stability of cyclic prodrugs of opioid peptides was lower in rat plasma than in human plasma [202]. Moreover, cholinesterase activity in human blood is more important than carboxylesterase whereas in rat blood, carboxylesterase is dominant [203]. Novartis published a comparison of the biotransformation of a methylcarbonate derivative of cyclosporin A and the metabolism by esterases was about 8 times greater in rat than human lung slices [204]. Despite a similar expression profile for carboxylesterase 1 in rat and human lungs [205], there are interspecies differences in metabolic activity of the lung. Therefore, an IPRL model can only show that the conjugates are likely to improve the pharmacokinetic parameters C_{max} and t_{max}, but it does not predict to what extent these parameters would be improved in humans.

Further experiments could help predict the human situation. Firstly, a comparison between the conjugate hydrolysis rates in rat and human lung homogenates would give a good indication of the conjugate stability in human lung tissues. Secondly, *in vivo* rat pharmacokinetic profiles could be used to predict the human situation, using advanced simulation packages based on a 2 compartmental approach [35].

IV.4. Conclusion

In this section, a comparison was drawn between the pharmacokinetic profiles of prednisolone and two ester conjugates, in the isolated and perfused rat lung, after nebulisation administration of the compounds.

The conjugates decreased the relative maximum perfusate concentration (C_{max}) by a factor of 2.2 and 3.0 for $mPEG_{2000}$-$Pred_2$ and PEG_{2000}-$Pred_2$ respectively, compared to prednisolone. According to simulations, t_{max} was also increased by 26 and 45% for $mPEG_{2000}$-$Pred_2$ and PEG_{2000}-$Pred_2$ respectively, compared to prednisolone. The improved pharmacokinetic parameters (longer t_{max}, lower C_{max} for the same dose) observed with the conjugates would significantly decrease the systemic exposure to the drug and potentially lower the associated side effects.

There are two marketed inhaled corticosteroids that are activated by esterase: 17-beclomethasone dipropionate and ciclesonide. Both prodrugs are administered as inactive compounds and cleaved to generate the active molecule. PEG-prednisolone conjugates were retained in the lung during the time frame of the experiment (one hour), whereas beclomethasone dipropionate [197] and ciclesonide [206] are both rapidly found in blood after inhalation. The two prodrugs are rapidly activated (cleaved) in lung and plasma [196] [207] and then conjugated to fatty acid to accumulate in the lung. In comparison to existing prodrugs, the conjugation to a large hydrophilic polymer such as PEG, provides a sustained release of the drug in lung tissue, by accumulation of the inactive conjugate in the airways.

Metabolised PEG conjugates were only hydrolysed in the lung to release prednisolone that then crossed the airway epithelium, since neither PEG nor the conjugates were recovered in perfusate.

Chapter V. General conclusion

V.1. An improved pharmacokinetic profile

The development of ester conjugates of PEG and inhaled drugs was illustrated in this thesis and ended up with the production of a lead model compound: a diester of PEG (2000 Da) and prednisolone (PEG_{2000}-$Pred_2$). The aim of the project was to improve the pharmacokinetic profile of a drug after inhalation administration, and this was successfully achieved. The rationale for the conjugate design was based on a rapid passive diffusion of small molecules through the lung epithelium. The conjugation of such a drug to a large hydrophilic polymer did ensure that the inactive conjugate stayed in lung fluids before hydrolysis occurred and released the free, active ingredient.

V.2. A drug development journey

A large number of conjugates could have been designed *in silico* by changing the four parameters that characterised the conjugates. The type of polymer, the molecular weight, the linker, and the drug could be varied, expanding the design space. The actual production of drug conjugates was narrowed to one polymer (PEG), one type of linker (ester), two well known drugs (prednisolone, and salbutamol) and three or four polymer molecular weights and end groups for respectively PEG-salbutamol and PEG-prednisolone. After the successful production of seven drug ester conjugates (Chapter II), the number of potential candidates was down to the four PEG-prednisolone since PEG-salbutamol were unstable at biological pHs (III.3.2). After a basic cytotoxicity screening, the number

of potential candidates was reduced to three since PEG_{3400}-$Pred_2$ induced some cell membrane damage (III.3.3, p. 160). According to the pharmacokinetic profiles obtained with the Isolated and Perfused Rat Lung, the best candidate was PEG_{2000}-$Pred_2$ since it considerably decreased C_{max} and increased t_{max}.

V.3. Further work

Safety and efficacy of the conjugates have to be assessed *in vivo* to ensure an efficient and safe disposition of the oxidised polymer after cleavage and the functionality of the released drug. The drug safety could be studied by examining slices of fixed rat lung after single exposure (acute toxicology) and repeated exposure (chronic exposure) to the conjugates. The efficacy could be assessed with the Sephadex-induced rat lung injury. This model has been developed to study lung inflammation of rats following intravenous injection or intratracheal instillation of suspension of saline containing Sephadex particles. The resulting inflamed lungs are characterised by granulomas, presence of neutrophils and eosinophils, and local increase in TNF-α (Tumor necrosis factor alpha). It has been used to illustrate the anti inflammatory properties of various compounds such as coumarin derivatives. [208, 209]. The drug effect has to be assessed following administration of the conjugates, and the correlation between prolonged delivery of the active drug in the lung and prolonged effect must be ascertained. The delivery of such conjugates has to be studied too. Although nebulisation was the more relevant mode of inhalation for the purpose of this work, the shelf life of such conjugates in aqueous solution, even at low pH, is too short and the use of nebulisation devices is not convenient for the patients. Therefore, solid formulations should be considered. The production

of solid particles of PEG-conjugates and lactose may be troublesome since PEG is a sticky polymer with a low melting point [210], but this could be overcome with the use of copolymer as excipients, or because the polymer is conjugated to a high melting point drug [211]. Suspension or solution of PEG conjugates in hydrofluoroalkane (HFA) could be studied for pressurised metered dose inhalers, since PEG_{1000} is currently used as a valve lubricant in the formulation of Symbicort [27].

V.4. Room for improvements

The project proved the concept and illustrated the benefits of polymer-drug conjugation for inhaled delivery of drugs. Despite the promising results for PEG-prednisolone conjugates, the other investigated molecule, salbutamol, did not provide conjugates stable enough for the purpose of this work. The drug properties appeared to be of primary importance for the stability of the conjugates, especially the amine group of salbutamol was responsible for catalysing ester hydrolysis, and the resulting conjugates were highly unstable. Thus, such amine containing compounds could benefit from other types of linker such as amide or carbamate. Such conjugations would result in more stable compounds, with similar hydrolysis pathways of ester [212, 213]. Depending on the drug chemical structure, other linkers such as carbonate ester [214], acetal or orthoester [215, 216] could potentially be of interest. The stability of these linkers in physiological condition is unpredictable but they can undergo hydrolysis and release the active drug. Ester or amide bond seem the more promising linkers since carboxylesterases can hydrolyse these chemical bonds [217-219], especially with the presence of carboxylesterase 1

and 2 in the lung [205]. Particularly, small peptide chains could be used as linkers [220] between polymer and drug, and the drug cleaved by lung proteases [221, 222], mainly produced by inflammatory cells [223].

The stability of drug conjugates towards enzymatic hydrolysis could be increased by the addition of sterically hindered groups around the ester or amide bond [224, 225].

The relative low drug loading of the polymer could be improved by the use of branched polymers and one molecule of hydrophilic polymer could be conjugated to several molecules of drugs [226-228].

The use of such a conjugation strategy for compounds delivered by inhalation could be of the greatest interest for drugs with low aqueous solubility [229]. Indeed, PEG conjugation would improve solubility in lung fluids and limit the risk for immunological responses [230], the drug would then be released in a controlled manner.

Drug acting locally with systemic side effects would most definitely benefit from PEG ester conjugation. As demonstrated with PEG-prednisolone conjugates, for a given dose, the maximum concentration in the systemic circulation (perfusate *ex vivo*, blood *in vivo*) was significantly lowered when using the conjugate. This feature could benefit most inhaled locally acting drugs, especially chemotherapeutic drugs whose effectiveness is limited by systemic side effects [231, 232].

Chapter VI. Appendices

Appendix 1. Supplementary information for II.3.1, PEG oxidation

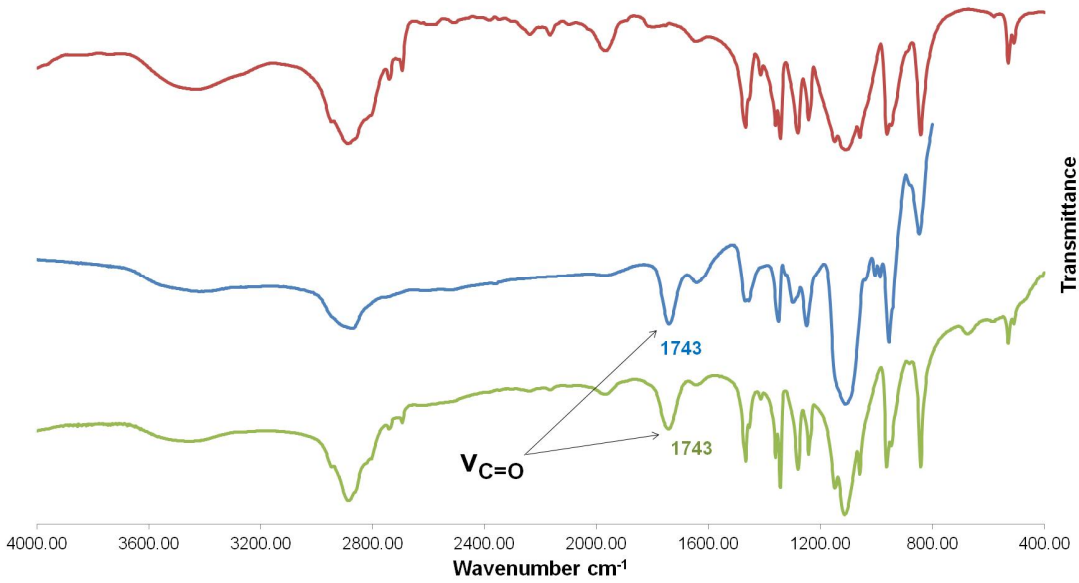

Fig.VI.1. IR spectra for PEG_{3400}, $PEG_{2000}COOH$ and $PEG_{1000}COOH$
— $PEG_{3400}OH$, — $PEG_{1000}COOH$, — $PEG_{2000}COOH$

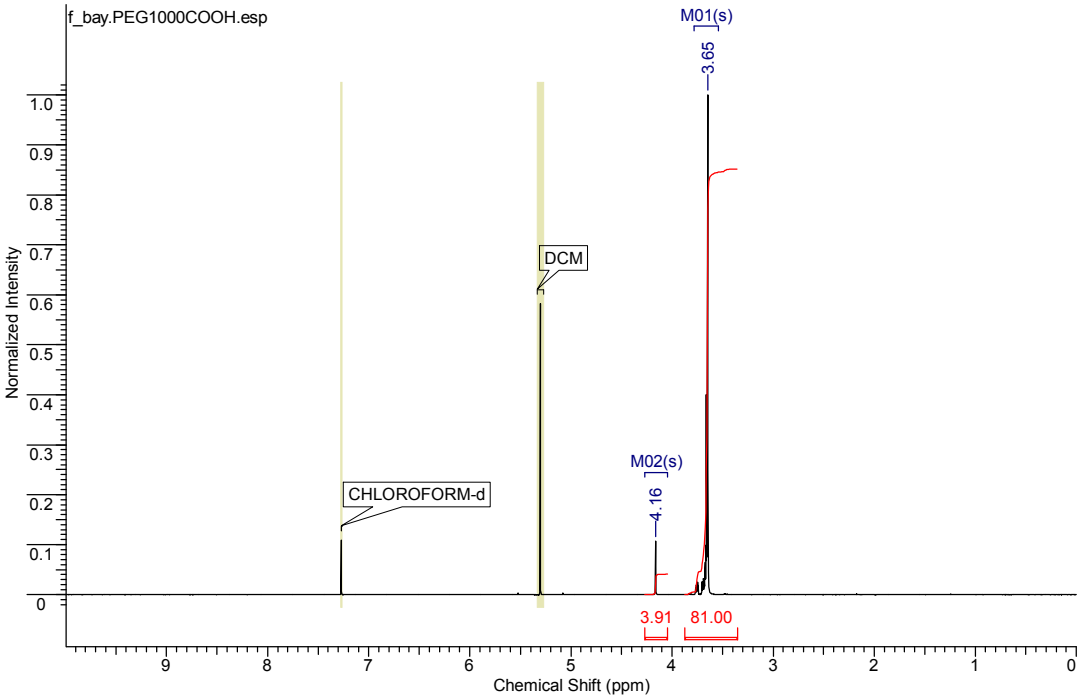

Fig.VI.2. ^{1}HNMR for oxidised $PEG_{1000}COOH$
Spectrum acquired on a Bruker DPX 400 spectrometer, 64 scans, in $CDCl_3$

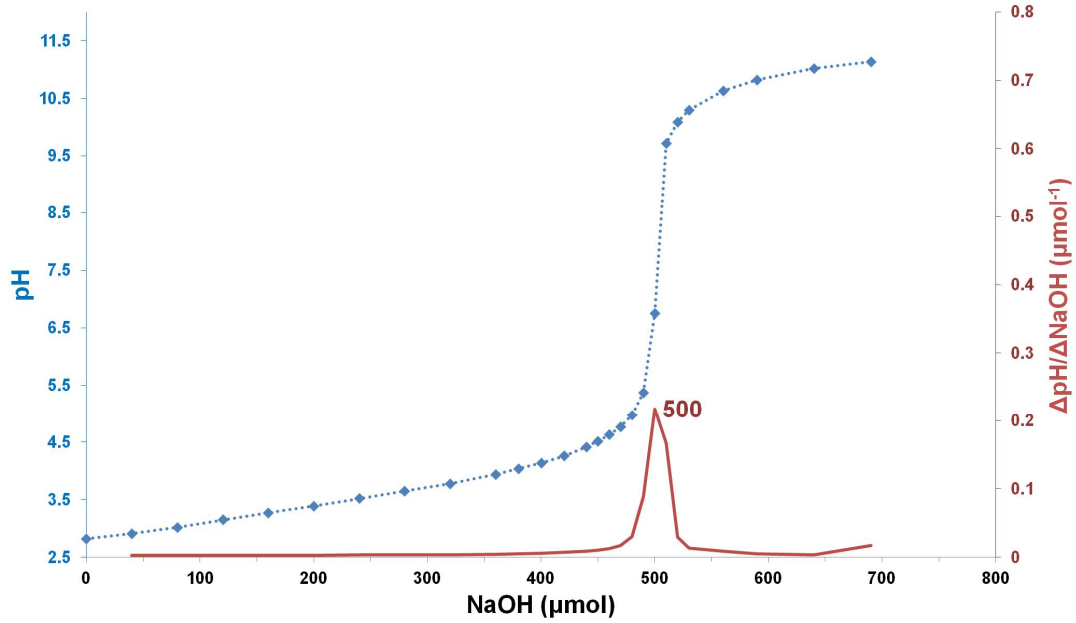

Fig.VI.3. Acid titration of $PEG_{1000}COOH$
-♦- pH, — ΔpH/ΔNaOH

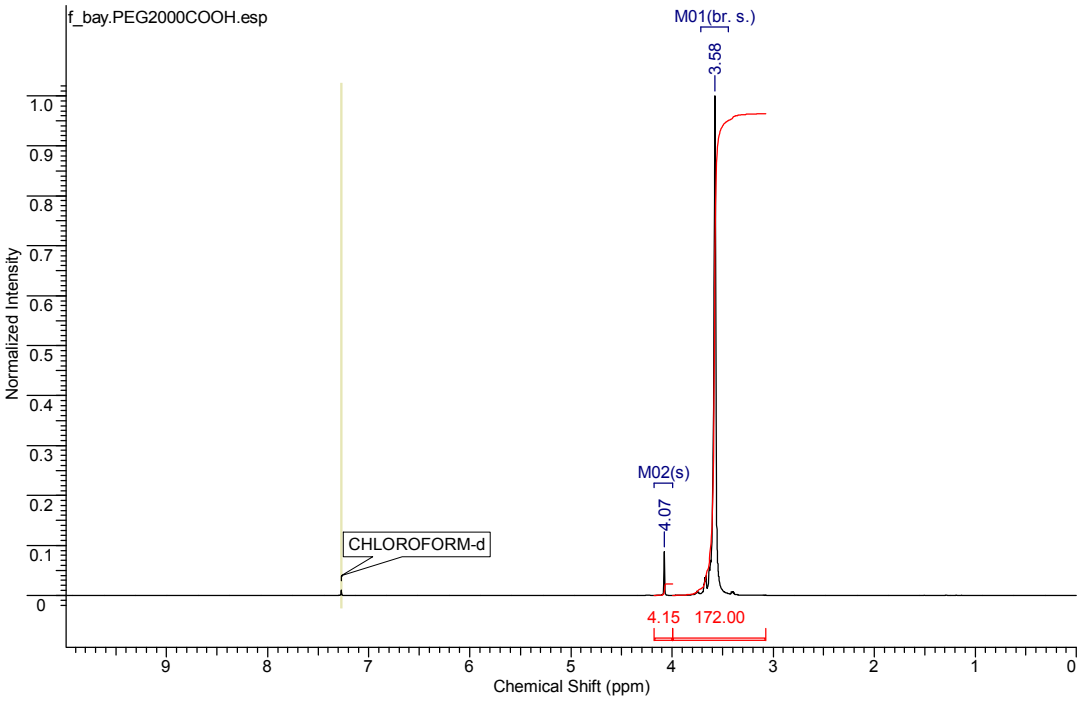

Fig.VI.4. $^{1}HNMR$ for $PEG_{2000}COOH$
Spectrum acquired on a Bruker AV(III)400 spectrometer, 64 scans, in $CDCl_3$

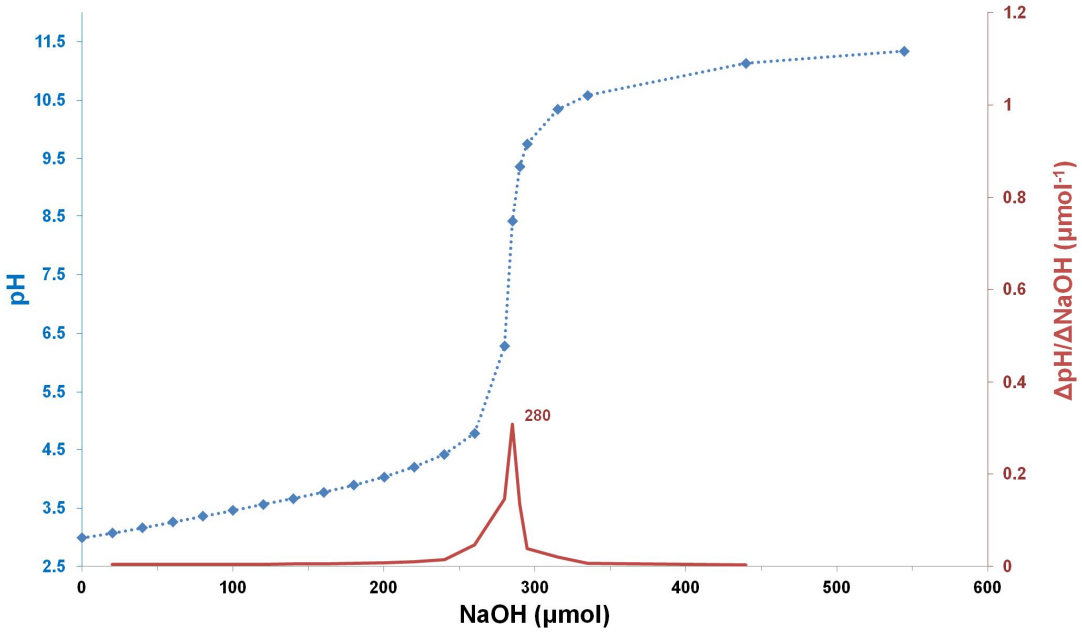

Fig.VI.5. Acid titration for $PEG_{2000}COOH$
-♦- pH, — ΔpH/ΔNaOH

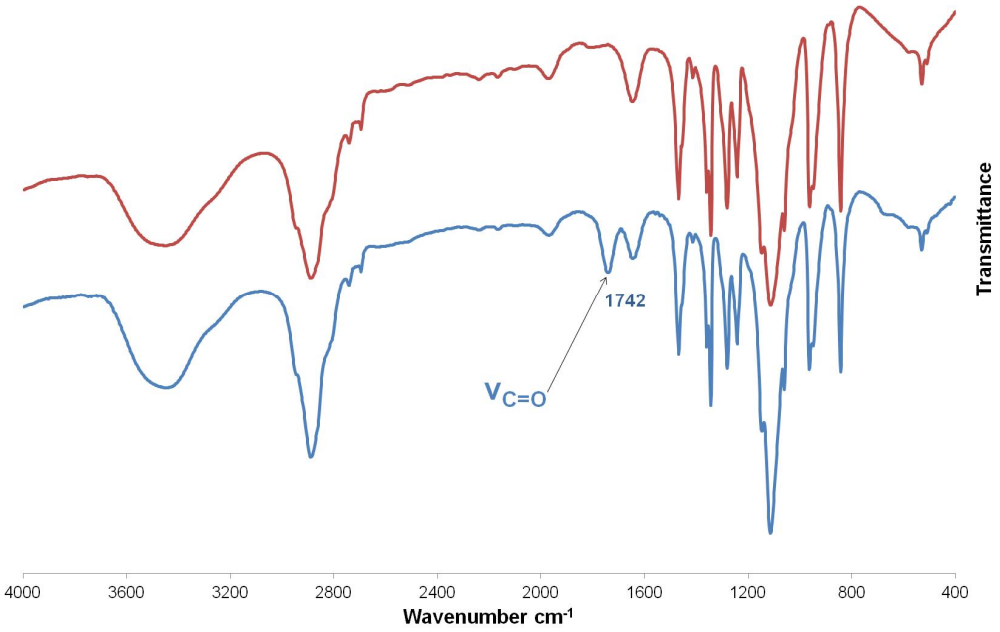

Fig.VI.6. IR spectra for $mPEG_{2000}$ and $mPEG_{2000}COOH$
— $mPEG_{2000}OH$, — $mPEG_{2000}COOH$

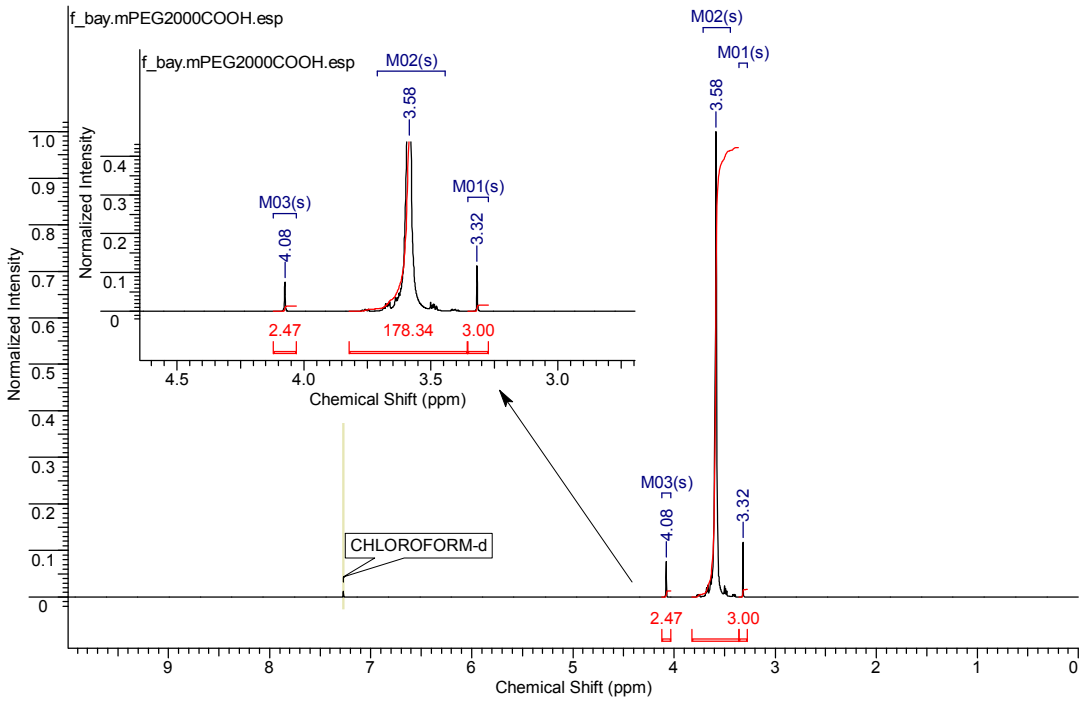

Fig.VI.7. ^{1}HNMR for $mPEG_{2000}COOH$
Spectrum acquired on a Bruker AV(III)400 spectrometer, 64 scans, in $CDCl_3$

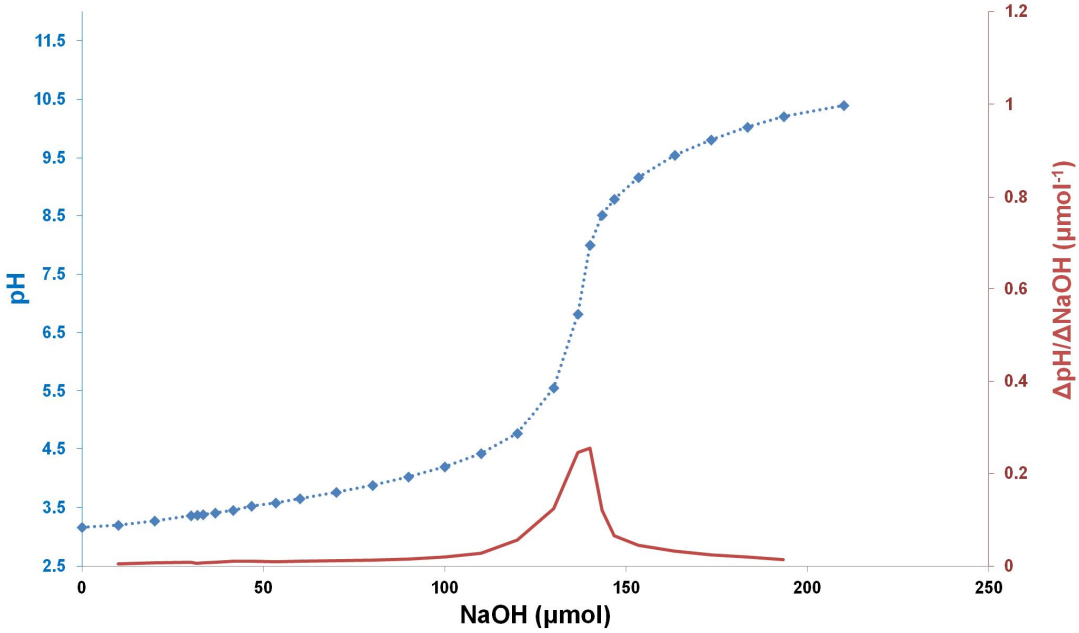

Fig.VI.8. Acid titration for $mPEG_{2000}COOH$
-♦- pH, — ΔpH/ΔNaOH

Appendix 2. Supplementary information for PEG-prednisolone, acyl chloride route

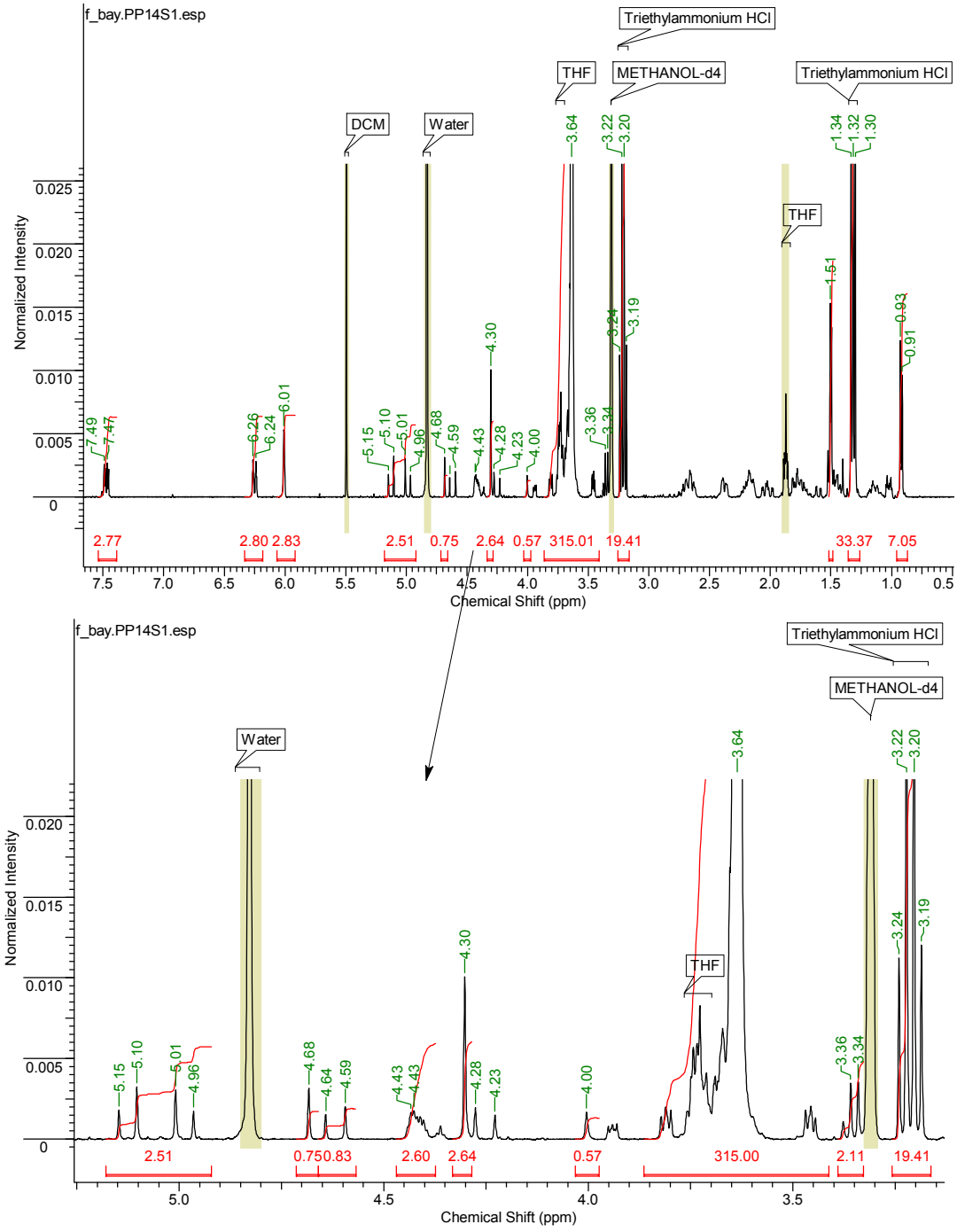

Fig.VI.9. ^{1}HNMR spectrum for PP14 crude
Spectrum acquired on a Bruker AV(III)400 spectrometer, 64 scans, in MeOD

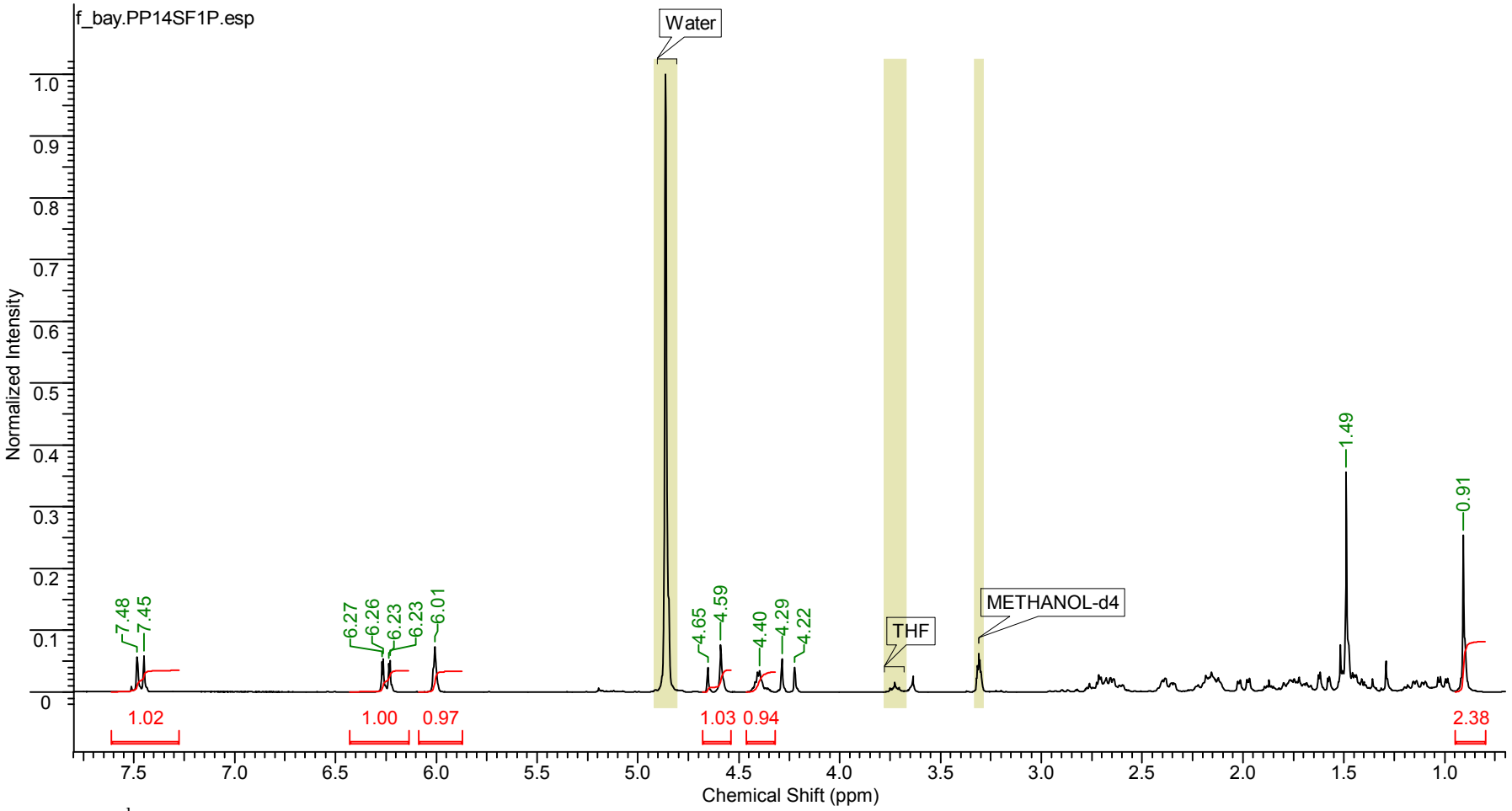

Fig.VI.10. [1]HNMR for PP14SF1
Spectrum acquired on a Bruker DPX 300 spectrometer, 64 scans, in MeOD

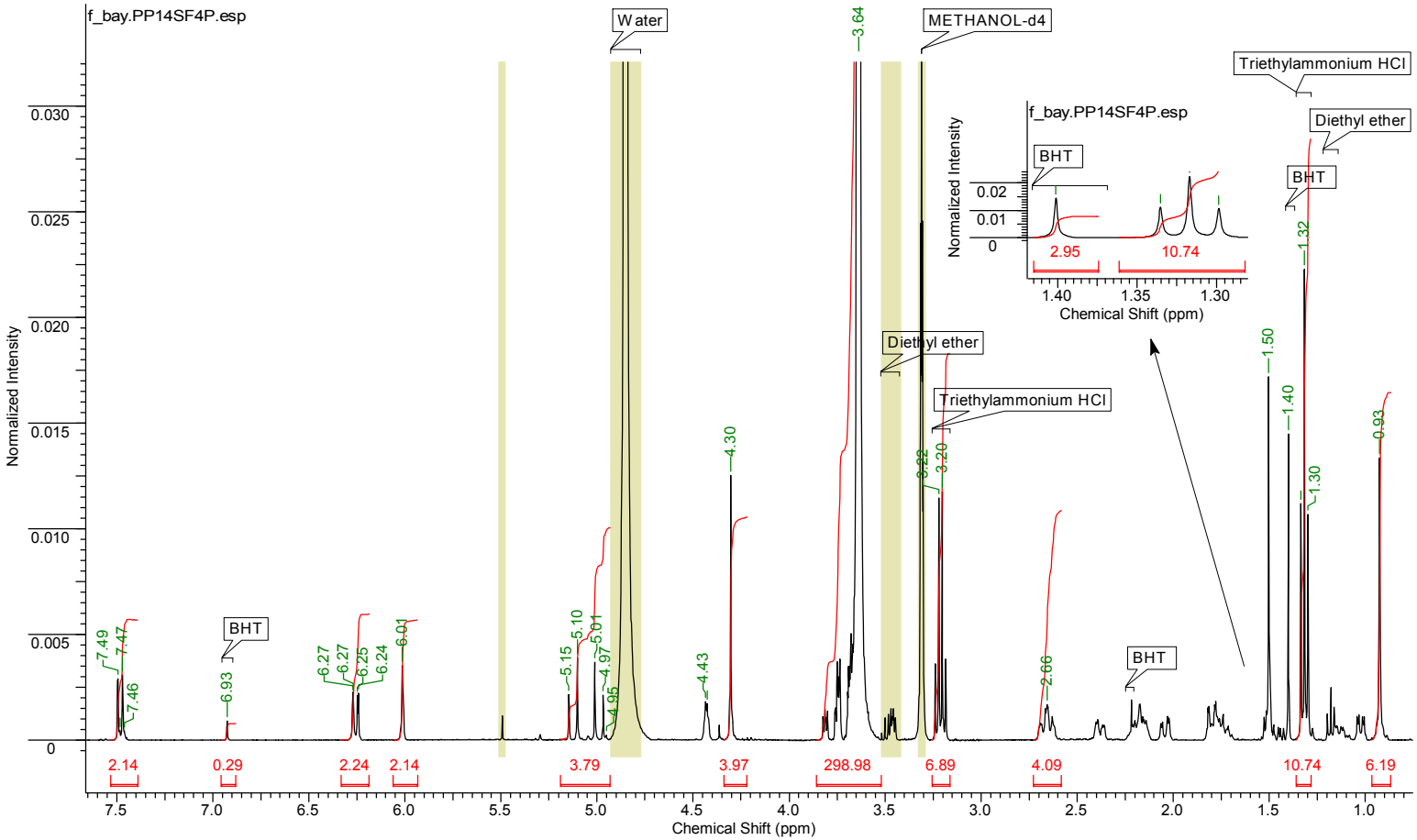

Fig.VI.11. [1]HNMR for PP14SF4
Spectrum acquired on a Bruker DPX 400 spectrometer, 64 scans, in MeOD

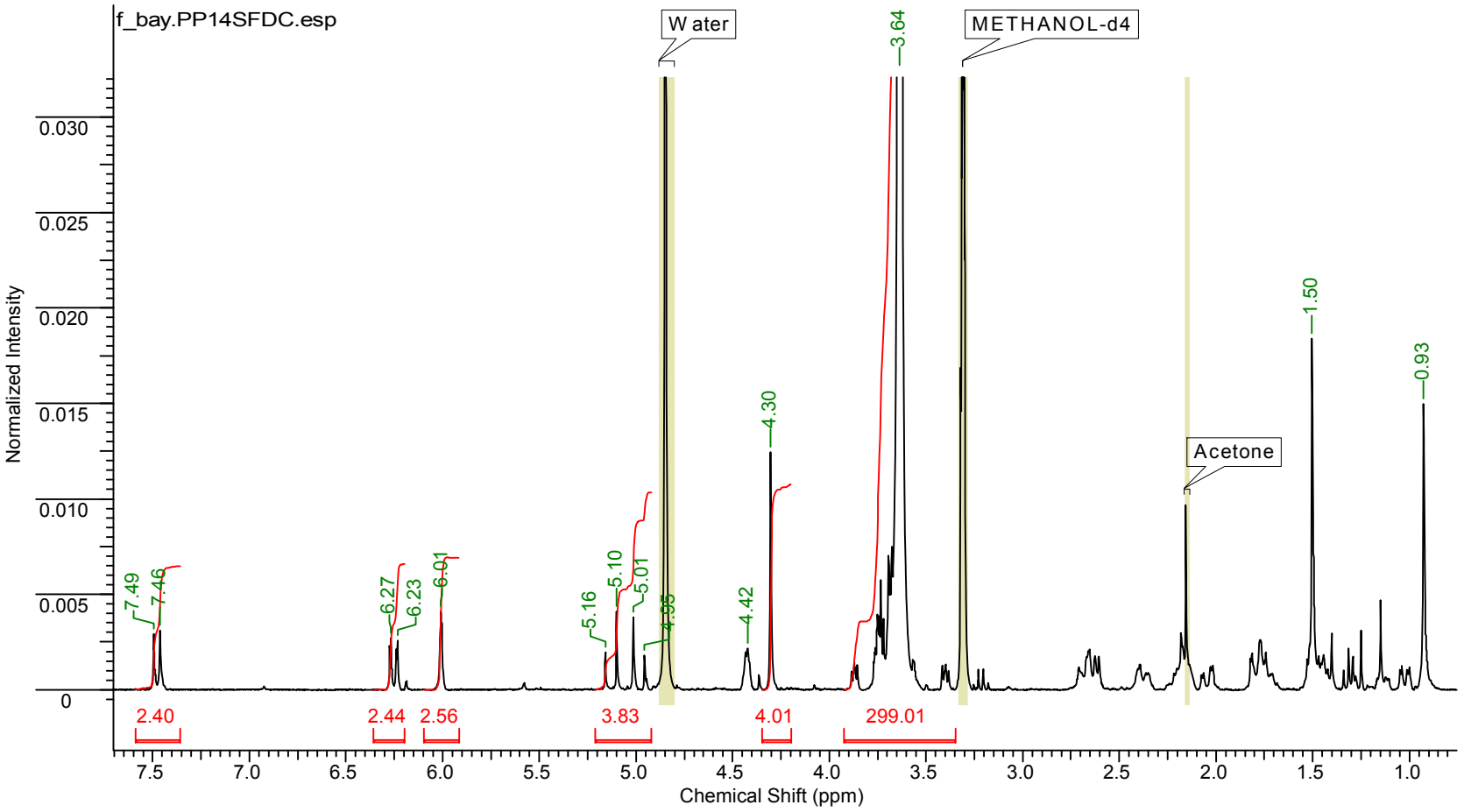

Fig.VI.12. ^{1}HNMR of PP14SFDC
Spectrum acquired on a Bruker DPX 300 spectrometer, 64 scans, in MeOD

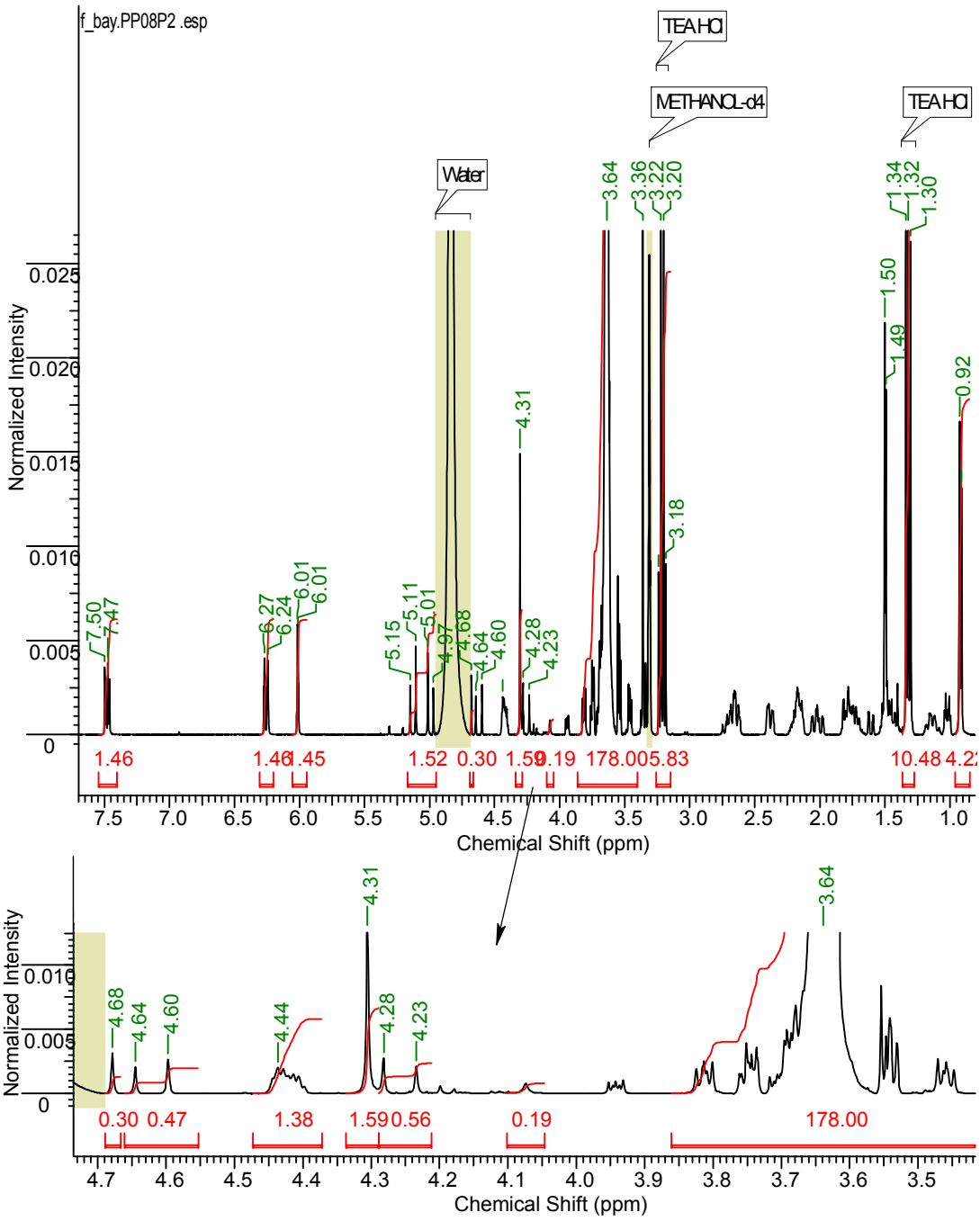

Fig.VI.13. ^{1}HNMR of crude PP08P2
Spectrum acquired on a Bruker AV(III)400 spectrometer, 64 scans, in MeOD

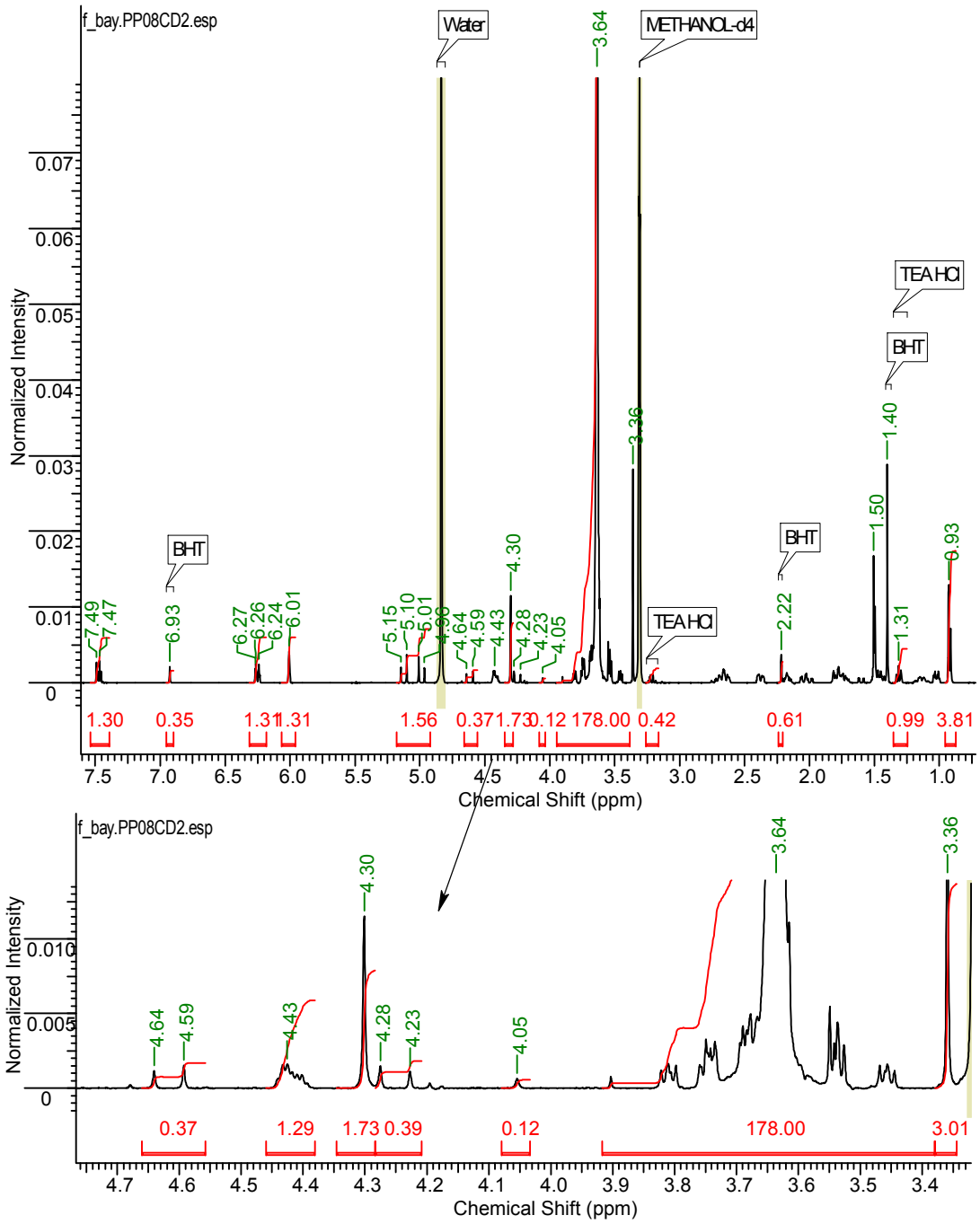

Fig.VI.14. 1HNMR of PP08DC2
Spectrum acquired on a Bruker AV(III)400 spectrometer, 16 scans, in MeOD

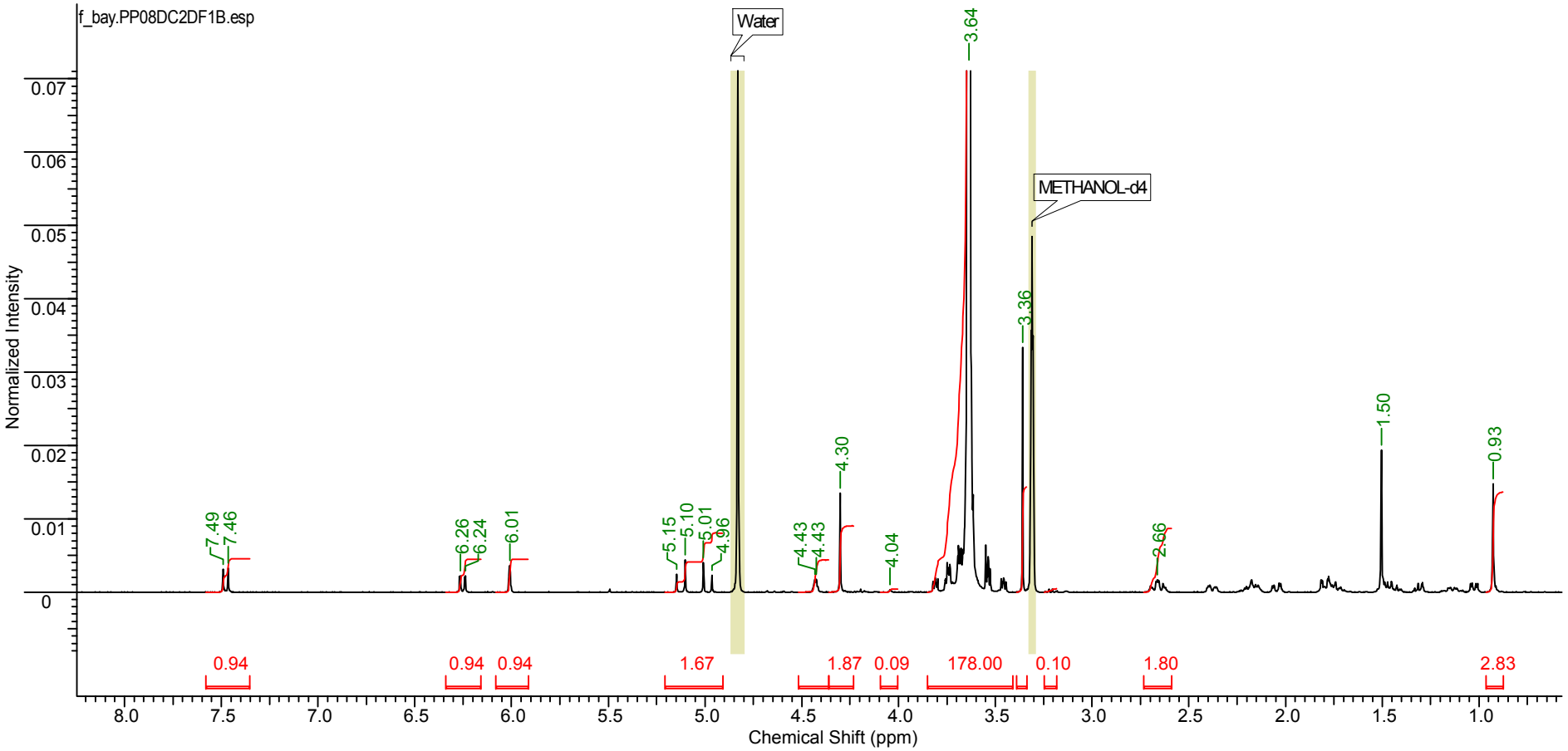

Fig.VI.15. 1HNMR of PP08DC2DF1B

Spectrum acquired on a Bruker AV(III)400 spectrometer, 64 scans, in MeOD

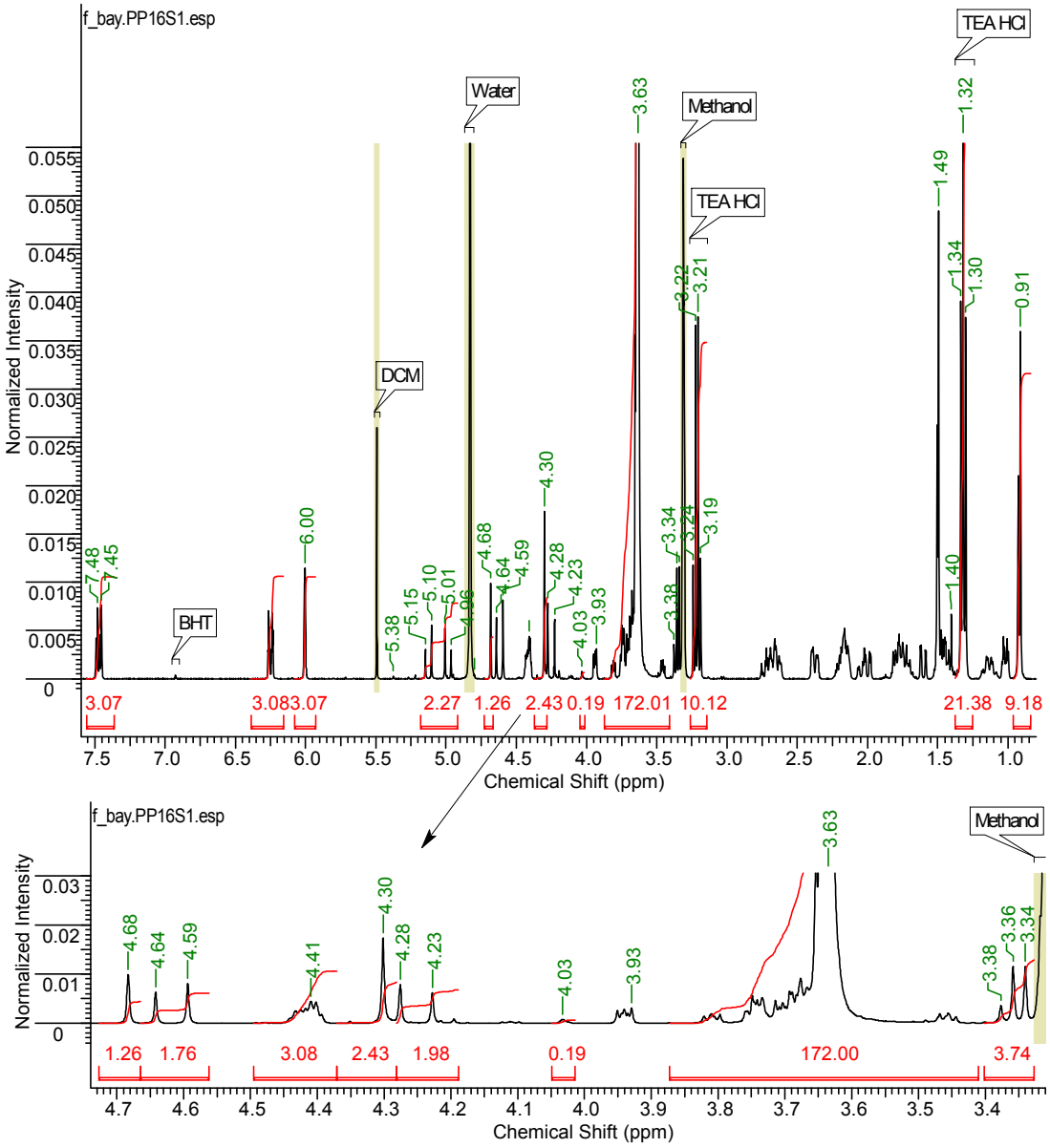

Fig.VI.16. ^{1}HNMR of crude PP16S1
Spectrum acquired on a Bruker AV(III)400 spectrometer, 64 scans, in MeOD

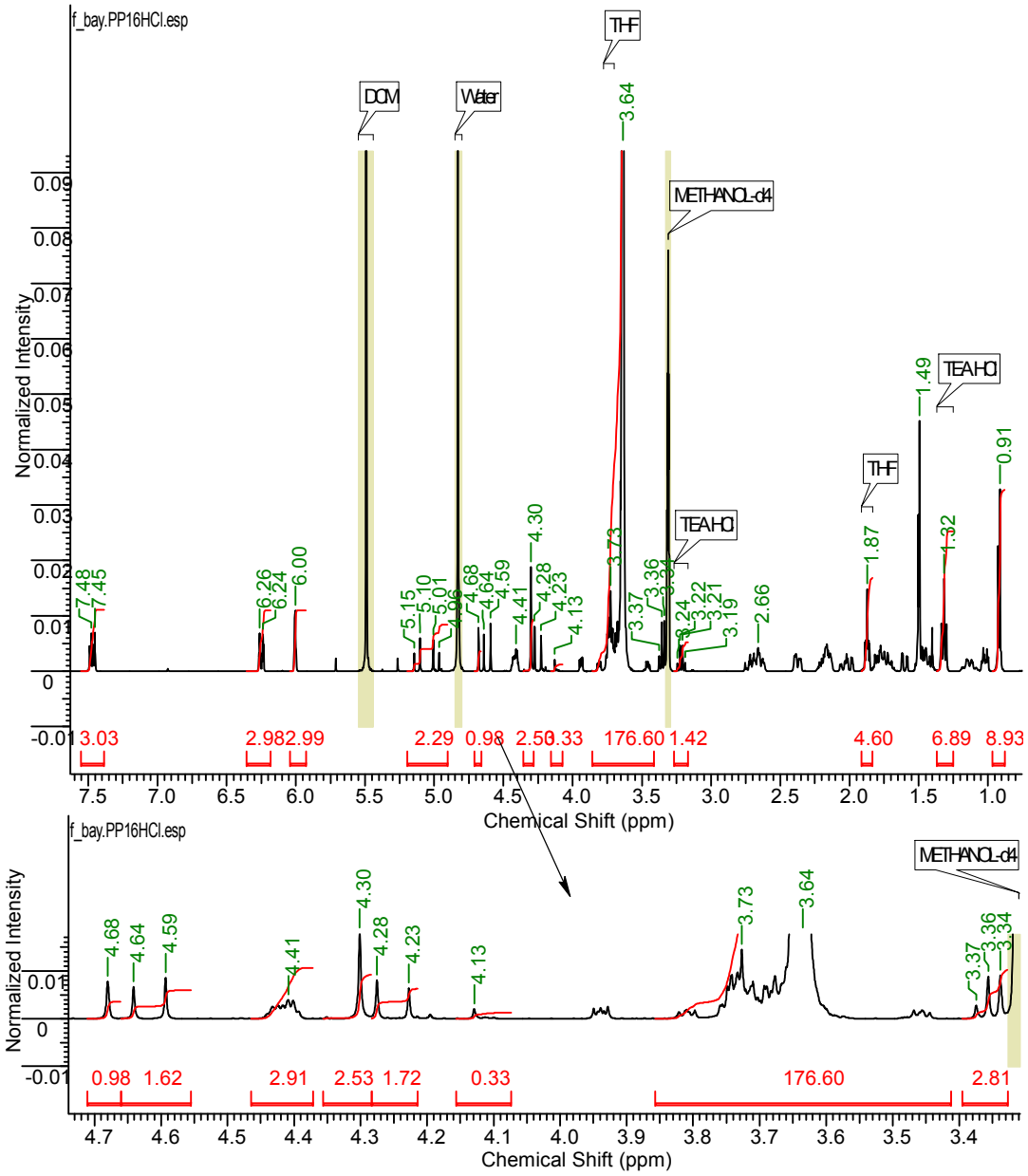

Fig.VI.17. ^{1}HNMR of PP16HCl
Spectrum acquired on a Bruker AV(III)400 spectrometer, 16 scans, in MeOD

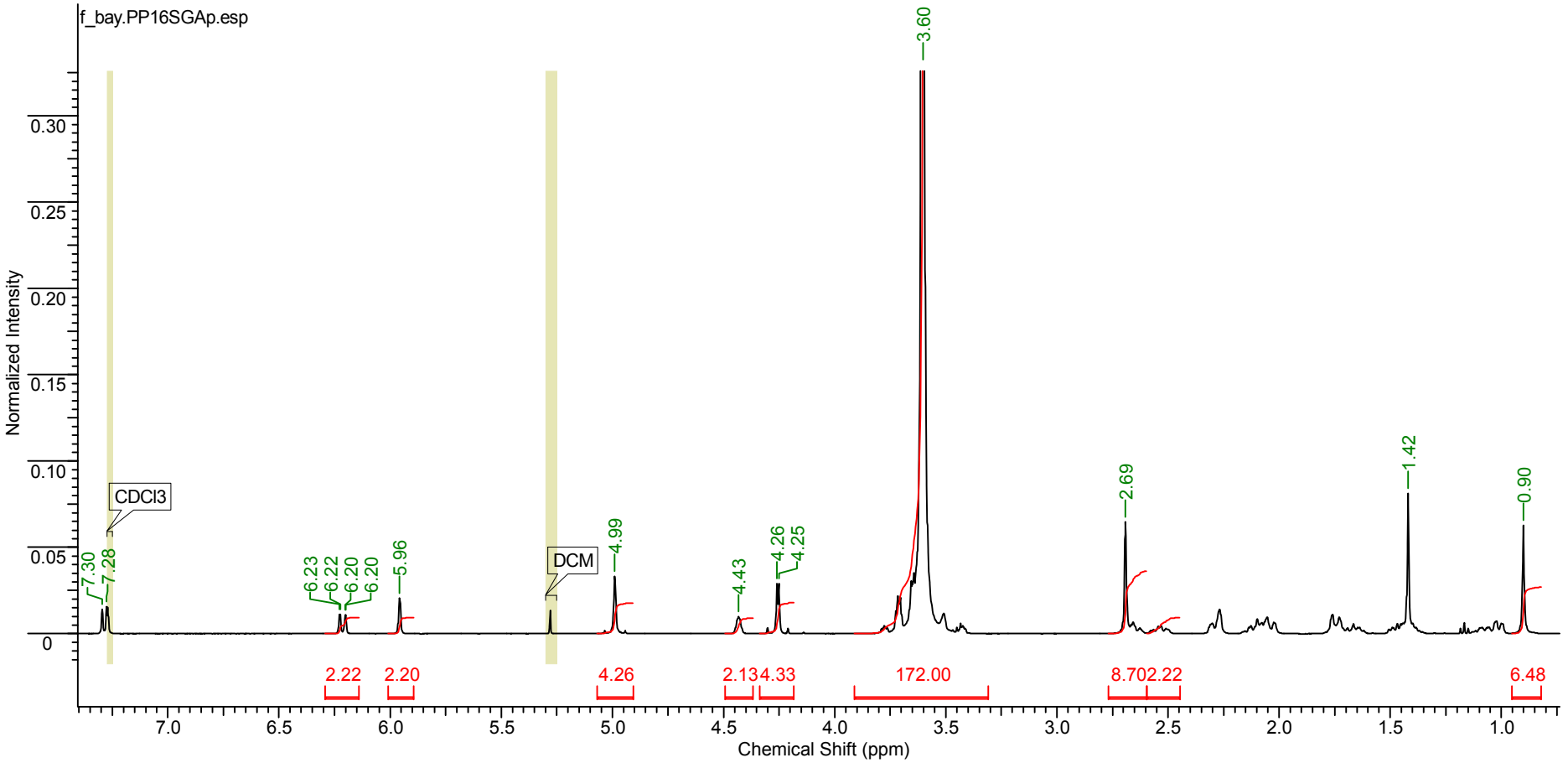

Fig.VI.18. ^{1}HNMR of PP16SGAp
Spectrum acquired on a Bruker AV(III)400 spectrometer, 64 scans, in $CDCl_3$

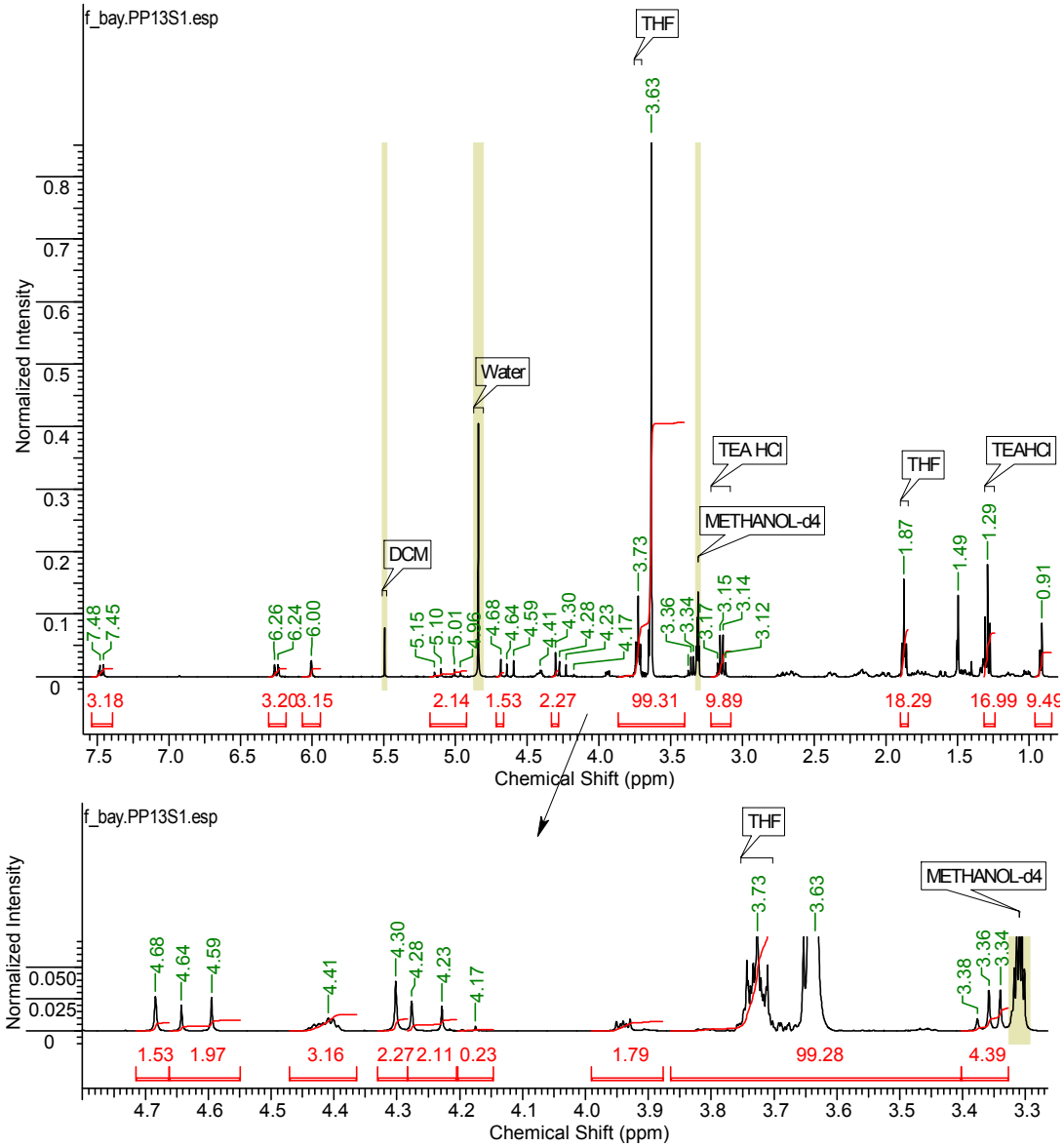

Fig.VI.19. ^{1}HNMR of crude PP13S1
Spectrum acquired on a Bruker DPX 400 spectrometer, 64 scans, in MeOD

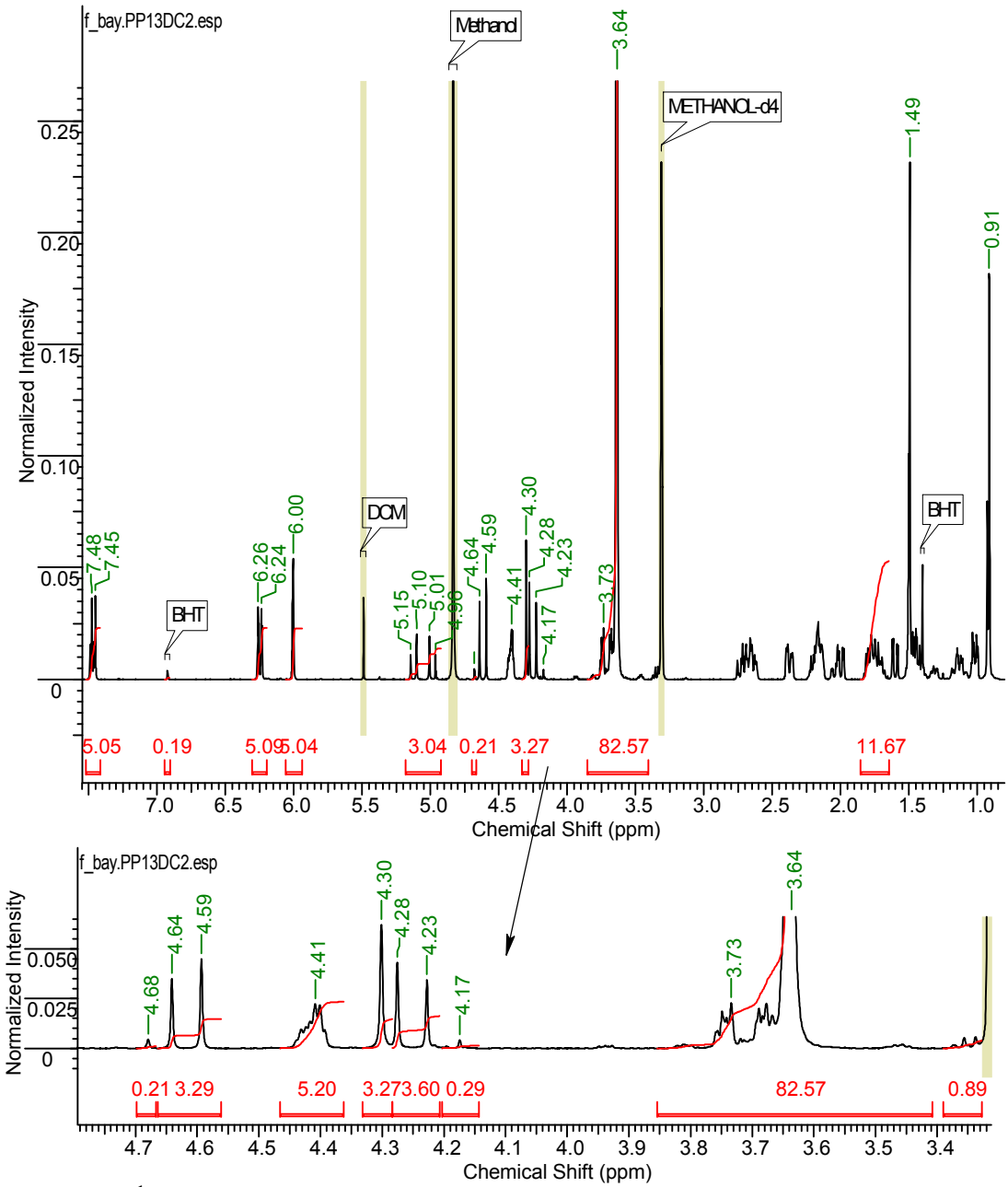

Fig.VI.20. ^{1}HNMR of PP13DC2

Spectrum acquired on a Bruker AV(III)400 spectrometer, 64 scans, in MeOD

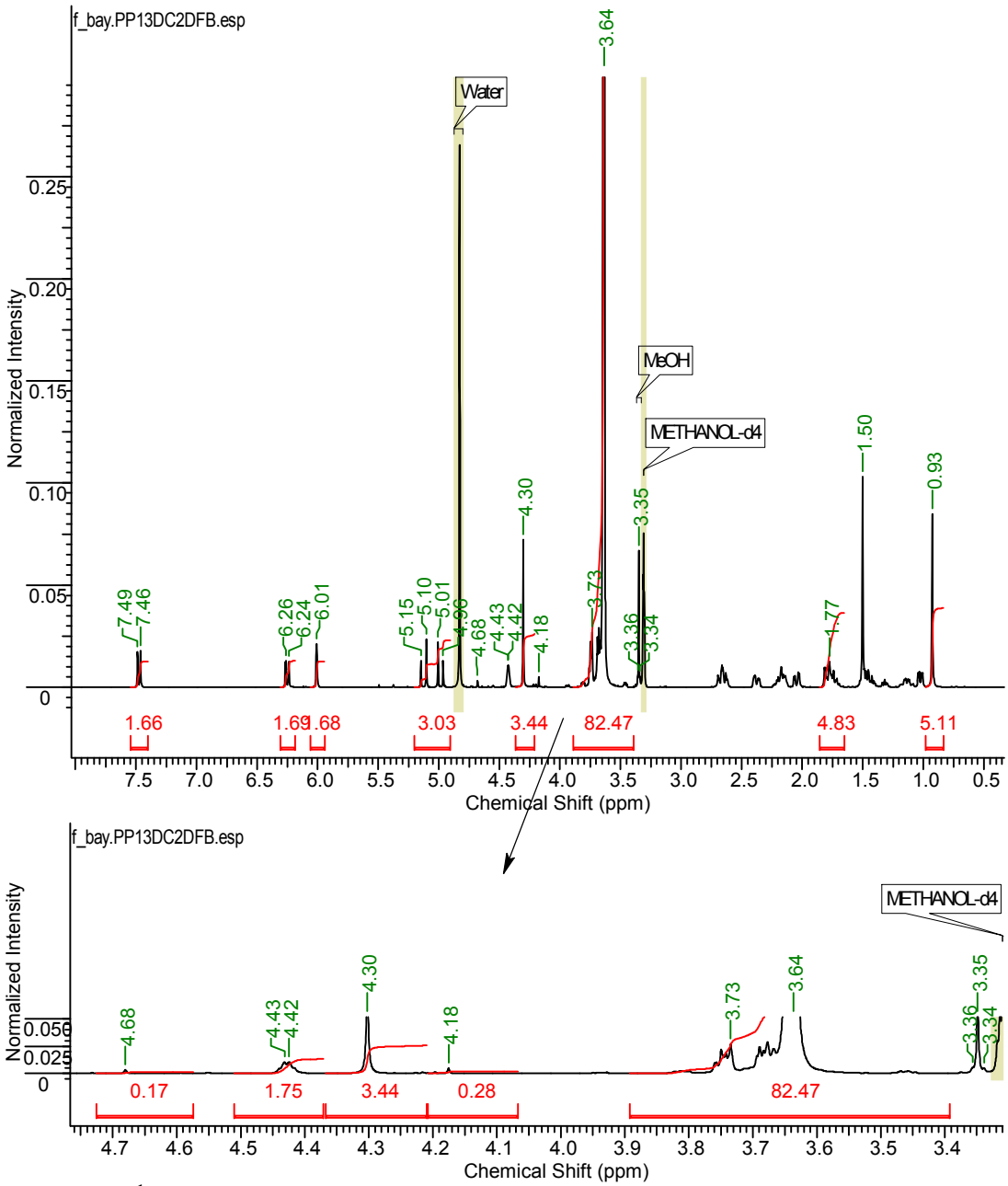

Fig.VI.21. ^{1}HNMR of PP13DC2DFB
Spectrum acquired on a Bruker AV(III)400 spectrometer, 64 scans, in MeOD

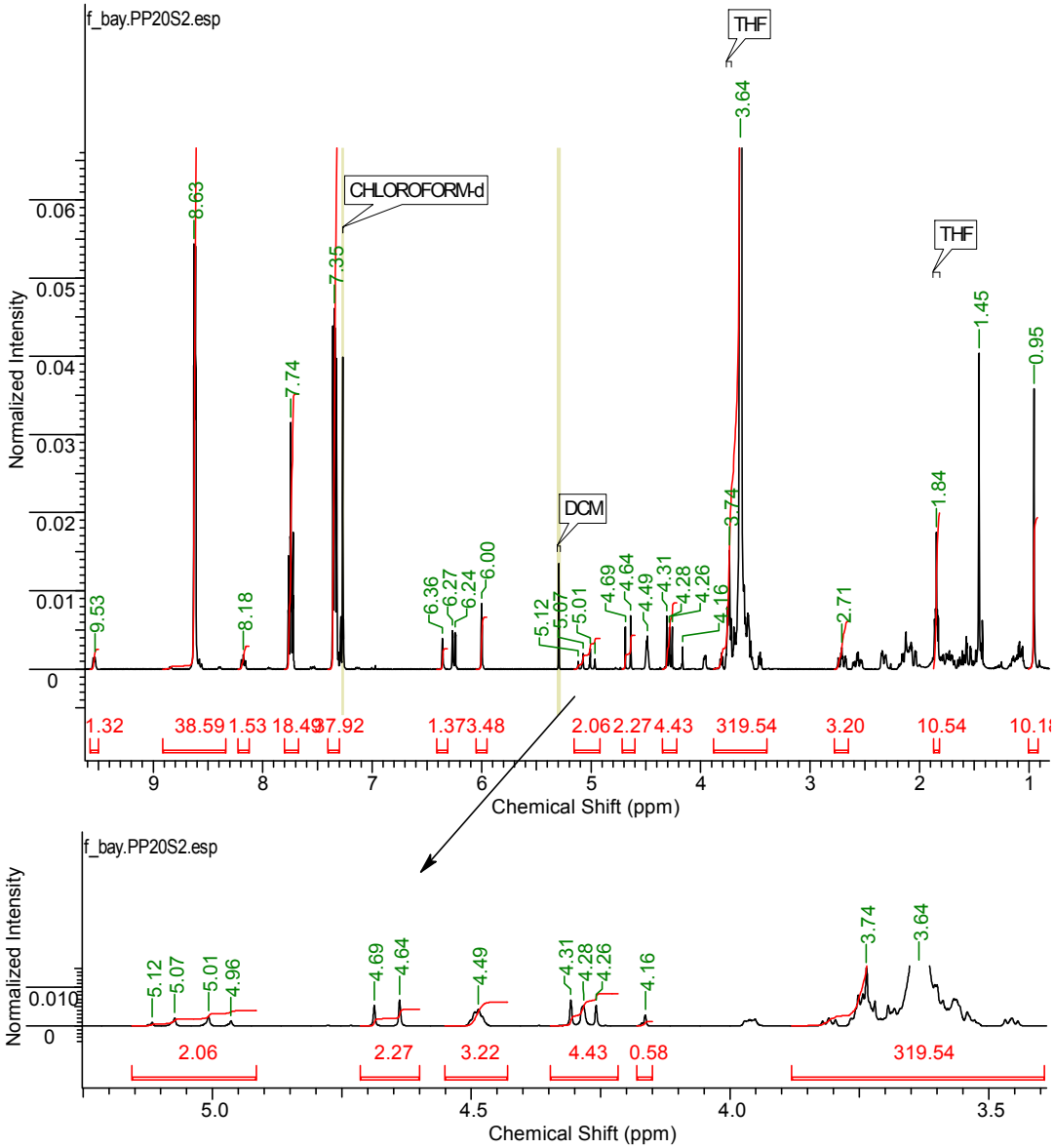

Fig.VI.22. ^{1}HNMR of PP20S2
Spectrum acquired on a Bruker AV(III)400 spectrometer, 64 scans, in $CDCl_3$

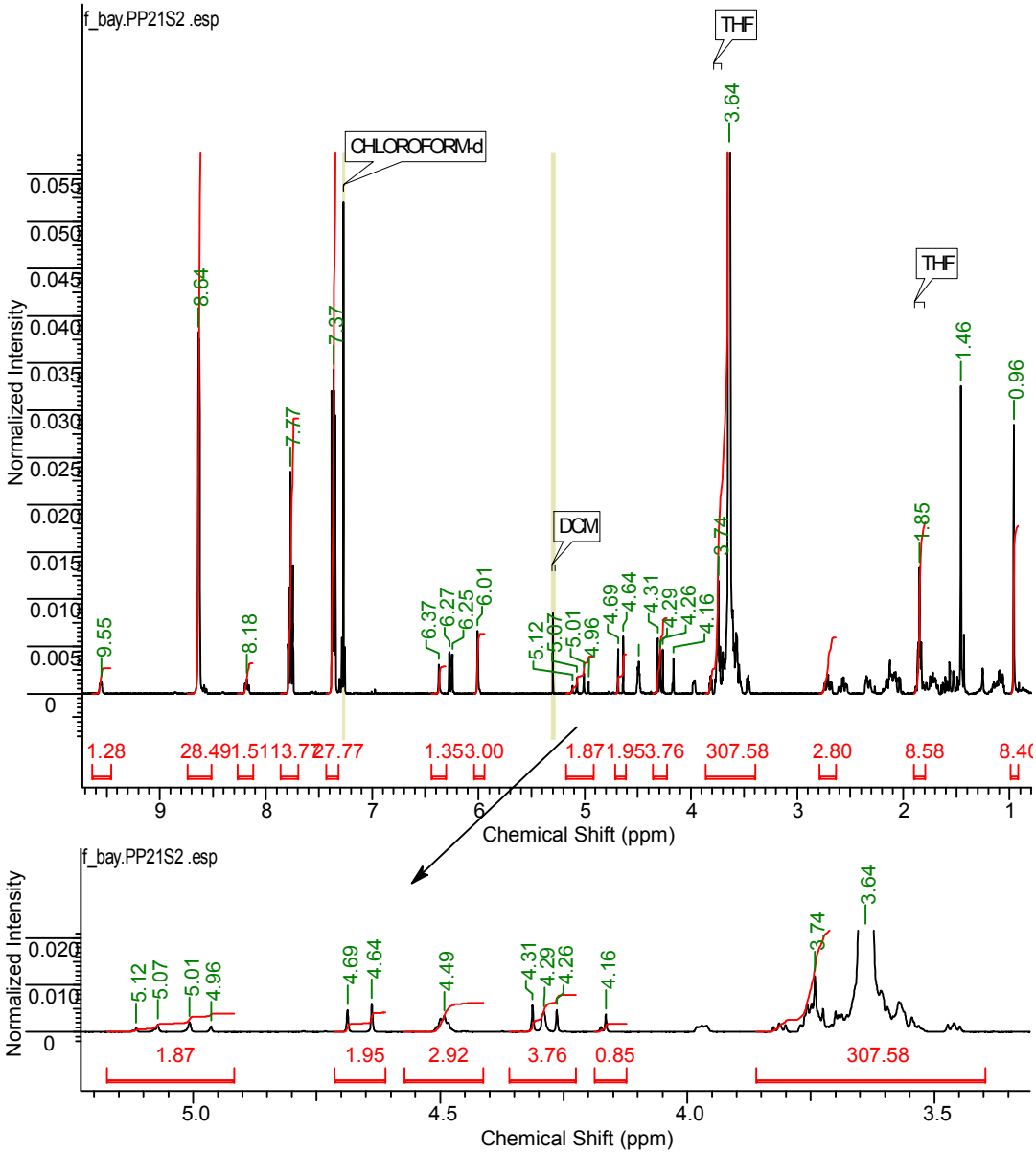

Fig.VI.23. ^{1}HNMR of PP21S2
Spectrum acquired on a Bruker AV(III)400 spectrometer, 64 scans, in $CDCl_3$

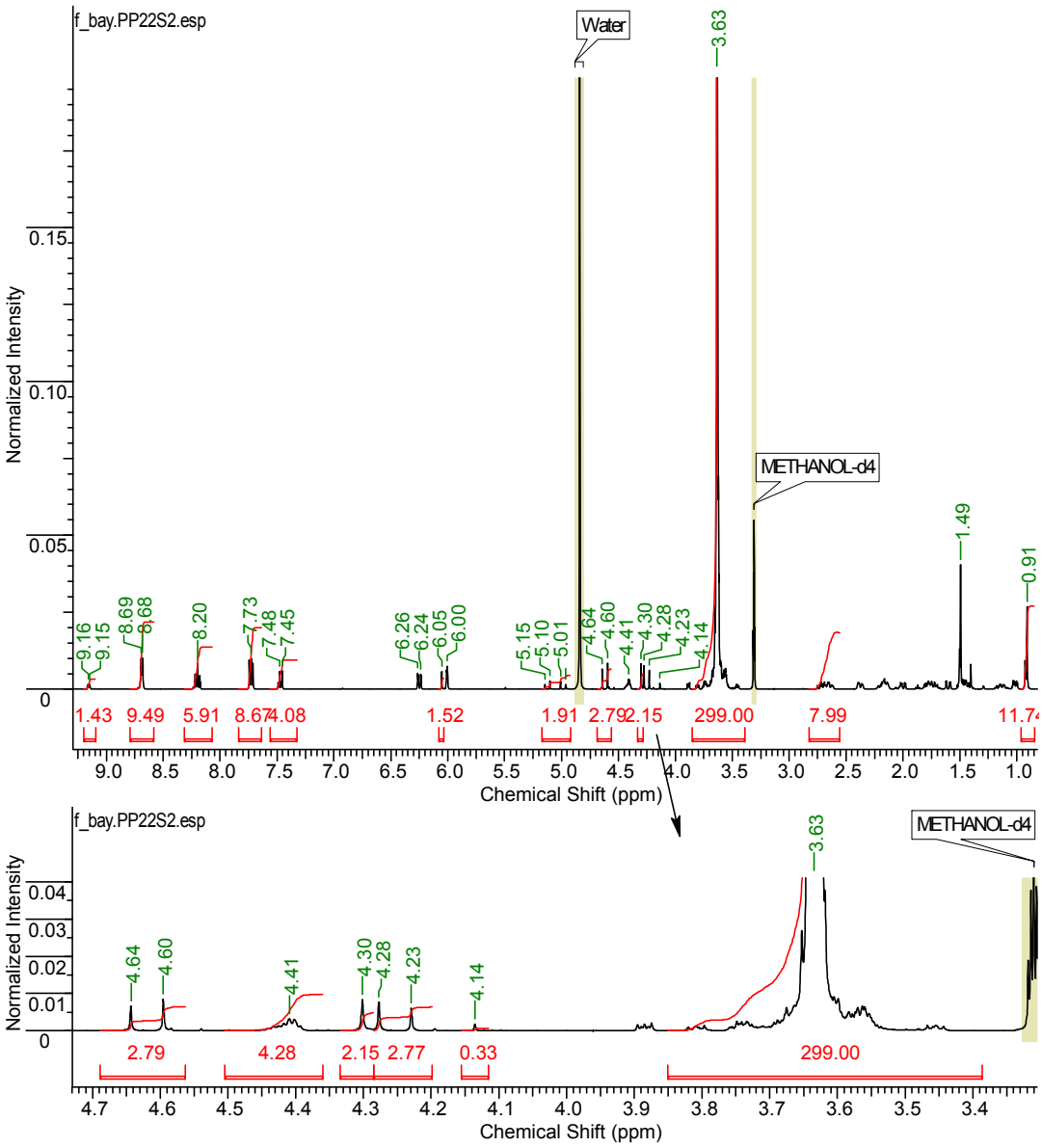

Fig.VI.24. ^{1}HNMR of PP22S2
Spectrum acquired on a Bruker DPX 400 spectrometer, 64 scans, in MeOD

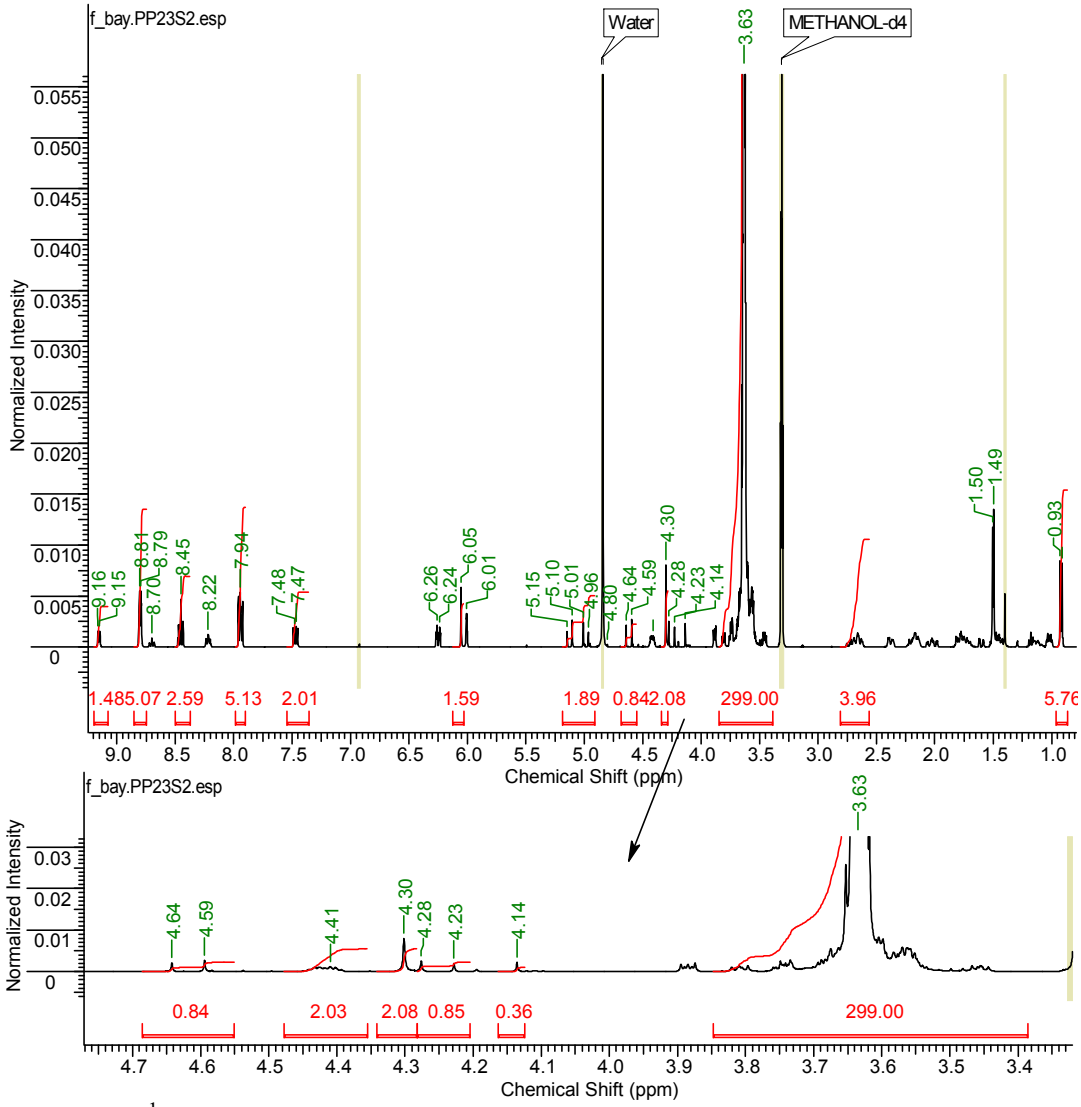

Fig.VI.25. ^{1}HNMR of PP23S2
Spectrum acquired on a Bruker DPX 400 spectrometer, 64 scans, in MeOD

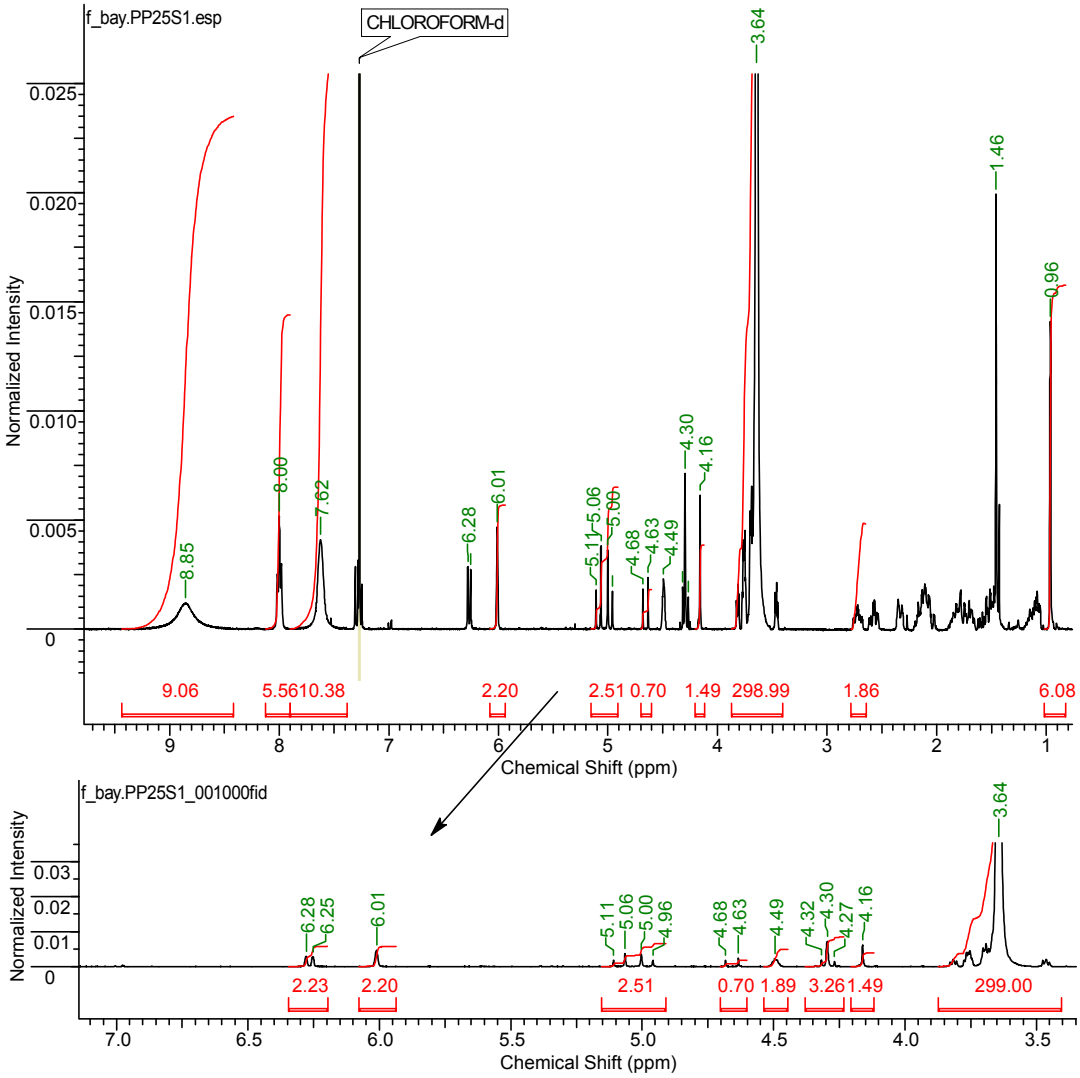

Fig.VI.26. ^{1}HNMR of PP25S1
Spectrum acquired on a Bruker AV(III)400 spectrometer, 64 scans, in $CDCl_3$

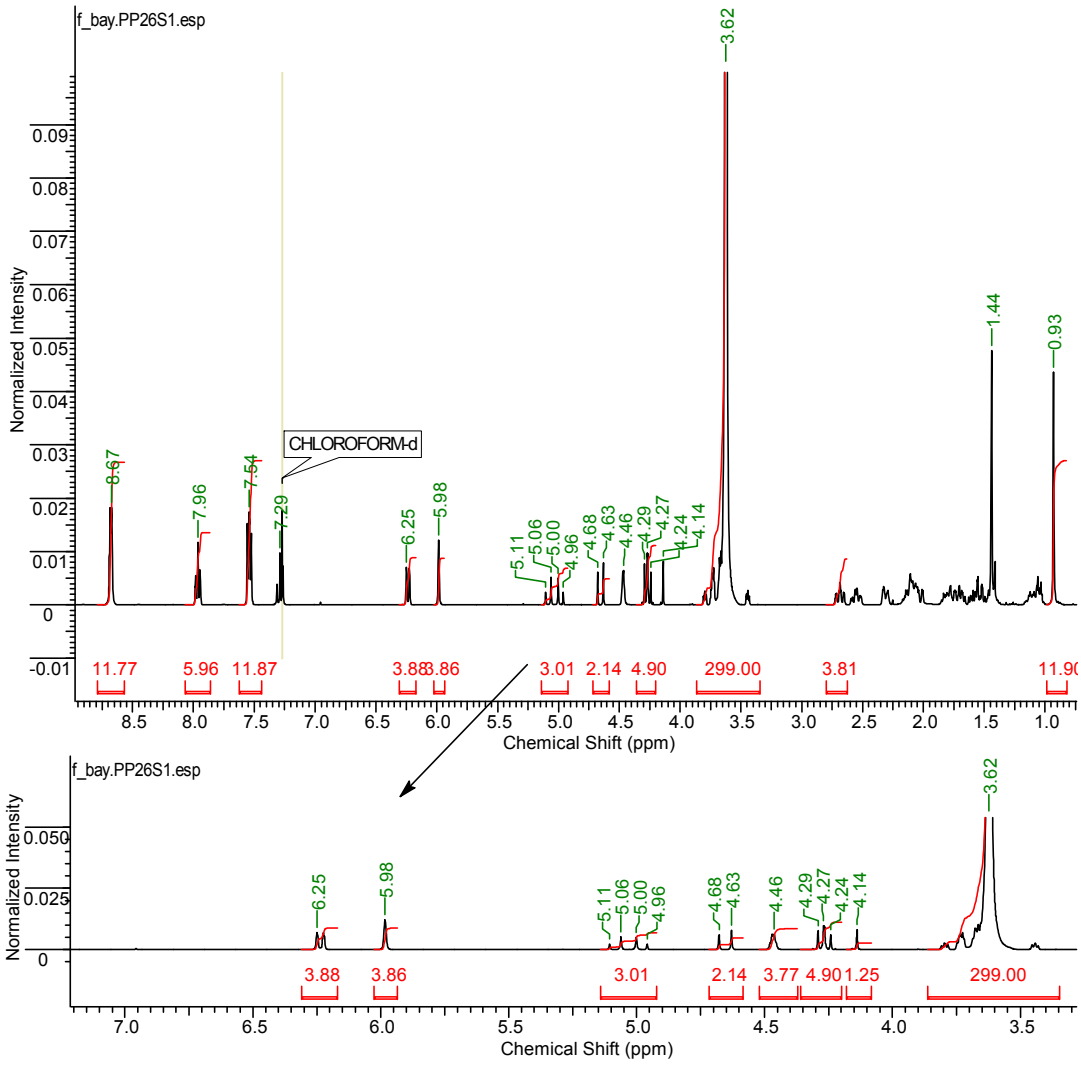

Fig.VI.27. ^{1}HNMR of PP26S1
Spectrum acquired on a Bruker AV(III)400 spectrometer, 64 scans, in $CDCl_3$

Appendix 3. Supplementary information for PEG-prednisolone, Mukaiyama route

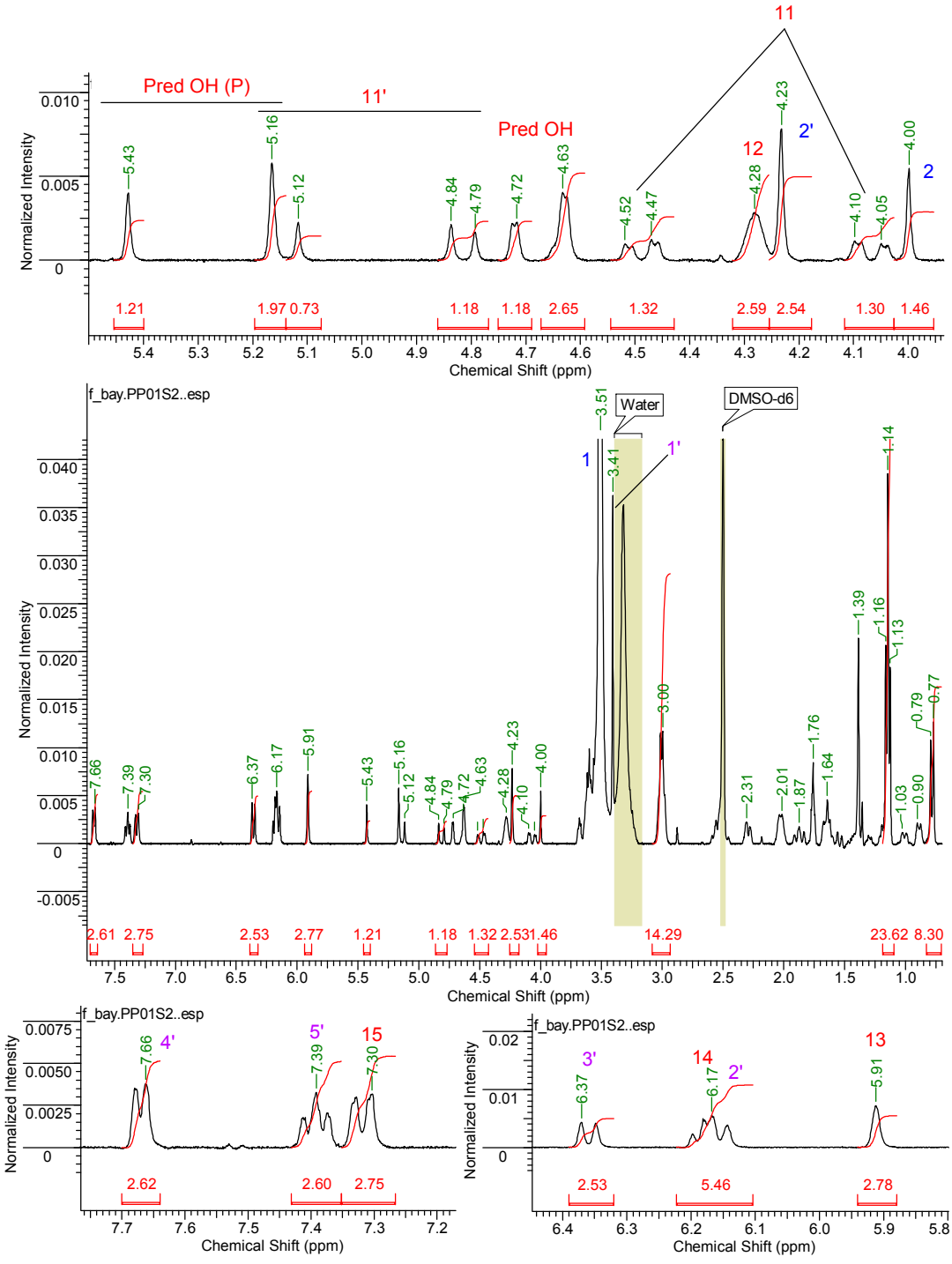

Fig.VI.28. ^{1}HNMR for the crude PP01S1
Spectrum acquired on a Bruker AV(III)400 spectrometer, 16 scans, in DMSO-d_6

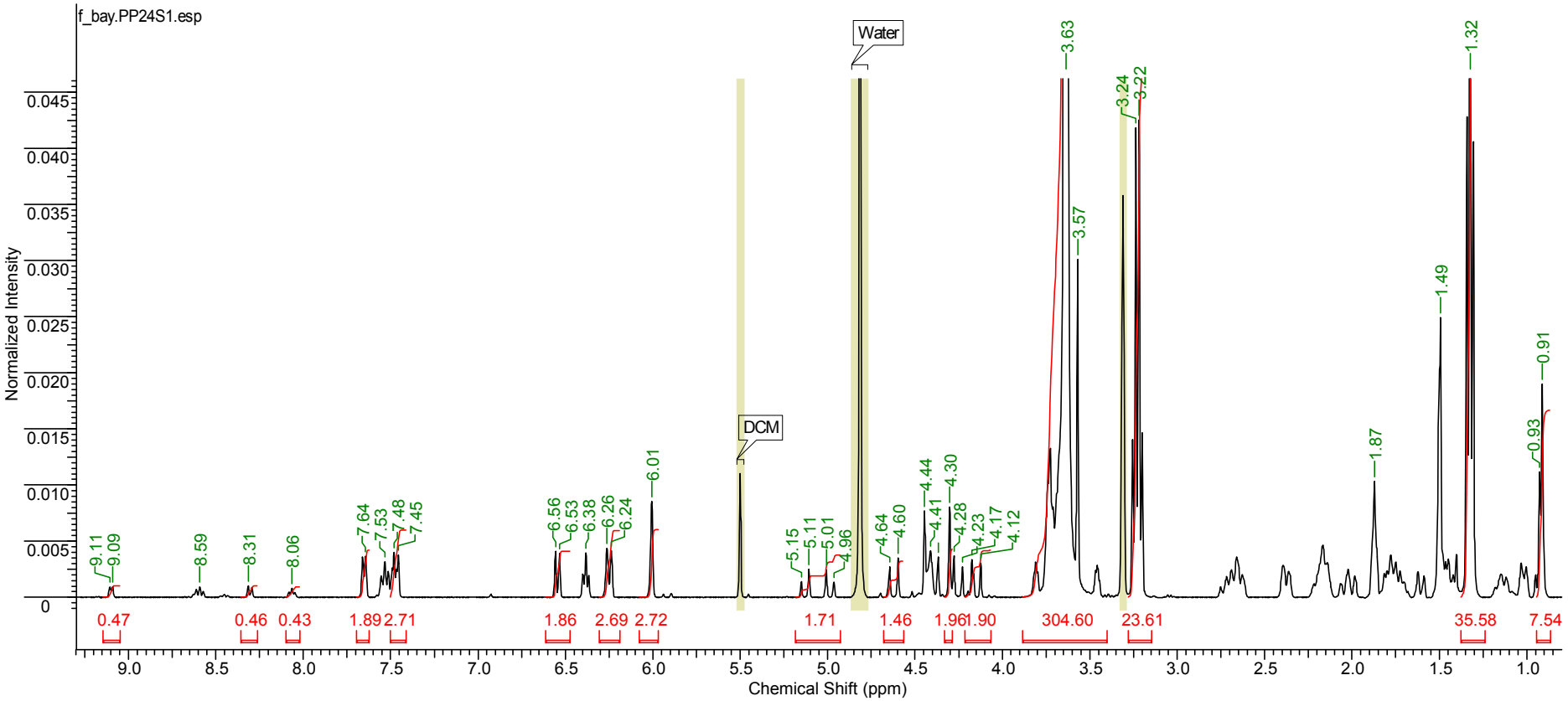

Fig.VI.29. [1]HNMR for the crude PP24S1
Spectrum acquired on a Bruker AV(III)400 spectrometer, 64 scans, in MeOD

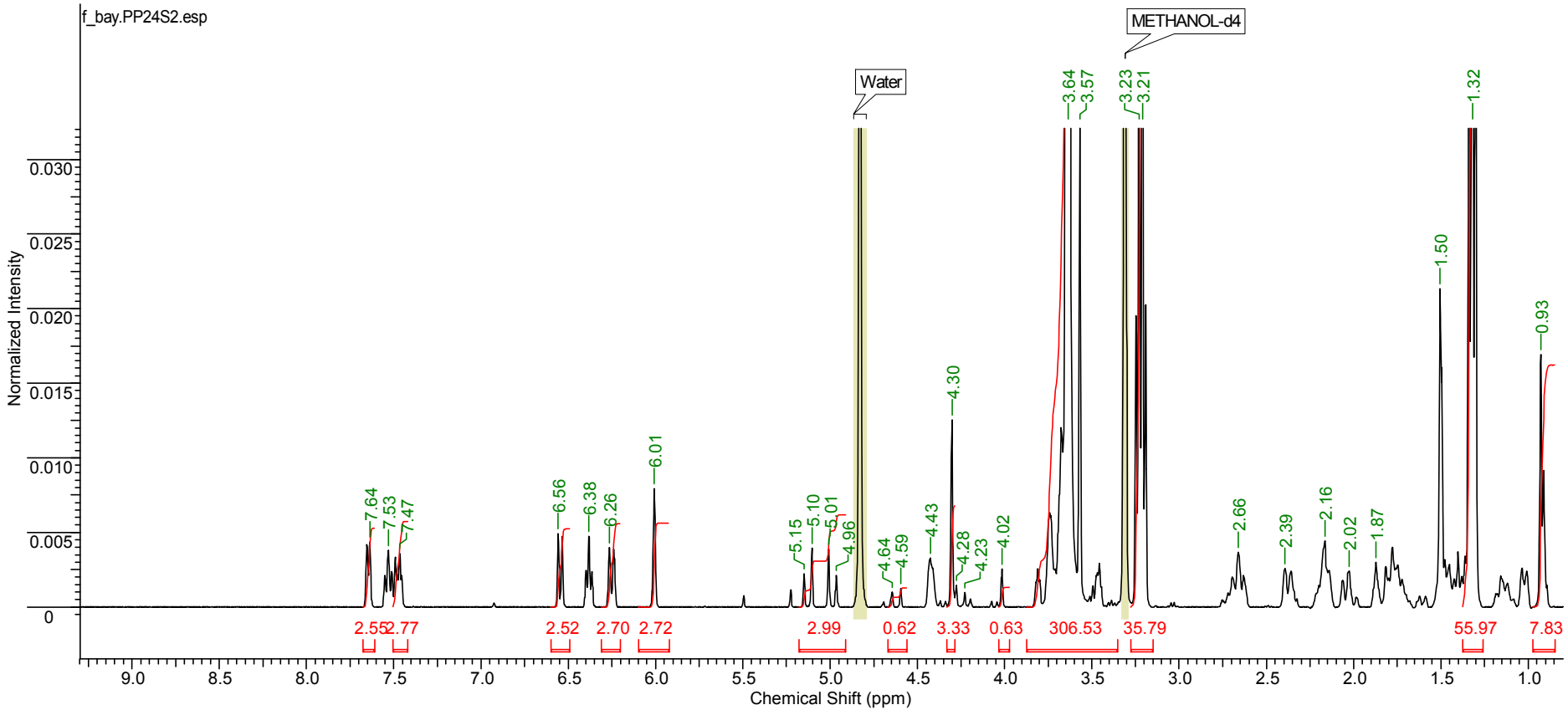

Fig.VI.30. [1]HNMR for the crude PP24S2
Spectrum acquired on a Bruker AV(III)400 spectrometer, 64 scans, in MeOD

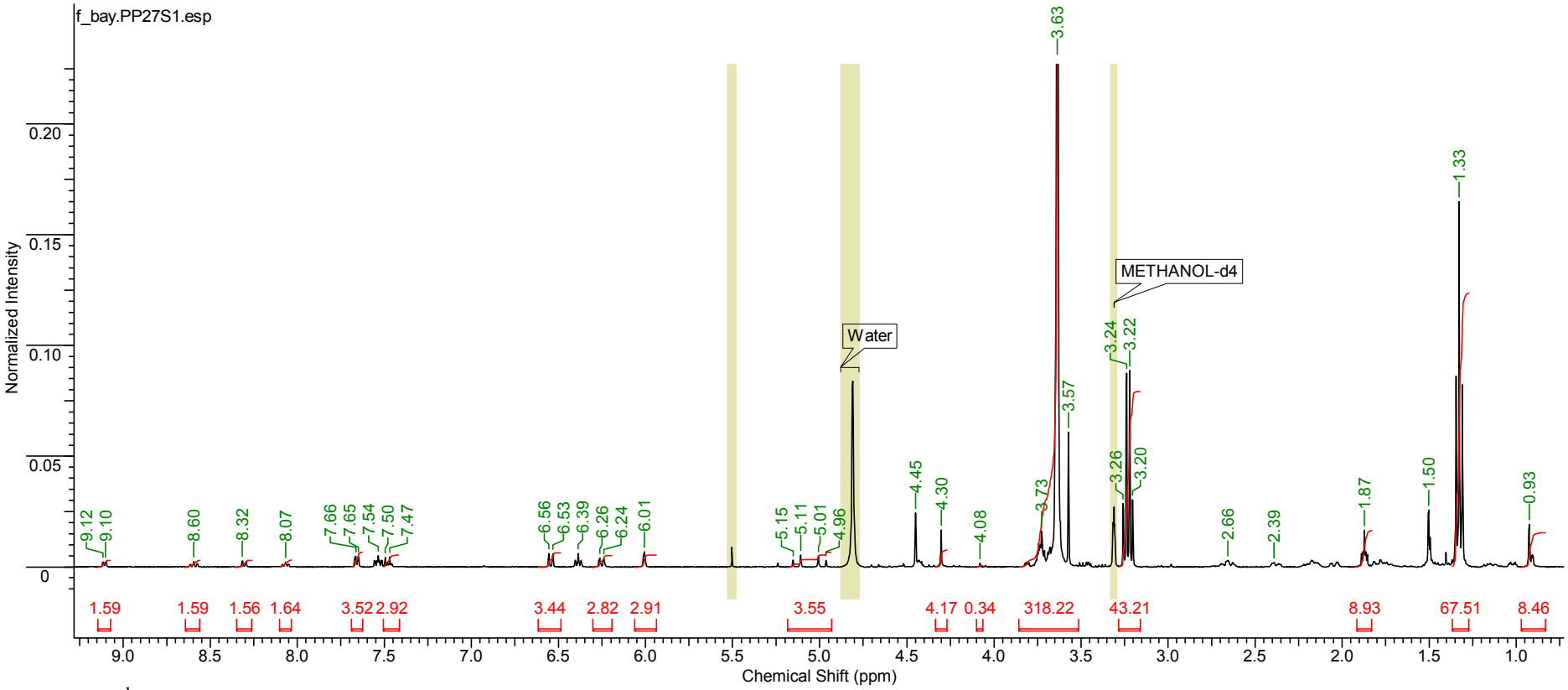

Fig.VI.31. ^{1}HNMR for the crude PP27S1

Spectrum acquired on a Bruker AV(III)400 spectrometer, 64 scans, in MeOD

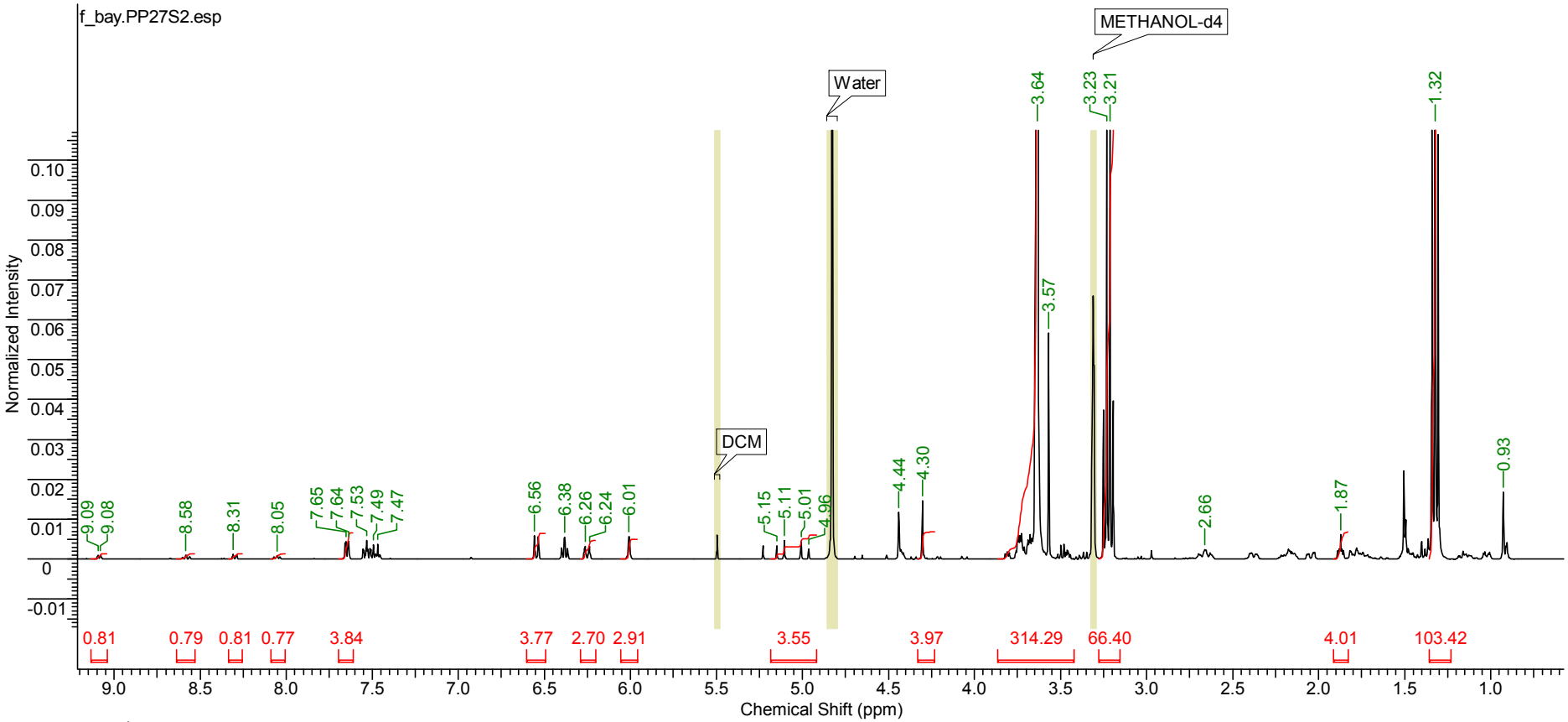

Fig.VI.32. [1]HNMR for the crude PP27S2
Spectrum acquired on a Bruker AV(III)400 spectrometer, 64 scans, in MeOD

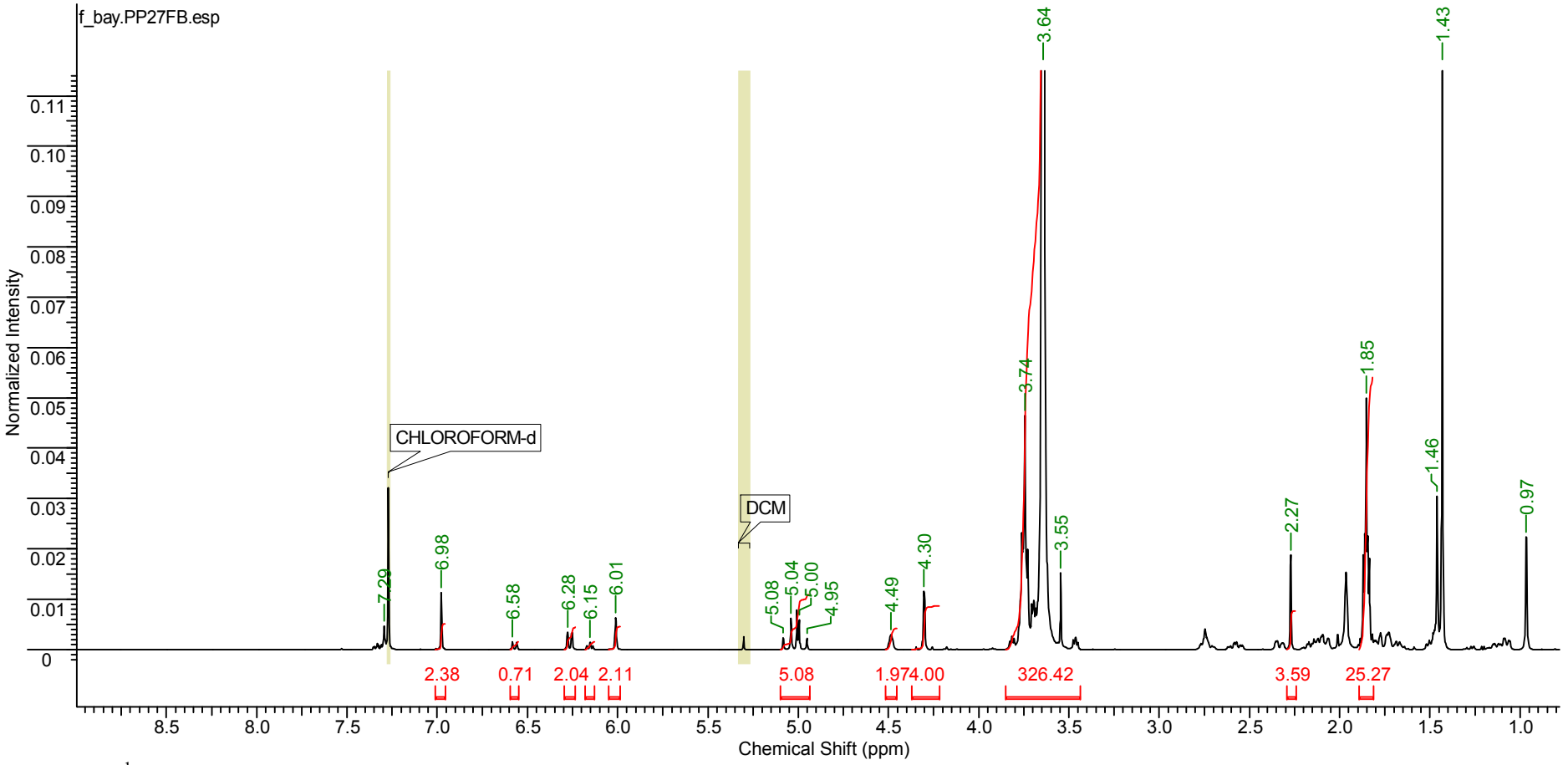

Fig.VI.33. ^{1}HNMR of PP27FB

Spectrum acquired on a Bruker AV(III)400 spectrometer, 64 scans, in $CDCl_3$

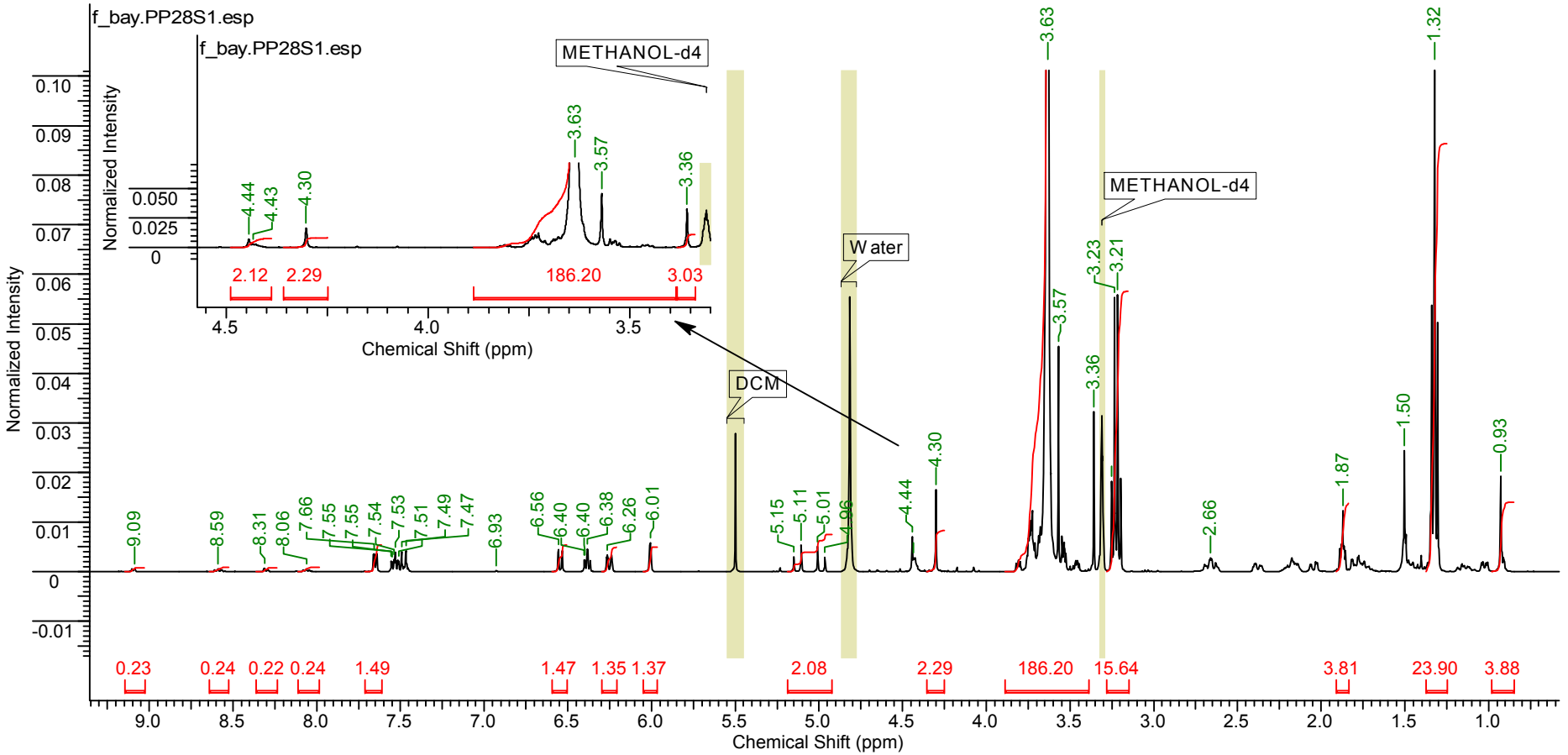

Fig.VI.34. [1]HNMR for the crude PP28S1
Spectrum acquired on a Bruker AV(III)400 spectrometer, 64 scans, in MeOD

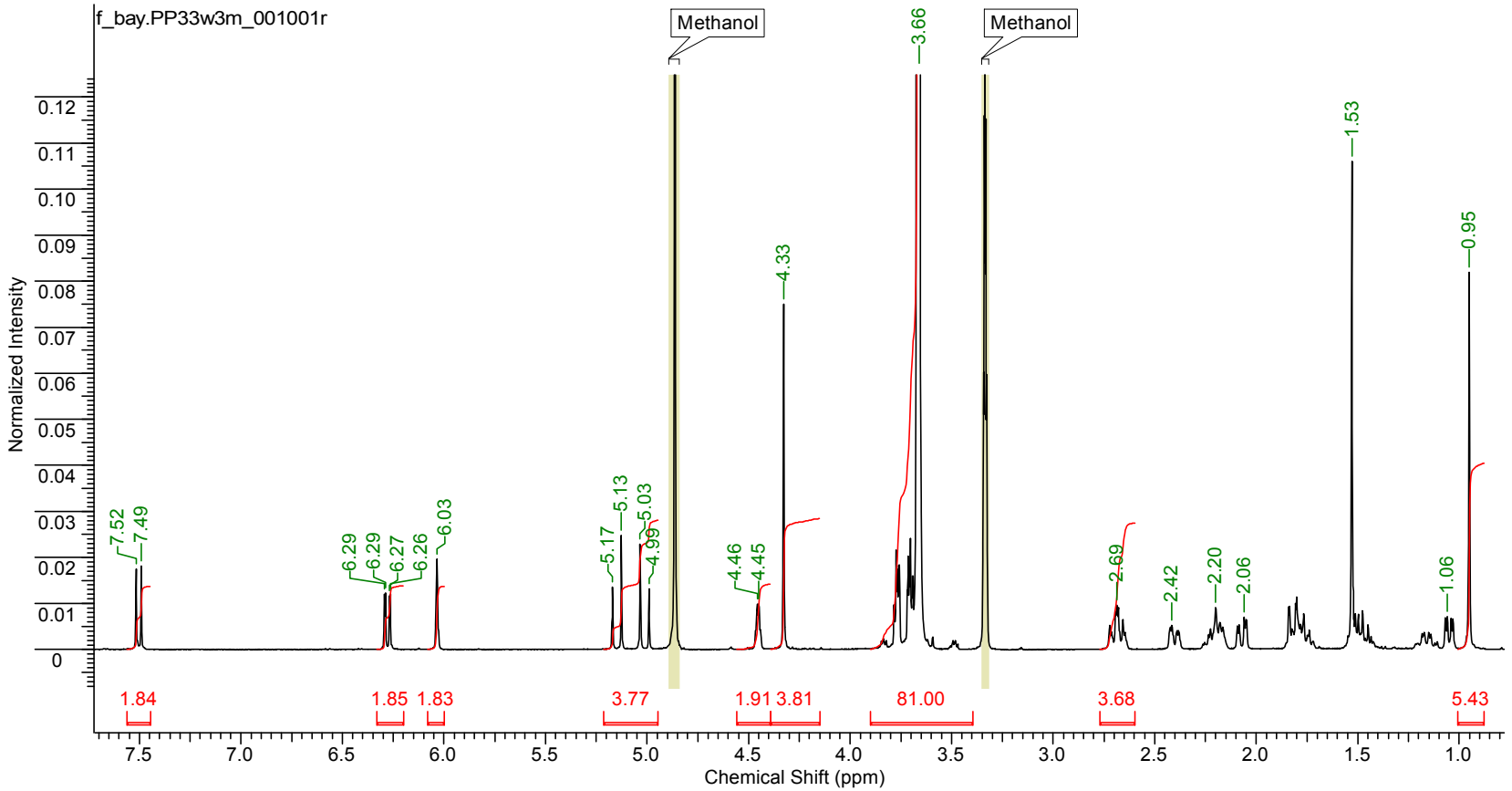

Fig.VI.35. ^{1}HNMR spectrum for PP33w3 (PEG_{1000}-$Pred_2$)
Spectrum acquired on a Bruker AV(III)400 spectrometer, 16 scans, in MeOD

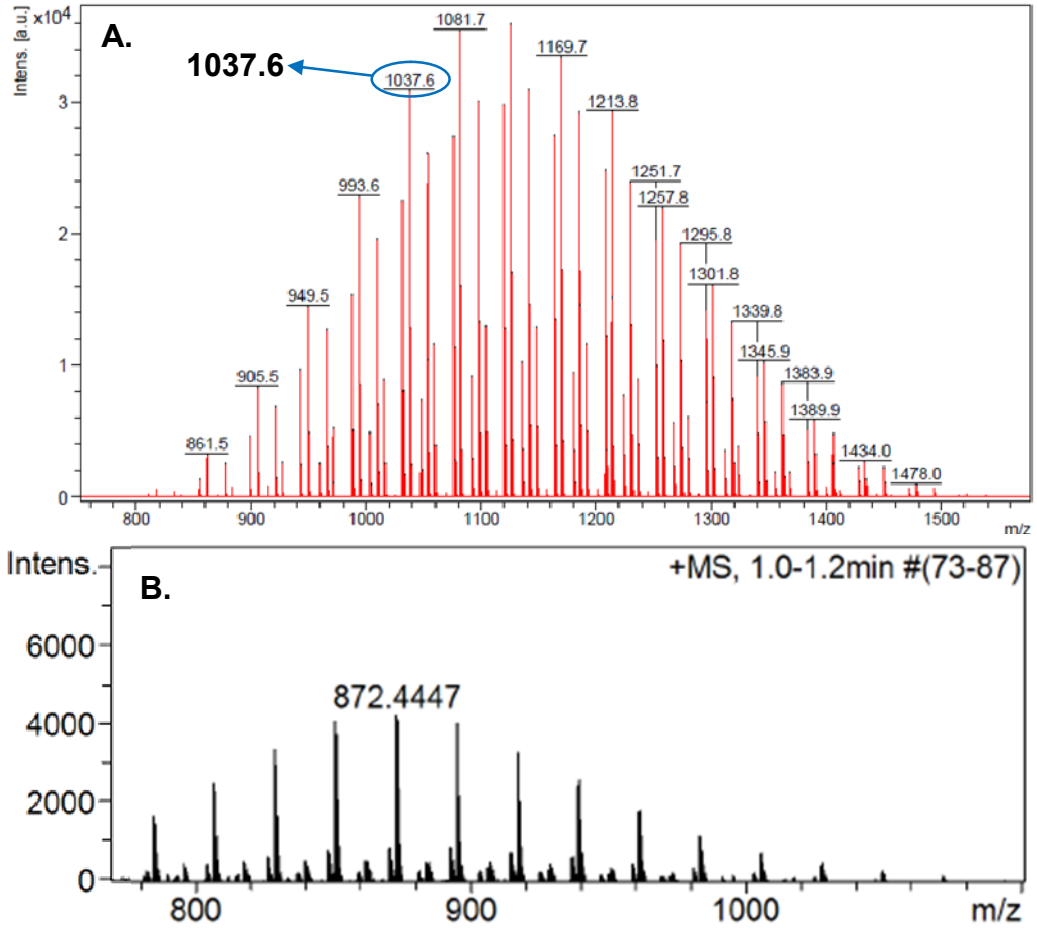

A. MALDI ionisation of oxidised PEG_{1000} produced singly charged ions (successive PEG signals 44 mass units apart), with ion abduct of mass m_1.

$$1037.6 = m_{PEG} + m_1$$

$$m_{PEG} = 1037.6 - m_1$$

B. ESI ionisation of PP33 produced doubly charged ions (successive PEG signals 22 mass units apart), with ion abducts of sodium (23 Da) and m_1.

$$872.4 = \frac{m_{PP} + m_{Na^+} + m_1}{2}$$

$$m_{PP} = 2 \times 872.4 - 23 - m_1$$

$$m_{PP} = 1721.8\ Da - m_1$$

$$\Delta mass = m_{PP} - m_{PEG}$$

$$= 1721.8 - m_1 - (1037.6 - m_1)$$

$$\Delta mass = 684.2\ Da$$

The mass difference ($\Delta mass$) between the conjugate and oxidised PEG was therefore 684.2 Da.

Fig.VI.36. Mass spectrometry analyses of **A.** $PEG_{1000}COOH_2$ and **B.** PP33w3 (PEG_{1000}-$Pred_2$)

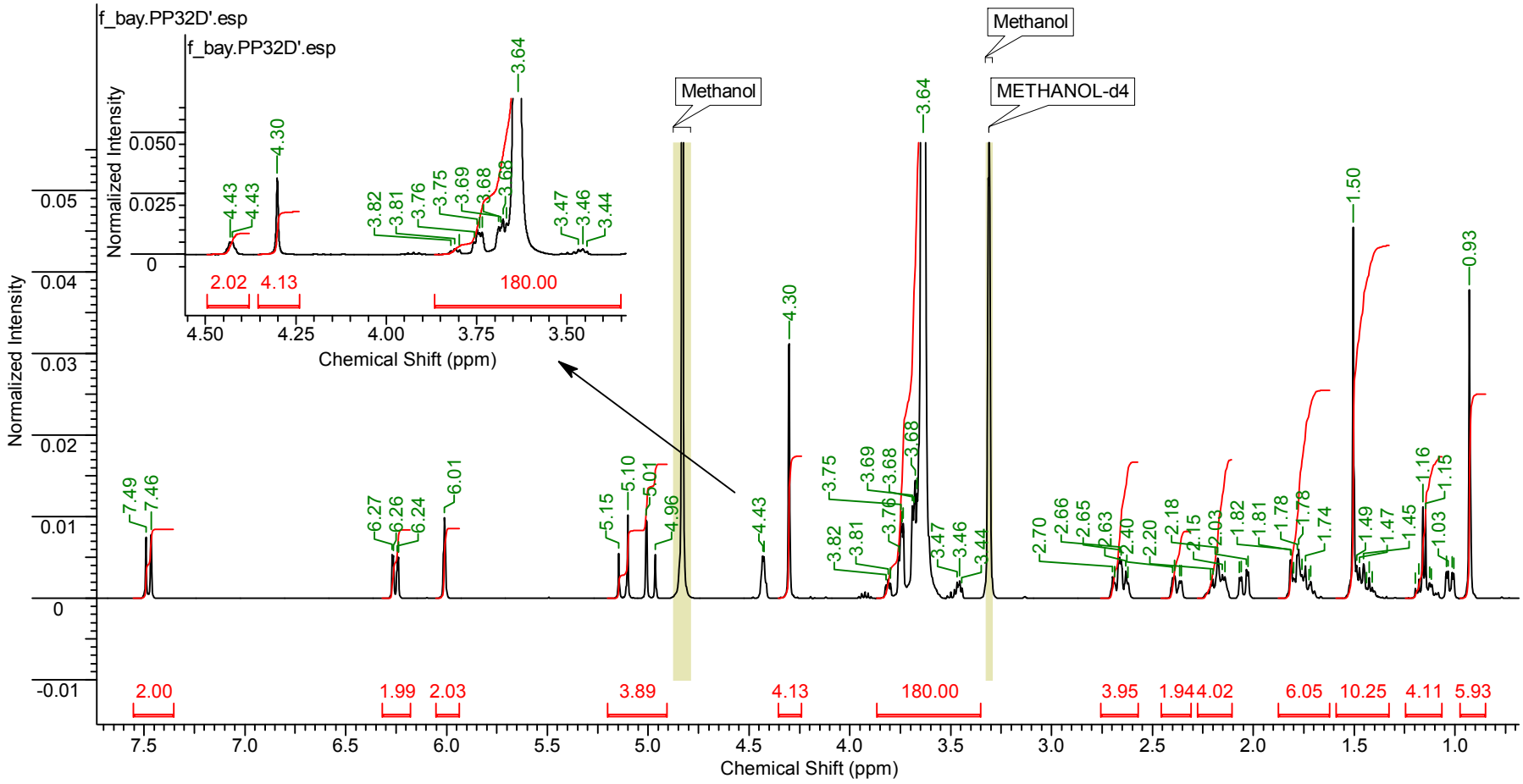

Fig.VI.37. 1HNMR spectrum for PP32D (PEG_{2000}-$Pred_2$)
Spectrum acquired on a Bruker AV(III)400 spectrometer, 16 scans, in MeOD

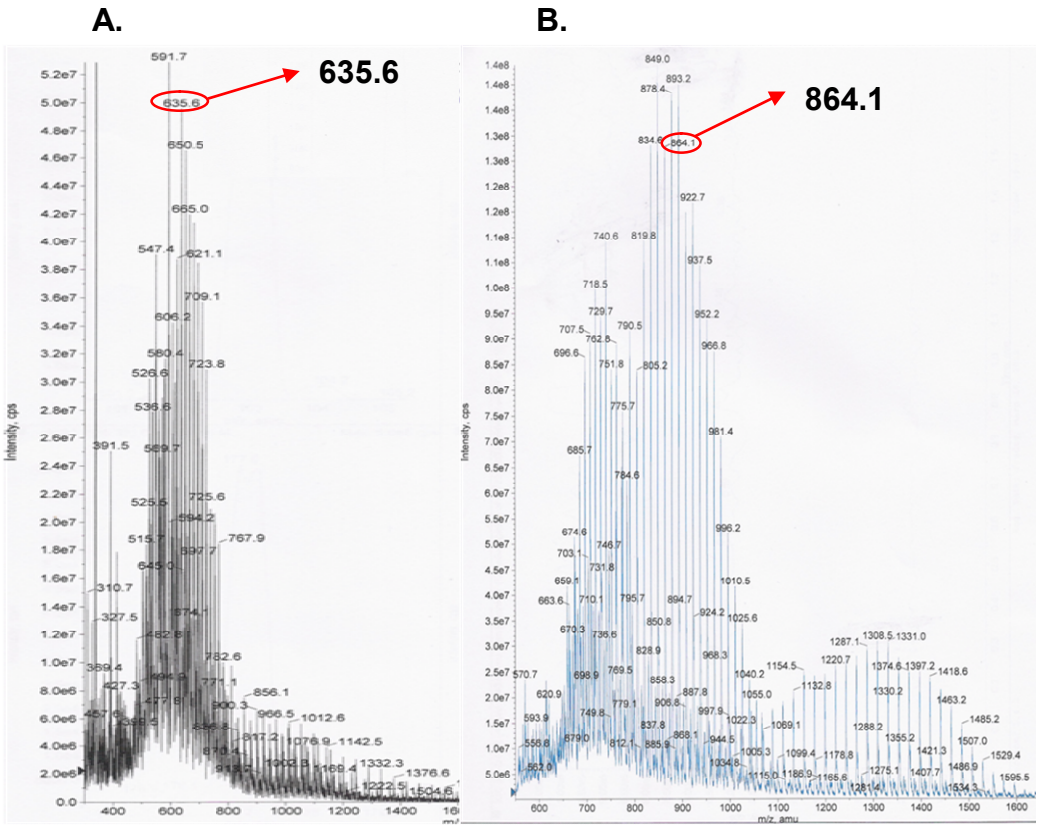

A. ESI ionisation of oxidised PEG_{2000} produced triply charged ions (successive PEG signals 14.7 mass units apart), with ion abducts of mass m_1 ($m_1 \geq 3$ amu).

$$635.6 = \frac{m_{PEG} + m_1}{3}$$

$$m_{PEG} = 1906.8 - m_1$$

B. ESI ionisation of PP32 produced mainly triply charged ions (successive PEG signals 14.7 mass units apart), with ion abducts of mass m_1 ($m_1 \geq 3$ amu).

$$864.1 = \frac{m_{PP} + m_1}{3}$$

$$m_{PP} = 2592.3 - m_1$$

$$\Delta mass = m_{PP} - m_{PEG}$$

$$= 2592.3 - m_1 - (1906.8 - m_1)$$

$$\Delta mass = 685.5\ Da$$

The mass difference ($\Delta mass$) between the conjugate and oxidised PEG was therefore 685.5 Da.

Fig.VI.38. Mass spectrometry analyses of **A.** $PEG_{2000}COOH_2$ and **B.** PP32D (PEG_{2000}-$Pred_2$)

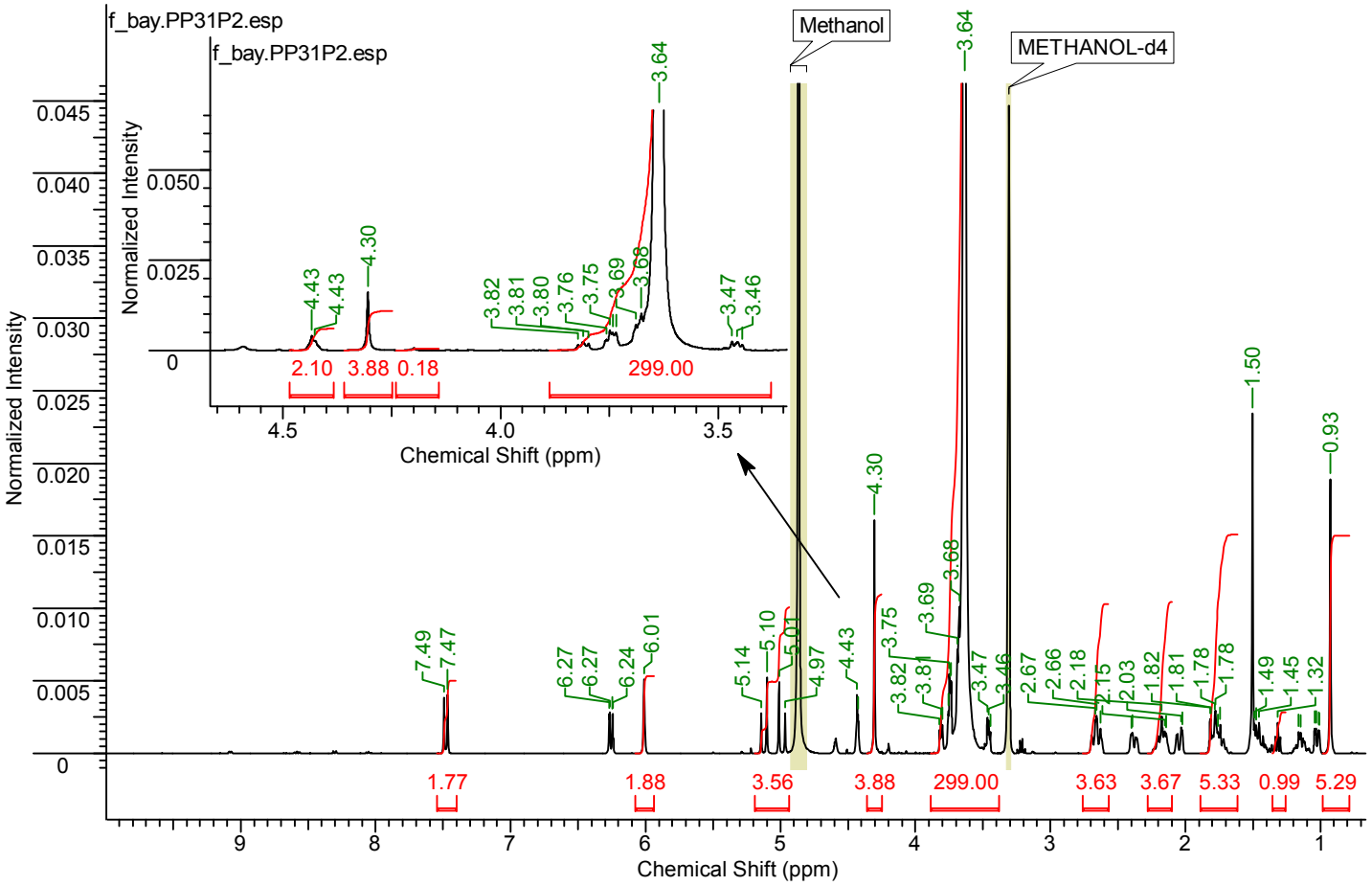

Fig.VI.39. 1HNMR spectrum for PP31P2 (PEG_{3400}-$Pred_2$)
Spectrum acquired on a Bruker AV(III)400 spectrometer, 64 scans, in MeOD

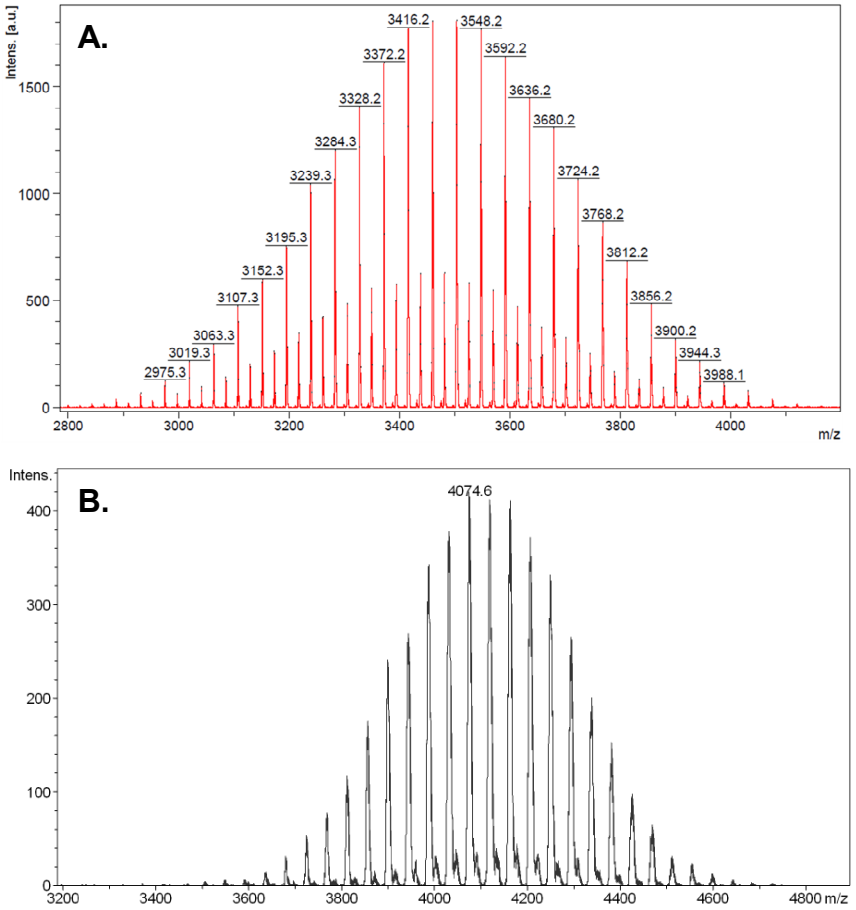

A. MALDI ionisation of oxidised PEG_{3400} produced singly charged ions (successive PEG signals 44 mass units apart), with ion abduct of mass m_1.

$$3416.2 = m_{PEG} + m_1$$

$$m_{PEG} = 3416.2 - m_1$$

B. MALDI ionisation of oxidised PP31 produced singly charged ions (successive PEG signals 44 mass units apart), with ion abduct of mass m_2.

$$4118.5 = m_{pp} + m_2$$

$$m_{PP} = 4118.5 - m_2$$

$$\Delta mass = m_{PP} - m_{PEG} = 4118.5 - m_2 - (3416.2 - m_1)$$

$$\Delta mass = 702.3 - m_2 + m_1$$

Assuming that PEG ion abduct was H^+ (m_1 = +1 amu), and PP31 ion abduct was NH_4^+ (m_2 = +18 amu), the mass difference ($\Delta mass$) between the conjugate and oxidised PEG was therefore 685.3 Da:

$$\Delta mass = 702.3 - 18 + 1$$

Fig.VI.40. Mass spectrometry analyses of **A.** $PEG_{3400}COOH_2$ and **B.** PP31P2 (PEG_{3400}-$Pred_2$)

Appendix 4. Supplementary information for PEG-salbutamol ester conjugation

A. Proton numbering and Carbon lettering of salbutamol sulfate

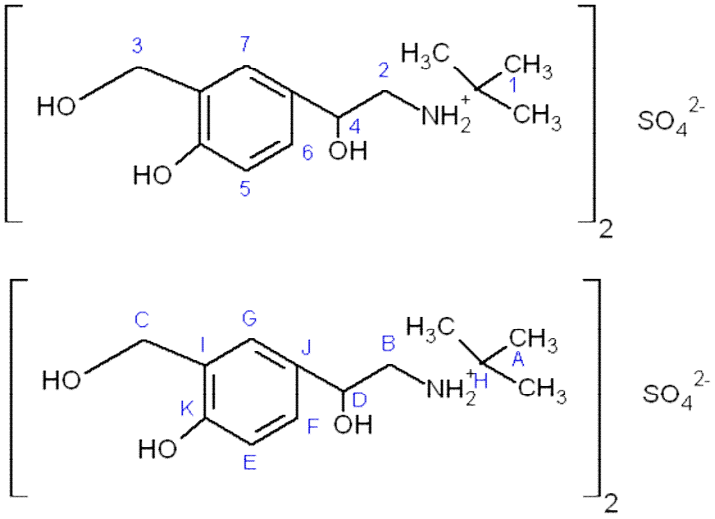

B. ^{1}HNMR of salbutamol sulfate

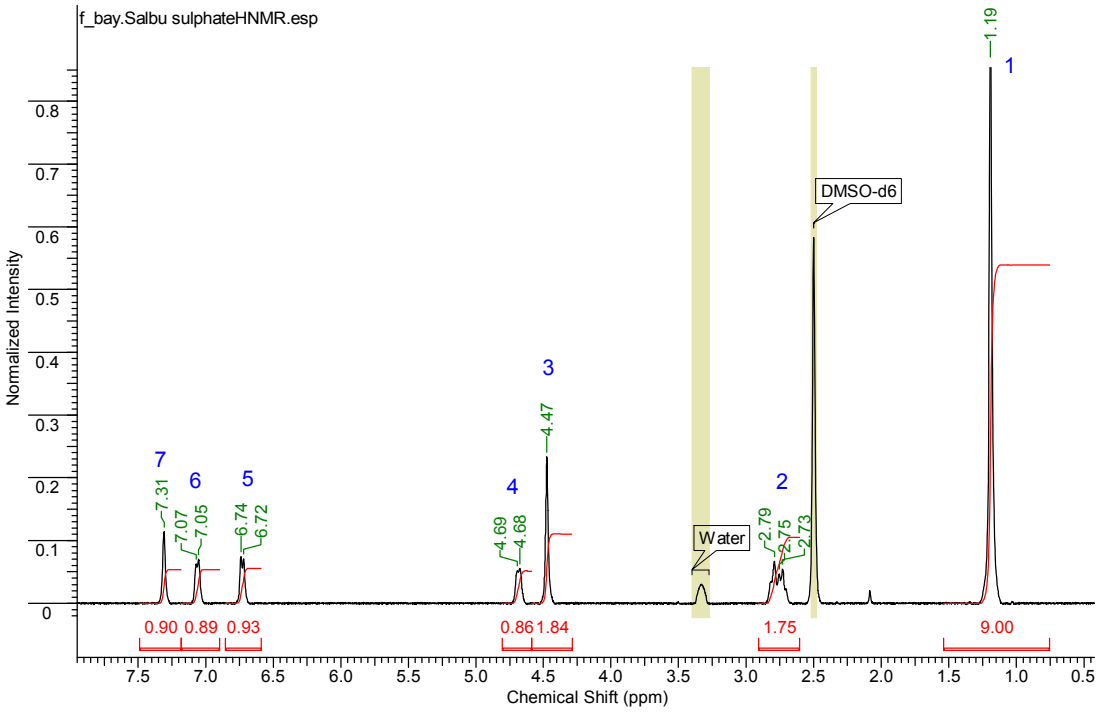

Spectrum acquired on a Bruker AV(III)400 spectrometer, 16 scans, in DMSO-d_6

C.HMQC of salbutamol sulfate

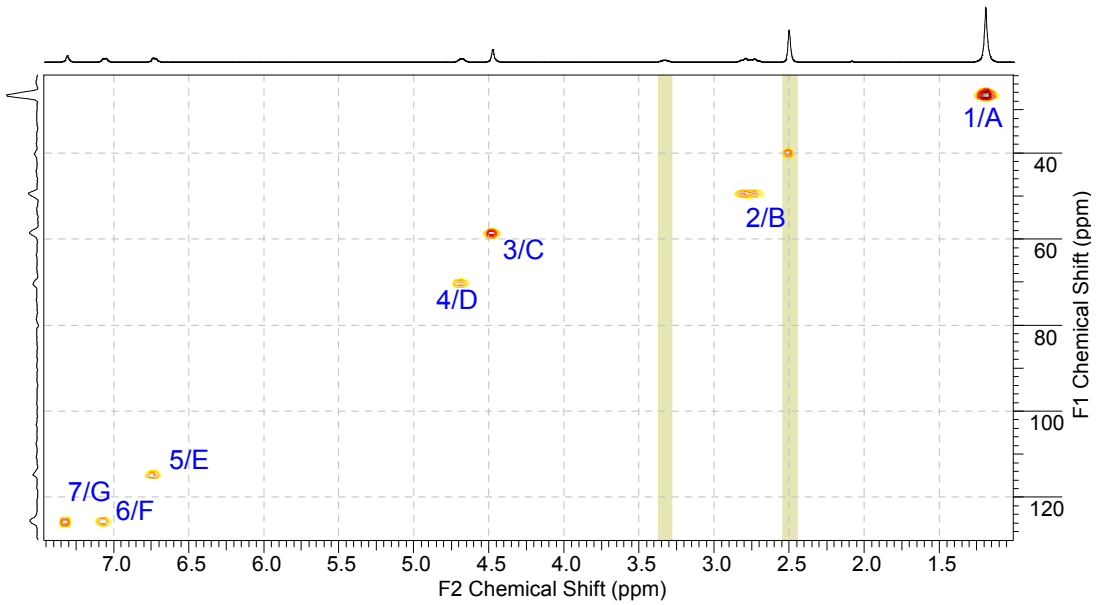

Spectra acquired on a Bruker AV(III)400 spectrometer in DMSO-d_6

D.HMBC of salbutamol sulfate

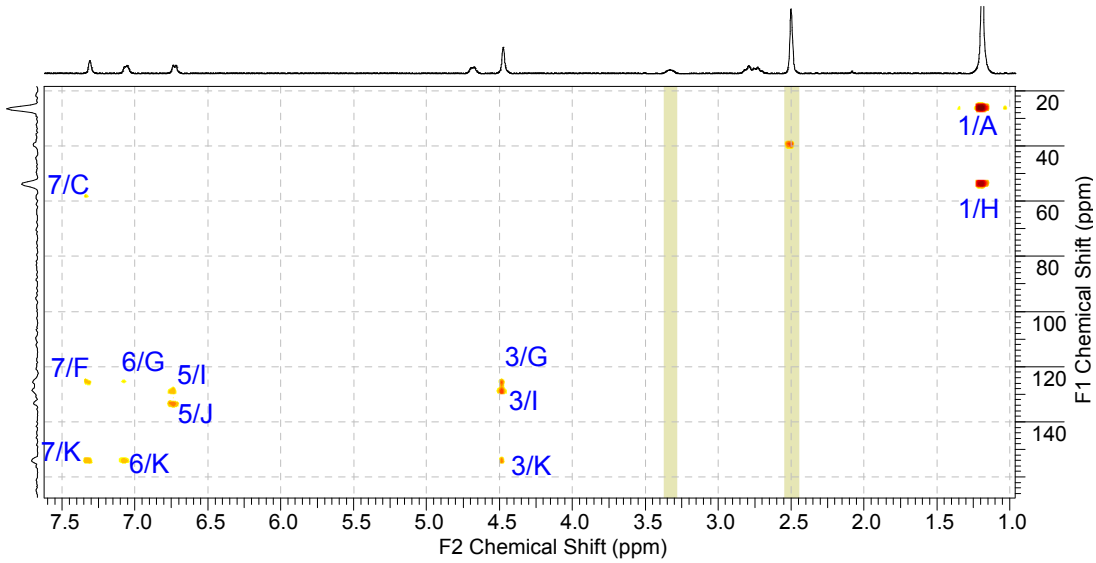

Spectra acquired on a Bruker AV(III)400 spectrometer in DMSO-d_6

Fig.VI.41. Salbutamol sulfate 2DNMR chemical shifts assignment

A. Proton numbering and Carbon lettering of salbutamol free base

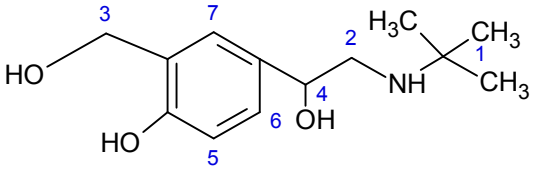

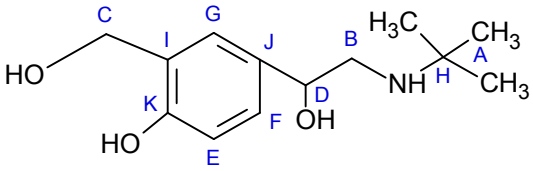

B. ^{1}HNMR of salbutamol free base

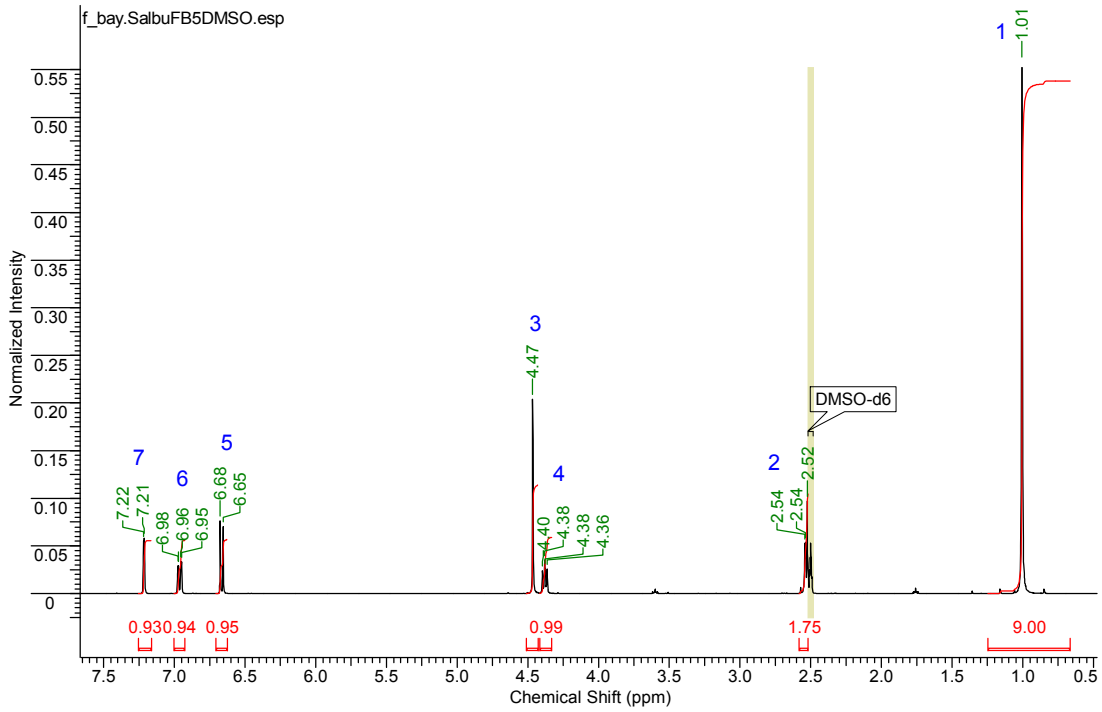

Spectrum acquired on a Bruker AV(III)400 spectrometer, 16 scans, in DMSO-d_6

C. HMQC of salbutamol free base

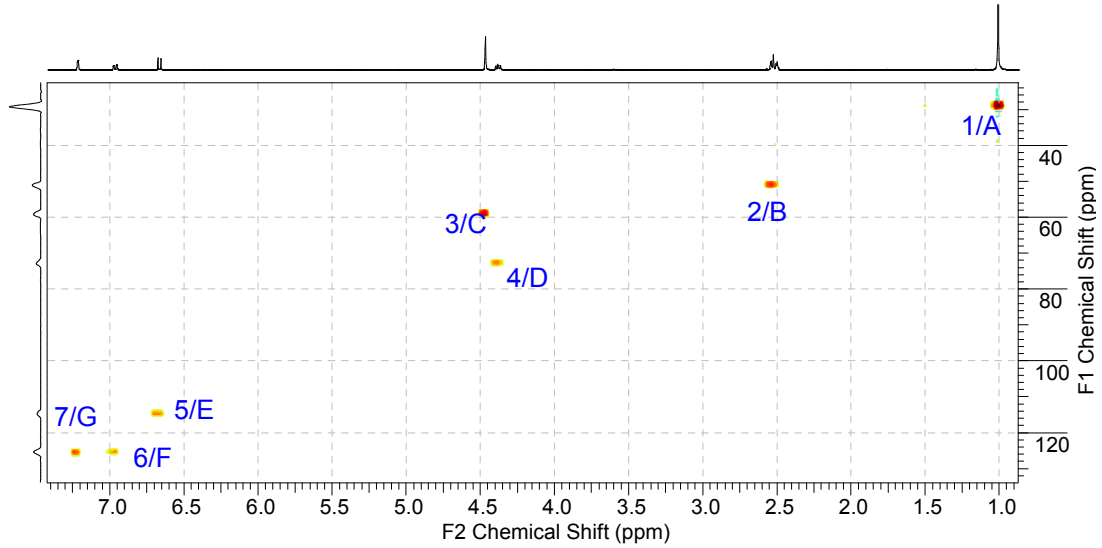

Spectra acquired on a Bruker AV(III)400 spectrometer in DMSO-d_6

D. HMBC of salbutamol free base

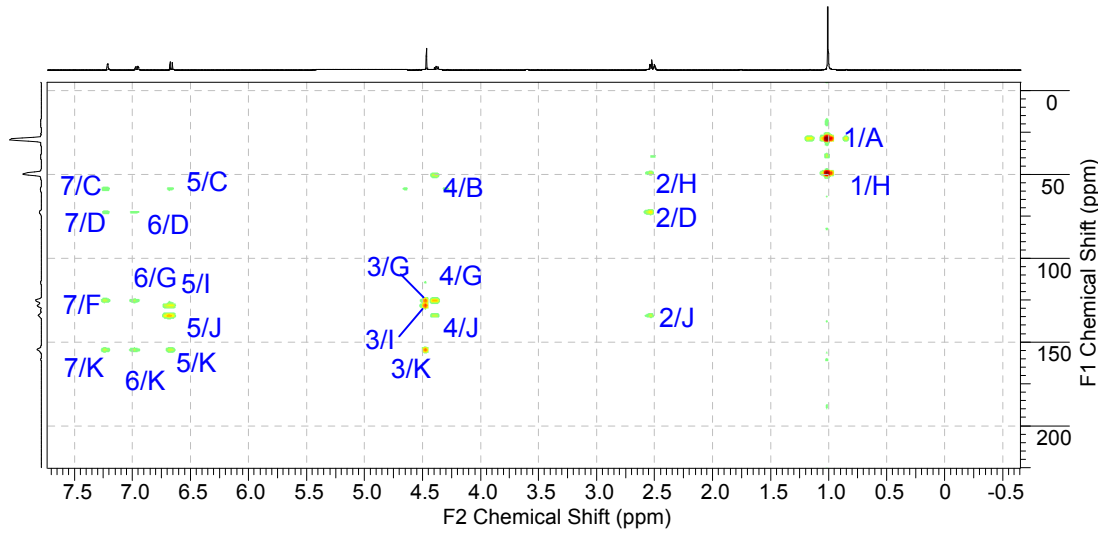

Spectra acquired on a Bruker AV(III)400 spectrometer in DMSO-d_6

Fig.VI.42. Salbutamol free base 2DNMR chemical shifts assignment

A. Proton numbering and Carbon lettering of salbutamol dodecyl sulfate

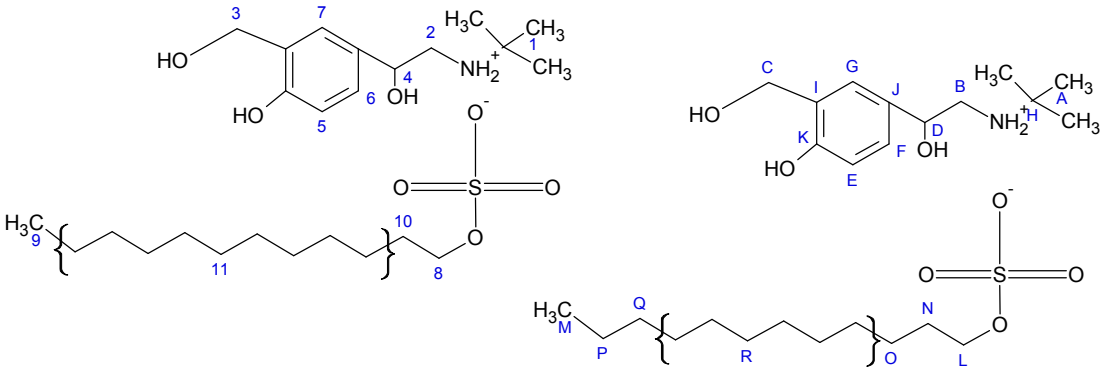

B. ^{1}HNMR of salbutamol dodecyl sulfate

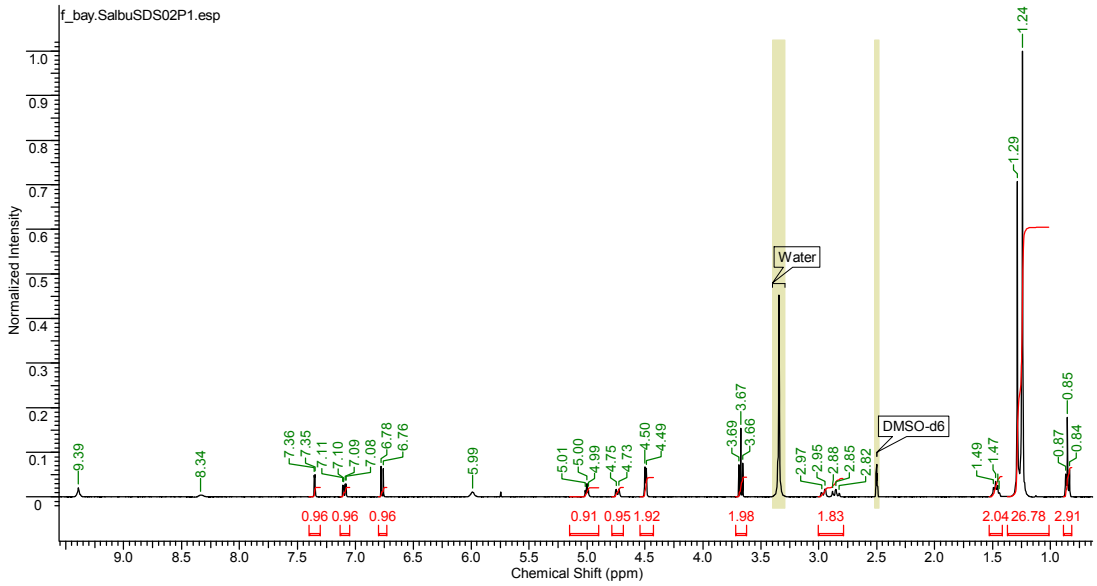

Spectrum acquired on a Bruker AV(III)400 spectrometer, 16 scans, in DMSO-d_6

C. HMQC of salbutamol dodecyl sulfate

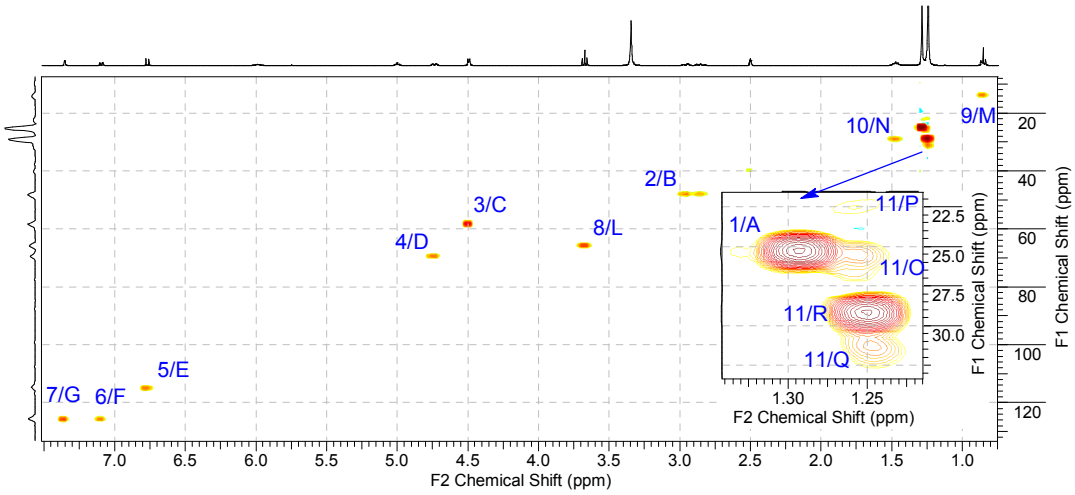

Spectra acquired on a Bruker AV(III)400 spectrometer in DMSO-d_6

D. HMBC of salbutamol dodecyl sulfate

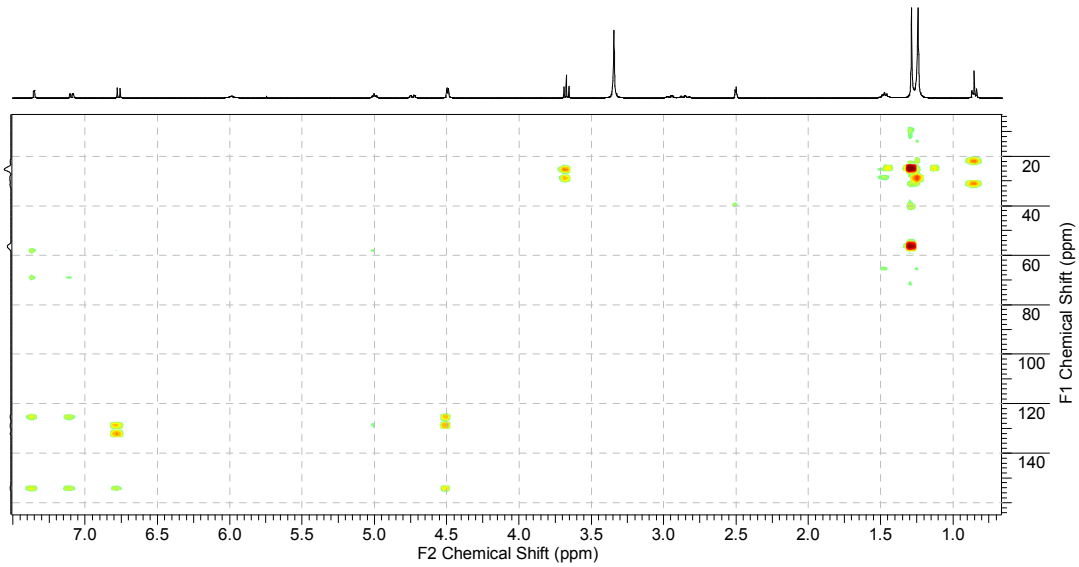

Spectra acquired on a Bruker AV(III)400 spectrometer in DMSO-d_6

Fig.VI.43. Salbutamol dodecyl sulfate 2DNMR chemical shifts assignment

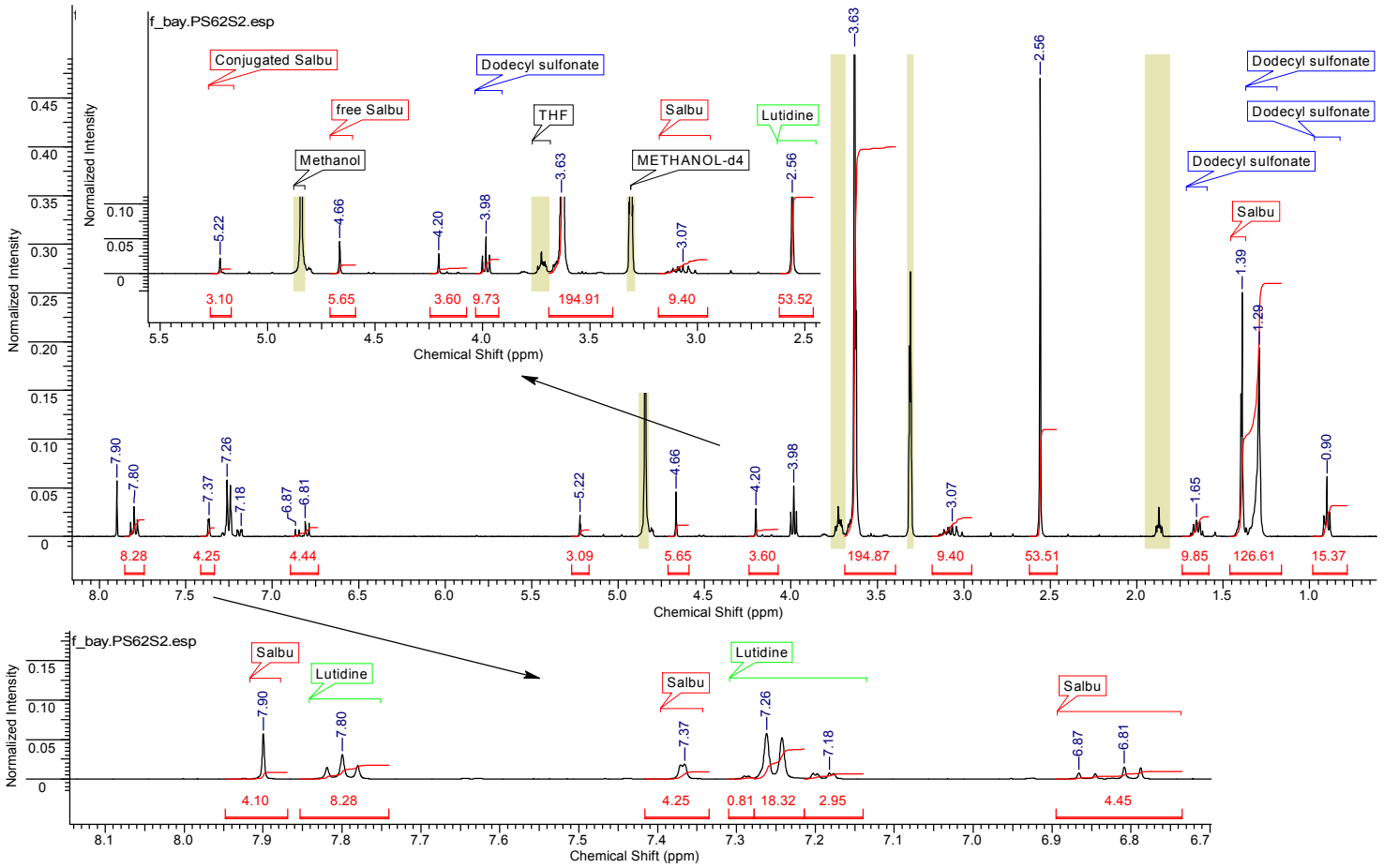

Fig.VI.44. ^{1}HNMR of PS62S2
Spectrum acquired on a Bruker AV(III)400 spectrometer, 16 scans, in MeOD

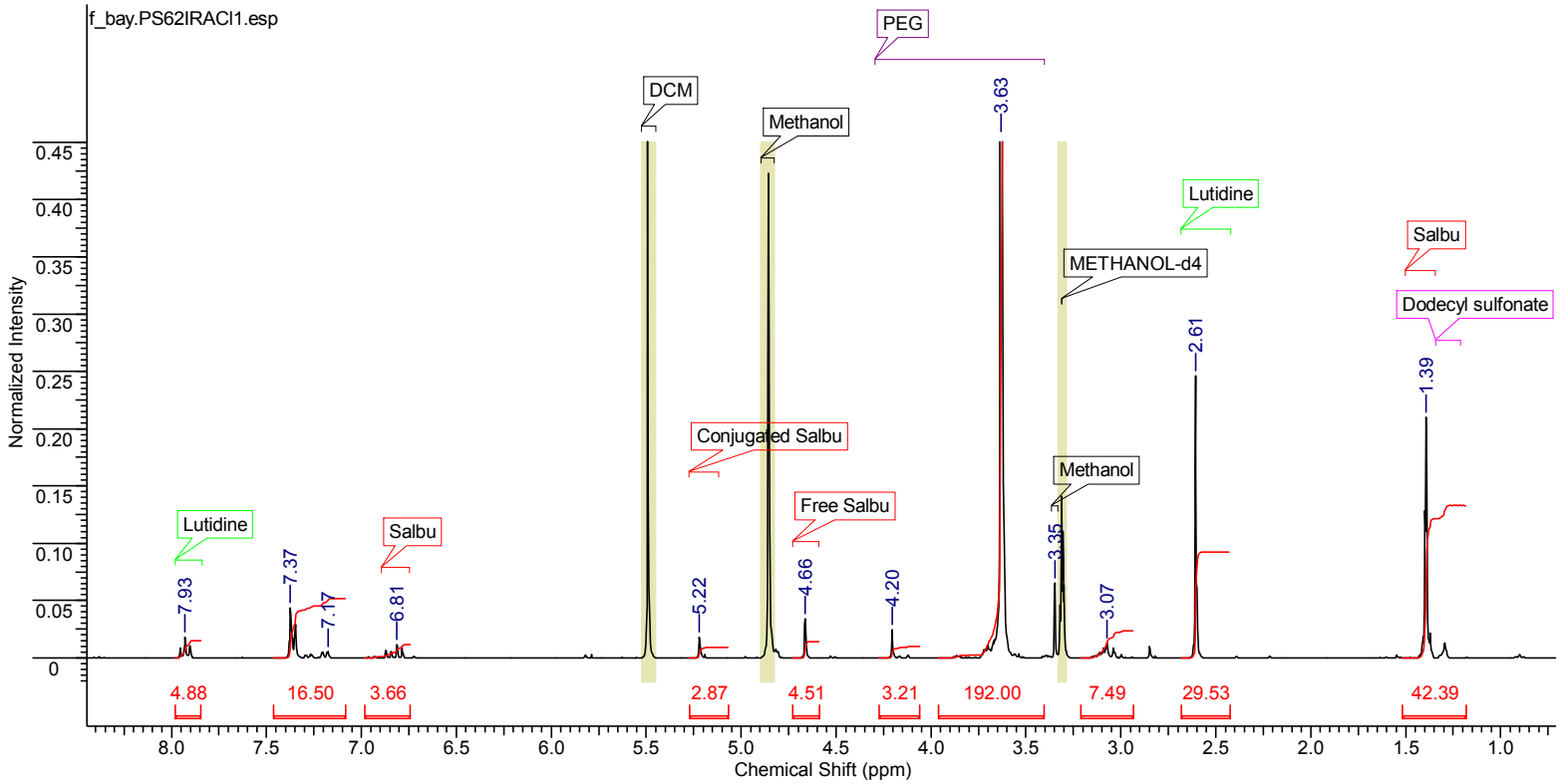

Fig.VI.45. ^{1}HNMR of PS62IRACl1
Spectrum acquired on a Bruker DPX 300 spectrometer, 16 scans, in MeOD

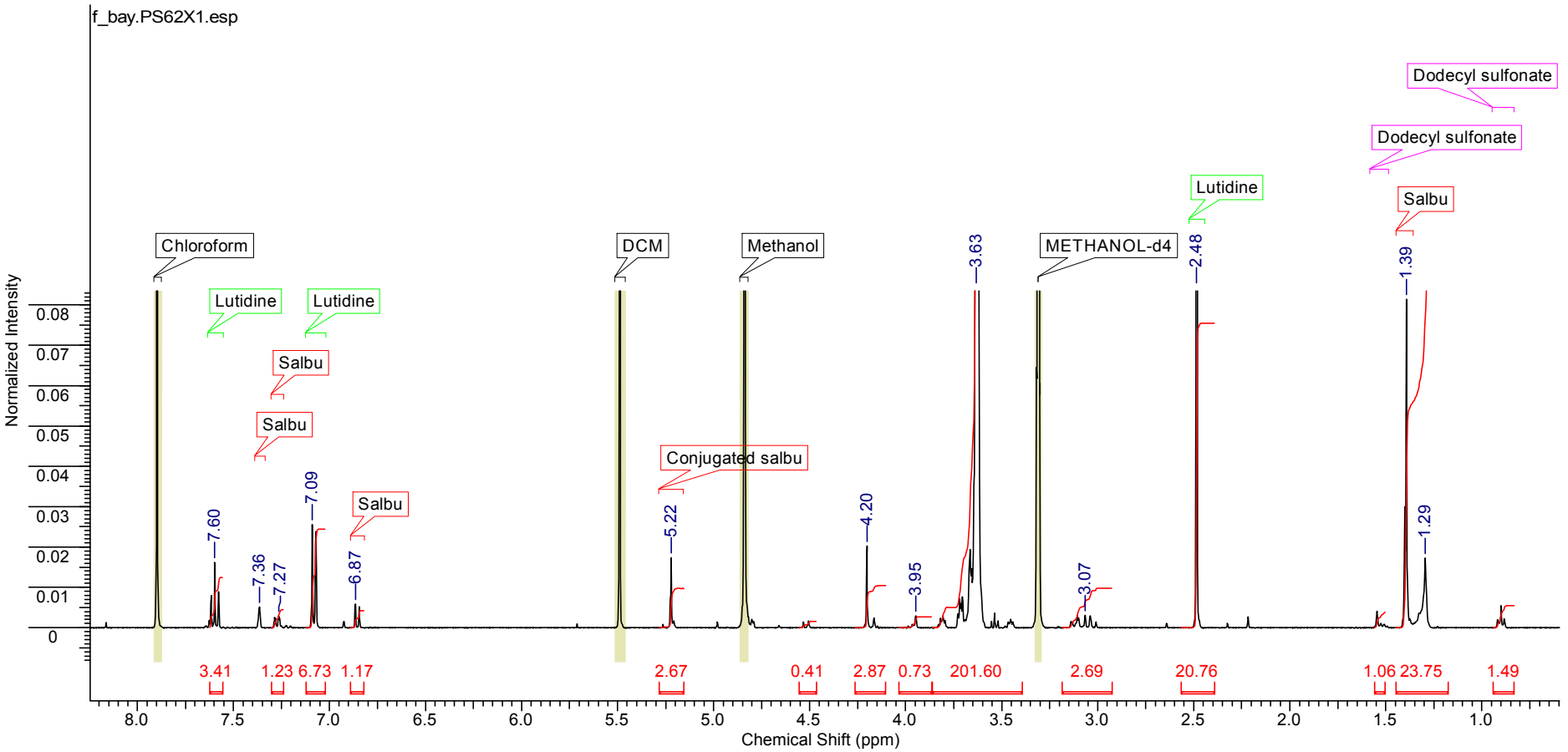

Fig.VI.46. ^{1}HNMR of PS62X1

Spectrum acquired on a Bruker AV(III)400 spectrometer, 16 scans, in MeOD

A. Proton numbering and carbon lettering of PEG_{2000}-Salbu

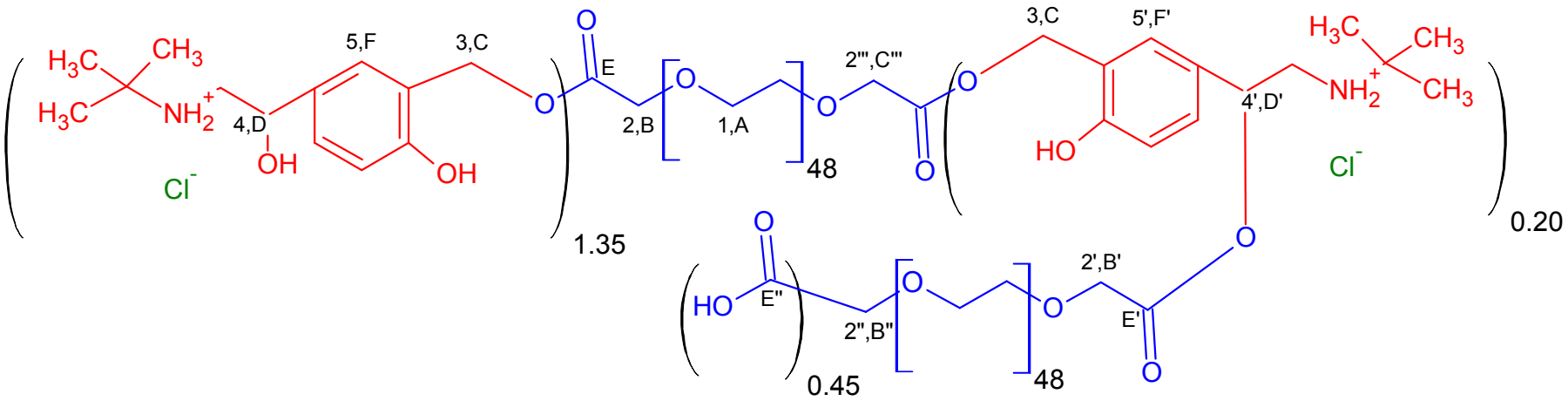

B. ^{1}HNMR of purified PEG_{2000}-Salbu

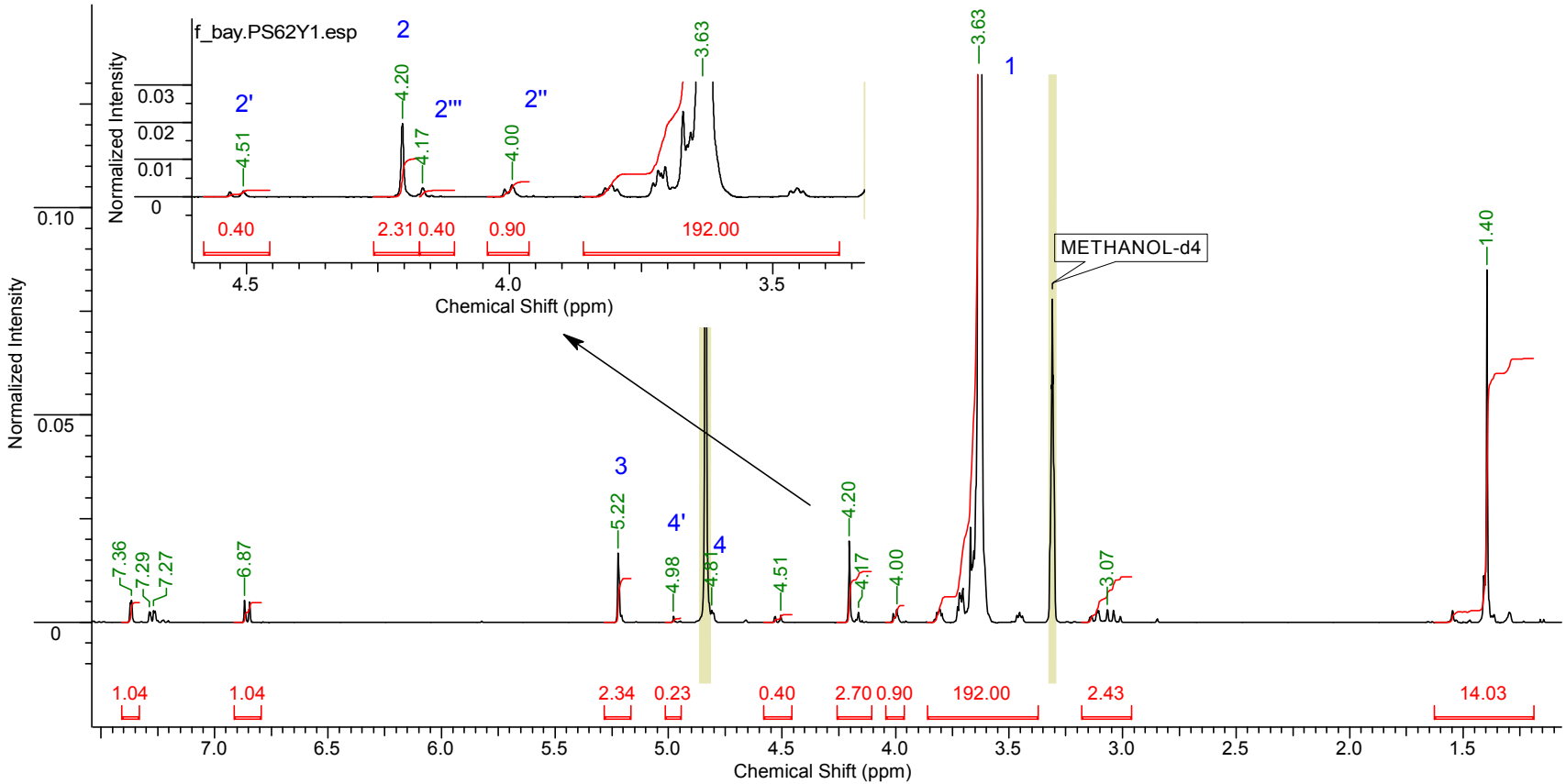

Spectrum acquired on a Bruker AV(III)400 spectrometer, 16 scans, in MeOD

C. HMQC NMR of purified PEG_{2000}-Salbu

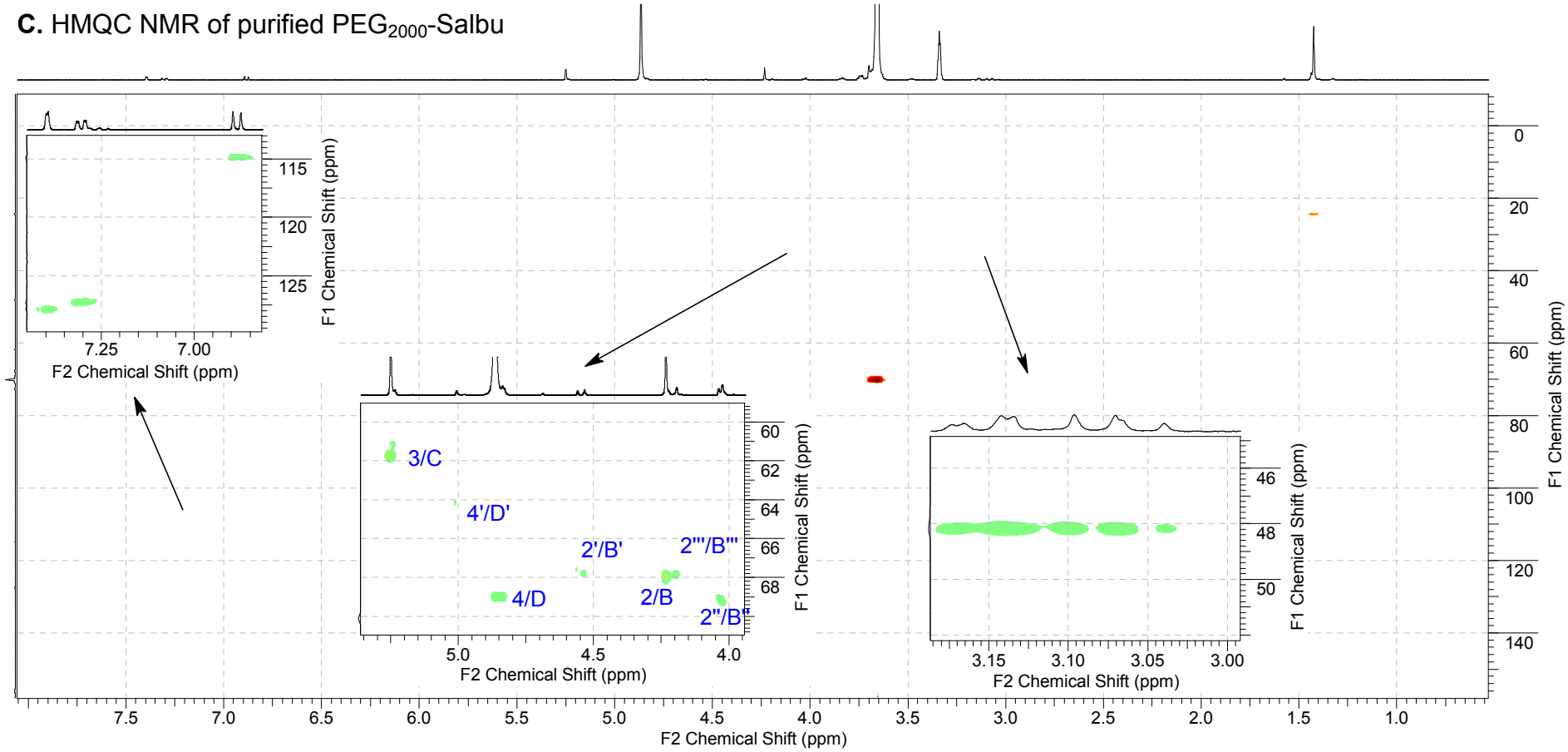

Spectra acquired on a Bruker AV(III)400 spectrometer in MeOD

D. HMBC NMR of purified PEG_{2000}-Salbu

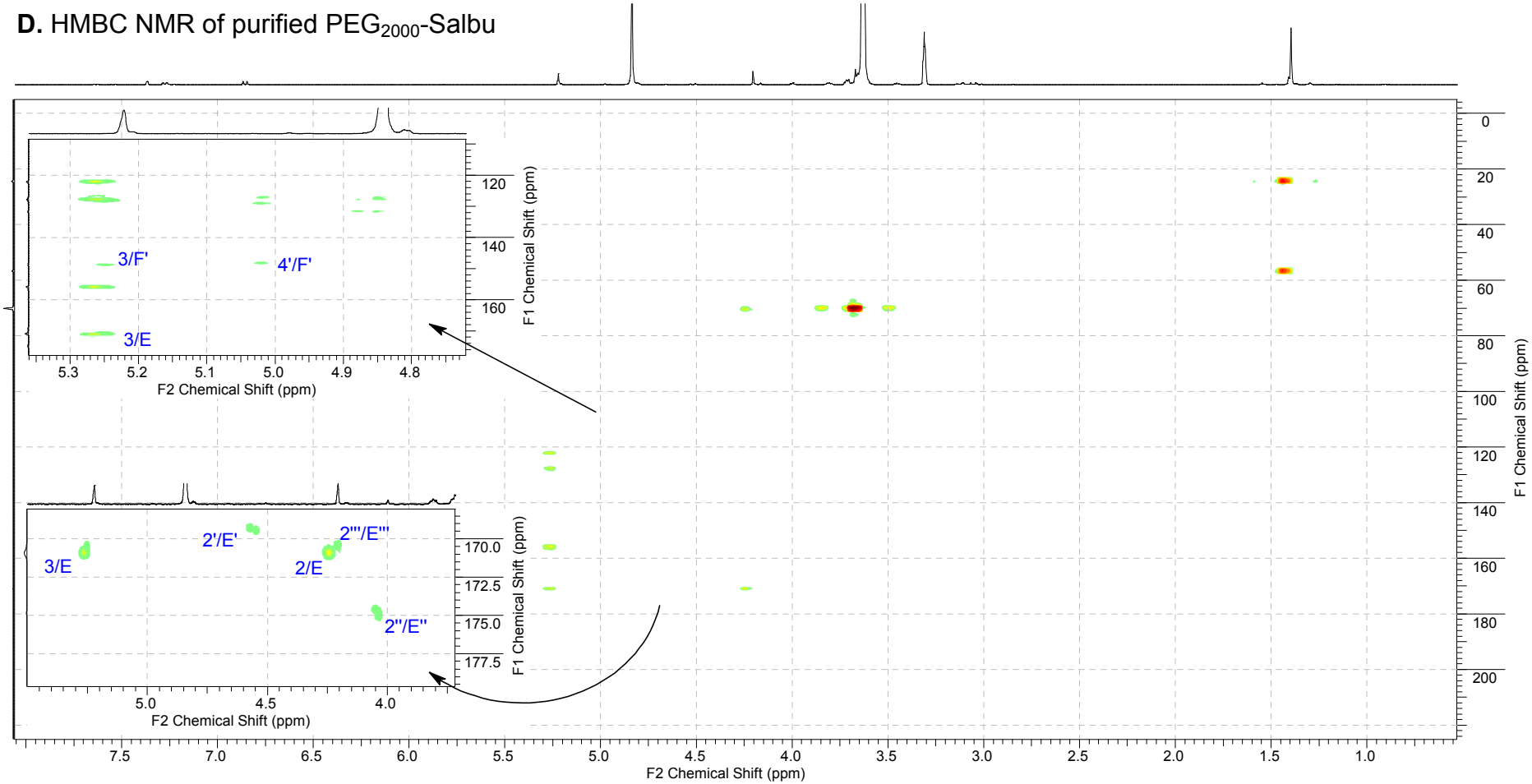

Spectra acquired on a Bruker AV(III)400 spectrometer in MeOD

Fig.VI.47. NMR analysis of purified PEG_{2000}-salbutamol ester

The integration values were defined such as the sum of the proton signals for PEG α carbon (PEG-C$\underline{H_2}$-CO-O-) was 4 H. The following signals were identified as such protons:

-Position 2'' (0.90 H) was a signal for unconjugated PEG, it is correlated to an α carbon at 69.14 ppm (B') and in HMBC, to a carbonyl at 174.90ppm (E').

-Position 2 (2.31 H) and 2''' (0.40 H) were signals for PEG conjugated to the primary hydroxyl group of salbutamol. The signals for the PEG α carbon (PEG-$\underline{C}H_2$-CO-O-Salbu) were respectively at 68.00 ppm (B) and 67.83 ppm (B'''). The corresponding carbonyl signals were measured in HMBC at 170.96 ppm (E) and 170.41 ppm (E'''). This carbonyl signals were also correlated to salbutamol protons in position 3, next to the primary hydroxyl group.

-Position 2' (0.40 H) was a signal for PEG conjugated to the secondary hydroxyl group of salbutamol. The signal for the PEG α carbon (PEG-$\underline{C}H_2$-CO-O-Salbu) was at 67.83 ppm (B'), and the corresponding carbonyl signal was measured in HMBC at 169.51 ppm (E'), consistent with an ester. This carbonyl signal was not correlated with any salbutamol proton signal, making the site of esterification more difficult to identify.

The salbutamol signal in position 4' (0.23 H) was conjugated to a carbon signal at 64.25 ppm (D'). This signal shares only one carbon signal in HMBC with the proton in position 3: F' at 148.55 ppm, which was dramatically shifted compared to F (127.88 ppm), correlated to the signals in positions 3 and 4.

The integral values of the proton signal in position 4' (0.23 H) was half of these of 2' and 2''' (0.40 H), confirming the proposed structure.

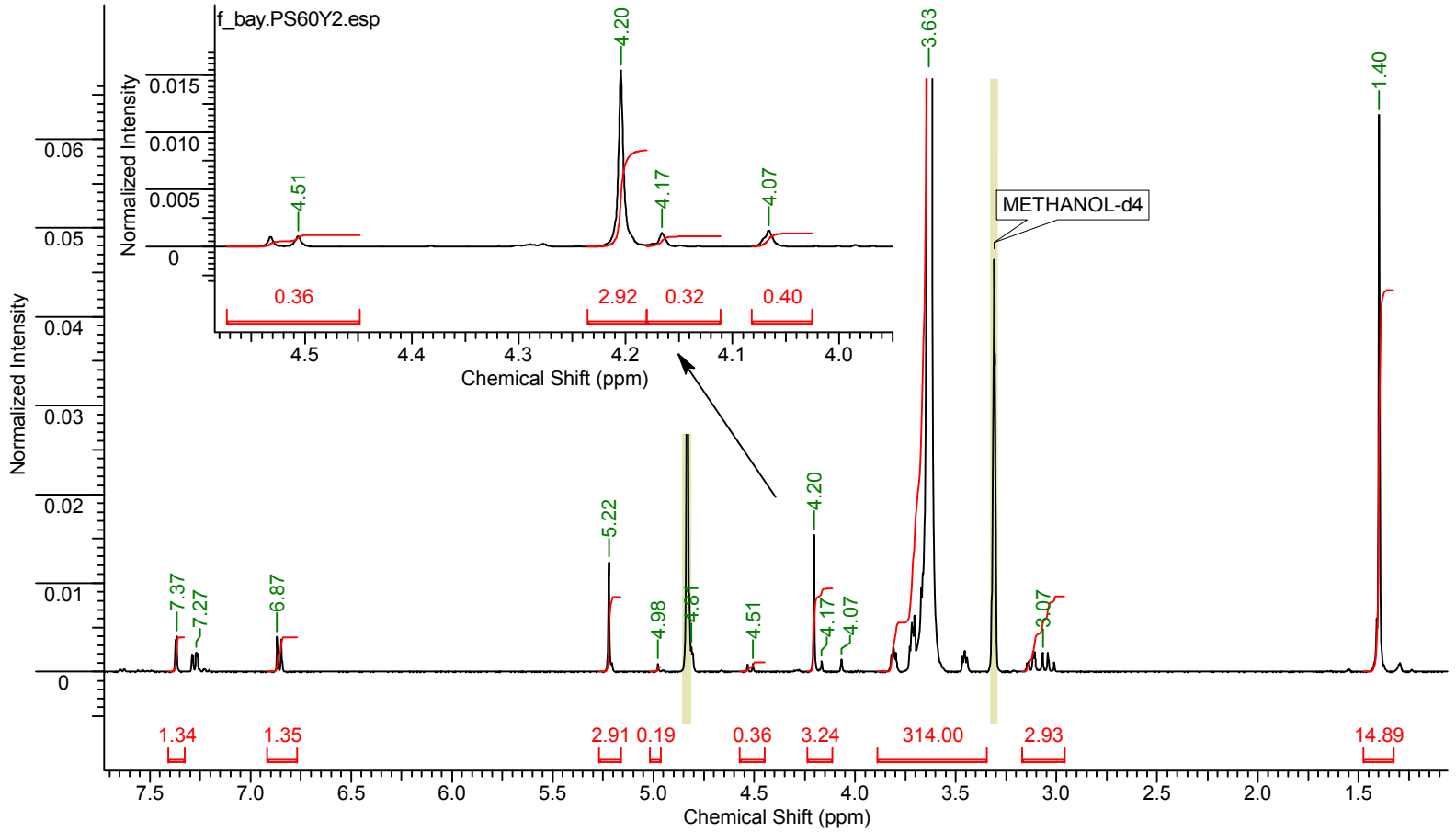

Fig.VI.48. ^{1}HNMR of purified PEG_{3400}-salbutamol ester
Spectrum acquired on a Bruker AV(III)400 spectrometer, 16 scans, in MeOD

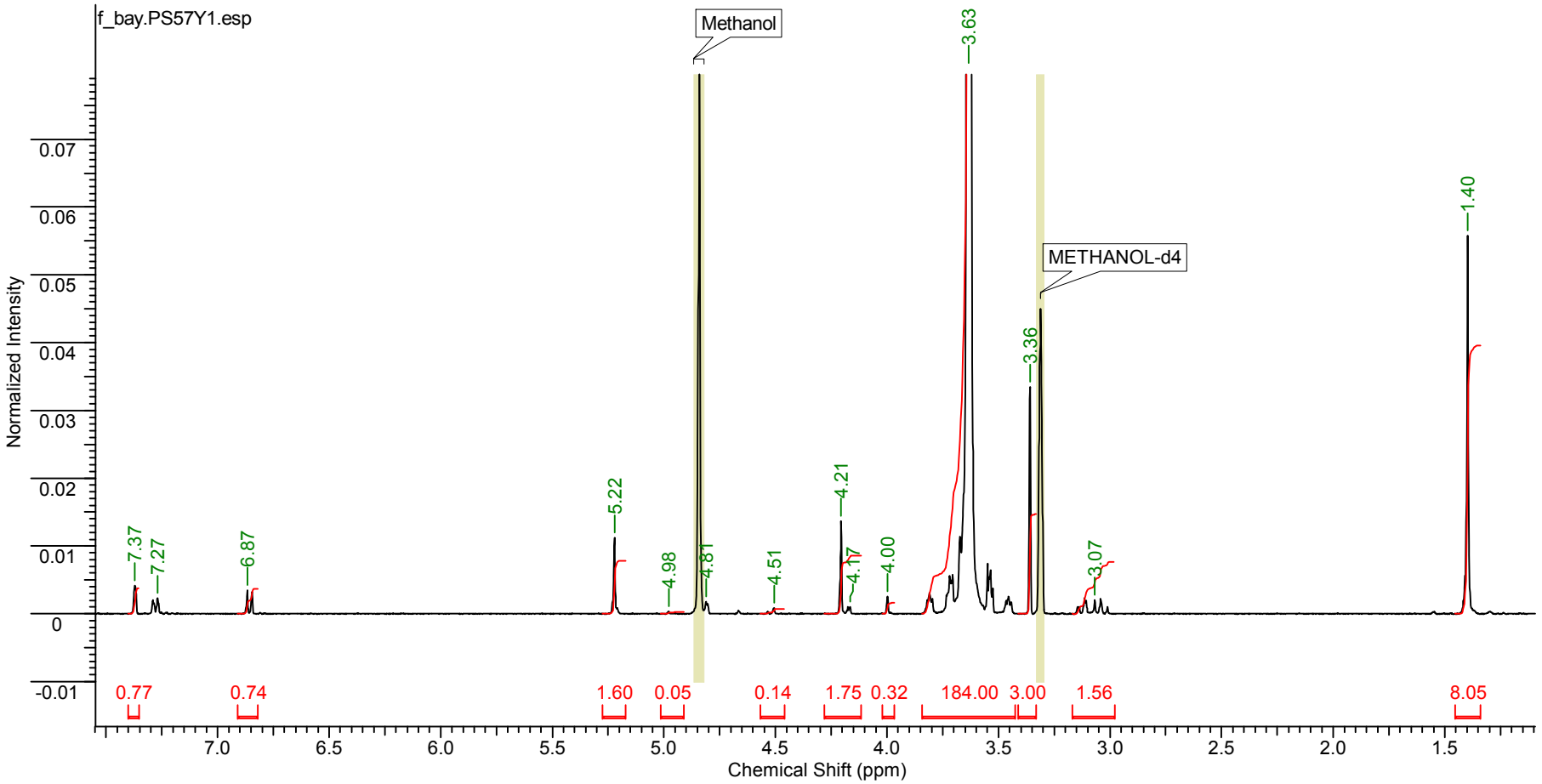

Fig.VI.49. ^{1}HNMR of purified $mPEG_{2000}$-salbutamol ester
Spectrum acquired on a Bruker AV(III)400 spectrometer, 16 scans, in MeOD

Appendix 5. Supplementary information for PEG-prednisolone HPLC-UV calibration solutions

Table. VI.1.Calibration solution preparation for PP28

Solution	Volume of Pred stock	Volume of PP28 stock	Volume of methanol	[Conjugate]	[Prednisolone]
	µL	µL	µL	mM	mM
Pred-PP28 TA	64	64	172	6.83	6.40
Solution	**Volume of Pred-PP28 TA**		**Volume of methanol**	**[Conjugate]**	**[Prednisolone]**
	µL		**µL**	**mM**	**mM**
Pred-PP28 T1	64		336	1.09	1.02

Solution	Volume of standard	Volume of methanol	[Conjugate]	[Prednisolone]
	µL	µL	µM	µM
Pred-PP28 T2	200 µL of T1	200	546.02	511.94
Pred-PP28 T3	200 µL of T2	200	273.01	255.97
Pred-PP28 T4	200 µL of T3	200	136.50	127.98
Pred-PP28 T5	200 µL of T4	200	68.25	63.99
Pred-PP28 T6	200 µL of T5	200	34.13	32.00
Pred-PP28 T7	200 µL of T6	200	17.06	16.00
Pred-PP28 T8	200 µL of T7	200	8.53	8.00
Pred-PP28 T9	200 µL of T8	200	4.27	4.00
Pred-PP28 T10	200 µL of T9	200	2.13	2.00
Pred-PP28 T11	200 µL of T10	200	1.07	1.00
Pred-PP28 T12	200 µL of T11	200	0.53	0.50
Pred-PP28 T13	200 µL of T12	200	0.27	0.25
Pred-PP28 T14	200 µL of T13	200	0.13	0.12
Pred-PP28 T15	200 µL of T14	200	0.07	0.06

Table. VI.2.Calibration solution preparation for PP29

Solution	Volume of Pred stock	Volume of PP29 stock	Volume of methanol	[Conjugate]	[Prednisolone]
	µL	µL	µL	mM	mM
Pred-PP29 RA	64	64	172	3.20	6.40
Solution	**Volume of Pred-PP29 RA**		**Volume of methanol**	**[conjugate]**	**[Prednisolone]**
	µL		**µL**	**mM**	**mM**
Pred-PP29 R1	32		168	0.51	1.02

Solution	Volume of standard	Volume of methanol	[Conjugate]	[Prednisolone]
	µL	µL	µM	µM
Pred-PP29 R2	200 µL of R1	200	256.07	511.94
Pred-PP29 R3	200 µL of R2	200	128.03	255.97
Pred-PP29 R4	200 µL of R3	200	64.02	127.98
Pred-PP29 R5	200 µL of R4	200	32.01	63.99
Pred-PP29 R6	200 µL of R5	200	16.00	32.00
Pred-PP29 R7	200 µL of R6	200	8.00	16.00
Pred-PP29 R8	200 µL of R7	200	4.00	8.00
Pred-PP29 R9	200 µL of R8	200	2.00	4.00
Pred-PP29 R10	200 µL of R9	200	1.00	2.00
Pred-PP29 R11	200 µL of R10	200	0.50	1.00
Pred-PP29 R12	200 µL of R11	200	0.25	0.50

Table. VI.3.Calibration solution preparation for PP31

Solution	Volume of Pred stock	Volume of PP28 stock	Volume of methanol	[Conjugate]	[Prednisolone]
	µL	µL	µL	mM	mM
Pred-PP31 RA	64	64	172	3.20	6.40
Solution	**Volume of Pred-PP31 RA**		**Volume of methanol**	**[Conjugate]**	**[Prednisolone]**
	µL		**µL**	**mM**	**mM**
Pred-PP31 R1	32		172	0.50	1.00

Solution	Volume of standard	Volume of methanol	[Conjugate]	[Prednisolone]
	µL	µL	µM	µM
Pred-PP31 R2	200 µL of R1	200	250.94	501.90
Pred-PP31 R3	200 µL of R2	200	125.47	250.95
Pred-PP31 R4	200 µL of R3	200	62.73	125.48
Pred-PP31 R5	200 µL of R4	200	31.37	62.74
Pred-PP31 R6	200 µL of R5	200	15.68	31.37
Pred-PP31 R7	200 µL of R6	200	7.84	15.68
Pred-PP31 R8	200 µL of R7	200	3.92	7.84
Pred-PP31 R9	200 µL of R8	200	1.96	3.92

Appendix 6. Supplementary information for PEG-salbutamol calibration solutions

Table. VI.4.Calibration solution preparation for salbutamol sulfate

Solution	Volume of standard	Volume of methanol	[salbutamol]
	µL	µL	µM
Salbu XA	50 µL of stock	450	3003
Salbu X1	100 µL of XA	300	750.8
Salbu X2	200 µL of X1	200	375.4
Salbu X3	200 µL of X2	200	187.7
Salbu X4	200 µL of X3	200	93.8
Salbu X5	200 µL of X4	200	46.9
Salbu X6	200 µL of X5	200	23.5
Salbu X7	200 µL of X6	200	11.7

Salbu X8	200 µL of X7	200	5.9

Table. VI.5.Calibration solution preparation for PS57

Solution	Volume of salbu stock	Volume of PS57 stock	Volume of methanol	[conjugate]	[salbutamol]
	µL	µL	µL	µM	µM
Salbu-PS57 QA	**50**	50	400	3532	3003

Solution	Volume of standard	Volume of methanol	[conjugate]	[salbutamol]
	µL	µL	µM	µM
Salbu-PS57 Q1	100 µL of QA	400	706.5	600.6
Salbu-PS57 Q2	200 µL of Q1	200	353.2	300.3
Salbu-PS57 Q3	200 µL of Q2	200	176.6	150.2
Salbu-PS57 Q4	200 µL of Q3	200	88.3	75.1
Salbu-PS57 Q5	200 µL of Q4	200	44.2	37.5
Salbu-PS57 Q6	200 µL of Q5	200	22.1	18.8
Salbu-PS57 Q7	200 µL of Q6	200	11.0	9.4
Salbu-PS57 Q8	200 µL of Q7	200	5.5	4.7

Table. VI.6.Calibration solution preparation for PS60

Solution	Volume of standard	Volume of methanol	[conjugate]
	µL	µL	µM
PS60 WA	50 µL of stock	450	1875
PS60 W1	100 µL of WA	300	468.8
PS60 W2	200 µL of W1	200	234.4
PS60 W3	200 µL of W2	200	117.2
PS60 W4	200 µL of W3	200	58.6
PS60 W5	200 µL of W4	200	29.3
PS60 W6	200 µL of W5	200	14.6
PS60 W7	200 µL of W6	200	7.3

Appendix 7. Supplementary information for PEG-prednisolone *in vitro* hydrolysis study

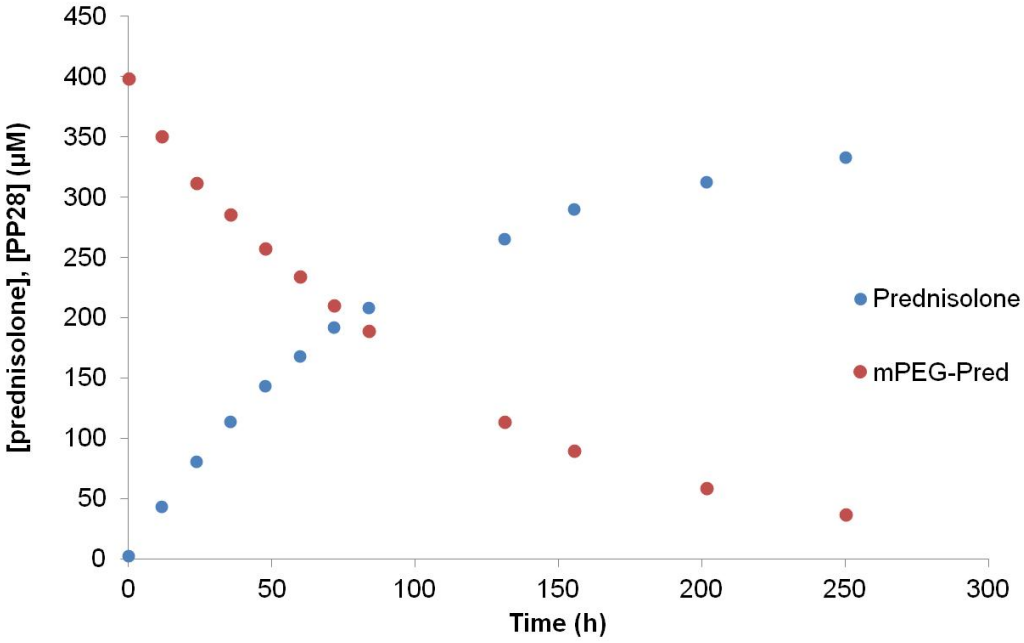

Fig.VI.50. Hydrolysis profile of PP28 ($mPEG_{2000}$-Pred) at pH 6.2

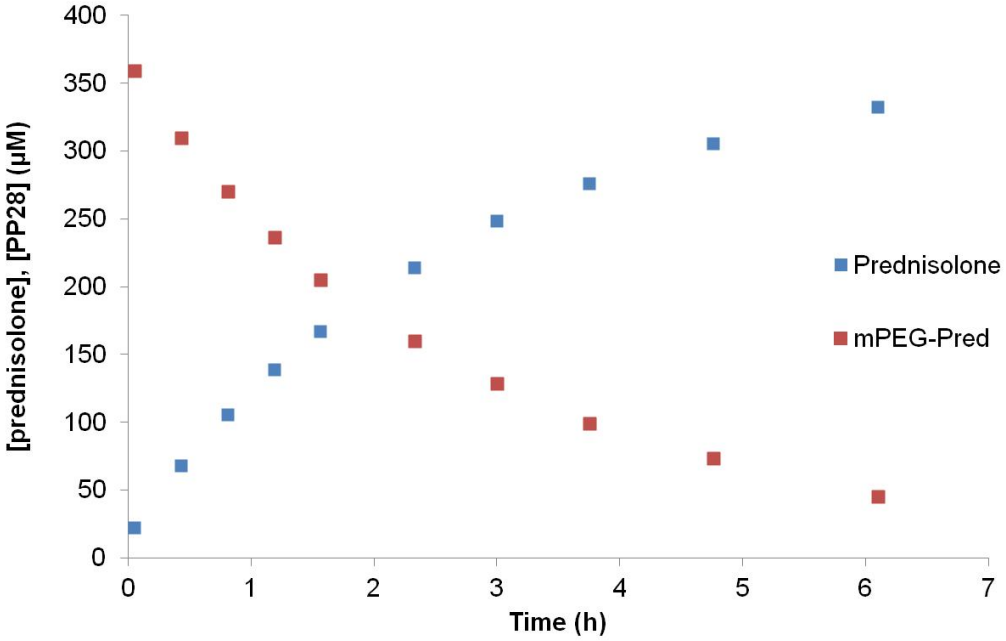

Fig.VI.51. Hydrolysis profile of PP28 ($mPEG_{2000}$-Pred) at pH 8.0

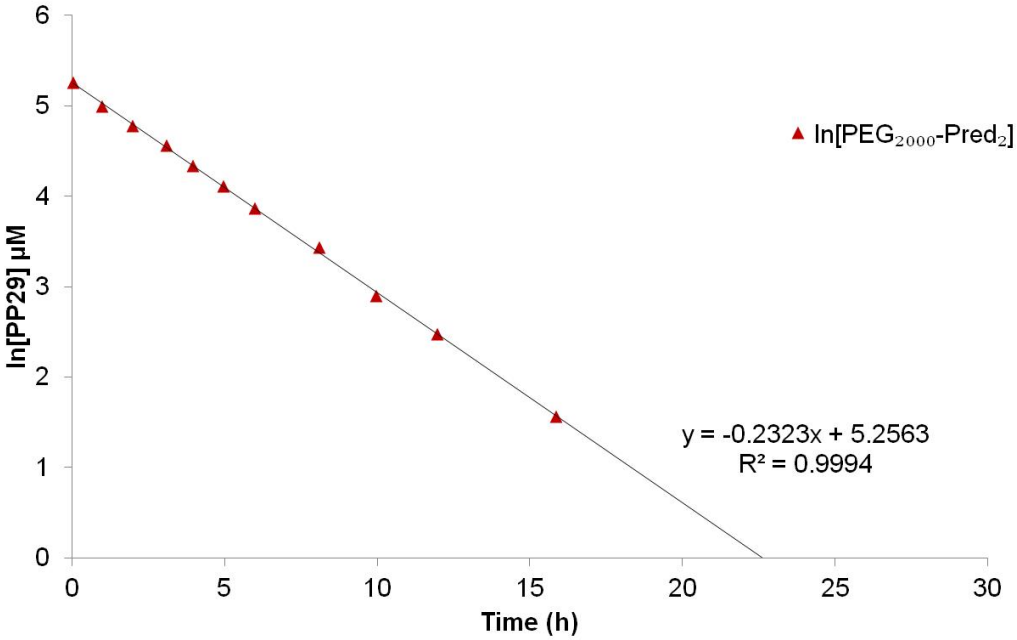

Fig.VI.52. Plot of ln[PP29] vs time at pH 7.4
Logarithm transformation and linear regression performed with Excel

Appendix 8. Supplementary information for hydrolysis with Calu-3

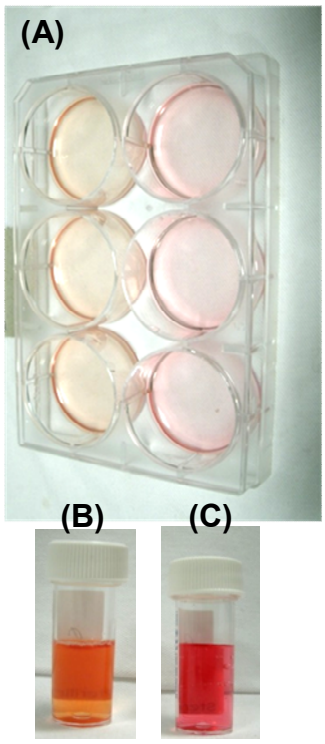

At the end of the experiments (III.3.4), the medium were pooled together and collected in 7 mL tubes (B and C). The difference in colour indicated a lower pH in the medium that contained the cells.

Fig.VI.53. Cell culture plate (A) and medium after hydrolysis test in the presence (B) or not (C) of cells

Appendix 9. Supplementary information for IPRL *ex vivo* methods

Table. VI.7.Perfusate composition: Krebs-Ringer bicarbonate buffer

Solute	mM	Solute	mM
NaCl	118.0	KH_2PO_4	1.2
KCl	4.7	HEPES	12.5
$CaCl_2$	2.5	Glucose	5.0
$MgSO_4$	1.2	BSA, fraction V	0.3 (2%)
$NaHCO_3$	24.9		

BSA: Bovine Serum Albumin, HEPES: Hydroxyethyl Piperazineethanesulfonic acid

(VI.1) ***Equations used to model the fate of prednisolone in IPRL experiments, using Berkeley Madonna terminology***

a. Prednisolone

$$k_{in} = \frac{Dose}{Duration} \cdot (1 - step\ (1, Duration))$$

$$\frac{dPred_l}{dt} = +k_{in} - \ k_{out} \cdot Pred_l$$

$$\frac{dPred_p}{dt} = + k_{out} \cdot Pred_l$$

kin (nmol.min^{-1}) is the 0 order constant of prednisolone administration in the lung, *Dose* (nmol) is the total administered dose, *Duration* (min) is the administration time, $Pred_l$ (nmol) is the amount of prednisolone in the lung, $Pred_p$ (nmol) is the cumulative amount of prednisolone in perfusate, k_{out} (min^{-1}) is the 1st order constant of prednisolone permeability from the lung.

b. mPEG-Pred$_l$

$$k_{in} = \frac{Dose}{Duration} \cdot (1 - step\ (1, Duration))$$

$$\frac{dPP1_l}{dt} = +k_{in} - \ k_1 \cdot PP1_l$$

$$\frac{dPred_l}{dt} = + k_1 \cdot PP1_l - k_{out} \cdot Pred_l$$

$$\frac{dPred_p}{dt} = + k_{out} \cdot Pred_l$$

k_{in} (nmol.min^{-1}) is the 0 order constant of prednisolone administration in the lung, *Dose* (nmol) is the total administered dose, *Duration* (min) is the administration time, $PP1_l$ (nmol) is the amount of conjugate in the lung, k_1 (min^{-1}) is the first order rate constant of the conjugate hydrolysis, $Pred_l$ (nmol) is the amount of prednisolone in the lung, $Pred_p$ (nmol) is the cumulative amount of prednisolone in perfusate, k_{out} (min^{-1}) is the 1st order constant of prednisolone permeability from the lung.

c. PEG-Pred$_2$

$$k_{in} = \frac{Dose}{Duration} \cdot (1 - step\,(1, Duration))$$

$$\frac{dPP2_l}{dt} = +k_{in} - \ k_2 \cdot PP2_l$$

$$\frac{dPred_l}{dt} = +\,2\,k_2 \cdot PP2_l - k_{out} \cdot Pred_l$$

$$\frac{dPred_p}{dt} = +\,k_{out} \cdot Pred_l$$

k_{in} (nmol.min^{-1}) is the 0 order constant of prednisolone administration in the lung, *Dose* (nmol) is the total administered dose, *Duration* (min) is the administration time, $PP2_l$ (nmol) is the amount of conjugate in the lung, k_2 (min^{-1}) is the first order rate constant of the conjugate hydrolysis, $Pred_l$ (nmol) is the amount of prednisolone in the lung, $Pred_p$ (nmol) is the cumulative amount of prednisolone in perfusate, k_{out} (min^{-1}) is the 1st order constant of prednisolone permeability from the lung.

Appendix 10. Supplementary information for IPRL *ex vivo* results

A. Prednisolone

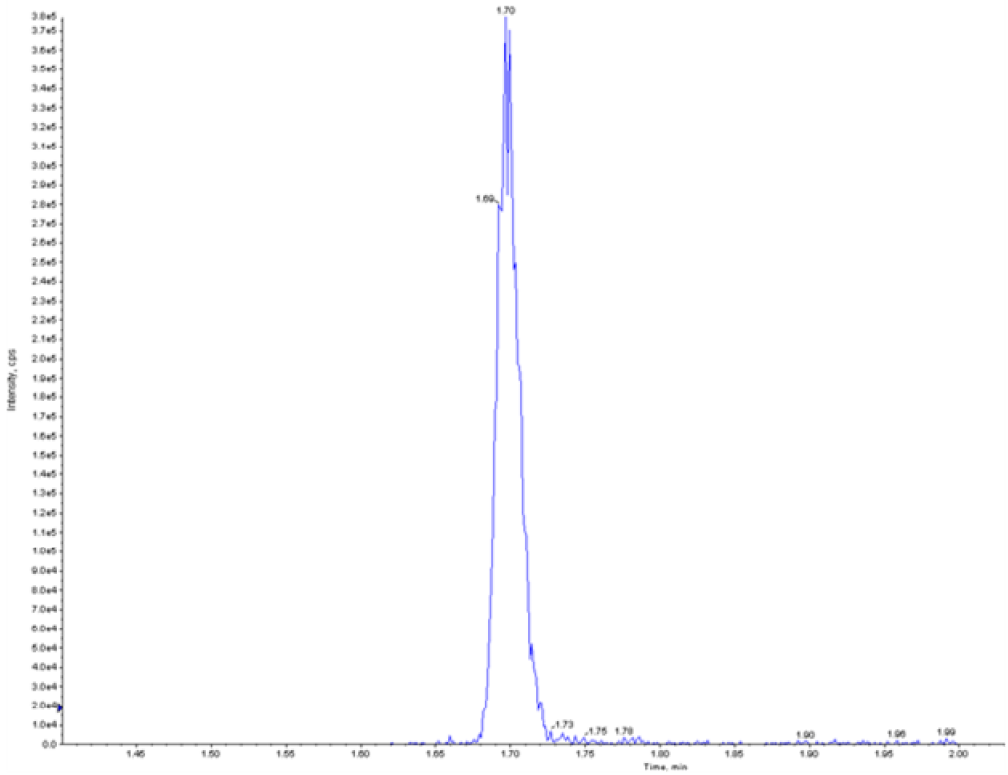

B. Dexamethasone

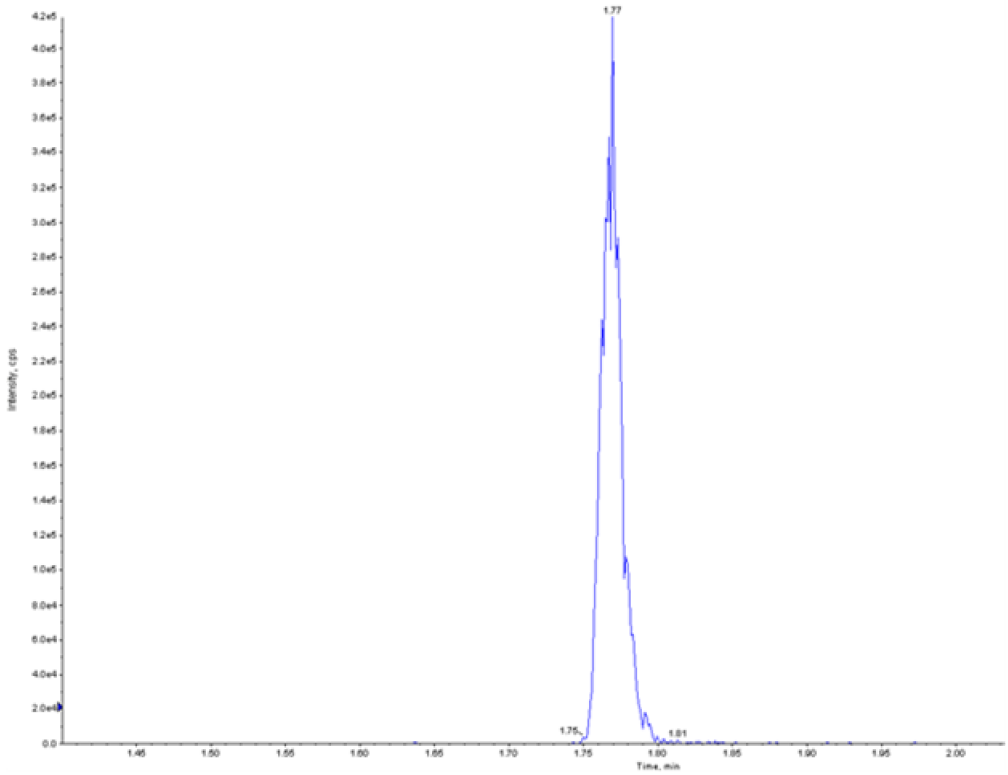

C. $mPEG_{2000}$-Pred

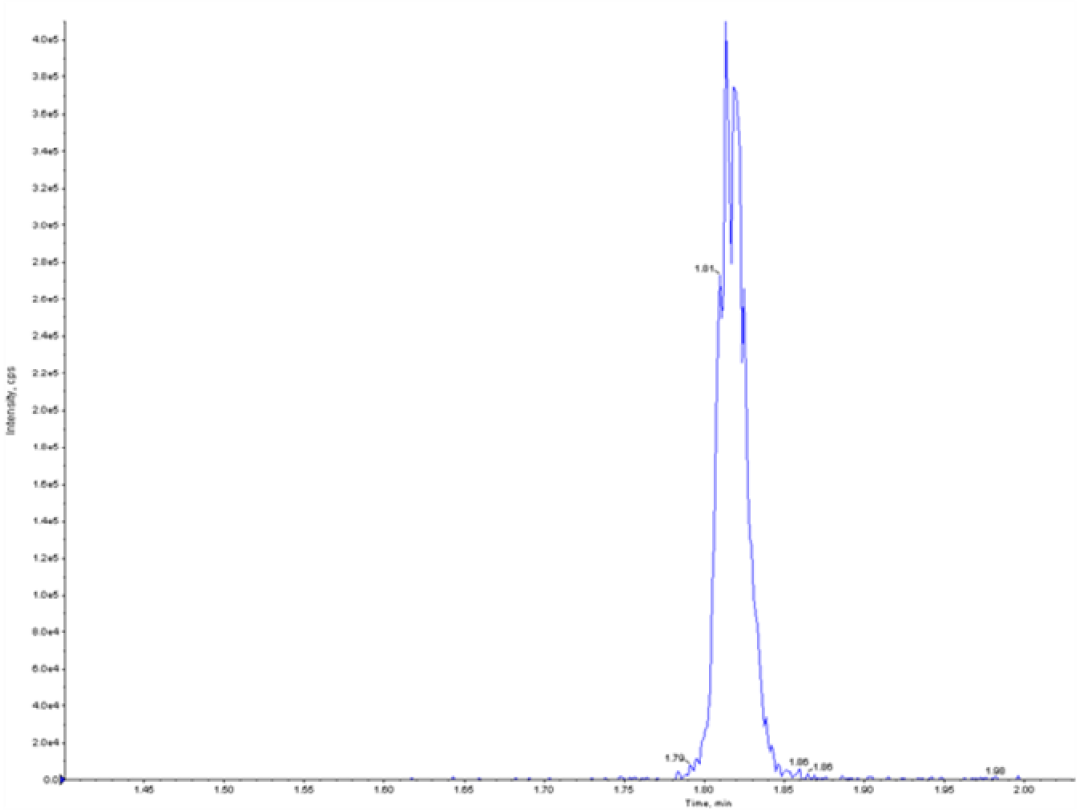

D. PEG_{2000}-$Pred_2$

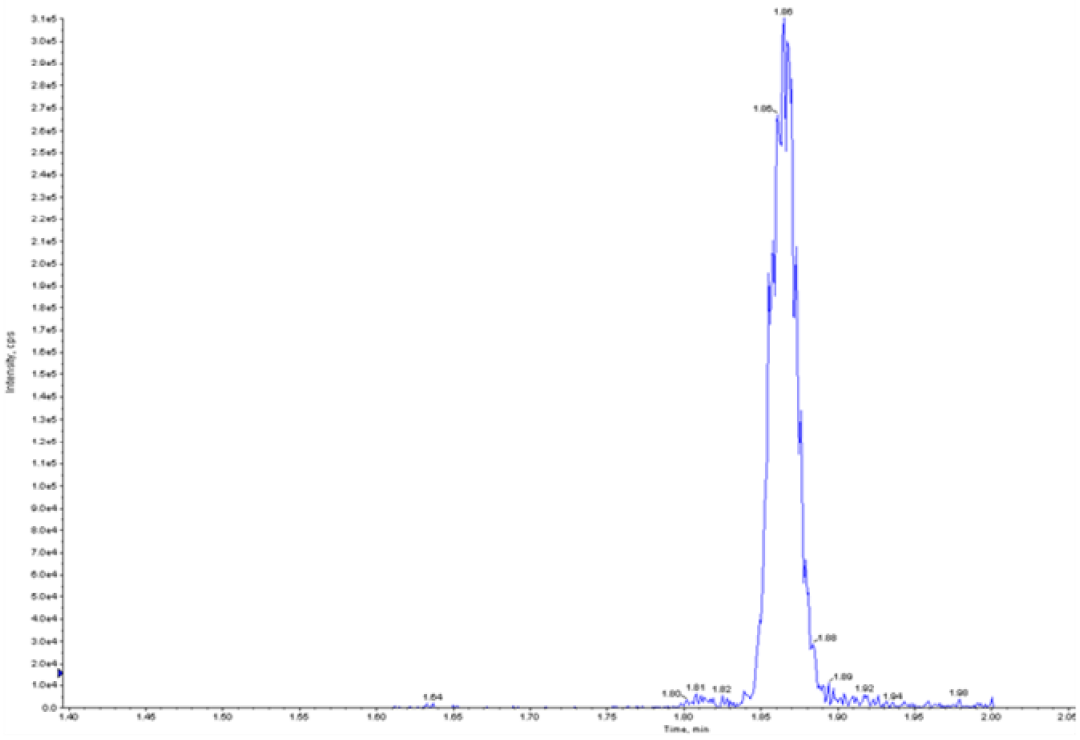

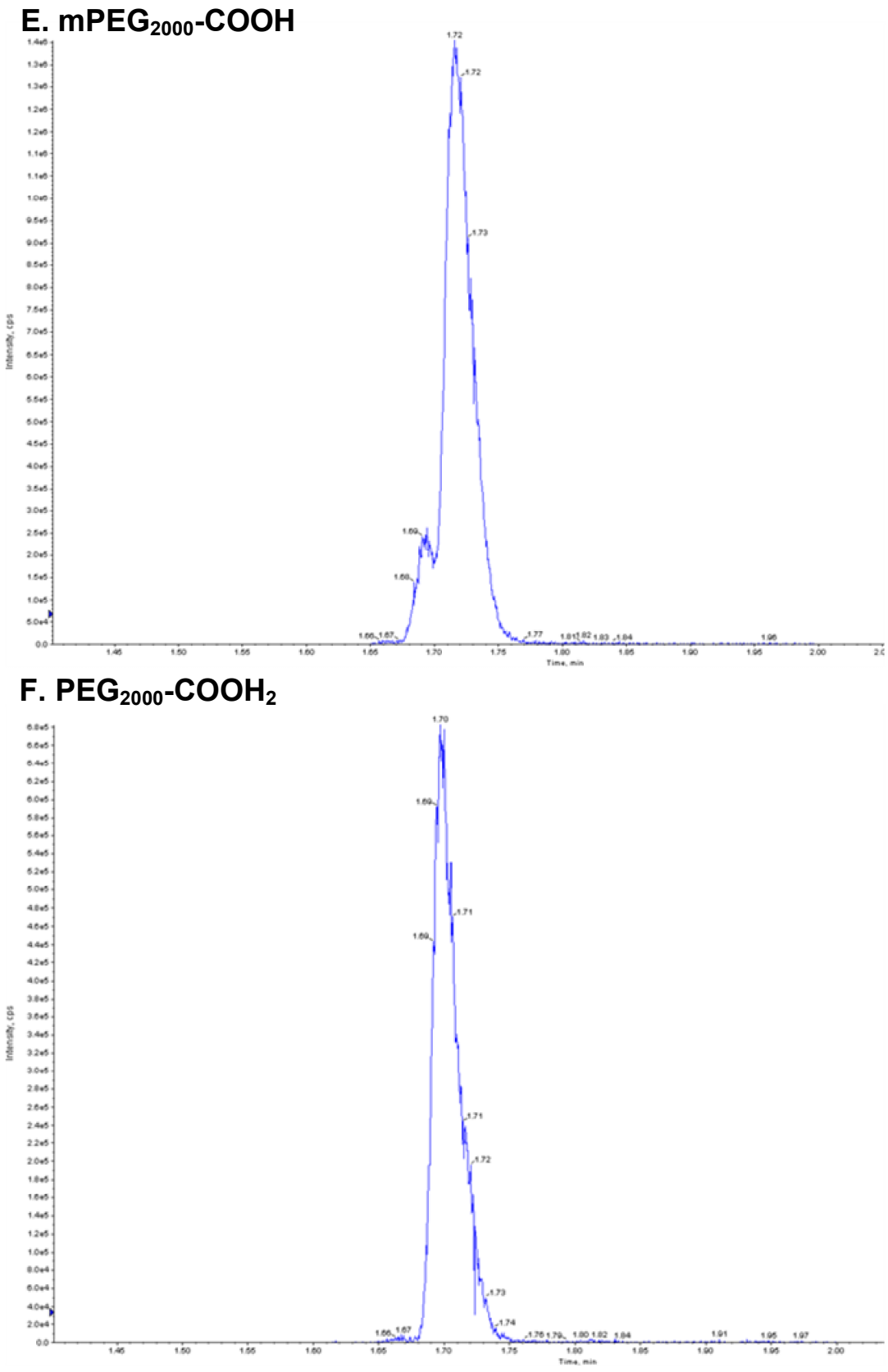

Fig.VI.54. Chromatogram of LC-MS/MS analysis of prednisolone, dexamethasone, mPEG-Pred$_1$, PEG-Pred$_2$, mPEGCOOH, PEGCOOH$_2$

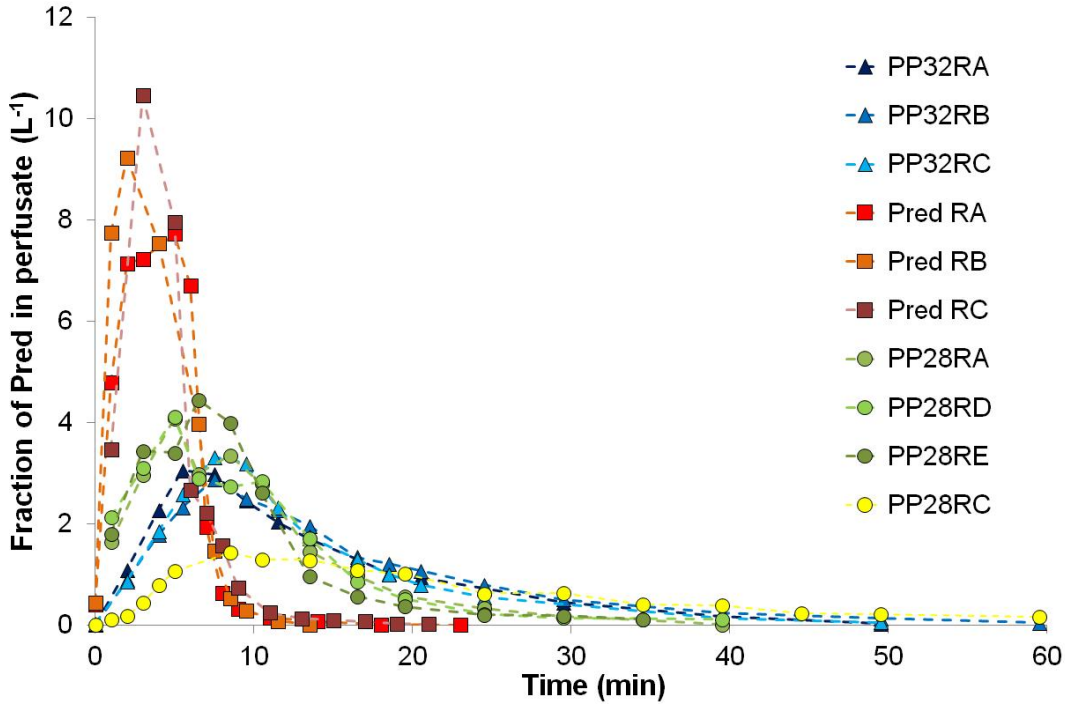

Fig.VI.55. Fraction of prednisolone in perfusate for prednisolone, mPEG-Pred, PEG-$Pred_2$

Each individual measured concentration (nmol.L^{-1}) was divided by the total dose administered during the experiment (nmol) to give relative fractions of prednisolone in perfusate (L^{-1})

Table. VI.8.Determination of prednisolone absorption rate from the lung using Berkeley Madonna

	INPUT	OUTPUT		
Experiment	**Dose nmol**	**infusion time (min)**	**k_{out} (min^{-1})**	**$t_{1/2}$ (min)**
Pred RA	153.45	2.9	0.504007	1.375273
Pred RB	93.83	1.6	0.52691	1.315494
Pred RC	72.04	1.9	0.423745	1.635765

A.

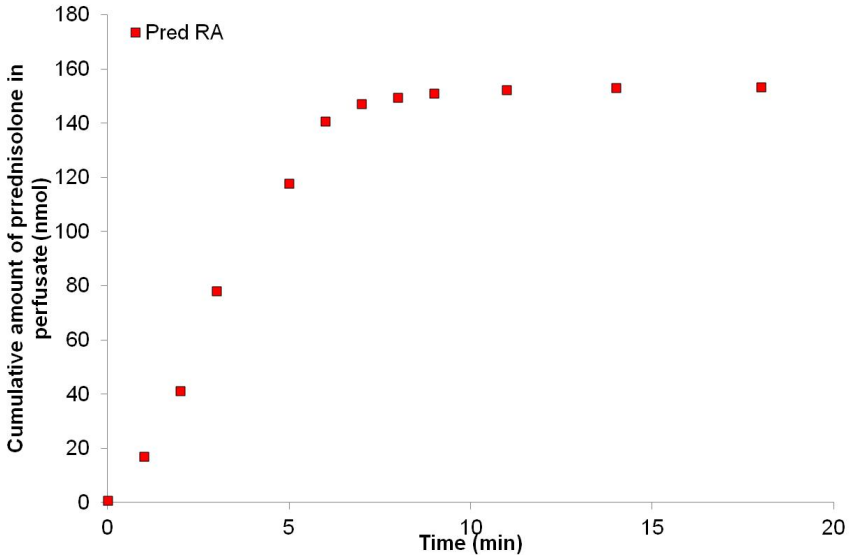
Pred RA
Cumulative amount of prrednisolone in perfusate (nmol)
Time (min)
0
20
40
60
80
100
120
140
160
180
0
5
10
15
20

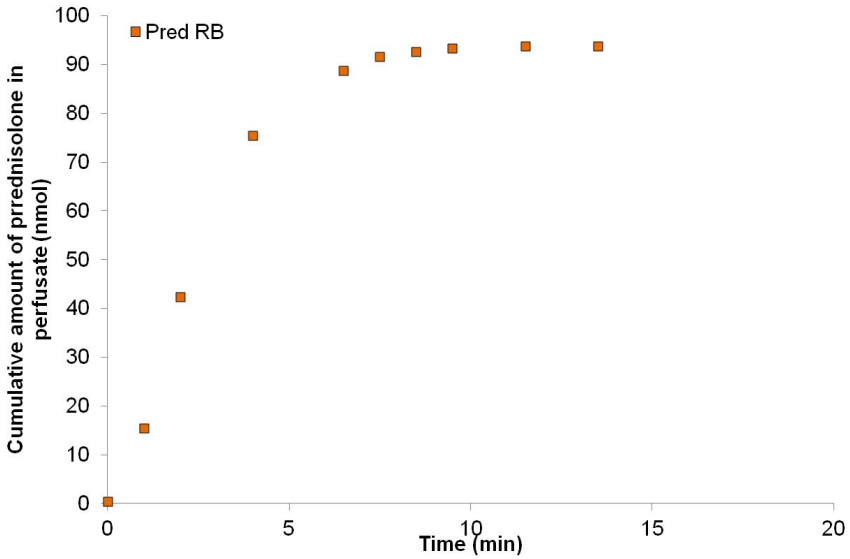
Pred RB
Cumulative amount of prrednisolone in perfusate (nmol)
Time (min)
0
10
20
30
40
50
60
70
80
90
100
0
5
10
15
20

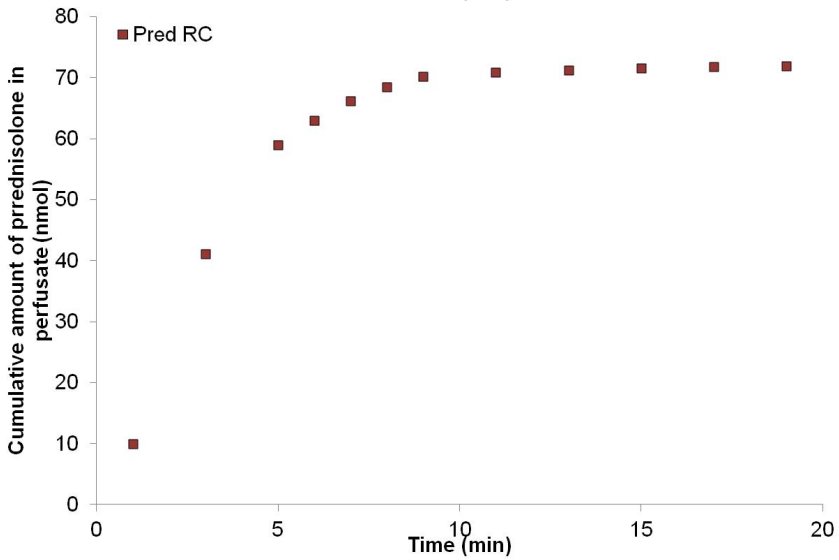
Pred RC
Cumulative amount of prrednisolone in perfusate (nmol)
Time (min)
0
10
20
30
40
50
60
70
80
0
5
10
15
20

B.

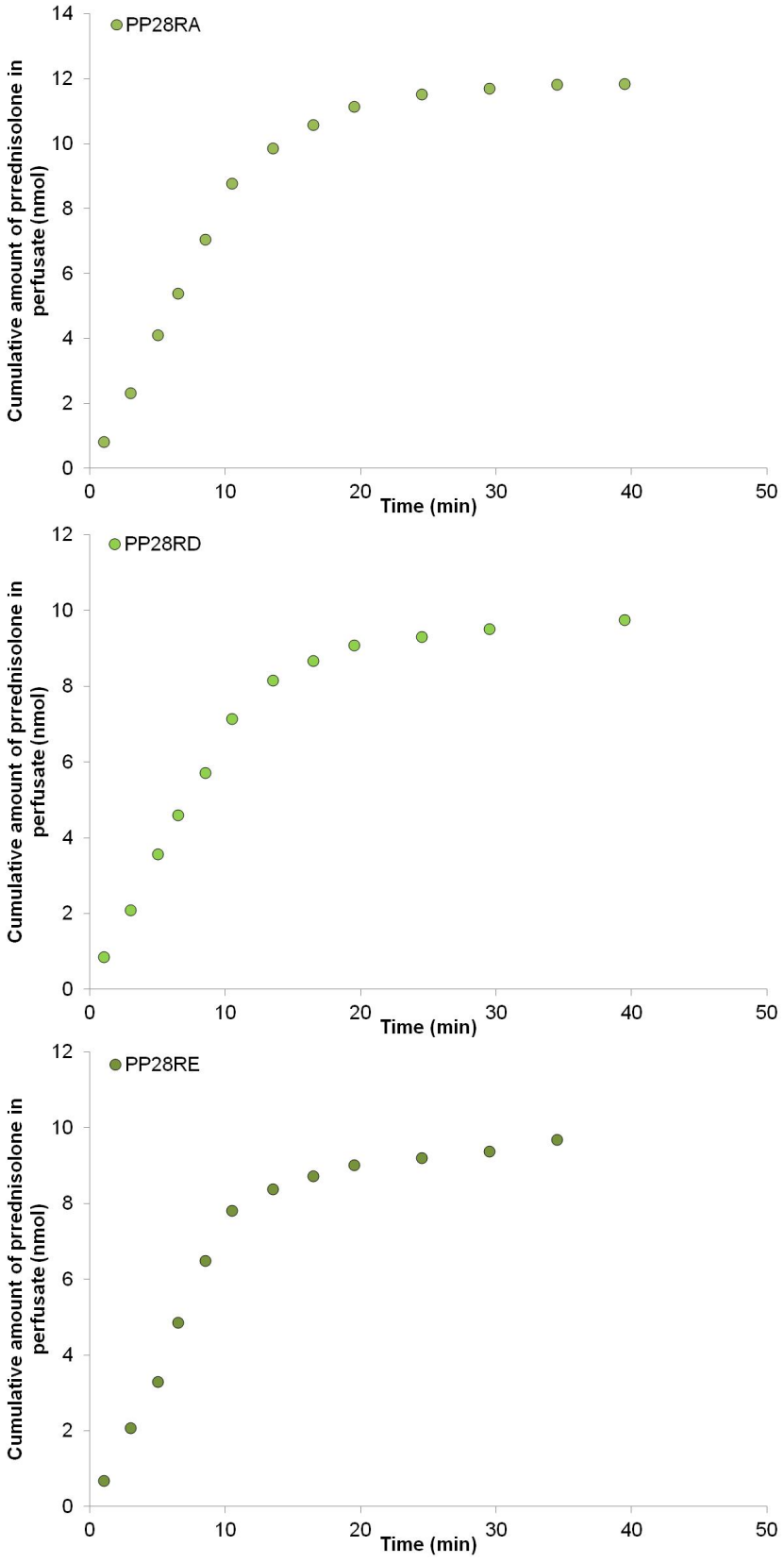
PP28RA
Cumulative amount of prrednisolone in perfusate (nmol)
Time (min)
PP28RD
Cumulative amount of prrednisolone in perfusate (nmol)
Time (min)
PP28RE
Cumulative amount of prrednisolone in perfusate (nmol)
Time (min)

C.

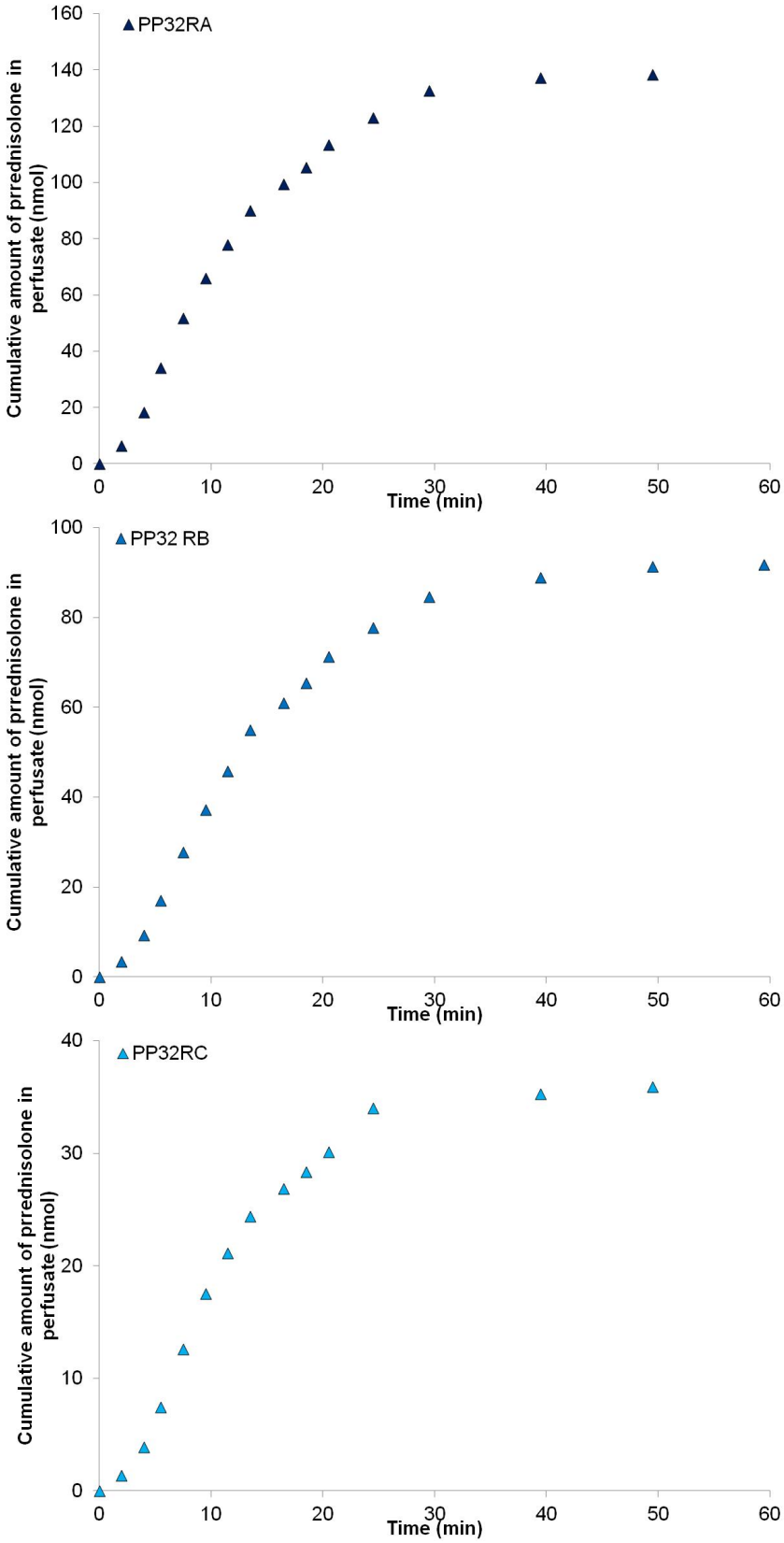

Fig.VI.56. Cumulative plots of prednisolone in perfusate for prednisolone (**A**), mPEG-Pred$_1$ (**B**), PEG-Pred$_2$ (**C**) IPRL experiments

Chapter VII. References

[1] J.S. Patton, P.R. Byron, Inhaling medicines: delivering drugs to the body through the lungs. Nature Reviews Drug Discovery 6(1) (2007) 67-74.
[2] E.R. Weibel, D.M. Gomez, Architecture of human lung. Science 137(3530) (1962) 577-585.
[3] A.B. Lansley, Mucociliary clearance and drug-delivery via the respiratory-tract. Adv. Drug Deliv. Rev. 11(3) (1993) 299-327.
[4] J.S. Patton, Mechanisms of macromolecule absorption by the lungs. Adv. Drug Deliv. Rev. 19(1) (1996) 3-36.
[5] N.R. Labiris, M.B. Dolovich, Pulmonary drug delivery. Part I: Physiological factors affecting therapeutic effectiveness of aerosolized medications. Br. J. Clin. Pharmacol. 56(6) (2003) 588-599.
[6] E.R. Weibel, Morphological basis of alveolar-capillary gas exchange. Physiol Rev. 53(2) (1973) 419-495.
[7] P.R. Byron, J.S. Patton, Drug-delivery via the respiratory-tract. J. Aerosol Med.-Depos. Clear. Eff. Lung 7(1) (1994) 49-75.
[8] G. Igor, The ascent of pulmonary drug delivery. J. Pharm. Sci. 89(7) (2000) 940-945.
[9] T.B. Op't Holt, Evolution of the inhalation of vapors and aerosols in the care of asthma and other respiratory diseases. Journal of Asthma & Allergy Educators 2(2) (2011) 75-80.
[10] J.S. Patton, in: B.-P. Karoline and L. Henrik (Eds.), Pulmonary Drug Delivery, Editio Cantor Verlag, Aulendorf, 2007.
[11] A. Safdar, S.A. Shelburne, S.E. Evans, B.F. Dickey, Inhaled therapeutics for prevention and treatment of pneumonia. Expert Opinion on Drug Safety 8(4) (2009) 435-449.
[12] G. Ryan, M. Singh, K. Dwan, Inhaled antibiotics for long-term therapy in cystic fibrosis. Cochrane Database Syst Rev.(3) (2011) 86.
[13] P. Greally, P. Whitaker, D. Peckham, Challenges with current inhaled treatments for chronic Pseudomonas aeruginosa infection in patients with cystic fibrosis. Curr. Med. Res. Opin. 28(6) (2012) 1059-1067.
[14] M.J. Shelton, M. Lovern, J. Ng-Cashin, L. Jones, E. Gould, J. Gauvin, K.A. Rodvold, Zanamivir pharmacokinetics and pulmonary penetration into epithelial lining fluid following intravenous or oral inhaled administration to healthy adult subjects. Antimicrobial Agents and Chemotherapy 55(11) (2011) 5178-5184.
[15] A. Poms, M. Kingman, Inhaled treprostinil for the treatment of pulmonary arterial hypertension. Critical Care Nurse 31(6) (2011) e1-e10.
[16] R.L. Benza, W. Seeger, V.V. McLaughlin, R.N. Channick, R. Voswinckel, V.F. Tapson, I.M. Robbins, H. Olschewski, L.J. Rubin, Long-term effects of inhaled treprostinil in patients with pulmonary arterial hypertension: The TReprostinil sodium Inhalation Used in the Management of Pulmonary arterial Hypertension (TRIUMPH) study open-label extension. The Journal of Heart and Lung Transplantation 30(12) (2011) 1327-1333.
[17] A.S. Monto, A. Webster, O. Keene, Randomized, placebo-controlled studies of inhaled zanamivir in the treatment of influenza A and B: pooled efficacy analysis. Journal of Antimicrobial Chemotherapy 44(suppl 2) (1999) 23-29.

[18] F.G. Hayden, L.V. Gubareva, A.S. Monto, T.C. Klein, M.J. Elliott, J.M. Hammond, S.J. Sharp, M.J. Ossi, Inhaled zanamivir for the prevention of influenza in families. New England Journal of Medicine 343(18) (2000) 1282-1289.
[19] J. Jakobsson, Desflurane: a clinical update of a third-generation inhaled anaesthetic. Acta Anaesthesiol. Scand. 56(4) (2012) 420-432.
[20] J. Hukkanen, P. Jacob, N.L. Benowitz, Metabolism and disposition kinetics of nicotine. Pharmacological Reviews 57(1) (2005) 79-115.
[21] I. Gately, Tobacco: a cultural history of how an exotic plant seduced civilization, Simon & Schuster UK Ltd, London, 2001.
[22] F. Ungaro, I. d' Angelo, A. Miro, M.I. La Rotonda, F. Quaglia, Engineered PLGA nano- and micro-carriers for pulmonary delivery: challenges and promises. Journal of Pharmacy and Pharmacology 64(9) (2012) 1217-1235.
[23] G.S. Mack, Pfizer dumps Exubera. Nat Biotech 25(12) (2007) 1331-1332.
[24] E.C. Walvoord, A. De La Peña, S. Park, B. Silverman, L. Cuttler, S.R. Rose, G. Cutler, S. Drop, J.J. Chipman, Inhaled growth hormone (GH) compared with subcutaneous GH in children with GH deficiency: pharmacokinetics, pharmacodynamics, and safety. Journal of Clinical Endocrinology and Metabolism 94(6) (2009) 2052-2059.
[25] N.R. Labiris, M.B. Dolovich, Pulmonary drug delivery. Part II: The role of inhalant delivery devices and drug formulations in therapeutic effectiveness of aerosolized medications. Br. J. Clin. Pharmacol. 56(6) (2003) 600-612.
[26] C. Ocallaghan, P.W. Barry, The science of nebulised drug delivery. Thorax 52 (1997) S31-S44.
[27] S. Da Rocha, R.P., B. Bharatwaj, S. Saiprasad, in: S. a. Hickey (Ed.), Controlled Pulmonary Drug Delivery, Springer, New York, 2011, pp. 165-201.
[28] L. Wu, S.R.P. da Rocha, Applications of the atomic force microscope in the development of propellant-based inhalation formulations. KONA Powder Part. J. 26 (2008) 106-128.
[29] T.M. Crowder, M.J. Donovan, in: S. a. Hickey (Ed.), Controlled Pulmonary Drug Delivery, Springer, New York, 2011, pp. 203-222.
[30] W. Wong, D.F. Fletcher, D. Traini, H.-K. Chan, J. Crapper, P.M. Young, Particle aerosolisation and break-up in dry powder inhalers. 1: evaluation and modelling of venturi effects for agglomerated systems. Pharmaceutical Research 27(7) (2010) 1367-1376.
[31] S.K. Vaswani, P.S. Creticos, Metered dose inhaler: past, present, and future. Annals of Allergy, Asthma & Immunology 80(1) (1998) 11-23.
[32] D.A. Groneberg, C. Witt, U. Wagner, K.F. Chung, A. Fischer, Fundamentals of pulmonary drug delivery. Respir. Med. 97(4) (2003) 382-387.
[33] C. Darquenne, Aerosol deposition in health and disease. Journal of Aerosol Medicine and Pulmonary Drug Delivery 25(3) (2012) 140-147.
[34] P. Zanen, L.T. Go, J.W.J. Lammers, Optimal particle size for β_2 agonist and anticholinergic aerosols in patients with severe airflow obstruction. Thorax 51(10) (1996) 977-980.
[35] R.M. Jones, A. Harrison, A new methodology for predicting human pharmacokinetics for inhaled drugs from oratracheal pharmacokinetic data in rats. Xenobiotica 42(1) (2012) 75-85.
[36] B. Olsson, E. Bondesson, L. Borgstrom, S. Edsbacker, S. Eirefelt, K. Ekelund, L. Gustavsson, T. Hegelund-Myrback, in: S. a. Hickey (Ed.), Controlled Pulmonary Drug Delivery, Springer, New York, 2011, pp. 21-50.

[37] J.A. Bond, Metabolism and elimination of inhaled drugs and airborne chemicals from the lungs. Pharmacology and Toxicology, Supplement 72(3) (1993) 36-47.
[38] S. Edsbäcker, C.J. Johansson, Airway selectivity: An update of pharmacokinetic factors affecting local and systemic disposition of inhaled steroids. Basic and Clinical Pharmacology and Toxicology 98(6) (2006) 523-536.
[39] J.S. Patton, C.S. Fishburn, J.G. Weers, The lungs as a portal of entry for systemic drug delivery. Proceedings of the American Thoracic Society 1(4) (2004) 338-344.
[40] M. Gumbleton, G. Al-Jayyoussi, A. Crandon-Lewis, D. Francombe, K. Kreitmeyr, C.J. Morris, M.W. Smith, Spatial expression and functionality of drug transporters in the intact lung: Objectives for further research. Adv. Drug Deliv. Rev. 63(1-2) (2011) 110-118.
[41] C. Bosquillon, Drug transporters in the lung - Do they play a role in the biopharmaceutics of inhaled drugs? J. Pharm. Sci. 99(5) (2010) 2240-2255.
[42] J.S. Patton, J.D. Brain, L.A. Davies, J. Fiegel, M. Gumbleton, K.J. Kim, M. Sakagami, R. Vanbever, C. Ehrhardt, The particle has landed-characterizing the fate of inhaled pharmaceuticals. Journal of Aerosol Medicine and Pulmonary Drug Delivery 23(SUPPL. 2) (2010) S71-S87.
[43] M. Rowland, T.n. Tozer, Clinical pharmacokinetic. Concepts and applications, Williams & Wilins, Philadelphia London, 1995.
[44] H.W. Kelly, Establishing a therapeutic index for the inhaled corticosteroids: Part I. Pharmacokinetic/pharmacodynamic comparison of the inhaled corticosteroids. Journal of Allergy and Clinical Immunology 102(4) (1998) S36-S51.
[45] C.A. Sorkness, Establishing a therapeutic index for the inhaled corticosteroids: Part II - Comparisons of systemic activity and safety among different inhaled corticosteroids. Journal of Allergy and Clinical Immunology 102(4) (1998) S52-S64.
[46] P. Hogger, Dose response and therapeutic index of inhaled corticosteroids in asthma. Curr. Opin. Pulm. Med. 9(1) (2003) 1-8.
[47] J. Rosenborg, P. Larsson, Z. Rott, C. BÃ–Cskei, M. Poczi, G. JuhÃ Sz, Relative therapeutic index between inhaled formoterol and salbutamol in asthma patients. Respir. Med. 96(6) (2002) 412-417.
[48] D.S. Millan, S.A. Ballard, S. Chunn, J.A. Dybowski, C.K. Fulton, P.A. Glossop, E. Guillabert, C.A. Hewson, R.M. Jones, D.J. Lamb, C.M. Napier, T.A. Payne-Cook, E.R. Renery, M.D. Selby, M.F. Tutt, M. Yeadon, Design and synthesis of long acting inhaled corticosteroids for the treatment of asthma. Bioorganic & Medicinal Chemistry Letters 21(19) (2012) 5826-5830.
[49] X.M. Zeng, G.P. Martin, C. Marriott, The controlled delivery of drugs to the lung. Int. J. Pharm. 124(2) (1995) 149-164.
[50] H.S.M. Ali, P. York, N. Blagden, S. Soltanpour, W.E. Acree, A. Jouyban, Solubility of budesonide, hydrocortisone, and prednisolone in ethanol plus water mixtures at 298.2 K. J. Chem. Eng. Data 55(1) (2010) 578-582.
[51] L. Thorsson, S. Edsbacker, A. Kallen, C.G. Lofdahl, Pharmacokinetics and systemic activity of fluticasone via Diskus (R) and pMDI, and of budesonide via Turbuhaler (R). Br. J. Clin. Pharmacol. 52(5) (2001) 529-538.
[52] C. Dalby, T. Polanowski, T. Larsson, L. Borgstrom, S. Edsbacker, T.W. Harrison, The bioavailability and airway clearance of the steroid component of

budesonide/formoterol and salmeterol/fluticasone after inhaled administration in patients with COPD and healthy subjects: a randomized controlled trial. Respir. Res. 10 (2009).
[53] A. Ryrfeldt, N.O. Bodin, Physiological disposition of ibuterol, terbutaline and isoproterenol after endotracheal instillation to rats. Xenobiotica 5(9) (1975) 521-529.
[54] I. Kass, T.S. Mingo, Bitolterol mesylate (WIN-32784) aerosol - a new long-acting bronchodilator with reduced chronotropic effects. Chest 78(2) (1980) 283-287.
[55] B. Axelsson, P. Bäckman, P. Strandberg, R. Brattsand, in: L. Claude (Ed.), Inhaled Steroids in Asthma - Optimising Effects in the Airways, Vol. 163, Marcel Dekker, New York, 2002, pp. 565-576.
[56] J. Swaminathan, C. Ehrhardt, in: S. a. Hickey (Ed.), Controlled Pulmonary Drug Delivery, Springer, New York, 2011, pp. 313-334.
[57] M.M. Bailey, C.J. Berkland, Nanoparticle formulations in pulmonary drug delivery. Med. Res. Rev. 29(1) (2009) 196-212.
[58] M. Chougule, B. Padhi, A. Misra, Nano-liposomal dry powder inhaler of tacrolimus: Preparation, characterization, and pulmonary pharmacokinetics. Int. J. Nanomed. 2(4) (2007) 675-688.
[59] O.R. Hung, S.C. Whynot, J.R. Varvel, S.L. Shafer, M. Mezei, Pharmacokinetics of inhaled liposome-encapsulated fentanyl. Anesthesiology 83(2) (1995) 277-284.
[60] N.V. Koshkina, V. Knight, B.E. Gilbert, E. Golunski, L. Roberts, J.C. Waldrep, Improved respiratory delivery of the anticancer drugs, camptothecin and paclitaxel, with 5% CO2-enriched air: pharmacokinetic studies. Cancer Chemother. Pharmacol. 47(5) (2001) 451-456.
[61] P. Sheth, P.B. Myrdal, in: S. a. Hickey (Ed.), Controlled Pulmonary Drug Delivery, Springer, New York, 2011, pp. 237-263.
[62] P. Sheth, P.B. Myrdal, in: S. a. Hickey (Ed.), Controlled Pulmonary Drug Delivery, Springer, New York, 2011, pp. 265-282.
[63] S. Al-Qadi, A. Grenha, D. Carrión-Recio, B. Seijo, C. Remuñán-López, Microencapsulated chitosan nanoparticles for pulmonary protein delivery: In vivo evaluation of insulin-loaded formulations. Journal of Controlled Release 157(3) (2012) 383-390.
[64] I. Kim, H.J. Byeon, T.H. Kim, E.S. Lee, K.T. Oh, B.S. Shin, K.C. Lee, Y.S. Youn, Doxorubicin-loaded highly porous large PLGA microparticles as a sustained-release inhalation system for the treatment of metastatic lung cancer. Biomaterials 33(22) (2012) 5574-5583.
[65] H. Karmouty-Quintana, F. Tamimi, T.K. McGovern, L.M. Grover, J.G. Martin, J.E. Barralet, Sustained steroid release in pulmonary inflammation model. Biomaterials 31(23) (2010) 6050-6059.
[66] Y.-J. Son, J.P. Mitchell, J.T. McConvill, in: S. a. Hickey (Ed.), Controlled Pulmonary Drug Delivery, Springer, New York, 2011, pp. 383-415.
[67] S. Khorasanizade, M. Shams, B.M. Mansoori, Calculation of aerosol deposition in human lung airways using Horsfield geometric model. Adv. Powder Technol. 22(6) (2011) 695-705.
[68] Horsfield.K, G. Dart, D.E. Olson, G.F. Filley, G. Cumming, Models of human bronchial tree. Journal of Applied Physiology 31(2) (1971) 207-217.

[69] A. Schmidt, S. Zidowitz, A. Kriete, T. Denhard, S. Krass, H.O. Peitgen, A digital reference model of the human bronchial tree. Computerized Medical Imaging and Graphics 28(4) (2004) 203-211.
[70] C.N. Guo, S.R. Gillespie, J. Kauffman, W.H. Doub, Comparison of delivery characteristics from a combination metered-dose inhaler using the Andersen Cascade Impactor and the Next Generation Pharmaceutical Impactor. J. Pharm. Sci. 97(8) (2008) 3321-3334.
[71] C.R. Lambre, M. Aufderheide, R.E. Bolton, B. Fubini, H.P. Haagsman, P.M. Hext, M. Jorissen, Y. Landry, J.P. Morin, B. Nemery, P. Nettesheim, J. Pauluhn, R.J. Richards, A.E.M. Vickers, R. Wu, In vitro tests for respiratory toxicity - The report and recommendations of ECVAM Workshop 18. Atla-Alternatives to Laboratory Animals 24(5) (1996) 671-681.
[72] B. Forbes, C. Ehrhardt, Human respiratory epithelial cell culture for drug delivery applications. European Journal Of Pharmaceutics And Biopharmaceutics 60(2) (2005) 193-205.
[73] M. Sakagami, In vivo, in vitro and ex vivo models to assess pulmonary absorption and disposition of inhaled therapeutics for systemic delivery. Adv. Drug Deliv. Rev. 58(9-10) (2006) 1030-1060.
[74] M. Madlova, C. Bosquillon, D. Asker, P. Dolezal, B. Forbes, In-vitro respiratory drug absorption models possess nominal functional P-glycoprotein activity. Journal of Pharmacy and Pharmacology 61(3) (2009) 293-301.
[75] S. Endter, D. Francombe, C. Ehrhardt, M. Gumbleton, RT-PCR analysis of ABC, SLC and SLCO drug transporters in human lung epithelial cell models. Journal of Pharmacy and Pharmacology 61(5) (2009) 583-591.
[76] B. Forbes, Human airway epithelial cell lines for in vitro drug transport and metabolism studies. Pharmaceutical Science and Technology Today 3(1) (2000) 18-27.
[77] B.I. Florea, M.L. Cassara, H.E. Junginger, G. Borchard, Drug transport and metabolism characteristics of the human airway epithelial cell line Calu-3. Journal of Controlled Release 87(1-3) (2003) 131-138.
[78] S.A. Cryan, N. Sivadas, L. Garcia-Contreras, *In vivo* animal models for drug delivery across the lung mucosal barrier. Adv. Drug Deliv. Rev. 60(7) (2008) 858-858.
[79] K. Yamada, Y. Yamamoto, K. Yanagihara, N. Araki, Y. Harada, Y. Morinaga, K. Izumikawa, H. Kakeya, H. Hasegawa, S. Kohno, S. Kamihira, *In vivo* efficacy and pharmacokinetics of biapenem in a murine model of ventilator-associated pneumonia with Pseudomonas aeruginosa. Journal of infection and chemotherapy : official journal of the Japan Society of Chemotherapy 18(4) (2012) 472-478.
[80] L.N. Somers GI, Lowdon BM, Jones AE, Freathy C, Ho S, Woodrooffe AJ, Bayliss MK, Manchee GR., A comparison of the expression and metabolizing activities of phase I and II enzymes in freshly isolated human lung parenchymal cells and cryopreserved human hepatocytes. Drug Metab Dispos. 35(10) (2007) 1797-1805.
[81] B.M. Liederer, R.T. Borchardt, Enzymes involved in the bioconversion of ester-based prodrugs. J. Pharm. Sci. 95(6) (2006) 1177-1195.
[82] S. Kudo, Differentiation of Clara cells and pneumocytes of the rat by means of enzymehistochemistry and immunohistochemistry. Anatomical Record 238(1) (1994) 49-56.

[83] N.M. Heller, R.P. Schleimer, Newly recognised glucocorticoid targets. in: L. Claude (Ed.), Lung Biology in Health and Disease, Vol. 163, Marcel Dekker, New York, 2002, pp. 137-164.
[84] G.B. Faulds, N. Subramaniam, J. Liden, S. Okret, W.J. Jusko, C. Stellato , N.M. Heller, R.P. Schleimer, in: L. Claude (Ed.), Inhaled Steroids in Asthma, Vol. 163, Marcel Dekker, New York, 2002, pp. 37-166.
[85] G.A. Rossi, F. Cerasoli, M. Cazzola, Safety of inhaled corticosteroids: room for improvement. Pulmonary Pharmacology and Therapeutics 20(1) (2007) 23-35.
[86] M. Johnson, Beta2 -adrenoceptors: mechanisms of action of beta2-agonists. Paediatric Respiratory Reviews 2(1) (2001) 57-62.
[87] TEVA, Proair HFA label. Horsham, 2010.
[88] T. Riley, J. Riggs-Sauthier, The benefits and challenges of PEGylating small molecules. Pharmaceutical Technology 32(7) (2008) 88-94.
[89] J. Khandare, T. Minko, Polymer-drug conjugates: progress in polymeric prodrugs. Progress in Polymer Science 31(4) (2006) 359-397.
[90] G. Pasut, F.M. Veronese, Polymer-drug conjugation, recent achievements and general strategies. Progress in Polymer Science 32(8-9) (2007) 933-961.
[91] D. Gaikwad, S. Dhawale, J. Khandare, M. Patil, T. Khade, B. Gavitre, K. Bobe, V. Kulkarni, U. Gaikwad, Polymer-drug conjugates: recent achievements. Research Journal of Pharmaceutical, Biological and Chemical Sciences 2(2) (2011) 200-208.
[92] R.B. Greenwald, PEG drugs: an overview. Journal of Controlled Release 74(1-3) (2001) 159-171.
[93] E. Markovsky, H. Baabur-Cohen, A. Eldar-Boock, L. Omer, G. Tiram, S. Ferber, P. Ofek, D. Polyak, A. Scomparin, R. Satchi-Fainaro, Administration, distribution, metabolism and elimination of polymer therapeutics. Journal of Controlled Release 161(2) (2012) 446-460.
[94] R. Webster, E. Didier, P. Harris, N. Siegel, J. Stadler, L. Tilbury, D. Smith, PEGylated proteins: evaluation of their safety in the absence of definitive metabolism studies. Drug Metab Dispos. 35(1) (2007) 9-16.
[95] R. Webster, V. Elliott, B.K. Park, D. Walker, M. Hankin, P. Taupin, F.M. Veronese, Birkhäuser Basel, 2009, pp. 127-146.
[96] D.R. Klonne, D.E. Dodd, P.E. Losco, C.M. Troup, T.R. Tyler, 2-week aerosol inhalation study on polyethylene glycol-(PEG)-3350 in F344 rats. Drug Chem. Toxicol. 12(1) (1989) 39-48.
[97] H. Gursahani, J. Riggs-Sauthier, J. Pfeiffer, D. Lechuga-Ballesteros, C.S. Fishburn, Absorption of polyethylene glycol (PEG) polymers: the effect of PEG size on permeability. J. Pharm. Sci. 98(8) (2009) 2847-2856.
[98] R.B. Greenwald, C.W. Gilbert, A. Pendri, C.D. Conover, J. Xia, A. Martinez, Drug delivery systems: water soluble taxol 2'-poly(ethylene glycol) ester prodrugs - Design and in vivo effectiveness. Journal of Medicinal Chemistry 39(2) (1996) 424-431.
[99] R.B. Greenwald, A. Pendri, C. Conover, C. Gilbert, R. Yang, J. Xia, Drug delivery systems. 2. Camptothecin 20-o-poly(ethylene glycol) ester transport forms. Journal of Medicinal Chemistry 39(10) (1996) 1938-1940.
[100] G. Yousefi, S.M. Foroutan, A. Zarghi, A. Shafaati, Synthesis and characterization of methotrexate polyethylene glycol esters as a drug delivery system. Chemical & Pharmaceutical Bulletin 58(2) (2010) 147-153.

[101] Q.S. Zhou, X.H. Jiang, J.R. Yu, K.J. Li, Synthesis and characterization of PEG-scutellarin conjugates, a potential PEG ester prodrug for the oral delivery of scutellarin. Chinese Chemical Letters 17(1) (2006) 85-88.
[102] M. Zacchigna, G. Di Luca, V. Maurich, E. Bocca, Syntheses, chemical and enzymatic stability of new poly(ethylene glycol)-acyclovir prodrugs. Farmaco 57(3) (2002) 207-214.
[103] S.M. Foroutan, D.G. Watson, Synthesis and characterisation of polyethylene glycol conjugates of hydrocortisone as potential prodrugs for ocular steroid delivery. Int. J. Pharm. 157(1) (1997) 103-111.
[104] R.B. Greenwald, A. Pendri, C.D. Conover, C. Lee, Y.H. Choe, C. Gilbert, A. Martinez, J. Xia, D. Wu, M.-m. Hsue, Camptothecin-20-PEG ester transport forms: the effect of spacer groups on antitumor activity. Bioorganic & Medicinal Chemistry 6(5) (1998) 551-562.
[105] F.M. Veronese, P. Caliceti, A. Pastorino, O. Schiavon, L. Sartore, L. Banci, L.M. Scolaro, Preparation, physico-chemical and pharmacokinetic characterization of monomethoxypoly(ethylene glycol)-derivatized superoxide dismutase. Journal of Controlled Release 10(1) (1989) 145-154.
[106] G. Tojo, M. Fernández, in: G. Tojo (Ed.), Springer New York, 2006, pp. 79-103.
[107] R. Atkins, F. Carey, 1990, pp. 371-374.
[108] B. Neises, W. Steglich, Simple method for the esterification of carboxylic acids. Angewandte Chemie International Edition in English 17(7) (1978) 522-524.
[109] X.-Q. Li, F.-T. Meng, H. Guang, Z.-G. Su, A simple and efficient method for synthesis of carboxymethylated polyethyleneglycol. Journal of Chemical Research 2005 (2005) 280-281.
[110] K. Saigo, M. Usui, K. Kikuchi, E. Shimada, T. Mukaiyama, New method for preparation of carboxylic esters. Bulletin of the Chemical Society of Japan 50(7) (1977) 1863-1866.
[111] A.P. Ijzerman, T. Bultsma, H. Timmerman, J. Zaagsma, The ionization of β_2-adrenoceptor agonists: a method for unravelling ionization schemes. Journal of Pharmacy and Pharmacology 36(1) (1984) 11-15.
[112] R. Imboden, G. Imanidis, Effect of the amphoteric properties of salbutamol on its release rate through a polypropylene control membrane. European Journal of Pharmaceutics and Biopharmaceutics 47(2) (1999) 161-167.
[113] S.O. Ko, M.A. Schlautman, E.R. Carraway, Effects of solution chemistry on the partitioning of phenanthrene to sorbed surfactants. Environmental Science & Technology 32(22) (1998) 3542-3548.
[114] G.P. Moss, The nomenclature of steroids. European Journal of Biochemistry 186(3) (1989) 429-458.
[115] S. Rachwal, E. Pop, M.E. Brewster, Structural studies of loteprednol etabonate and other analogs of prednisolone using NMR techniques. Steroids 61(9) (1996) 524-530.
[116] The Japanese Pharmacopoeia Sixteenth Edition, The Ministry of Health Labour and Welfare, 2011, p. 1918.
[117] J.A. Dean, Lange's Handbook of Chemistry (15th Edition). McGraw-Hill, 1999.
[118] H.R.H. Ali, H.G.M. Edwards, J. Kendrick, I.J. Scowen, Vibrational spectroscopic study of salbutamol hemisulphate. Drug Testing and Analysis 1(1-2) (2009) 51-56.

[119] D.W. Straughan, J.H. Fentem, M. Balls, In Vitro Methods in Pharmaceutical Research, Academic Press, San Diego, 1996, pp. 1-13.
[120] B. Kane, Z. Borrill, T. Southworth, A. Woodcock, D. Singh, Reduced exhaled breath condensate pH in asthmatic smokers using inhaled corticosteroids. Respirology 14(3) (2009) 419-423.
[121] K. Kostikas, G. Papatheodorou, K. Ganas, K. Psathakis, P. Panagou, S. Loukides, pH in expired breath condensate of patients with inflammatory airway diseases. American Journal of Respiratory and Critical Care Medicine 165(10) (2002) 1364-1370.
[122] J.C. Ojoo, S.A. Mulrennan, J.A. Kastelik, A.H. Morice, A.E. Redington, Exhaled breath condensate pH and exhaled nitric oxide in allergic asthma and in cystic fibrosis. Thorax 60(1) (2005) 22-26.
[123] J.F. Hunt, K.Z. Fang, R. Malik, A. Snyder, N. Malhotra, T.A.E. Platts-Mills, B. Gaston, Endogenous airway acidification - Implications for asthma pathophysiology. American Journal of Respiratory and Critical Care Medicine 161(3) (2000) 694-699.
[124] R. Koczulla, S. Dragonieri, R. Schot, R. Bals, S.A. Gauw, C. Vogelmeier, K.F. Rabe, P.J. Sterk, P.S. Hiemstra, Comparison of exhaled breath condensate pH using two commercially available devices in healthy controls, asthma and COPD patients. Respir. Res. 10 (2009).
[125] K.A. Foster, M.L. Avery, M. Yazdanian, K.L. Audus, Characterization of the Calu-3 cell line as a tool to screen pulmonary drug delivery. Int. J. Pharm. 208(1-2) (2000) 1-11.
[126] R.M.D.P.A.K.M. Isabelle Pezron, Insulin aggregation and asymmetric transport across human bronchial epithelial cell monolayers (Calu-3). J. Pharm. Sci. 91(4) (2002) 1135-1146.
[127] C.I. Grainger, L.L. Greenwell, D.J. Lockley, G.P. Martin, B. Forbes, Culture of Calu-3 cells at the air interface provides a representative model of the airway epithelial barrier. Pharmaceutical Research 23(7) (2006) 1482-1490.
[128] M.E. Cavet, M. West, N.L. Simmons, Transepithelial transport of the fluoroquinolone ciprofloxacin by human airway epithelial Calu-3 cells. Antimicrobial Agents and Chemotherapy 41(12) (1997) 2693-2698.
[129] C. Ehrhardt, C. Kneuer, C. Bies, C.M. Lehr, K.J. Kim, U.U. Bakowsky, Salbutamol is actively absorbed across human bronchial epithelial cell layers. Pulmonary Pharmacology & Therapeutics 18(3) (2005) 165-170.
[130] J. Fiegel, C. Ehrhardt, U.F. Schaefer, C.M. Lehr, J. Hanes, Large porous particle impingement on lung epithelial cell monolayers - Toward improved particle characterization in the lung. Pharmaceutical Research 20(5) (2003) 788-796.
[131] G. Borchard, M.L. Cassara, P.E.H. Roemele, B.I. Florea, H.E. Junginger, Transport and local metabolism of budesonide and fluticasone propionate in a human bronchial epithelial cell line (Calu-3). J. Pharm. Sci. 91(6) (2002) 1561-1567.
[132] J. Brillault, W.V. De Castro, T. Harnois, A. Kitzis, J.C. Olivier, W. Couet, P-glycoprotein-mediated transport of moxifloxacin in a Calu-3 lung epithelial cell model. Antimicrobial Agents and Chemotherapy 53(4) (2009) 1457-1462.
[133] L. Bordenave, R. Bareille, F. Lefebvre, C. Baquey, A comparison between 51chromium release and LDH release to measure cell membrane integrity: Interest for cytocompatibility studies with biomaterials. Journal of Applied Biomaterials 4(4) (1993) 309-315.

[134] T.C. McIlvaine, A buffer solution for colorimetric comparison. Journal of Biological Chemistry 49(1) (1921) 183-186.
[135] P.J. Elving, J.M. Markowitz, I. Rosenthal, Preparation of buffer systems of constant ionic strength. Analytical Chemistry 28(7) (1956) 1179-1180.
[136] C. Mohan, Buffers: a guide for the preparation and use of buffers in biological systems, Darmstadt, 2003.
[137] E. Euranto, Chapter 11. Esterification and ester hydrolysis. The chemistry of carboxylic acids and esters (1969) 505-588.
[138] Y. Huang, J. Lu, X. Gao, J. Li, W. Zhao, M. Sun, D.B. Stolz, R. Venkataramanan, L.C. Rohan, S. Li, PEG-derivatized embelin as a dual functional carrier for the delivery of paclitaxel. Bioconjugate Chemistry 23(7) (2012) 1443-1451.
[139] P. Kallinteri, S. Higgins, G.A. Hutcheon, C.B. St. Pourçain, M.C. Garnett, Novel functionalized biodegradable polymers for nanoparticle drug delivery systems. Biomacromolecules 6(4) (2005) 1885-1894.
[140] B. Capon, Neighbouring group participation. Quarterly Reviews, Chemical Society 18(1) (1964) 45-111.
[141] L.J. Edwards, The hydrolysis of aspirin. A determination of the thermodynamic dissociation constant and a study of the reaction kinetics by ultra-violet spectrophotometry. Transactions of the Faraday Society 46 (1950) 723-735.
[142] L.J. Edwards, The hydrolysis of aspirin. Part 2. Transactions of the Faraday Society 48 (1952) 696-699.
[143] E.R. Garrett, The kinetics of solvolysis of acyl esters of salicyclic acid. Journal of the American Chemical Society 79(13) (1957) 3401-3408.
[144] A.R. Fersht, A.J. Kirby, Structure and mechanism in intramolecular catalysis. Hydrolysis of substituted aspirins. Journal of the American Chemical Society 89(19) (1967) 4853-4857.
[145] A.R. Fersht, A.J. Kirby, Hydrolysis of aspirin. Intramolecular general base catalysis of ester hydrolysis. Journal of the American Chemical Society 89(19) (1967) 4857-4863.
[146] A.J. Kirby, G.J. Lloyd, Intramolecular general base catalysis of intramolecular nucleophilic catalysis of ester hydrolysis. Journal of the Chemical Society, Perkin Transactions 2(6) (1974) 637-642.
[147] A.R. Fersht, A.J. Kirby, Intramolecular nucleophilic catalysis of ester hydrolysis by the ionized carboxyl group. The hydrolysis of 3,5-dinitroaspirin anion. Journal of the American Chemical Society 90(21) (1968) 5818-5826.
[148] T.C. Bruice, S.J. Benkovic, A comparison of the bimolecular and intramolecular nucleophilic catalysis of the hydrolysis of substituted phenyl acylates by the dimethylamino group. Journal of the American Chemical Society 85(1) (1963) 1-8.
[149] P. Chetoni, P. Crotti, M.F. Saettone, Albuterol prodrugs for ocular administration - Synthesis and evaluation of the physicochemical and IOP-depressant properties of 3 albuterol triesters. Int. J. Pharm. 105(2) (1994) 147-155.
[150] P.C. Seville, C. Simons, G. Taylor, P.A. Dickinson, Prodrug to probe solution HFA pMDI formulation and pulmonary esterase activity. Int. J. Pharm. 195(1-2) (2000) 13-16.
[151] T.C. Bruice, J.M. Sturtevant, Imidazole catalysis. 5. The intramolecular participation of the imidazolyl group in the hydrolysis of some esters and the amide

of gamma-(4-imidazolyl)-butyric acid and 4-(2'-acetoxyethyl)-imidazole. Journal of the American Chemical Society 81(11) (1959) 2860-2870.
[152] S.A. Bernhard, J.H. Carter, E. Katchalski, M. Sela, Y. Shalitin, A. Berger, Co-operative effects of functional groups in peptides .1. Aspartyl-serine derivatives. Journal of the American Chemical Society 84(12) (1962) 2421-2434.
[153] A. Agren, U. Hedsten, B. Jonsson, Hydrolysis of protolytic esters. Acta Chemica Scandinavica 15(7) (1961) 1532-1554.
[154] B. Hansen, Kinetics of alkaline hydrolysis of aminoalkyl esters of carboxylic acids. Acta Chemica Scandinavica 16(8) (1962) 1927-1935.
[155] G. Aksnes, P. Froyen, Hydrogen bonding ionization and rate hydrolysis of aliphatic ammonium esters. Acta Chemica Scandinavica 20(6) (1966) 1451-1455.
[156] E.R. Garrett, Evidence for general base catalysis in an ester hydrolysis. 2. Hydrolysis of an aminoalkyl acetylsalicylate. Journal of the American Chemical Society 80(15) (1958) 4049-4056.
[157] G. Aksnes, P. Froyen, Alkaline hydrolysis of positively charged methyl and p-nitrophenyl esters of dimethyl- and trimethylglycine. Acta Chemica Scandinavica 21(6) (1967) 1507-1510.
[158] A. Buur, H. Bundgaard, V.H.L. Lee, Prodrugs of propranolol: hydrolysis and intramolecular aminolysis of various propranolol esters and an oxazolidin-2-one derivative. Int. J. Pharm. 42(1-3) (1988) 51-60.
[159] P. Li, K. Zhao, S. Deng, D.W. Landry, Nonenzymatic hydrolysis of cocaine via intramolecular acid catalysis. Helvetica Chimica Acta 82(1) (1999) 85-89.
[160] C.G. Zhan, S.X. Deng, J.G. Skiba, B.A. Hayes, S.M. Tschampel, G.C. Shields, D.W. Landry, First-principle studies of intermolecular and intramolecular catalysis of protonated cocaine. Journal of Computational Chemistry 26(10) (2005) 980-986.
[161] T. Ehtezazi, D. Allanson, I. Jenkinson, C. O'Callaghan, Effect of oropharyngeal length in drug lung delivery via suspension pressurized metered dose inhalers. Pharmaceutical Research 23(6) (2006) 1364-1372.
[162] R. Donnelly, J.P. Seale, Clinical pharmacokinetics of inhaled budesonide. Clin. Pharmacokinet. 40(6) (2001) 427-440.
[163] A.H. deBoer, G.K. Bolhuis, D. Gjaltema, P. Hagedoorn, Inhalation characteristics and their effects on in vitro drug delivery from dry powder inhalers .3. The effect of flow increase rate (FIR) on the in vitro drug release from the Pulmicort 200 Turbuhaler. Int. J. Pharm. 153(1) (1997) 67-77.
[164] Kim. CS, Hu. SC, DeWitt. P, G. TR, Assessment of regional deposition of inhaled particles in human lungs by serial bolus delivery method. J Appl Physiol. 81(5) (1996) 2203-2213.
[165] G. Pasut, F. Canal, L. Dalla Via, S. Arpicco, F.M. Veronese, O. Schiavon, Antitumoral activity of PEG-gemcitabine prodrugs targeted by folic acid. Journal of Controlled Release 127(3) (2008) 239-248.
[166] O. Schiavon, G. Pasut, S. Moro, P. Orsolini, A. Guiotto, F.M. Veronese, PEG-Ara-C conjugates for controlled release. European Journal of Medicinal Chemistry 39(2) (2004) 123-133.
[167] M. Canevari, I. Castagliuolo, P. Brun, M. Cardin, M. Schiavon, G. Pasut, F.M. Veronese, Poly(ethylene glycol)-mesalazine conjugate for colon specific delivery. Int. J. Pharm. 368(1-2) (2009) 171-177.

[168] F. Bettio, M. Canevari, C. Marzano, F. Bordin, A. Guiotto, F. Greco, R. Duncan, F.M. Veronese, Synthesis and biological in vitro evaluation of novel PEG-psoralen conjugates. Biomacromolecules 7(12) (2006) 3534-3541.
[169] S. Zalipsky, Chemistry of polyethylene-glycol conjugates with biologically-active molecules. Adv. Drug Deliv. Rev. 16(2-3) (1995) 157-182.
[170] R.A. Robinson, The primary neutral salt effect in the catalytic hydrolysis of ethyl acetate. Transactions of the Faraday Society 26 (1930) 217-226.
[171] J.I. Hoppe, J.E. Prue, Metal-ion catalysis and specific kinetic salt effects in the alkaline hydrolysis of half-esters of dicarboxylic acids. Journal of the Chemical Society(APR) (1957) 1775-1781.
[172] F. Bayard, T. Calande, D.I. Pritchard, W. Thielemans, S. Young, S. Paine, C. Bosquillon, Esterase activity in the Human Bronchial Epithelial Calu-3 Cell Line. Journal of Pharmacy and Pharmacology 62(10) (2010) 1316-1317.
[173] W.M. Russell, R.L. Burch, The principles of humane experimental technique, London, 1959.
[174] M. Balls, The principles of humane experimental technique: timeless insights and unheeded warnings. Altex-Alternatives to Animal Experimentation 27(2) (2010) 144-148.
[175] A.M. Goldberg, The principles of humane experimental technique: is it relevant today? Altex-Alternatives to Animal Experimentation 27(2) (2010) 149-151.
[176] A. Tronde, C. Bosquillon, B. Forbes, The isolated perfused lung for drug absorption studies. Biotechnology: Pharmaceutical Aspects (2008) 135-163.
[177] C.u.A. Fernandes, R. Vanbever, Preclinical models for pulmonary drug delivery. Expert Opinion on Drug Delivery 6(11) (2009) 1231-1245.
[178] A. Tronde, B. Norden, A.B. Jeppsson, P. Brunmark, E. Nilsson, H. Lennernas, U.H. Bengtsson, Drug absorption from the isolated perfused rat lung-correlations with drug physicochemical properties and epithelial permeability. J. Drug Target. 11(1) (2003) 61-74.
[179] Y.N. Pang, M. Sakagami, P.R. Byron, The pharmacokinetics of pulmonary insulin in the in vitro isolated perfused rat lung: Implications of metabolism and regional deposition. European Journal of Pharmaceutical Sciences 25(4-5) (2005) 369-378.
[180] Y.N. Pang, M. Sakagami, P.R. Byron, Insulin self-association: effects on lung disposition kinetics in the airways of the isolated perfused rat lung (IPRL). Pharmaceutical Research 24(9) (2007) 1636-1644.
[181] A. Tronde, G. Baran, S. Eirefelt, H. Lennernas, U.H. Bengtsson, Miniaturized nebulization catheters: a new approach for delivery of defined aerosol doses to the rat lung. J. Aerosol Med.-Depos. Clear. Eff. Lung 15(3) (2002) 283-296.
[182] P. Ewing, S.J. Eirefelt, P. Andersson, A. Blomgren, A. Ryrfeldt, P. Gerde, Short inhalation exposures of the isolated and perfused rat lung to respirable dry particle aerosols; The detailed pharmacokinetics of budesonide, formoterol, and terbutaline. Journal of Aerosol Medicine and Pulmonary Drug Delivery 21(2) (2008) 169-180.
[183] P. Ewing, A. Ryrfeldt, C.O. Sjöberg, P. Andersson, S. Edsbäcker, P. Gerde, Vasoconstriction after inhalation of budesonide: A study in the isolated and perfused rat lung. Pulmonary Pharmacology and Therapeutics 23(1) (2010) 9-14.
[184] E. Selg, F. Acevedo, R. Nybom, B. Blomgren, A. Ryrfeldt, P. Gerde, Delivering horseradish peroxidase as a respirable powder to the isolated, perfused,

and ventilated lung of the rat: the pulmonary disposition of an inhaled model biopharmaceutical. Journal of Aerosol Medicine and Pulmonary Drug Delivery 23(5) (2010) 273-284.
[185] Y.S. Nam, I.K. Kwon, Y. Lee, K.B. Lee, Quantitative monitoring of corticosteroids in cosmetic products manufactured in Korea using LC-MS/MS. Forensic Science International 220(1-3) (2012) e23-e28.
[186] V.A. Frerichs, K.M. Tornatore, Determination of the glucocorticoids prednisone, prednisolone, dexamethasone, and cortisol in human serum using liquid chromatography coupled to tandem mass spectrometry. Journal of Chromatography B-Analytical Technologies in the Biomedical and Life Sciences 802(2) (2004) 329-338.
[187] S. Basavaraj, H.A.E. Benson, C. Cruickshank, D.H. Brown, Y. Chen, Development of a liquid chromatography/mass spectrometry methodology to separate, detect, characterize and quantify PEG-resveratrol prodrugs and the conjugation reaction precursors and intermediates. Rapid Commun. Mass Spectrom. 25(11) (2011) 1543-1551.
[188] P. Gerde, P. Ewing, L. Låstbom, Å. Ryrfeldt, J. Waher, G. Lidén, A novel method to aerosolize powder for short inhalation exposures at high concentrations: isolated rat lungs exposed to respirable Diesel soot. Inhalation Toxicology 16(1) (2004) 45-52.
[189] L.Y. Yeo, J.R. Friend, M.P. McIntosh, E.N.T. Meeusen, D.A.V. Morton, Ultrasonic nebulization platforms for pulmonary drug delivery. Expert Opinion on Drug Delivery 7(6) (2010) 663-679.
[190] K.A. Johnson, R.S. Goody, The original Michaelis constant: translation of the 1913 Michaelis-Menten paper. Biochemistry 50(39) (2011) 8264-8269.
[191] G.E. Briggs, J.B.S. Haldane, A note on the kinetics of enzyme action. Biochemical Journal 19(2) (1925) 338-339.
[192] A.E. Vatter, O.K. Reiss, J.K. Newman, Lindquis.K, Groenebo.E, Enzymes of lung. I. Detection of esterase with a new cytochemical method. Journal of Cell Biology 38(1) (1968) 80-98.
[193] O. Vondeimling, M. Muller, E. Eisenhardt, The non-specific esterases of mouse lung. Histochemistry 78(2) (1983) 271-284.
[194] N.W. McCracken, P.G. Blain, F.M. Williams, Nature and role of xenobiotic metabolizing esterases in rat-liver, lung, skin and blood. Biochemical Pharmacology 45(1) (1993) 31-36.
[195] M. Jendbro, C.J. Johansson, P. Strandberg, H. Falk-Nilsson, S. Edsbacker, Pharmacokinetics of budesonide and its major ester metabolite after inhalation and intravenous administration of budesonide in the rat. Drug Metabolism and Disposition 29(5) (2001) 769-776.
[196] K. Foe, K.F. Brown, J.P. Seale, Comparative kinetics of metabolism of beclomethasone propionate esters in human lung homogenates and plasma. J. Pharm. Sci. 89(9) (2000) 1143-1150.
[197] P.T. Daley-Yates, A.C. Price, J.R. Sisson, A. Pereira, N. Dallow, Beclomethasone dipropionate: absolute bioavailability, pharmacokinetics and metabolism following intravenous, oral, intranasal and inhaled administration in man. Br. J. Clin. Pharmacol. 51(5) (2001) 400-409.
[198] T. Nonaka, R. Nave, N. McCracken, A. Kawashimo, Y. Katsuura, Ciclesonide uptake and metabolism in human alveolar type II epithelial cells (A549). BMC Pharmacology 7(1) (2007).

[199] R. Nave, H. Watz, H. Hoffmann, H. Boss, H. Magnussen, Deposition and metabolism of inhaled ciclesonide in the human lung. European Respiratory Journal 36(5) (2010) 1113-1119.
[200] N.W. McCracken, P.G. Blain, F.M. Williams, Human xenobiotic metabolizing esterases in liver and blood. Biochemical Pharmacology 46(7) (1993) 1125-1129.
[201] Y. Yoshigae, T. Imai, A. Horita, H. Matsukane, M. Otagiri, Species differences in stereoselective hydrolase activity in intestinal mucosa. Pharmaceutical Research 15(4) (1998) 626-631.
[202] J.Z. Yang, W. Chen, R.T. Borchardt, *In vitro* stability and in vivo pharmacokinetic studies of a model opioid peptide, H-Tyr-D-Ala-Gly-Phe-D-Leu-OH (DADLE), and its cyclic prodrugs. Journal of Pharmacology and Experimental Therapeutics 303(2) (2002) 840-848.
[203] E.V. Rudakova, N.P. Boltneva, G.F. Makhaeva, Comparative analysis of esterase activities of human, mouse, and rat blood. Bulletin of Experimental Biology and Medicine 152(1) (2011) 73-75.
[204] A.E.M. Vickers, R.M. Jimenez, M.C. Spaans, V. Pflimlin, R.L. Fisher, K. Brendel, Human and rat lung biotransformation of cyclosporin A and its derivatives using slices and bronchial epithelial cells. Drug Metabolism and Disposition 25(7) (1997) 873-880.
[205] M. Hosokawa, Structure and catalytic properties of carboxylesterase isozymes involved in metabolic activation of prodrugs. Molecules 13(2) (2008) 412-431.
[206] A. Drollmann, R. Nave, V.W. Steinijans, E. Baumgärtner, T.D. Bethke, Equivalent pharmacokinetics of the active metabolite of ciclesonide with and without use of the AeroChamber Plus^{TM} spacer for inhalation. Clin. Pharmacokinet. 45(7) (2006) 729-736.
[207] E. Mutch, R. Nave, N. McCracken, K. Zech, F.M. Williams, The role of esterases in the metabolism of ciclesonide to desisobutyryl-ciclesonide in human tissue. Biochemical Pharmacology 73(10) (2007) 1657-1664.
[208] R.-F. Guo, P.A. Ward, J.A. Jordan, M. Huber-Lang, R.L. Warner, M.M. Shi, Eotaxin expression in Sephadex-induced lung injury in rats. The American Journal of Pathology 155(6) (1999) 2001-2008.
[209] Z. Li, J. Hu, M. Sun, H. Ji, S. Chu, G. Liu, N. Chen, Anti-inflammatory effect of IMMLG5521, a coumarin derivative, on Sephadex-induced lung inflammation in rats. International Immunopharmacology 14(2) (2012) 145-149.
[210] F. Tewes, L. Tajber, O.I. Corrigan, C. Ehrhardt, A.M. Healy, Development and characterisation of soluble polymeric particles for pulmonary peptide delivery. European Journal of Pharmaceutical Sciences 41(2) (2010) 337-352.
[211] D.O. Corrigan, O.I. Corrigan, A.M. Healy, Predicting the physical state of spray dried composites: Salbutamol sulphate/lactose and salbutamol sulphate/polyethylene glycol co-spray dried systems. Int. J. Pharm. 273(1-2) (2004) 171-182.
[212] W.H. Brown, C.F. Foote, B.L. Iverson, E.V. Anslyn, in: L. Lockwood (Ed.), Organic chemistry, Cengage Learning, Inc, Mason, OH, 2011, pp. 649-679.
[213] A.L. Simplicio, J.M. Clancy, J.F. Gilmer, Prodrugs for amines. Molecules 13(3) (2008) 519-547.
[214] J. Ostergaard, C. Larsen, Bioreversible derivatives of phenol. 1. The role of human serum albumin as related to the stability and binding properties of carbonate

esters with fatty acid-like structures in aqueous solution and biological media. Molecules 12(10) (2007) 2380-2395.
[215] T.H. Fife, General acid catalysis of acetal, ketal, and ortho ester hydrolysis. Accounts of Chemical Research 5(8) (1972) 264-272.
[216] P. Deslongchamps, Y.L. Dory, S.G. Li, The relative rate of hydrolysis of a series of acyclic and six-membered cyclic acetals, ketals, orthoesters, and orthocarbonates. Tetrahedron 56(22) (2000) 3533-3537.
[217] P.H. Morgan, I.G. Nair, Hydrolysis of a synthetic amide substrate by human C1 esterase (C1s). Journal of Immunology 119(1) (1977) 19-25.
[218] R. Mentlein, E. Heymann, Hydrolysis of ester- and amide-type drugs by the purified isoenzymes of nonspecific carboxylesterase from rat liver. Biochemical Pharmacology 33(8) (1984) 1243-1248.
[219] S. Takai, A. Matsuda, Y. Usami, T. Adachi, T. Sugiyama, Y. Katagiri, M. Tatematsu, K. Hirano, Hydrolytic profile for ester- or amide-linkage by carboxylesterases pI 5.3 and 4.5 from human liver. Biological and Pharmaceutical Bulletin 20(8) (1997) 869-873.
[220] A. Guiotto, M. Canevari, P. Orsolini, O. Lavanchy, C. Deuschel, N. Kaneda, A. Kurita, T. Matsuzaki, T. Yaegashi, S. Sawada, F.M. Veronese, Synthesis, characterization, and preliminary in vivo tests of new poly(ethylene glycol) conjugates of the antitumor agent 10-amino-7-ethylcamptothecin. Journal of Medicinal Chemistry 47(5) (2004) 1280-1289.
[221] V.H.J. van der Velden, A.R. Hulsmann, Peptidases: structure, function and modulation of peptide-mediated effects in the human lung. Clin. Exp. Allergy 29(4) (1999) 445-456.
[222] I. Garcia-Verdugo, D. Descamps, M. Chignard, L. Touqui, J.M. Sallenave, Lung protease/anti-protease network and modulation of mucus production and surfactant activity. Biochimie 92(11) (2005) 1608-1617.
[223] C.C. Taggart, C.M. Greene, T.P. Carroll, S.J. O'Neill, N.G. McElvaney, Elastolytic proteases. American Journal of Respiratory and Critical Care Medicine 171(10) (2005) 1070-1076.
[224] M.J. Taraszka, Relative enzymatic hydrolysis rates of lincomycin esters. I. soluble esters. J. Pharm. Sci. 60(9) (1971) 1414-1417.
[225] C. Mignat, D. Heber, H. Schlicht, A. Ziegler, Synthesis, opioid receptor affinity, and enzymatic hydrolysis of sterically hindered morphine 3-esters. J. Pharm. Sci. 85(7) (1996) 690-694.
[226] G. Pasut, S. Scaramuzza, O. Schiavon, R. Mendichi, F.M. Veronese, PEG-epirubicin conjugates with high drug loading. Journal of Bioactive and Compatible Polymers 20(3) (2005) 213-230.
[227] M. Zacchigna, F. Cateni, S. Drioli, G.M. Bonora, Multimeric, multifunctional derivatives of poly(ethylene glycol). Polymers 3(3) (2011) 1076-1090.
[228] H. Zhao, B. Rubio, P. Sapra, D. Wu, P. Reddy, P. Sai, A. Martinez, Y. Gao, Y. Lozanguiez, C. Longley, L.M. Greenberger, I.D. Horak, Novel prodrugs of SN38 using multiarm poly(ethylene glycol) linkers. Bioconjugate Chemistry 19(4) (2008) 849-859.
[229] C.A. Lipinski, F. Lombardo, B.W. Dominy, P.J. Feeney, Experimental and computational approaches to estimate solubility and permeability in drug discovery and development settings. Adv. Drug Deliv. Rev. 46(1-3) (2001) 3-26.
[230] A. Tronde, B. Norden, H. Marchner, A.K. Wendel, H. Lennernas, U.H. Bengtsson, Pulmonary absorption rate and bioavailability of drugs in vivo in rats:

structure-absorption relationships and physicochemical profiling of inhaled drugs. J. Pharm. Sci. 92(6) (2003) 1216-1233.
[231] W.H. Roa, S. Azarmi, M.H.D.K. Al-Hallak, W.H. Finlay, A.M. Magliocco, R. Löbenberg, Inhalable nanoparticles, a non-invasive approach to treat lung cancer in a mouse model. Journal of Controlled Release 150(1) (2011) 49-55.
[232] P. Zarogoulidis, E. Eleftheriadou, I. Sapardanis, V. Zarogoulidou, H. Lithoxopoulou, T. Kontakiotis, N. Karamanos, G. Zachariadis, M. Mabroudi, A. Zisimopoulos, K. Zarogoulidis, Feasibility and effectiveness of inhaled carboplatin in NSCLC patients. Invest. New Drugs 30(4) (2011) 1628-1640.